



PREDIS

PREDIS – Proceedings of May Workshop 2023

Date 29.9.2023

Dissemination level Public Version Final

Editors Sami Naumer and Maria Oksa

VTT Technical Research Centre of Finland Ltd
Kivimiehentie 3, Espoo, Finland

sami.naumer@vtt.fi

maria.oksa@vtt.fi



This project has received funding from the European Union's Euratom research and training programme 2019-2020 under grant agreement No 945098.

TABLE OF CONTENTS

| | | |
|-------|--|----|
| 1 | OVERVIEW | 5 |
| 2 | OVERVIEW OF STRATEGIC IMPLEMENTATION (WP2)..... | 6 |
| 3 | OVERVIEW OF KNOWLEDGE MANAGEMENT (WP3)..... | 9 |
| 4 | SCIENTIFIC PROGRESS IN INNOVATIONS IN METALLIC TREATMENT AND CONDITIONING (WP4) | 12 |
| 4.1 | Defining Europe-wide Needs and Opportunities for Management of Metallic Waste Streams (Task 4.3.)..... | 12 |
| 4.2 | Development and optimisation of decontamination processes (Task 4.4.)..... | 15 |
| 4.2.1 | Metallic waste surrogates preparation | 15 |
| 4.2.2 | Decontamination of metallic waste using chemical solutions..... | 16 |
| 4.2.3 | Decontamination of metallic samples using a gel technology avoiding secondary liquid waste..... | 20 |
| 4.2.4 | Secondary waste treatment..... | 22 |
| 4.3 | Optimisation of metallic waste characterisation and procedures for waste minimisation and recycling (Task 4.5)..... | 24 |
| 4.3.1 | Classification of the metallic waste streams of the different types of reactors | 24 |
| 4.3.2 | Characterization and sorting of metallic waste in different management routes | 27 |
| 4.3.3 | Development of new radiochemical procedures for DTM radionuclides..... | 28 |
| 4.4 | Encapsulation of reactive metals in magnesium phosphate cement-based matrices (Task 4.6.) | 33 |
| 4.4.1 | Development of magnesium phosphate cement formulations | 33 |
| 4.4.2 | Magnesium phosphate cement cost optimization | 34 |
| 4.4.3 | Behavior of magnesium phosphate cement under irradiation | 35 |
| 4.4.4 | Leaching behaviour of magnesium phosphate cement pastes | 36 |
| 4.4.5 | Al corrosion in magnesium phosphate cements..... | 38 |
| 4.4.6 | Steel corrosion in magnesium phosphate cements..... | 40 |
| 4.4.7 | Be corrosion in magnesium phosphate cements..... | 41 |
| 5 | SCIENTIFIC PROGRESS INNOVATIONS IN LIQUID ORGANIC WASTE TREATMENT AND CONDITIONING (WP5)..... | 44 |
| 5.1 | Geopolymer cements for the immobilisation of radioactive liquid organic wastes | 44 |
| 5.2 | Robustness tests for immobilization of oils in alkali activated slag | 45 |
| 5.3 | Robustness tests and optimization of BFS based geopolymers (Task 5.3) | 48 |
| 5.4 | Encapsulation of Neostane oil and TBP/Dodecane using the mix formulation (KIPT formulation) (Task 5.3)..... | 51 |
| 5.5 | Study of conditioning matrix durability – leaching experiments with BFS formulation and engine oil as waste | 54 |
| 5.6 | Study of the effects of gamma irradiation on the behavior of GP | 56 |
| 5.7 | Durability of alkali activated slag bearing organic liquid waste | 57 |
| 5.8 | PREDIS 4th Workshop GSL WP5 update..... | 59 |
| 5.9 | Study of direct conditioning process coordination (Task 5.3)..... | 61 |

| | | |
|----------|--|------------|
| 5.10 | Study of direct conditioning matrix performances: Study of thermal behaviour and "fire hazard" (Task 5.4) | 64 |
| 5.11 | Geopolymer cements for the immobilisation of radioactive liquid organic wastes | 67 |
| 5.12 | Results of oil and liquid scintillation immobilization with>NNL formulation | 69 |
| 5.13 | Innovations in liquid organic waste treatment and conditioning | 71 |
| 5.14 | Study of direct conditioning process..... | 74 |
| 5.15 | Study of conditioning matrix performances | 75 |
| 6 | SCIENTIFIC PROGRESS IN INNOVATIONS IN SOLID ORGANIC WASTE TREATMENT AND CONDITIONING (WP6)..... | 77 |
| 6.1 | PREDIS 4th Workshop GSL WP6 update | 77 |
| 6.2 | Densification and encapsulation of ashes from incineration of RSOW from IRIS process: characterizations of the samples and launch of the short term durability tests (WP6, tasks 3, 4, 5 and 6)..... | 80 |
| 6.3 | Gasification of Solid Organic Radioactive Waste..... | 83 |
| 6.4 | Stability and Physico-Chemical Characterisation of Reconditioned Waste Forms Relevant to Radioactive Wastes..... | 86 |
| 6.5 | Immobilization of thermally treated ionic exchange resins in geopolymer matrices | 88 |
| 6.6 | Immobilization of molten salt residue using alkali-activated and cement-based materials..... | 90 |
| 6.7 | Characterisation of the ash and their encapsulation after thermal treatment of IER..... | 93 |
| 6.8 | Physico-chemical characterization of the resulting waste forms | 98 |
| 6.9 | Short and long-term leaching tests with HIPed ashes (Task 6.6) | 101 |
| 6.10 | Geopolymer characterization from immobilization of MSO waste | 102 |
| 6.11 | Oxidative pyrolysis and Fenton-like wet oxidation of spent ion-exchange resins..... | 105 |
| 6.12 | Encapsulation of treated organic wastes into tuff-based geopolymeric matrix | 109 |
| 6.13 | Leachability of nuclides of wastes conditioned in tuff-based geopol-ymeric matrix..... | 112 |
| 7 | SCIENTIFIC PROGRESS OF INNOVATIONS IN CEMENTED WASTE HANDLING AND PREDISPOSAL STORAGE (WP7) | 115 |
| 7.1 | Radiation detection tools for radwaste characterization & monitoring | 115 |
| 7.2 | Embedded Monitoring System | 119 |
| 7.3 | Experimental characterizations of old waste drums | 121 |
| 7.4 | CONDITIONING MONITORING FOR CEMENTED WASTE PACKAGE IN PREDISPOSAL STORAGE.... | 124 |
| 7.5 | Demonstration and implementation of monitoring technologies | 125 |

1 Overview

Maria Oksa (VTT), maria.oksa@vtt.fi

Keywords: waste, treatment, predisposal, safety, radioactive, nuclear, science and technology, monitoring, packages, material science

PREDIS May Workshop 2023 in short

EU project PREDIS – ‘Predisposal management of radioactive waste’ organised its third annual workshop in Mechelen, Belgium, 22.-26.5.2023 with 170 registered participants, most attending in-person. The workshop started with the students’ session holding topical presentations on waste acceptance systems, solid organic waste treatment and conditioning fundamentals, geopolymers for treatment and conditioning of liquid organic waste, metallic nuclear waste challenges and their treatment options and innovations in sensors, data and digital twins. The second and third days of the workshops were focusing on project implementation in strategic topics, knowledge management, technical and scientific tasks and collaboration with EURAD EJP. The PREDIS project has advanced tremendously on scientific and technical developments as well as in strategic implementation and knowledge management during the three first years of the project. These advancements were presented during the open workshop and panel discussion, and the extended abstracts of these presentations are included into this report. The project will end in August 2024 and the final results will be presented in the PREDIS Final Conference in Avignon, France, 3.-7.6.2024.

The current status of ‘innovations in cemented waste handling and predisposal storage’ presentation included the developments in the tasks related to testing and monitoring, digital twin, data and decision and demonstration. This work package performs for example investigation of conventional and innovative NDE (non-destructive evaluation) and monitoring techniques, with the aim of integrity testing of relevant technologies using full-size package mock-ups. One target is building the condition monitoring system of predisposal storage with decision platform. For the ‘innovations in solid organic waste treatment and conditioning’ work package, the presentations were focused on the work performed on demonstrating the reliability of alkaline binders, verifying the matrix performance of conditioned waste according to a set of uniformed waste acceptance criteria and demonstrating the thermal treatment methods leading to a significant volume reduction and safe reconditioned waste packages. The presented advancements on work package ‘innovations in liquid organic waste treatment and conditioning’ were showing results on implementing geopolymers and related alkali-activated materials as mineral binders, development of direct conditioning solutions and assessing technical and economic requirements. ‘Innovations in metallic radioactive waste management’ presentations consisted of development of innovative and optimised characterization techniques, demonstration of decontamination processes and development of conditioning matrices for reactive metallic wastes.

Welcome to get more information and details of the PREDIS technical progress and results in this proceedings report! The general status of each work package is shortly introduced, following technical and scientific presentations of selected specific topics and in all work packages, where the younger generation participatings were also presenting their work.

Acknowledgements

This project has received funding from the Euratom research and training programme 2019-2020 under grant agreement No 945098.

2 Overview of Strategic Implementation (WP2)

Anthony Banford, NNL, UK, anthony.w.banford@uknnl.com

Keywords: include SRA, LCA-LCC, WAC keywords

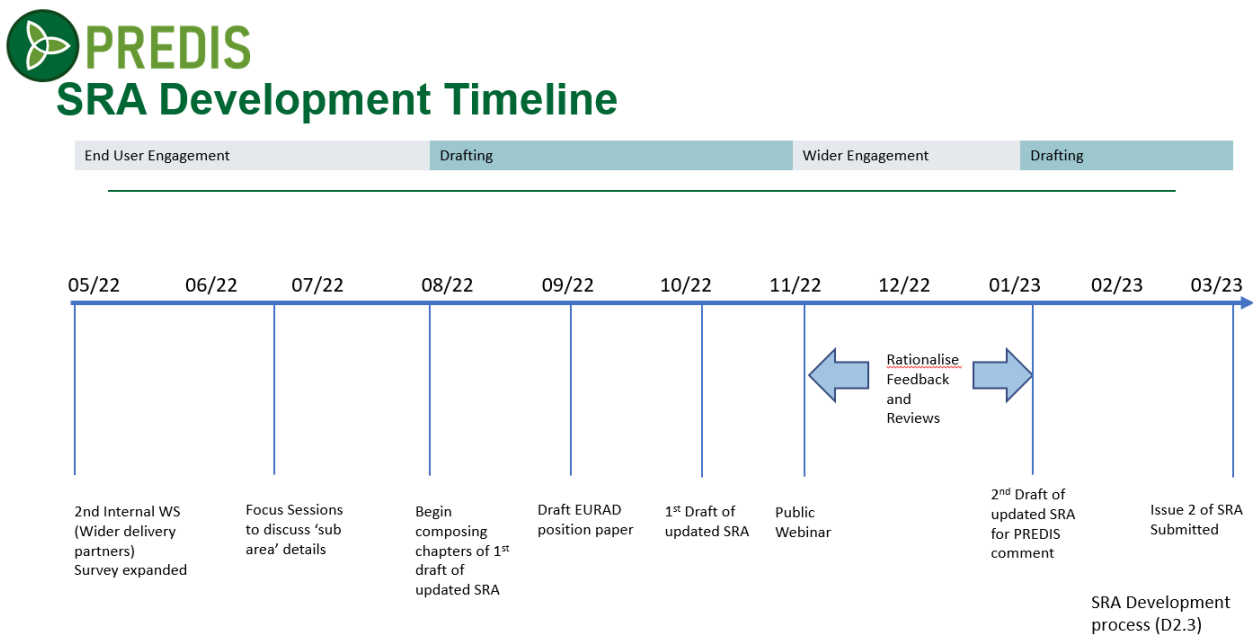
1. Introduction

In WP2 there are a number of activities that are being carried out during the lifetime of the project. These include the establishment of a predisposal stakeholder community (Task 2.1), the development of a Predisposal Strategic Research Agenda (SRA) (Task 2.2), further development work on Waste Acceptance Systems (WAS & WAC) (Task 2.3), general internal and external project governance improvements (Task 2.4), developments in Life Cycle Assessment (Task 2.5) and a predisposal Gap Analysis – (complete) (Task 2.6).

2. Description of work and main findings

Task 2.1 led by SCK CEN has seen 25 approved PREDIS end users and 177 stakeholders mapped from 33 different countries over all 5 continents.

Task 2.2 led by NNL and the main task over the previous period has been the update to the Issue 1 of the PREDIS Strategic Research Agenda (SRA). This activity commenced in Winter 2021. and the team of PREDIS partners that were allocated to the task discussed and formulated the approach taken to obtain the needs and opportunities from the stakeholders to be included in the updated SRA. That approach included a series of engagements using mixed methods to obtain the opinions ahead of drafting the report. Initially a targeted survey was developed to be issued to the PREDIS end users and stakeholders. Following that a number of workshops and sessions took place to expand on the input of the stakeholders and obtain further details and opinions.

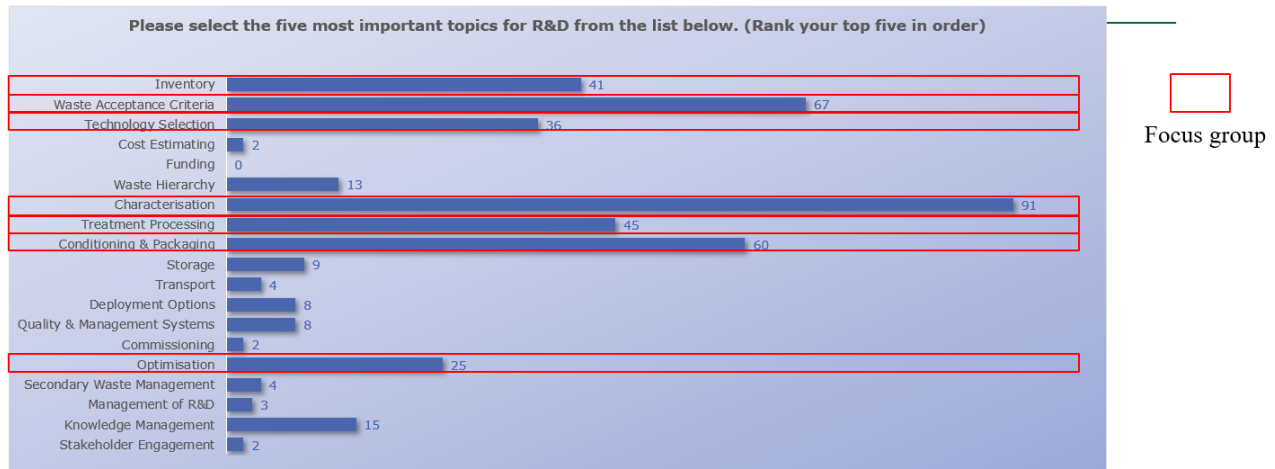


This project has received funding from the Euratom research and training programme 2019-2020 under grant agreement No 945098.

Figure 1. PREDIS Strategic Research Agenda Update Development Timeline.

The team led on individual topic areas and drafted the paper during the summer of 2022. A webinar followed in November 2022 where the findings were reflected to the stakeholder to check alignment. Following this a review period took place to finalise the paper which was published on the PREDIS website in May 2023.

Results and Priorities




 This project has received funding from the Euratom research and training programme 2019-2020 under grant agreement No 945098.

Figure 2. PREDIS SRA Survey Results and Priorities.

Figure 2 shows the results of the end-user and stakeholder survey of technical topics, with the seven most important topics highlighted in red.

Future activities in the coming year under the SRA task include the publication of a journal paper, horizon scanning for relevant upcoming disruptive technology, and the incorporation of the findings of research undertaken within the PREDIS project into the SRA document.

Task 2.3 led by CvRez delivered a WAC focused session consisted of six presentations summarizing results of recent activities and bringing information about progress of a twin project EURAD-ROUTES, the end user view on achieved results, and the identification of perspective directions for WAC development (Strategic Research Agenda).

The three recent deliverables were discussed including:

- 'State of the art of waste form characterisation' bringing together the most significant recent innovations in the area of waste characterisation, and focusing on the characterisation of radiological parameters,
- 'Preliminary assessment of the effectiveness of characterisation methods' describing the characterisation methods in terms of their efficiency and usefulness, and
- 'Overview of waste form qualification approaches' summarizing the interfaces between waste form qualification (WFQ) and safety, including safety case, specifying the relation of WFQ to WAC, commenting the experience from national practice.

As well as the upcoming document – 'Guidance on formulating generic waste acceptance criteria'.

The parallel EURAD-ROUTES project assessed the (i) current use of WAC, (ii) possibilities for sharing experience on waste management with/without WAC available, and (iii) R&D needs and opportunities for collaboration. The last one identified the following items as the most challenging for future studies:

- Common analysis on disposal strategy for wastes that do not meet WAC for existing or planned facilities,
- Comparison and standardisation of radionuclides and their speciation to account for in characterisation & WAC,
- Benchmarking exercises for WAC-development,
- Characterisation methods to determine compliance of particular wastes with WAC, and
- Sampling and characterisation methodologies to obtain representative data.

Some of the benefits that have been seen namely in utilizing the knowledge acquired in the national programme allowing the optimisation of national facilities and plans for new ones. Vice versa, recommendation

for a future EURAD project include request for benchmarking of generic, and preliminary/specific disposal WAC, comparison and standardization of radionuclides considered in WAC, and harmonization of WAC aiming at sharing predisposal facilities and activities.

The final discussions examined possibilities to support sharing experience while implementing a project. While a questionnaire remains the main source of information, potential approaches to ease the position of a respondent include using mixed methods well planned in advance of the engagement using simple and focused questions, tables rather than text requests, address only knowledgeable experts, preference of face-to-face meetings/workshops and creating teams to put together required info or focus groups from representatives of project partners, or establishing a discussion forum processing the required information.

During the session a poll was organised requesting opinion of respondents on Where do you see the most significant gaps/needs for establishing a Waste Acceptance System. The results are displayed in the following figure.

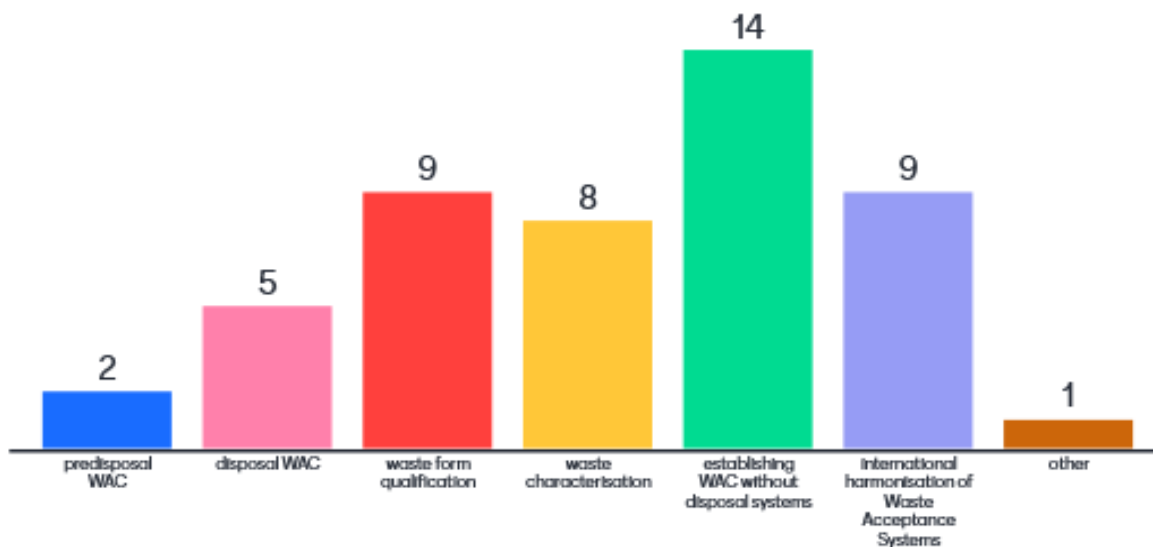


Figure 3. PREDIS Annual Meeting Mechelen 2023 WAC Survey poll results.

3. Summary

The updated Issue 2 of the PREDIS SRA is available on the PREDIS website here:

https://predis-h2020.eu/wp-content/uploads/2023/05/PREDIS-SRA_Milestone-Report-2.4_May-2023.pdf

The work on the next updated version of the SRA to capture the findings and next steps from the PREDIS Technical work packages and any outcomes from the planned Horizon Scanning activities.

References

- [1] A. Wareing, Strategic Research Agenda 16/05/2023 version 2, PREDIS, 2023

3 Overview of Knowledge Management (WP3)

P. Carbol (EC, JRC), A. Valls (AMPHOS21), J. Faltejsek (UJV)

Paul Carbol, European Commission (JRC), Germany, paul.carbol@ec.europa.eu

Alba Valls, AMPHOS21, Spain

Jiri Faltejsek, UJV, Czech Republic

Keywords: Radioactive waste management, Predisposal activities, Knowledge management, State-of-Knowledge, Training, Mobility, Students

1. Introduction

Knowledge management activities are a crucial component of the PREDIS project. The four activities: (a) KM programme management, (b) State-of-Knowledge document production, (c) training activities, and (d) mobility actions are the central topics, but also extended KM topics such as identifying end-users needs, student group coaching, preparation of a glossary and dissemination are handled in this work package (Figure 4).

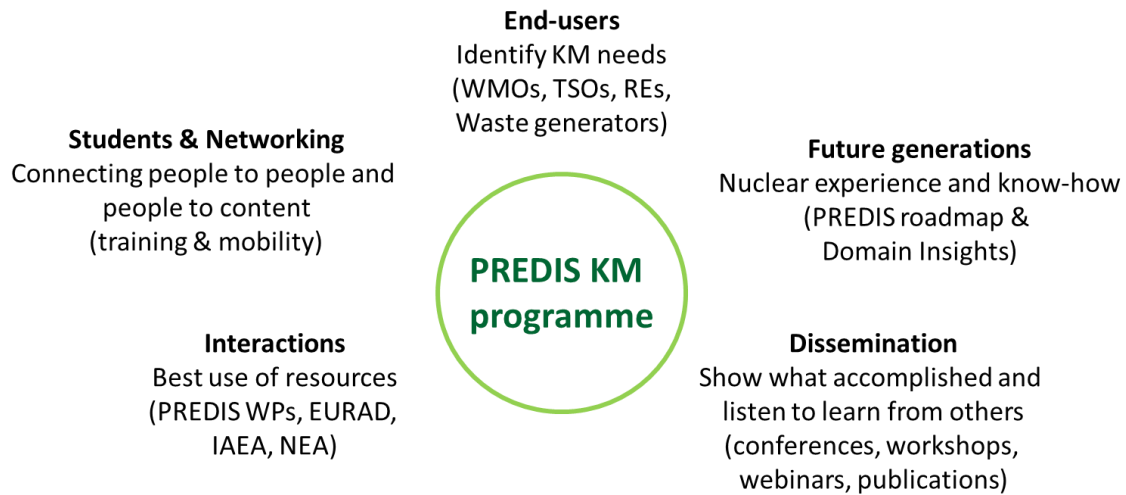


Figure 4. Extended KM activities in PREDIS.

2. Description of work and main findings

State-of-Knowledge document production schedule is now set with all Domain Insights (DI) authors, reviewers and time plan defined. Nonetheless, the time plan has been revised several times and some DI documents are behind the schedule. All efforts are on delivering all of them within the PREDIS project (August 2024). Nevertheless, to be formatted, cross-referenced and introduced in the EURAD Wiki requires that the DI's be finalised before March-April 2024. The identified needed coherence between content in the PREDIS SRA and the DI documents is still possible to be achieved as the SRA is still open for changes, being now in the phase of socialising.

Training activities are progressing well. So far, four courses have been organised and two are under development, while one course need to be defined, based on end-users needs. An overview of all courses:

- PREDIS Overview, Innovation in Predisposal Radioactive Waste Management, 9-10 June 2022, 3h, online, 81 participants
- Management of low and intermediate level wastes, 7-9 September 2022, in presence, Rež, Czech Republic, 21 participants
- Practical-theoretical training session on GENIE 2k & ISOCS for waste characterisation, 21-24 November 2022, Jose Cabrera NPP, Spain, in presence, 9 participants
- Basic knowledge on Predisposal of radioactive wastes, 22 May 2023, in presence, Mechelen, Belgium, 23 participants
- Joint PREDIS-EURAD training course on Waste Acceptance Criteria (WAC), 4-8 September 2023, in presence, Prague, Czech Republic, 40 participants

- RadWaste Management by ORANO, 4 days, in presence, La Hague, France, 20 students
- Theme 2 – Predisposal, Domain Insights lectures, 2024, 2 days, online, open to all
- LCA used in predisposal radioactive waste management, proposed.

Discussions are ongoing concerning the course on Life-Cycle-Analysis (LCA) applied in the RWM as a potential last course, as no such course is given in Europe to the knowledge of the WP2 LCA/LCC team.

Mobility actions are well used and mobility are still asked for. The mobility activities supported by PREDIS are; (a) visit to partners or industry, (b) internship/exchange programme, (c) training course participation and (d) attending technical events (i.e. conference, workshop). It could be concluded that students in some WP were more active applying for mobility and that mobility between partners within a WP was most popular, followed by cross-WP actions, and visiting partners external to PREDIS. Even though the mobility KPI have been reached the mobility programme will continue as long as resources are available. Based on the response from students that mobility is slightly more important than trainings, some budget was transferred from the training budget to the mobility budget.

Student group activities are ongoing with one student representative and 38 active students. The total number of students is 48, taking into account those that has already left the PREDIS project.

Case studies is a new activity, initiated in PREDIS on request of IAEA and will involve all WPs, foremost the technical work packages. WP1 showed some examples and will take the lead on this activity.

Dissemination of KM activities has been progressing with four performed presentations (IGD-TP Symposium in Switzerland, SNS2022 Annual Meeting in Spain, WM2023 in USA, OECD/NEA in France and SNS2023 in Spain) [1-4] and two planned (ICEM2023 in Germany and the Spanish Nuclear Society 48th Annual Meeting 2023, in Spain) [5,6].

3. Summary

The key performance indicators set for the KM WP of training new experts in the field of predisposal waste management technologies has been achieved. The targeted number of PhD and PostDoc students was set to 15 and the current status is 38 students. Furthermore, the number of mobilities between partners was set to 20 and so far, the number reached is 22 completed mobility actions. There is an active student group in PREDIS that are present at some KM WP meetings and co-decides on training (La Hague training was specifically requested by the students). PREDIS knowledge management activities are presented globally.

There is an increased awareness that the Domain Insights document production needs to be stimulated to reach the set goals of 12 DIs by the end of 2023.

Acknowledgements

The authors would like to acknowledge the great support by Erika Holt and Maria Oksa, as well as all the WP leaders contributing to a successful KM in PREDIS. Without the support from the partners inside the KM WP the KM programme would not work. Many thanks to Jess McWilliams (Sheffield University) for keeping together and leading the PREDIS student group.

References

- [1] HAVLOVA V., VALLS A., CARBOL P., HOLT E., OKSA M., BANFORD A., ABDELOUS A., FOURNIER M., MENNECART T., NIEDERLEITHINGER E., KENT J., LO FRANO R.: Knowledge Management in Predisposal of Radioactive waste (PREDIS EU project). IGD-TP Symposium, Zürich, Switzerland, 20-22.09.2022
- [2] VALLS A., VACLAVA V., CARBOL, P., DURO, L.: Gestión del conocimiento en el proyecto europeo PREDIS (Knowledge Management within PREDIS). 47^a Reunión Anual de la Sociedad Nuclear Española (Spanish Nuclear Society Annual Meeting), Cartagena, Spain, 26-30.09.22
- [3] BELMANS N., COECK M., HAVLOVA V., VALLS A., HOLT E.: Implementing training and mobility in EU Projects EURAD and PREDIS. WM2023 Symposium, Arizona, USA, 28.2.2023
- [4] CARBOL P.: Updates in EURAD (/PREDIS) knowledge management activities. OECD-NEA 3rd Plenary Meeting of the Working Party on Information, Data and Knowledge Management (WP-IDKM), Paris, France, 7-8.02.2023.

- [5] MIKSOVA, J., BELMANS, N., CARBOL, P., HOLT, E., VALLS A., FALTEJSEK, J.: Lessons Learned From Implementing Training and Mobility Programmes Within EC H2020 Projects EURAD and PREDIS. ICEM (International Conference on Environmental Remediation and Radioactive Waste Management) Stuttgart, Germany, 3-6.10.2023.
- [6] VALLS A., CARBOL P., HOLT E., THEODON L., DURO L.: La gestión del conocimiento en la gestión de residuos radiactivos. Aplicación y evolución en proyectos europeos (Knowledge Management in the frame of radwaste management. Application and evolution within European projects). 48ª Reunión Anual de la Sociedad Nuclear Española (Spanish Nuclear Society Annual Meeting), Toledo, Spain, 4-6.10.2023.

4 Scientific progress in Innovations in metallic treatment and conditioning (WP4)

PREDIS project is developing technologies for treatment and conditioning of radioactive waste such as metallic waste as well as radioactive organic waste whether liquid (RLOW) or solid (RSOW). The WP4 focus is on on steel and Ni-alloys radioactive metallic waste, which are major components in nuclear installations. These metallic wastes are often surface-contaminated in the form of corrosion layers of a few tens of micrometers retaining radionuclides including but not limited to activation corrosion products (Co-60, Ni-63, Fe-55) and fission products such as Cs-137.

4.1 Defining Europe-wide Needs and Opportunities for Management of Metallic Waste Streams (Task 4.3.)

Jenny Kent, Tim Harrison (Galson Sciences Ltd, UK), jek@galson-sciences.co.uk

Keywords: metal melting, metal decontamination, secondary waste, value assessment

1. Introduction

Task 4.3 is focused on understanding needs and opportunities for managing metallic radioactive waste.

Decommissioning of the current fleet of European civil nuclear power plants is expected to generate thousands of tonnes of radioactive metallic waste. Therefore, we need to develop more effective decontamination and remediation processes for metallic wastes, as well as optimising routes for recycling and reuse. The presentation summarised work completed over the past 12 months and plans for upcoming tasks, including:

- The potential for innovative application of non-nuclear metal melting technologies.
- A strategic analysis of the economic and environmental impacts of decontamination and metal melting, using Value Assessment.
- Evaluation of secondary waste produced by decontamination technologies.

2. Description of work and main findings

WP4 is investigating the potential for innovative application of non-nuclear metal melting technologies, which are particularly applicable to metallic wastes that cannot be decontaminated and recycled (i.e. activated decommissioning waste). The current induction melters for low-activity metallic wastes cannot accept metals with higher levels of activity, and this task involves engaging with the supply chain to compile information on the technology readiness level (TRL) of alternative melting technologies and evaluating their potential application to radioactive wastes. To date, information has been collected for:

- Induction Melting – the baseline technology currently used in nuclear industry to provide comparison point
- Vacuum Induction melting (provides improved homogenisation and greater control of off-gassing compared to induction melting)
- Electric and Plasma Arc Melting (provides wider material tolerances than induction melting, higher quality output for the same input but has lower energy efficiency)

WP4 is aiming to develop and optimise decontamination technologies for treatment of contaminated metallic waste. In the coming months, information on secondary wastes and the economic and environmental impacts of these technologies will be gathered to feed into a strategic analysis of the economic and environmental impacts of decontamination and metal melting. This will include identification of the costs and benefits of the potential opportunities for metal decontamination and melting, and application of the waste hierarchy in countries across Europe.

Value assessment provides a toolkit for decision makers (e.g. End Users) who are considering the merits of alternative technologies for treatment of their wastes. Value can be defined as “*the realisable benefit in safety, monetary and environmental outcomes that will arise from implementing this technology at a specified time*” [1]. There is a project milestone (MS25) to hold a Value Assessment Workshop as part of WP4.

Different contributors to “value” were discussed with WP4 partners, along with the criteria that can be used to assess waste stream – technology combinations to identify benefits and challenges (Figure 5) and it was noted that value needs to be considered across the full waste management lifecycle.

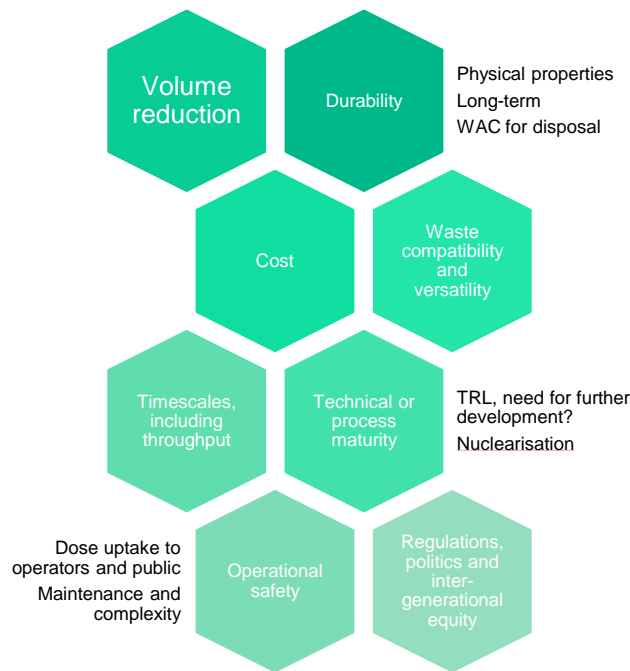


Figure 5. Criteria that will be considered in the PREDIS WP4 Value Assessment.

Similar Value Assessment workshops are included in the scope of other PREDIS WPs to demonstrate the costs and benefits of using the innovative approaches being developed in the PREDIS project. A consistent approach will be agreed across the PREDIS WPs in terms of methodology, approach and format of deliverables; follow-up coordination meetings are being scheduled in June/July 2023. The Value Assessment process shown in Figure 6 was used in the THERAMIN project and will be used as a starting point for these discussions. Consistency of scenarios and input data with the WP2 Life Cycle Analysis (LCA) was discussed and will be further explored with the team at University of Manchester leading that work prior to confirming the case studies to be chosen for Value Assessment. Key points to agree include a common start and end point and the use of comparative assessment against a baseline option.

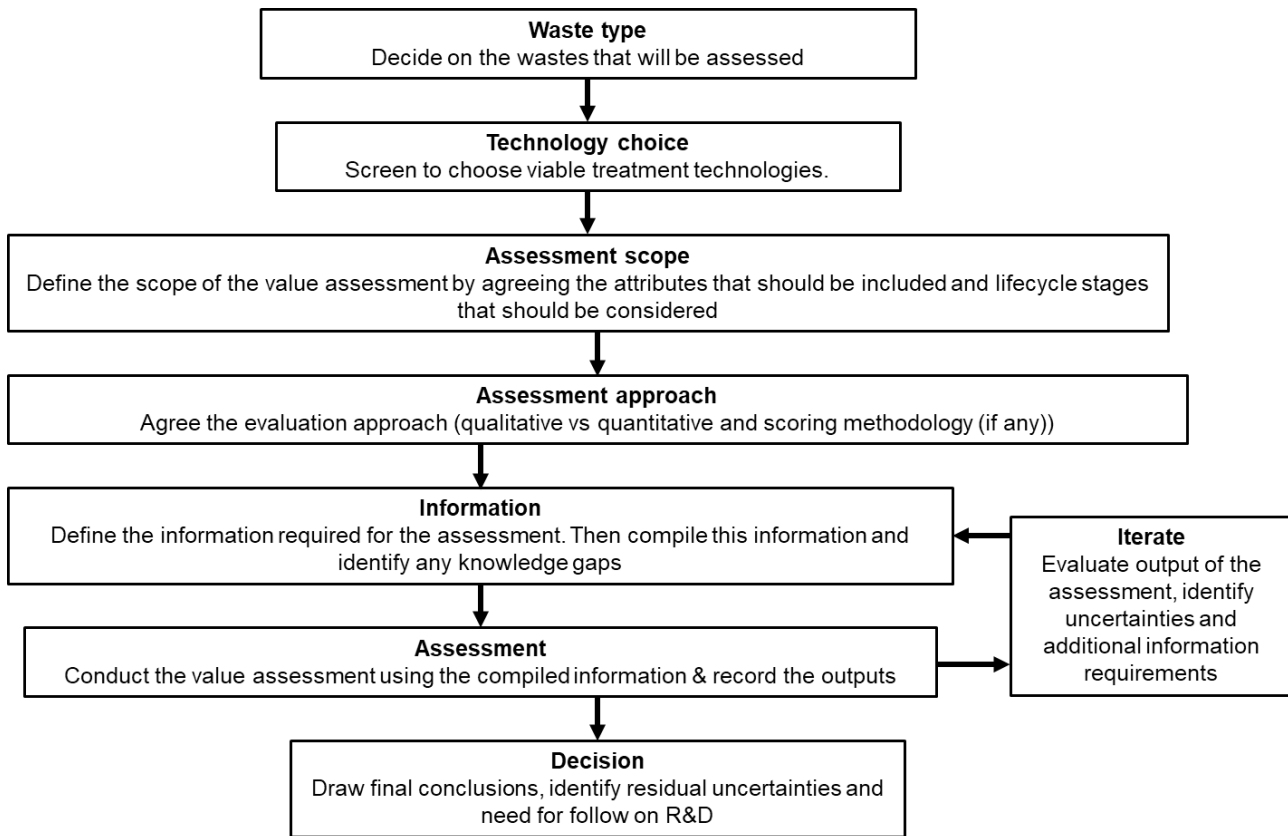


Figure 6. Value Assessment methodology used in the THERAMIN project [1].

Additional work is also planned in the coming months to apply the methodology developed by GSL in the MS24 report “ Report on Secondary Wastes to Inform Optimisation of the Metal Decontamination Processes” [2] to enhance the information included in the technology datasheets and support the Value Assessment workshop. This will include collation of information on the volume and disposability of secondary wastes generated by the decontamination processes being developed.

3. Way forward

Preparation of Deliverable 4.2 (Synthesis Report on Management of Metallic Waste Streams) was discussed. This report is due to be completed in May 2024 and preparation will begin later in 2023 to enable inputs and review comments to be provided by WP4 partners and End Users. The proposed outline presents the challenge being addressed by WP4, potential solutions and a comparative assessment against the current baseline. Key contents include:

- Inventory of metallic waste and challenges associated with their management.
- Metallic waste decontamination technologies.
- Metal melting technologies (non-nuclear).
- Secondary waste management – including volumes, characteristics and management routes.
- Economic and environmental impacts of decontamination and metal melting.

References

- [1] Galson Sciences Ltd, THERAMIN Project Deliverable D2.5: Value Assessment, March 2020. http://www.theramin-h2020.eu/downloads/THERAMIN%20D2_5%20Value%20Assessment.pdf
- [2] A. Fuller, PREDIS Milestone 24: Report on Secondary Wastes to Inform Optimisation of the Metal Decontamination Processes, August 2021.

4.2 Development and optimisation of decontamination processes (Task 4.4.)

1. Introduction

Task 4.4 is focused on understanding optimization techniques for the decontamination of metallic radioactive waste. Decommissioning of the current fleet of European civil nuclear power plants is expected to generate very large quantities of radioactive metallic waste. Therefore, there is a need to improve the decontamination processes for metallic wastes, and the associated secondary effluents with a goal to be able to recycle the metals in order to promote the concept of circular economy through LCA routes, whilst accounting for the Waste Acceptance Criteria (WAC).

The presentation summarised work completed to date, including:

- Decontamination strategy to be used as a guideline.
- Characterization of surrogate samples used for testing of decontamination techniques.
- Identification of decontamination techniques selected for testing and the parameters which can affect efficiencies.
- Demonstrated the efficacies of different conditions, which show promise in decontamination of such metals.
- Demonstrated the associated treatment techniques for the secondary liquid effluents generated.

2. Description of work and main findings

4.2.1 Metallic waste surrogates preparation

Thomas Carey, Anne Callow and Jessica Hopkin
thomas.carey@uknnl.com

3. Introduction

WP4 stakeholders are developing innovative decontamination technologies for the treatment and conditioning of metallic wastes where no or inadequate solutions are currently available. Common technical challenges exist in the development of these innovations, particularly centred around the technology's deployment, decontamination performance and secondary waste treatment. All these technical challenges need to be overcome if future offerings or services are to be made commercially available for the civil nuclear decommissioning market.

4. Description of work and main findings

Contamination of metallic surfaces can occur via range of different mechanisms and is dependent on the specific environment within a nuclear plant (e.g. temperature, pressure, pH, metal type etc.). Artificial coupons that replicate these contaminated are useful for 2 main reasons: i) to act as a benchmark for the assessment of decontamination techniques and ii) to further scientific understanding of the contamination mechanisms.

NNL have utilised their knowledge of UK's reprocessing plants to prepare artificial coupons, which reflected the contaminated and highly corroded metallic surfaces expected in plant infrastructure. These contaminated surfaces are highly complex and are currently not well understood by the industry. [1] Knowledge of these contaminated surfaces is required to enable effective decontamination and decommissioning planning.

Detailed characterisation of these coupons has been conducted using a suite of techniques including Energy-dispersive X-Ray Spectroscopy, Focused Ion Beam – Secondary Ion Mass Spectrometry, and Atom Probe Tomography. Successful characterisation provided an estimation of the contaminated layer on the corroded surface. Data showed contamination had not penetrate into the bulk metal matrix (defined as < 2 at% oxygen) beyond the nickel-enriched / oxygen saturated metal beneath the metal-oxide interface.

An iron-rich outer oxide was identified which had an Fe:Cr:O ratio indicative of (Fe,Cr)O₂. The following contaminating elements were associated with this phase and had a concentration of up to 3% : Zr, Nd, Gd, Ru, Pa, Cs, Ru and Sm. A deeper underlying Cr-rich layer was also identified which had the following associated contaminating elements up to 1.77%: Nd, Zr, Rb, Gd, Cs, Ru and Pd. The measured depth of contamination across the metal/oxide interface was 38 nm, although with respect to the surface of a single

corroded grain the depth was around 70–80 nm. A scientific publication is now in preparation based on this work.

The artificial coupons (discussed above) have been prepared and shared with WP4 collaborators (Subatech and CEA, France and UJV, Czech Republic). In parallel, SORC (Hungary) have shared artificial coupons which replicated the contaminated surfaces expected in the steam generators of PWR nuclear power plants. WP4 stakeholders have been demonstrating their decontamination innovations (as follows) on these common coupons to allow direct comparison of techniques:

- UJV, Czech Rep.– ionic liquids
- Subatech, France – Advance CORD
- CEA, France – chemical gel decontamination
- NNL, UK – electrochemical decontamination

In addition, Subatech and NNL have performed collaborative studies on optimising the treatment secondary waste arising from the CORD chemical decontamination technique.

5. Way forward

In the coming months all WP4 stakeholders will be finalising their collaborative practical assessments and will be publishing the new knowledge and technology progression gained.

Acknowledgements

NNL would like to thank all stakeholder involved in WP4, in addition to Sellafield Ltd for their support.

References

- [1] D.Barton, T. Johnson, A. Callow, T. Carey, S. Bibby, S. Watson, D. Engelberg, C. Sharrad, *A review of contamination of metallic surfaces within aqueous nuclear waste streams*, Progress in Nuclear Energy, 159 (2023) 104637, <https://doi.org/10.1016/j.pnucene.2023.104637>

4.2.2 Decontamination of metallic waste using chemical solutions

Aditya Rivonkar, Tomo Suzuki-Muresan, Abdessalam Abdelouas, Marcel Mokili, (IMT Atlantique, France)
contacts: rivonkar@subatech.in2p3.fr; robin@subatech.in2p3.fr

Keywords: decontamination, CORD process, radioactive metals, effluent treatment, radioactive waste, precipitation

1. Introduction

Chemical decontamination techniques are selected based on their ability to effectively treat intricate shapes and structures. Among these techniques, the chemical oxidation reduction decontamination (CORD) process is commonly employed for decontaminating metals composed of stainless steels or Ni-alloys. The CORD process consists of a two-step approach: initially, potassium permanganate in nitric acid is used to oxidise the Cr-Ni oxides, followed by the introduction of oxalic acid, which serves to break down any remaining permanganate and any generated MnO₂, while simultaneously reducing the Fe-Ni oxides^[1,2]. This two-step cycle can be repeated as necessary to achieve the desired decontamination level for the metals. Throughout the decontamination process, an effluent is produced, containing a significant amount of oxalic acid and dissolved metallic ions, including radionuclides. These effluents must also be decontaminated before any conditioning stage in order to reduce waste volumes. For this purpose, it is possible to use specific resins. However, this process is very costly because of the specificity of the resins and the complexity of the effluents. To reduce the decontamination costs, effluent can be pre-treated by precipitation^[3]. To do so, the first step is to destroy the oxalic acid to avoid any competition during the precipitation process. Then, it is possible to precipitate the metals and radionuclides in solution by adjusting the pH of the radioactive solution. As the complexes formed are pH-dependent, two precipitations (pH 8.5 and 12) are required to remove most of the metal cations present in solution. Finally, a last step of filtration is needed to remove the contaminated solid phase.

2. Description of work and main findings

Surrogate samples from nuclear reprocessing plants (for ex. Sellafield in the UK) were prepared by a WP4 partner, National Nuclear Laboratory (NNL) and sent to IMT Atlantique, for some collaborative studies. The stainless steel samples were prepared using the boiling acid technique, wherein the steel was dipped into 8M boiling nitric acid to oxidise the surface. To simulate the conditions of the Sellafield site, stable isotopes of various elements were mixed into the acid. The concentration and classification of these elements is given in Table 1. Some elements could not be measured or detected using ICP-MS, and are classified as not detected. The concentration of the base metal components on the surface of the oxide would be significantly higher than in Table 1 due to the contribution coming from the metal itself. These samples were characterised by NNL before being sent to IMT Atlantique.

Table 1. Composition of mixture used for preparation of samples.

| Classification | Element | Conc. (mol/L) | Classification | Element | Conc. (mol/L) |
|------------------------------|---------|---------------|--------------------------------|---------|---------------|
| Base metal components | Fe | 0.21 | Lanthanides | La | 0.04 |
| | Ni | 0.04 | | Ce | 0.09 |
| | Cr | 0.06 | | Pr | 0.04 |
| | Mo | 0.15 | | Nd | 0.13 |
| Transition elements | Y | 0.02 | | Sm | 0.03 |
| | Zr | 0.19 | | Eu | 0.01 |
| | Ru | 0.05 | Gd | 0.15 | |
| | Rh | 0.01 | Not detected / measured | Na | 0.02 |
| | Pd | 0.04 | | K | 0.02 |
| | Re | 0.03 | | Al | 0.03 |
| Other Elements | Rb | 0.02 | | N | 1.50 |
| | Sr | 0.04 | | P | 0.04 |
| | Cs | 0.09 | | | |
| | Ba | 0.05 | | | |
| | Te | 0.02 | | | |

The sample was treated using 3 cycles of the optimised CORD process, 3mM nitric acid and 15mM potassium permanganate followed by 18.5mM oxalic acid, with a volume/surface ratio of 0.4m². An aliquot was taken after each step of the process and was analysed using ICP-MS. For effluent treatment, all the effluents were gathered and treated by the precipitation process shown in Figure 7. The treatment was done with two different reagents in order to investigate the efficiency between hydroxide and sulphide precipitation^[4,5]. All reagent concentrations were set at 1M for this experiment and the stirring time was fixed at 1h for the precipitation. The concentrations of each cation were analysed by ICP-MS at each stage of the protocol.

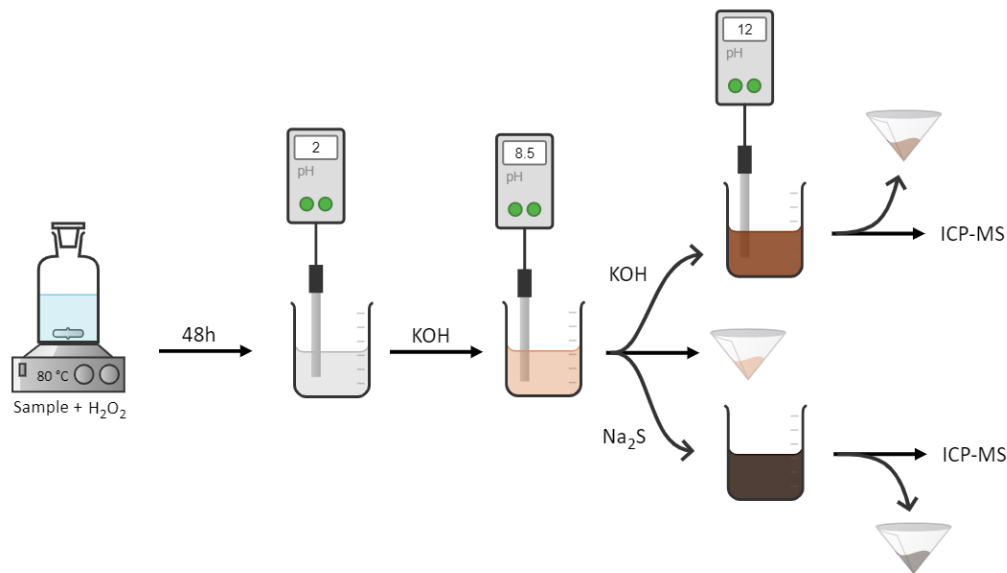


Figure 7. Precipitation protocol using two precipitant (KOH and Na₂S).

The dissolution of the base metal components by the CORD process is seen in Figure 8, with approximately 1.5mg/L of Cr dissolved, 1.8 mg/L of Fe 0.4mg/L of Ni and 0.04mg/L of Mo dissolved after 3 cycles. The overall dissolution could be summarised as follows:

- Base metal components
 - Chromium dissolution favoured in permanganate.
 - Iron, Nickel and Molybdenum dissolution favoured in oxalic acid.
- Transition elements
 - Rhenium favoured in permanganate.
 - Dissolution of the rest in oxalic acid.
- Other elements
 - Rubidium and Caesium favoured permanganate dissolution.
 - Dissolution of the rest in oxalic acid.
- Lanthanides
 - Dissolution favoured in oxalic acid.
- Others
 - Not measured/could not be detected using ICP-MS.

Apart from the base metal components, dissolution of the other elements occurred during the first cycle suggesting that these elements lie within the oxide layer and do not penetrate into the sub-surface, which confirms the results found during the physical characterization. The process was replicated on another sample with a 50% lower V/S ratio of 0.184m, and the results were similar. This was due to the very small oxide layer formed on the surface, a few tens of nanometers, as opposed to few micrometres in the case of NPPs.

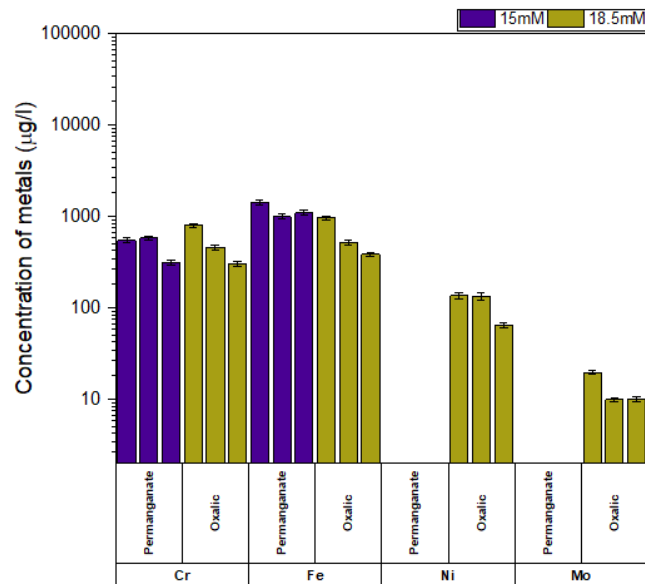


Figure 8. Liquid characterization of CORD solutions: Base metal components.

Figure 9 below highlights the importance of the choice of reagents and pH used to carry out the precipitation steps. Indeed, the different metals in solution do not precipitate under the same conditions. Most of the metals seem to be removed (>96%) as hydroxides at pH 8.5 (Fe, Y, Ru, Rh, Pd, Te, La, Ce, Pr, Nd, Sm, Eu, Gd) since some concentrations are below the detection limit (0.1µg/L) of ICP-MS. These include actinides and some transition metals. Other elements precipitate preferentially at a more basic pH, around 12 using KOH for Mn, Ni, Sr while Cr is more precipitated using Na₂S. Finally, the total concentration of metals in solution was reduced by 99.8 ± 0.1% either by adding KOH or Na₂S. An additional chromatographic resin step will be necessary to remove the last traces of metal but the process can lead to 99% reduction in the volume of resin required^[2].

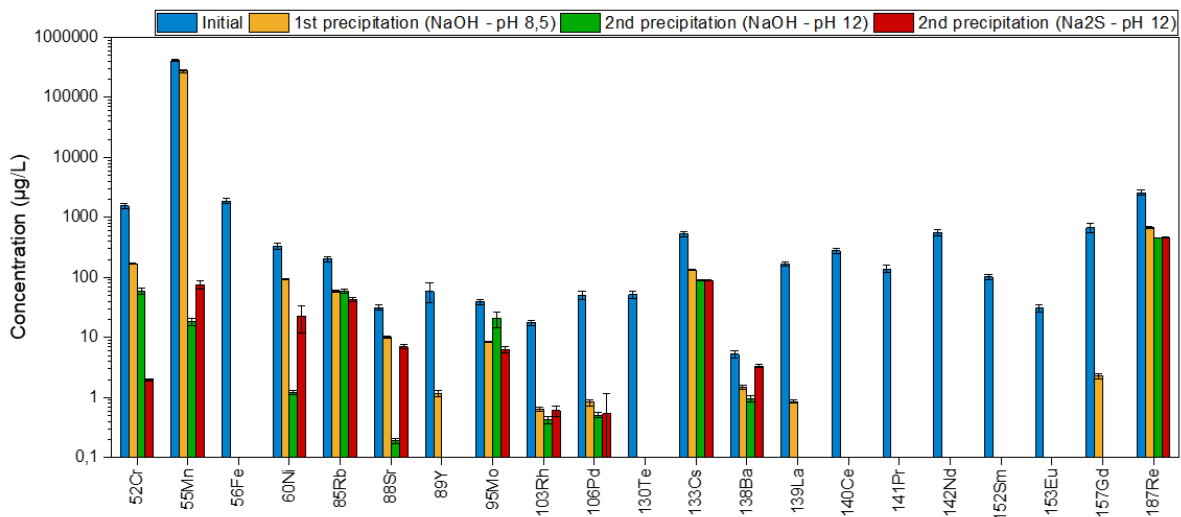


Figure 9. Liquid characterization of effluent after each stage of the precipitation protocol.

3. Summary and way forward

The CORD process is highly effective for treating metallic components in nuclear reprocessing sites. Its efficiency remains unaffected even with a 50% volume reduction, suggesting potential for further reduction which could not be completed in this study. Precipitation protocols require two pH levels to reduce metallic concentration due to solubility issues. Hydroxide precipitation is generally more effective than sulphide precipitation, except for chromium. Cationic resins are required to remove the remaining cations. Both processes are cost-effective, easy to apply, scalable, and generate WAC-friendly waste. Ongoing research

will also explore electrocoagulation and phosphate precipitation, as a means to reduce reagent volume requirements or to enhance the efficiency.

CORD and hydroxide precipitation have also been applied to radioactive Ni-alloy samples from NPP steam generators. The results of these studies are anticipated to be published in the forthcoming months, further expanding the knowledge and applicability of these decontamination processes.

References

- [1] H. Ocken, Decontamination Handbook. Report n°112352, 1999.
- [2] A. Rivonkar et al., Optimisation of the chemical oxidation reduction process (CORD) on surrogate stainless steel in regards to its efficiency and secondary wastes. Front. Nucl. Eng., p.1-13, 2022.
- [3] IAEA, Chemical precipitation processes for the treatment of aqueous radioactive waste. Technical Report N°337, 1992.
- [4] M. Marchioretto et al., Heavy metals precipitation in sewage sludge. Separation Science and Technology, 3393-3405, 2005.
- [5] N. Ain Zainuddin et al., Removal of Nickel, Zinc and Copper from Plating Process Industrial Raw Effluent Via Hydroxide Precipitation Versus Sulphide Precipitation. IOP Conference Series: Materials Science and Engineering, Volume 551, 2019.

4.2.3 Decontamination of metallic samples using a gel technology avoiding secondary liquid waste

Alban Gossard, Fabien Frances (CEA, France), Richard Katona (SORC, Hungary)
alban.gossard@cea.fr

Keywords: Gel, decontamination, electrochemical measurements

1. Introduction

A gels decontamination technology has been developed at the CEA, France [1]. Such gels are used for the decontamination of metallic surfaces and have the main advantage to produce only secondary solid waste. A Ce(IV)-nitric acid gel was proved to be efficient for the decontamination of non-oxidized stainless steel (SS). However, its application on strongly oxidized SS leads to inhomogeneous and non-controlled operations. To better evaluate the efficiency of the gel technology and understand their decontamination mechanisms, a methodology has been developed on a model system “Ce(IV)-nitric acid gel – non-oxidized SS” by coupling electrochemical tests and mass loss measurements.

2. Description of work and main findings

3. Evaluation of the corrosion rate considering a « infinite » contact (no drying) by electrochemical tests

A three-electrode electrochemical cell was used to measure the corrosion rate between stainless steel and gel decontamination technology. This evaluation is theoretical and assumes that the contact of the gel with the stainless steel is “infinite”, meaning that no drying occurs during the operation. The Radelkis OP-0830P saturated calomel reference electrode (SCE), stainless steel counter electrode and stainless steel 1.4571 working electrode were immersed in the decontamination gel. The electrochemical cell was connected to Voltalab PGZ201 potentiostat and the working electrode was polarised at a sweep rate of 1 mV/s. The potential range was +/- 200 mV. According to the Butler-Volmer equation the polarisation curve is as follows [2]:

$$i=i_0 \left(e^{\frac{\beta z_a F}{RT} \Delta E} - e^{-\frac{\alpha z_k F}{RT} \Delta E} \right) \quad (1)$$

In equation (1), i is the current density (mA/cm²), i_0 is the equilibrium current density (mA/cm²), α/β are the oxidation/reduction factors, z_a/z_k are the amount of the change in charge numbers, F is the Faraday constant,

T is the temperature, R is the universal gas constant and ΔE is the polarisation (mV). Polarisation curves of 1.4571 stainless steel using decontamination gel technology are shown in Figure 10.

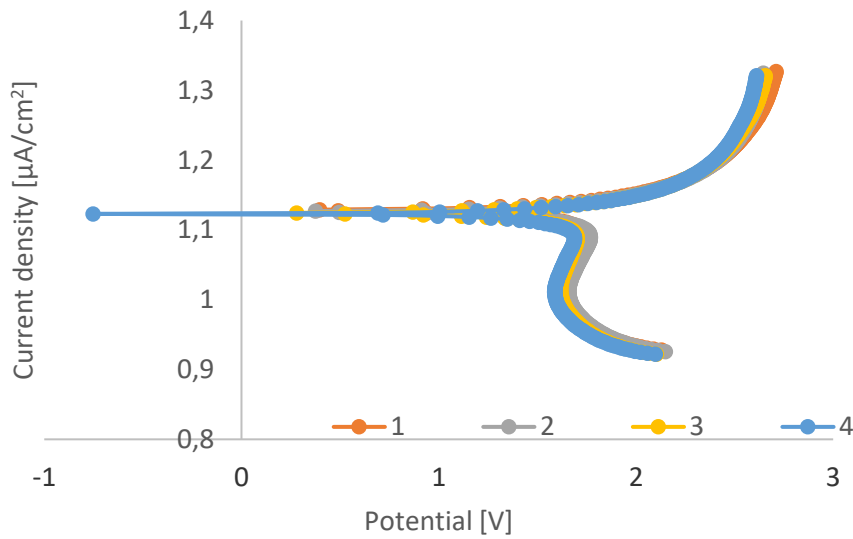


Figure 10. The polarisation curves of stainless steel (1.4571) using gel decontamination.

The potential and the equilibrium current densities were determined by Tafel extrapolation. The corrosion rate, CR (mm/year) was calculated from equation (2), where M is the molar mass (g/mol) and d is the density of the metal (g/cm³).

$$CR = i_0 \cdot \frac{M}{z} \cdot \frac{10}{d \cdot F} \quad (2)$$

The average corrosion rate was calculated as **3.62 +/- 0.38 mm/year**. A peak was observed in the cathodic part of the polarisation curves, which we assume to be a reduction of Ce(IV) ions induced by the reaction with the stainless steel surface. After the Ce (IV) ions had oxidised the metal, the acids cleaned the surface by dissolution, which is highlighted by the polarisation curve characteristics of the anodic part.

4. Evaluation of the dissolved thickness as a function of the gel-stainless steel contact time

Stainless steel substrates were prepared by first polishing and cleaning to obtain a smooth and non-oxidized surface. Then, samples were dipped in a bath of gel to deposit a millimeter thick gel layer on a known surface. The contact between the gel and the samples was varied from few hours until gel drying. After elimination of the gel (or solid residues in case of complete drying), the samples were washed again and the mass loss was determined. From these experimental values, the dissolved metal thickness was calculated as well as the corrosion rate using equation (3).

$$CR = \frac{\Delta m}{\text{surface} \cdot \text{density} \cdot \text{contact time}} \quad (3)$$

The results are reported in Figure 11.

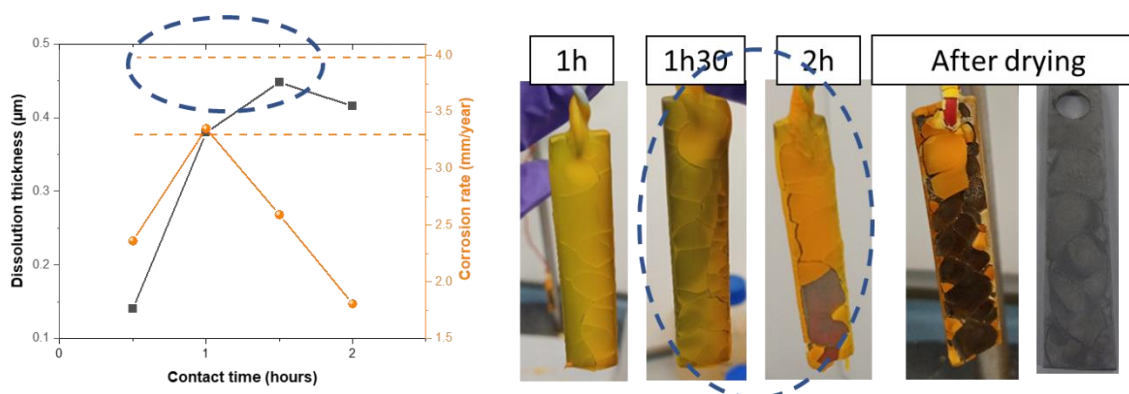


Figure 11. Evolution of the SS dissolution thickness as well as the calculated corrosion rate as a function of the gel-SS contact time and associated pictures.

It was observed that during the first hour the dissolved metal thickness logically increases with the contact time. More interestingly, **the corrosion rate determined from this mass loss evaluation is consistent with the corrosion rate obtained from electrochemical tests**, i.e. between 2.5 and 3.3 mm/year. Then, the dissolved thickness slowly evolves with time and the corrosion rate drastically drops. This decrease can be explained by the drying of the gel, which induces cracks and formation of solid residues. Because the samples were hung out, the drying residues detached from the substrate and fell, inducing some modifications on the contact surface between the gel and the SS substrate. Consequently, from this point, the evaluation of the dissolution thickness or corrosion rate is not pertinent anymore and only mass losses can be compared. After complete drying of the gel, the mass loss still increased, demonstrating that the metal dissolution continues but heterogeneously, which may explain the results observed on strongly oxidized samples.

It shall be noted that there was no significant modification of the metallic surface composition following the decontamination operation (only a slight oxidation observed with XRD analysis). Finally, SEM observations and/or AFM and/or optical profilometry analyses could be used to complete these data and illustrate the surface topography before and after decontamination.

5. Conclusions

A methodology to evaluate the efficiency of a model gel on a SS substrate has been developed by coupling electrochemical tests, mass loss measurements and surface characterization. To be definitively validated, this methodology could be applied to other gel formulations and/or other nature of metallic substrates.

References

- [1] A. Gossard, A. Lilin, S. Faure, Gels, coatings and foams for radioactive surface decontamination: State of the art and challenges for the nuclear industry, *Progress in Nuclear Energy*, 149 p.104255 2022.
- [2] D. Li, C. Lin, C. Batchelor-McAuley, L. Chen, R.G. Compton, Tafel analysis in practice, *Journal of Electroanalytical Chemistry*, 826 p.117-124 2018.

4.2.4 Secondary waste treatment

Martin Straka, Jiří Bárta (UJV-Rez, Czech Republic), martin.straka@ujv.cz

Keywords: ionic liquids, decontamination, corrosion layer

1. Introduction

The main goal of work conducted by UJV is to set up a fit to the purpose chemical decontamination process, in relation to the objective of Nickel alloys recycling while minimizing secondary waste and to optimize the treatment of waste streams. UJV team is studying the separation of radionuclides and other relevant elements from ionic liquids by electrodeposition within the framework of the development of general two-step separation process consisting of extraction of radionuclides from the decontamination solutions into ionic liquids and subsequent electrochemical separation using solid electrode.

At CTU, research is focused on liquid waste minimization by ionic liquids based processes. Main emphasis is put on recycling of chemicals and media used and potentially also possible returning of radionuclides for other use. Two-step separation method consisting of extraction of radionuclides from the decontamination solutions by using the ionic liquids, followed by the separation of radionuclides from ionic liquids by electrodeposition.

2. Description of work and main findings

Several ionic liquids were tested within the framework of this work and their electrochemical properties were described. It was proven that for the process, the effectivity or reproducibility of so-called 2nd generation ionic liquids (characterised mainly by their hydrophobicity) are most suitable for the usage in any process of this type. Most experiments were done with ionic liquids with [bis (trifluoro-methanesulfonyl) imide] (abbr. TSFI) anion proved to be usable.

Electrochemical characteristics of U, Co, Eu, Ni and Fe were measured, and it was concluded that the electrochemical window of the ionic liquids with TSFI anion were suitable to support the deposition of these elements on solid electrodes. Top of that, the electrochemical characteristics of complex system containing both U and Eu were measured and defined, see Figure 12. Current-modulated electrolysis was conducted to show that it is possible to separate uranium from europium in this way (in form of UO₂).

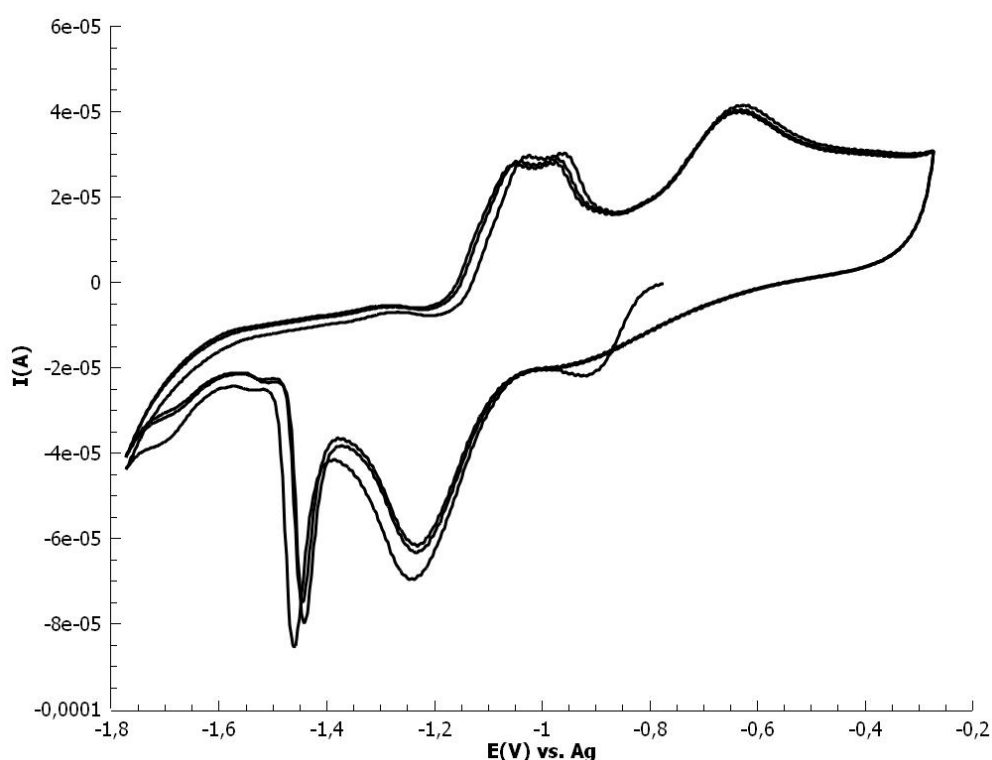


Figure 12. CV of the [BMIM][TSFI] / Eu, U system measured on Au working electrode, scan rate 50 mV/s.

Coupons with artificial corrosion layer containing several elements including Eu and Cs were prepared in NNL laboratories and transferred to the UJV Rez. Direct dissolution of the corrosion layer into ionic liquid was tested. It was found that all the elements of interested go to the ionic liquid, although the bubbles forming in case of the electrolytic current too high caused macro-particles of the corroded material fall down.

At CTU, liquid-liquid extraction was used for the separation of radionuclides from different types of aqueous phase (including the simulants of decontamination solutions). The effect of solvent (chloroform, imidazolium or ammonium based ionic liquid) with extractant on radionuclide extraction was studied in wide range of pH values. Representatives of activation products (Co, Fe), fission products (Sr, Mo, Tc) were tested in this work. Extraction efficiency varies depending on extracted radionuclide and its chemical properties. It was find out that [C4mim][NTf2] as ionic liquid with acceptable properties, can be used as solvent for metal extraction. Extraction of Co, Fe, Mo, Sr and Tc can be significantly enhanced by using ionic liquids as a solvent, where maximum distribution ratios were achieved.

3. Conclusions and way forward

Compared to previous period, uranium deposition was achieved and tested in higher detail. The modulated-current electrolysis was used for its separation from Eu.>NNL artificial coupons were tested, and its corrosion layer was dissolved (anodic dissolution) into IL.

For the future work, focus on quantitative parameters and optimization of the separation process will be studied and tested.

At CTU: the main conclusions are:

- Extraction with 8HQ or DCH18C6 in IL is suitable also at HCit + HOx concentrations present in common decontamination solutions
- Ionic liquids can be regenerated electrochemically (see UJV results)
- As whole procedure, extraction of radionuclides from model decontamination solution shows possibility to regenerate solution while concentrating them for the next step of electrochemical treatment

Acknowledgements

This work had additional support from the Centre of Advanced Applied Sciences (CAAS) (Project No: CZ.02.1.01/0.0/0.0/16_019/0000778) and the project No. TH01020381 (Technology agency of the Czech Republic under the EPSILON Programme).

4.3 Optimisation of metallic waste characterisation and procedures for waste minimisation and recycling (Task 4.5)

4.3.1 Classification of the metallic waste streams of the different types of reactors

Rita Plukiene, Elena Lagzdina, Marina Konstantinova (FTMC), Anastasia Savidou, Angelos Markopoulos, Dimitris Mavrikis (NCSR), Marie Charlotte Bornhöft, Eileen Langegger (DMT)
Contacts: rita.plukiene@ftmc.lt; savidou@ipta.demokritos.gr

Keywords: metallic radioactive waste, nuclide vector methodology, scaling factors, easy-to-measure (ETM) radionuclides, difficult-to-measure (DTM) radionuclides, γ -spectrometry, low energy emission, chemical separation and purification.

1. Introduction

The objective of Task 4.5 within the PREDIS project is the minimization of metallic radioactive waste (MRW) from decommissioning. The T4.5.1 subtask work was dedicated for classification of the waste streams of the different types of reactors. Waste classification involves the quantification of specified radionuclides in the waste materials to comply with disposal requirements and disposal site performance objectives. The aim of classification of the MRW streams of the different types of reactors is changing together with MRW activity: the higher activity MRW (HLW, ILW) needs classification related to radiation protection and best packaging concept, LLW and VLLW may need decontamination and declassification afterwards. Radionuclide generation and distribution in MRW at the different nuclear reactors (types: PWR, BWR, RBMK, VVER) was overviewed and compared. Pre-dismantling classification of MRW using modelling allows preliminary evaluation of the size of controlled areas and expected activities, while Nuclide Vector (NV) methodology applying scaling factors (SF) is used for classification of the low activity waste/ materials (LLW, VLLW, Exempt) [1]. Optimized NV is obtained by analysing and systemizing the information about radioactive metallic waste streams, identifying the optimal list of relevant radionuclides, describing inter-correlations between easy-to-measure (ETM) nuclides and difficult-to-measure (DTM) nuclides including multivariate analysis of the already measured data at the sites and numerical analysis of activation and contamination parts for the waste streams [2-3]. According to the level of activation the waste management route after dismantling (i.e. management as radioactive waste, unconditional clearance, clearance after decontamination e.g. sand blasting, clearance and melt, melt and clearance etc.) is selected [4].

2. Description of work and main findings

In the T4.5.1 subtask the work was dedicated for classification of the waste streams of the different types of reactors was carried out. Radionuclide generation and distribution in MRW at the different nuclear reactors (types: PWR, BWR, RBMK, VVER) was overviewed and compared. Due to the structural design of the different reactors, as Channel Reactor of High Power (RBMK), Boiling Water Reactor (BWR), Canada Deuterium Uranium (CANDU) and Pressurized Water Reactor (PWR) or Russian type of PWR – VVER, the radiation control area for MRW is different. In PWR technology, where only the reactor building and the reactor auxiliary building are in radiation control area, while in BWR also the turbines and the generator are located in radiation control area, for CANDU activated metal pressure tube, calandria tube, reactivity device, and reactivity device supporter were classified as greater than disposal criteria, whereas the structural components such as the calandria tank, reactivity device supporters, and side structural components was classified as low- and intermediate-level waste, for RBMK zones of different metal construction activation was determined accordingly to the neutron fluence [10, 11]. Metallic structures are made from various grades of steel and metal alloys during the construction of nuclear reactor. The choice of a specific type of material depends on the conditions in which the reactor will operate. The most commonly used materials are stainless steel, steel and various metal alloys such as zirconium for fuel rods and assemblies as resistant material to high temperatures and neutron activation. The materials used in the construction of the reactor become radioactive during neutron activation, and also can be contaminated with radioactive elements due to fuel leakage during normal reactor operation or incident events as well as from corrosion of activated materials. The main reactor materials differ depending on the reactor type: carbon steel or stainless steel are dominant in BWRs and Inconel or incoloy in PWRs. For BWR's the main metal activation products are ^{60}Co , ^{59}Ni , ^{63}Ni , ^{94}Nb , ^{14}C [12], for VVER also ^{55}Fe , ^{54}Mn , for RBMK type reactor. All these materials have impurities, the amount of which is regulated during production, and their permissible values are usually indicated in their passports. However, maximum permissible concentrations are often indicated only for main chemical elements. The other impurities can be obtained from similar reactor studies [13; 14] or can be determined from virgin samples using the instrumental neutron activation analysis or the prompt gamma activation analysis or inductively coupled plasma mass spectrometer or are measured and deducted from the comparison of modelling/measurement result [15]. Composition of activation radionuclide directly influences the choice of dismantling and management technologies afterwards.

For approximate estimation of the volume and activity generated annually by 1GWe in different type NPP, one can refer the information on long-lived ILW in [16] – the highest volumes and activities (~1PBq) belongs to Gas Cooled Reactor (GCR) (5000 m³) and RBMK (1500 m³) type reactors, the lowest activities (~0.1PBq) belongs to PWR (250 m³) and Pressurized Heavy Water Reactor (250 m³) reactors.

Reactor operations generate radioactive fission, activation, and corrosion products:

- Fission products (FP) appears due to cladding defect: volatile (Cs, Ba, Sr, Ce, Pr, Zr, Ru...) and actinides and U, which normally do not migrate. Amounts of nuclides depends on the length and position of the defect and the burn-up fraction of the defective fuel rod. FP usually are incorporated in the metallic oxides of the primary circuit surfaces.
- Activation products (AP) are chemical elements of the water coolant, air, moderator, biological shield or control tools (sensors) materials activated under the neutron flux (^{16}N , ^{17}N , ^3H , ^{41}Ar , ^{14}C , ^{60}Co , ^{55}Fe , ^{63}Ni ...). These activation products do not depend on fuel defect level and some of them are short-lived therefore are not a significant radiation source; Usually AP levels are determined using operating plant data. Due to the fact that uranium occurs as an impurity in the metallic materials, FP are also generated in the material itself. Like the AP, these FP are firmly embedded within the material and are not located as contamination on the surface.
- Corrosion Products (CP) come from the corrosion of the structure materials in contact with the primary coolant. The main CP responsible of dose rates are ^{60}Co and ^{58}Co , the others are ^{51}Cr , ^{54}Mn , ^{59}Fe . The prediction of the Co sources varies depending on the uncertainties about the transport, deposition and releasing mechanisms or kinetics of the nuclides and about their soluble or particular forms. [17]

Specific activity of FP, AP and CP nuclides in reactor coolant depends on many factors, such as the number of operating defective fuel elements, reactor power history, fuel burnup and efficiency of reactor coolant purification system, on the transport processes of these nuclides: release from fuel cladding defects, transport with coolant and sedimentation on particles in the coolant or internal surfaces of tubes and also the sediments can dissolve or erode from tube surfaces back to the coolant due to changing chemical or thermal-hydraulic conditions of the coolant [18,19]. These circumstances determine the change of the scaling factors between initial activities of radionuclides in the reactor metallic constructions. The processes are similar in BWR, PWR or RBMK in general, although due to different water chemistry, physical processes and complexity of the

reactor main circulation circuit, different final contamination of the main circulation circuit tubes internal surfaces can be observed [20].

The procedure for classification of the contaminated LLW, VLLW parts, i.e. SFs methodology, is similar for all types of reactors. For SFs determination, calculations based on correlations between DTM and ETM radionuclides (key isotopes) using statistical methods are performed [12]. The methodology is based on investigation of the functional dependence between activities of DTM nuclides and activities of ETM nuclides. If the correlation coefficient between these nuclides functional dependence is bigger than 0.5, then it is reasonable to calculate a Scaling Factor (SF) between DTM and ETM nuclides. In the case of log-normal distribution of data, “linear regression of logarithms” (i.e. linear correlation between DTM and ETM radionuclides log concentrations) is applied for calculation of a SF. If there is a lack of measured data, the “weighted arithmetic mean” method is applied. The main key radionuclides are usually ^{60}Co and ^{137}Cs , (in case of plutonium isotopes presence ^{241}Am is used as key radionuclide). A mathematical model and some graphical representations of the activity concentration data are needed to ensure that the SFs are correctly defined for each waste stream.

For SFs determination also are needed: determination of minimum number of samples to obtain statistically representative result; outlier analysis and data grouping, checking if the SF defined for different groups of samples are statistically compatible and, thus, can be considered as the same SF; reconstruction of data for samples collected in different periods of time is usually necessary after reactor shut-down and in case of significant fuel failure.

Periodically, the dataset used to calculate the SFs is checked to confirm that it is statistically compatible with new samples collected during the operational life of the facility.

During the operational phase, the necessary data to implement the SFs methodology is obtained as the waste is generated. During the decommissioning stage, the SFs program relies on new laboratory analyses coming from a sampling plan, which is based on previous existing characterizations (i.e. historical operational data, SFs determined during operation, site specific measurements taken after the operational life and before decommissioning).

In order to determine a representative nuclide vector for a defined set of metallic waste components that will form a waste stream when dismantled, it is necessary to cover a larger part of the systems that make up the stream in order to increase representativeness and experimentally confirm the system division into streams. Also, in order to optimize the scope and cost of the research program, technologically similar systems (i.e. systems that are interconnected because they are affected by flow of the same technological process liquid or gas, similar form, surface contamination peculiarities etc.) are combined into a group of systems that form a stream that will be characterized with one nuclide vector.

Optimized NV is obtained by analysing and systemizing the information about radioactive metallic waste streams, identifying the optimal list of relevant radionuclides (e.g., selection of ^{60}Co and ^{94}Nb for ZrNb alloys), describing inter-correlations between key nuclides and difficult to measure nuclides (^{59}Ni , ^{63}Ni and other nuclides from the list of radionuclides to be declared for dedicated disposal site) including multivariate analysis of the already measured data at the sites and numerical analysis of activation and contamination parts for the waste streams as shown in the Figure 13 chart.

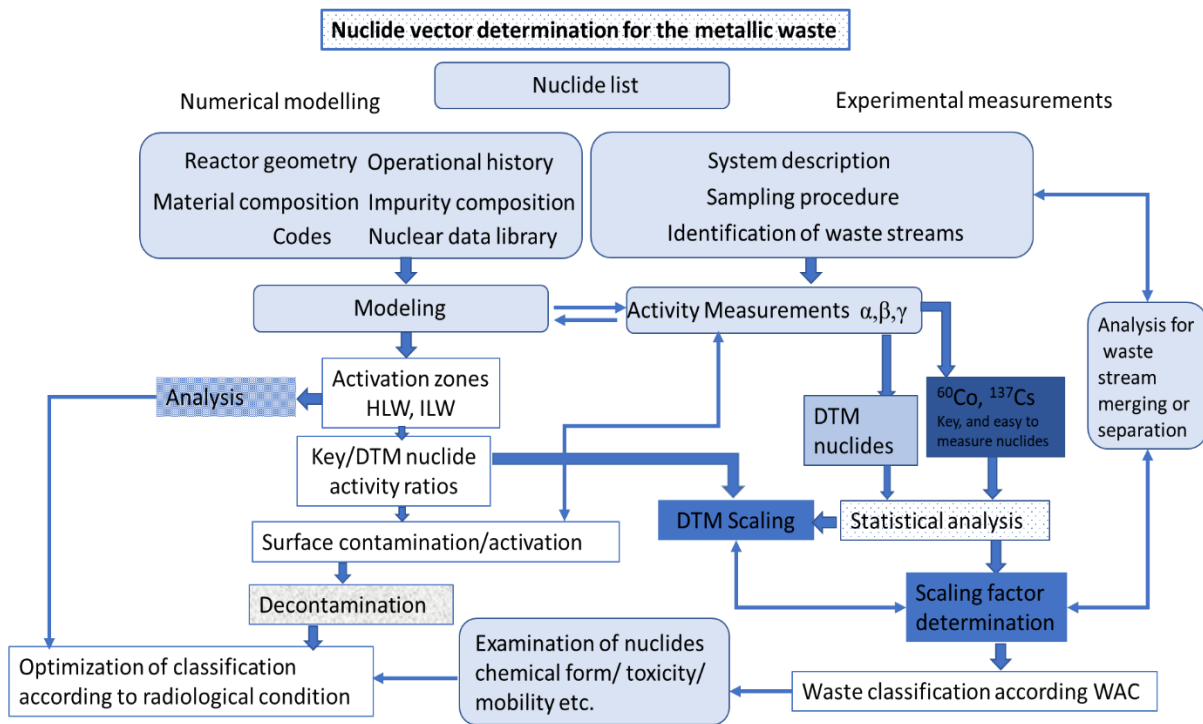


Figure 13. Chart of Nuclide Vector determination and optimization of classification.

3. Conclusions

During the research performed in T4.5.1 subtask on classification of the waste streams of the different types of reactors:

- the state-of-art scientific information on MRW classification and possible management routes was provided.
- optimized classification scheme according to waste acceptance criteria and waste disposal options was drawn
- the comparison of scaling factor approach at different member states is carrying out.

4.3.2 Characterization and sorting of metallic waste in different management routes

Fabiana Gentile, Filippo Gagliardi, Giulia Colavolpe (NUCLECO), Eileen Langegger, Marie-Charlotte Bornhoeft (DMT), Diego E. Hernando, José Luis Leganés Nieto (ENRESA), Rita Plukiene, Elena Lagzdina, Marina Konstantinova (FTMC)
jlen@enresa.es

1. Introduction

For efficient characterization of metallic ILW, LLW, VLLW by applying scaling factors simple non-destructive γ -spectrometry technique or combination of dose rate/ γ -spectrometry measurement is needed. In WP4 4.5.2 subtask investigation of non-destructive γ -spectrometry technique is performed. For determination of the management route of metallic waste containers a new set-up of non-destructive gamma spectrometry measurements is investigated. By applying this technique ETM radionuclides are determined and then by using the SFs for DTM radionuclides, the nuclide vectors of metallic radioactive waste are obtained. The uncertainty of the usually used non-destructive techniques is high due to the inhomogeneity of the density as well as the location of the sources within the container. For localization of the sources and more accurate estimation of radioactivity in waste containers, research based on the use of sectorial gamma scanning [5] and a system of plastic scintillation detectors [6] are carried out. Also, investigation of the γ -spectra of ^{60}Co (as activation) and ^{137}Cs (as surface contamination) sources in different metallic waste shielding geometries is performed estimating possibility to use peak shape/intensity and peak/Compton ratio of γ -spectra analysis and MCNP6 modelling for metallic waste surface activation identification [7-9].

2. Description of work

In WP4 4.5.2 subtask investigation of non-destructive γ -spectrometry technique is performed in order to define ETM radionuclides, which can be used latter on for MRW characterization by using the SFs for DTM radionuclides. A non-destructive gamma spectrometry technique focusing on the interpretation of gamma ray spectra resulting from radionuclides in activated and/or contaminated components is investigated. Specifically, a spectrum is produced by using MCNP simulations of gamma detector response to the activities of ETM gamma emitters that are known or can be determined in a component or a segment of metallic construction/waste. This spectrum is compared with the experimental spectrum to investigate if any peaks of other gamma emitters are hidden in the continuum or, in case of ^{90}Sr presence, if bremsstrahlung radiation is observed. This method aspires to achieve high measurement sensitivity for gamma emitters (especially in case of underwater measurements) and to be used for the strontium detection/ determination.

For characterization of low-activity metallic segments after dismantling, a non-destructive γ -spectrometry set-up is proposed, which allows reduction of: the range of the distances of the sources from the detector; the range of the source solid angles of detection; as well as the radiation attenuation range for different source locations. Regarding the measurement of 10-30 cm diameter straight or curved pipes of 0.3 cm wall thickness (wall thickness tolerance 0.1 cm) as well as flat and curved surfaces of thickness 0.3-2 cm (specific tolerance for each surface thickness), the measurement uncertainties related to activity inhomogeneities are lower than 30%. The detection efficiencies of ^{137}Cs and ^{60}Co for sufficient amount of metallic waste (about 100 kg) allow measurement in 1-2 min. The method is effective for determination of activities in activated and/ or contaminated metallic waste. The specific activities are determined by using the results of the measurements (i.e. activities of ETM radionuclides) and the SFs for activation and/or contamination produced DTM radionuclides.

Also, investigation of the γ -spectra of ^{60}Co (as activation) and ^{137}Cs (as surface contamination) sources in different metallic waste shielding geometries is performed estimating possibility to use peak shape/intensity and peak/Compton ratio of γ -spectra analysis and MCNP6 modelling for metallic waste surface activation identification [7-9].

3. Conclusions

During the research performed T4.5.2 subtask on innovative technique for MRW characterization:

- a non-destructive γ -spectrometry set-up inside a shielded chamber is proposed, which allows reduction of uncertainties related to activity inhomogeneities by 30% and determination of activities of ^{137}Cs and ^{60}Co at the level of clearance in 1-2 min for amount of MRW ~100 kg.
- surface contamination by ^{137}Cs source can be distinguished from the shape/intensity and peak/Compton ratio of γ -spectra analysis by using the modelling and measurement comparison.
- recommendations for application of new non-destructive γ -spectrometry set-up's for effective and efficient characterization of very low-level metallic waste in order to reduce the amount of MRW to be disposed of in final repositories will be introduced.

4.3.3 Development of new radiochemical procedures for DTM radionuclides

Anumaija Leskinen, Tommi Kekki (VTT), Mojmír Němec, Kateřina Čubová (CTU), Tomo Suzuki, Nicolas Bessagnet, Marcel Mokili, Abdesselam Abdelouas (IMTA)
suzuki@subatech.in2p3.fr; Anumaija.Leskinen@vtt.fi; mojmir.nemec@jfifi.cvut.cz

1. Introduction

The difficult to measure (DTM) radionuclides, require destructive radioanalytical techniques. Radionuclides of very low energy emission may be found in certain metallic radioactive waste as surface contaminants or neutron activated radionuclides in the base metal. The radionuclides are divided to easy-to-measure (ETM) and difficult-to-measure (DTM) radionuclides. These radionuclides have to be accurately quantified with a robust and validated radiochemical procedure. Four radionuclides have been selected: ^{59}Ni (7.6 \times 10⁵ y, β^+ , EC, EX-K α 1 = 6.93 keV (20%), EX-K α 2 = 6.91 keV (10%), E γ_{\pm} = 511 keV), ^{63}Ni (98.7 y, β^- , E_{max} = 66.98 keV (100%)), ^{41}Ca (7.6 \times 10⁴ y, EC, EEC = 421.64 keV (100%)), ^{93}Zr (1.61 \times 10⁶ y, β^- , E_{max} = 60.0 keV (73%) and 90.8 keV (27%)). The targets of the study is to provide a highly selective and efficient separation and purification, and to develop a sensitive to ultra-sensitive method of measurement, depending on the radionuclide. The utilised technologies are gamma spectrometry, liquid scintillation counting (LSC), and Inductively Coupled Plasma Mass spectrometry (ICP-MS).

2. Description of work and main findings

Regarding the development of new radiochemical procedures for DTM radionuclides, the general methodology is based on the separation-purification of sample (synthetic, or a solid containing the radionuclide source, or a surrogate), the conditioning to obtain the most suitable form for measurements (liquid form or deposition on filters), and the selection of an adapted analytical technique and the optimization of the detection efficiency prior to the measurement.

⁵⁹Ni / ⁶³Ni (VTT contribution)

The radiochemical method development of ⁵⁹Ni analysis focused on measurement target preparation and measurement as the radiochemical purification for ^{59/63}Ni has been developed earlier [21]. The ^{59/63}Ni purification procedure includes an anion exchange resin and Ni resin treatments to purify a ^{59/63}Ni fraction, which is eluted from the Ni resin using 3M HNO₃. The eluant solution is evaporated to approximately 2 ml and 1 ml is taken for ⁶³Ni measurement using LSC and 100 µl for yield measurements. The ⁵⁹Ni emits low energy x-rays and this study concentrated on detection of ⁵⁹Ni using broad energy gamma spectrometer. The self-attenuation of low energy x-rays is a challenge and consequently preparation of the measurement target is key. Preparation of the measurement target was imitated based on dimethylglyoxime (DMG) precipitation (technique utilised also in the Ni resin) and filtration on a filter according literature review. However, the results showed unreliable deposition of the precipitate resulting in unreliable measurement result (Figure 14). Next, a study was made to prepare the measurement target by evaporation of 1ml of the evaporated ^{59/63}Ni fraction on a filter (Figure 14) and the results showed good linearity between 20 Bq and 1000 Bq. In this modified method, the 2 ml evaporated fraction is divided as follows; 1 ml for ⁵⁹Ni measurement, 100 µl for the ⁶³Ni (volume increased if needed), and 100 µl for yield measurements. As ⁵⁹Ni standard solution is expensive, ⁵⁵Fe surrogate was used in preparation of a standard curve. Especially in steel, ⁶⁰Co interference is possible in Ni-fraction as they are chemically similar. Interference of ⁶⁰Co was studied and seen that below 250 Bq of ⁵⁵Fe, ⁶⁰Co began to cause interference. After preparation of the standard curve, real stainless steel samples were studied. Good decontamination was achieved (no ⁶⁰Co contamination) and additionally good correlation between ⁵⁹Ni and ⁶⁰Co Bq/g results. Next an intercomparison exercise is needed.

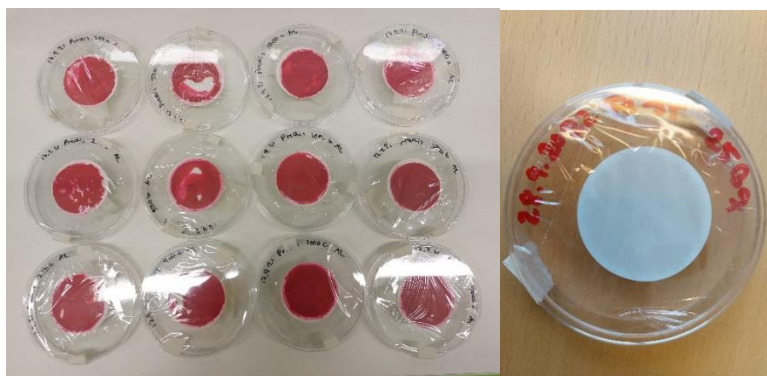


Figure 14. Measurement targets prepared using DMG precipitation (left) and evaporation (right).

⁵⁹Ni/⁶³Ni (CTU contribution)

Final steps regarding ^{59/63}Ni radiometric measurement are being developed focusing on electrodeposition of nickel from the eluted solution coming from final separation of nickel with dimethylglyoxime (DMG), what is a standard separation method used for nickel separation and analysis. The new proposed „back-end“ of the method uses galvanostatic deposition of nickel from weakly acidic chloride-sulphate system containing high concentration of boric acid (30g per L) acting like a buffer. The process runs at constant current density of 0.15 A.cm⁻² on stainless steel cathode as it is commonly used in electrodeposition for alpha spectrometry. The idea behind this development aims on measurement of the deposited nickel with low energy gamma spectrometry to get ⁵⁹Ni activity, then the cathode is immersed to the scintillation cocktail and ⁶³Ni is measured. In such arrangement it is supposed to be achieved better parameters of the whole analysis due to additional electrodeposition separation step, concentrating all the nickel from the initial sample reducing thus additional operation and division of the activity to two or more subsamples for separate ⁶³Ni and ⁵⁹Ni measurement, it is also possible to use bigger volume and nickel metal concentration in the eluate, or use nickel carrier. Currently, optimization aiming on high electrodeposition yields (> 95%) are taking place as well as active experiments with ⁶³Ni.

In parallel, experiments focused on behaviour of Ni and Ca in a caesium sputter source were done to find options of isobar suppression – a possible way to allow or improve measurement traces of ⁵⁹Ni and ⁴¹Ca with

accelerator mass spectrometry (Figure 15). In these cases, ^{59}Co and ^{41}K should be suppressed. In the experiments, fluoride target matrices – mixtures of metals or fluorides of the elements with PbF_2 in silver cathode were used and their mass spectra were compared also to the oxide ones. It was found that for ^{41}Ca , molecules $[\text{CaF}_3]^-$ and $[\text{CaF}_4]^-$ can be used, while potassium creates only $[\text{KF}]^-$ and $[\text{KF}_2]^-$ molecules. Unlike nickel, no heavier molecules than $[\text{CoF}_4]^-$ have been found, but the measurement should be repeated with higher sensitivity.

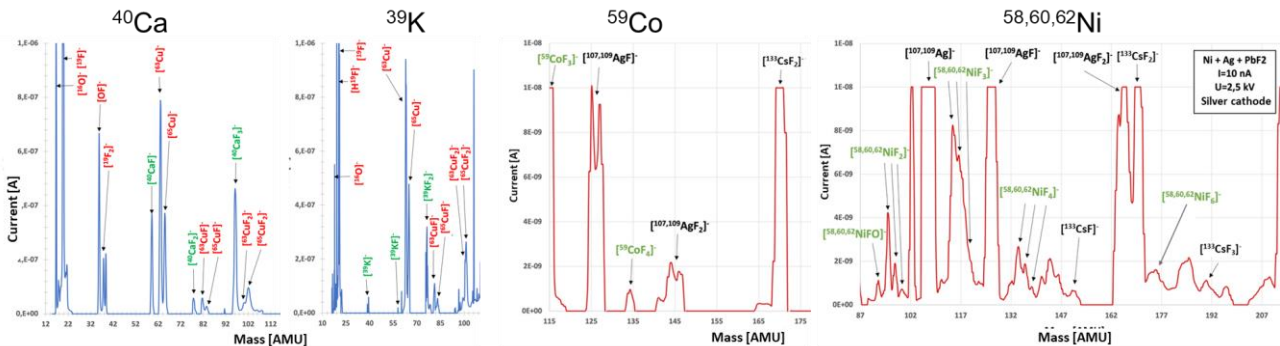


Figure 15. Mass spectra coming from caesium sputtering ion source in screening of suppression of ^{59}Ni and ^{41}Ca isobars.

^{93}Zr (IMT Atlantique contribution)

The evaluation of ^{93}Zr requires the development of a procedure of purification and separation to remove the contribution of Fe, Ni, Cr, Nb, and Mo coming from the digestion of the metallic sample during the sample preparation (Figure 16). Several series of samples containing Zr are prepared to evaluate this effect during the measurement of Zr by ICP-MS and LSC. Chromatographic separation resins (UTEVA, TK400) are used with non radioactive solutions and Inconel metal for the optimization of the protocols. The efficiency of Zr recovering is about 95% at the end of the treatment and almost 100% of the main elements Fe, Cr and Ni are retained in the resins. These tests confirm that almost 100% of Mn, Sb, Ce, Y, Nb and Mo are retained in resins.

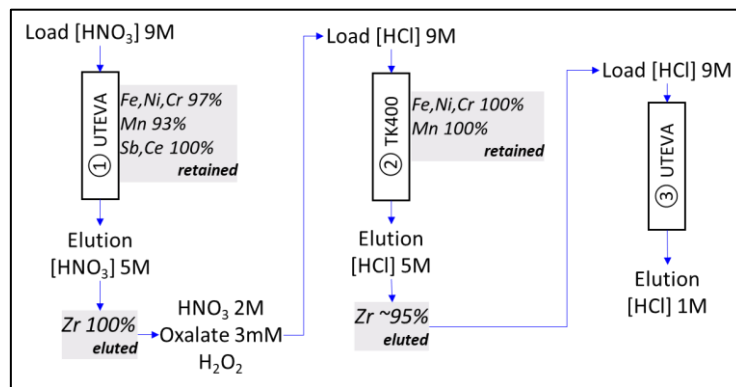


Figure 16. Separation and purification method for the extraction of Zr.

As the risk of unavailability of standard ^{93}Zr was identified, an alternative study was undertaken using ^{63}Ni as a close analogue in terms of beta emission energies. For this purpose, ^{63}Ni was measured by liquid scintillation under similar conditions as ^{93}Zr , i.e. from the last extraction condition by UTEVA (1M HCl). The following parameters were evaluated: effects of HCl concentration, stability of the scintillating liquid, evaluation of the background and determination of the counting efficiency. The results showed that the optimal conditions for ^{93}Zr detection are 8mL 1M HCl + 12mL AB and 8mL 0.1M HCl + 12mL LLT. Based on the ^{63}Ni measurements, the results were used to determine the theoretical counting efficiency of ^{93}Zr by theoretical calculation in collaboration with Sofia University. The preliminary conclusion shows that the counting efficiencies of ^{93}Zr are significantly different from those of ^{63}Ni meaning that the direct use of ^{63}Ni as a standard (method used in some publications [22-24]) leads to a systematic underestimation of the counting efficiency of ^{93}Zr by about 20%. To validate the simulation, standard source of ^{93}Zr is needed.

3. Conclusions

The optimisation for ^{59}Ni measurements, at VTT, using ^{55}Fe calibration curve achieve a satisfying detection limit, lower than originally expected (~20 Bq vs 100 Bq). The uncertainty due to ^{60}Co interference is seen below 250 Bq of ^{55}Fe and currently studied further. In the near future, intercomparison exercise with a real sample is discussed.

At CTU, electrodeposition of ^{59}Ni is optimised with good deposition efficiency between 80-90%, the goal it to reach >95%. The next step is to validate the parameters with ^{63}Ni and to measure the detection efficiency. The detection of ^{59}Ni with AMS and the contributions of interferences (^{59}Co) are evaluated to find options for best isobar suppression. Similarly, ^{41}Ca measurement by AMS is also in optimization regarding its isobaric interference with ^{41}K .

The protocol of separation and purification of ^{93}Zr is reached with a good recovery (~95%) and low detection limit by LSC of 0.04 Bq/g based on ^{63}Ni calibration curve used as a surrogate. This protocol needs a validation with a standard solution of ^{93}Zr . The optimization of metal digestion, such as Ni-alloys (Inconel) and Fe-alloys (stainless steel) is reached for non-oxidized samples, and it will be optimized in the future work for oxidized metallic samples.

Acknowledgements

The authors would like to thank S. CONINX, J. FEINHALS (DMT GmbH & Co. KG, Hamburg, Germany) which were partners of WP4 4.5.1 and co-authors of part of the work performed. The development of radiochemical procedures was also supported by the Finnish Research Programme on Nuclear Waste Management KYT 2022, the project No. CZ.02.1.01/0.0/16_019/0000728 funded by the Ministry of Education, Youth and Sports the Czech Republic and CTU grant no. SGS21/169/OHK4/3T/14 as well as the ANR LabCom TESMARAC programme (2020-2024). The authors would like to thank S. Happel from Triskem Company his expertise on chromatographic resin extractions, and P. Cassette from Sofia University for his expertise on theoretical evaluation of ^{93}Zr and ^{63}Ni spectra.

References

- [1] INTERNATIONAL ATOMIC ENERGY AGENCY, Classification of Radioactive Waste, IAEA Safety Standards Series No. GSG-1, IAEA, Vienna (2009).
- [2] R. Plukienė, A. Plukis, E. Lagzdina, M. Konstantinova, A. Savidou, S. Coninx, J. Feinhals, Classification of the metallic radioactive waste streams of the different types of reactors in PREDIS, International Conference on Radioactive Waste Management: Solutions for a Sustainable Future, IAEA Headquarters Vienna, Austria, 1–5 November 2021.
- [3] R. Plukienė, A. Plukis, E. Lagzdina, M. Konstantinova, A. Savidou, S. Coninx, J. Feinhals, Metallic radioactive waste classification for the different types of reactors considered in PREDIS, International Conference FISA 2022 / EURADWASTE '22, 30 May–3 June 2022, Lyon, France.
- [4] M.-Ch. Bornhoeft, G. Colavolpe, S. Coninx, H. D. Espejo, J. Feinhals, F. Gagliardi, F. Gentile, E. Lagzdina, N.J. L. Leganés, A. Leskinen, A. Markopoulos, D. Mavrikis, M. Němec, R. Plukiene, A. Savidou, T. Suzuki-Muresan, Optimization of metallic waste characterization and procedures for waste minimization and recycling in PREDIS project, International Conference on Radioactive Waste Management: Solutions for a Sustainable Future, IAEA Headquarters Vienna, Austria, 15-19 May 2023.
- [5] HAVENITH, A., FRITZSCHE, M., PASLER, D., HARTMANN, T., “Advance sectorial gamma scanning for the radiological characterization of radioactive waste packages”, *Atw. Intern. Zeitsch. fuer Kernen* **63** (2019) 160-166.
- [6] PASTENA, M., WEINHORST, B., KANISCH, G., PÉREZ LEZAMA, E., RADTKE, J., THOMAS, T., “A novel approach to the localization and estimation of radioactivity in contaminated waste packages via imaging techniques”, *Measurement Science and Technology* **32** 9 (2021) 1-15.
- [7] E. Lagzdina, D. Germanas, D. Lingis, J. Garankin, M. Konstantinova, R. Plukienė, A. Plukis, and V. Remeikis, Discrimination of surface and volume activity in metallic waste samples by using HPGe and CeBr3 detectors and MCNP modelling of γ -spectra, International Conference FISA 2022 / EURADWASTE '22, 30 May–3 June 2022, Lyon, France.
- [8] R. Plukiene, E. Lagzdina, D. Germanas, K. Mikalauskiene, M. Konstantinova, A. Plukis, A. Gudelis, V. Remeikis, Surface activity determination in metallic waste samples by using HPGe and CeBr3 detectors and MCNP modelling of γ -spectra, ICRM 2023, Bucharest, Romania, 27-31 March 2023.
- [9] E. Lagzdina, R. Plukienė, D. Germanas, K. Mikalauskiene, M. Konstantinova, A. Plukis, V. Remeikis, Modelling and experimental determination of surface and volume activity in different geometry metallic waste samples, ENYGF, Kraków, Poland, 8–12 May 2023.

- [10] Stade Decommissioning and dismantling of the nuclear power plant – from the nuclear power plant to the green lawn 3 ed. (2008). INIS: http://inis.iaea.org/search/search.aspx?orig_q=RN:47065581
- [11] DONG-KEUN C., HEUI-JOO C., RIZWAN A., GYUN-YOUNG H., Radiological characteristics of decommissioning waste from a CANDU reactor, *Nuc. Eng. Techn.* **43** 6 (2011) 583-592.
- [12] INTERNATIONAL ATOMIC ENERGY AGENCY, Determination and Use of Scaling Factors for Waste Characterization in Nuclear Power Plants, Nuclear Energy Series No. NW-T-1.18, IAEA, Vienna (2009).
- [13] INTERNATIONAL ATOMIC ENERGY AGENCY, The decommissioning of WWER type nuclear power plants, IAEA-TECDOC-1133, IAEA, Vienna (2000).
- [14] NARKUNAS E., SMAIZYS A., POSKAS P., Neutron Activation in the Metal Structures of an RBMK-1500 Reactor, *Nuclear Technology* **168** 2 (2009) 533–536.
- [15] BYLKIN, B.K., DAVYDOVA, G.B., ZVERKOV, Y.A., KRAYUSHKIN, A.V., NERETIN, Y.A., NOSOVSKY, A.V., SEYDA, V.A., SHORT S.M., Induced Radioactivity and Waste Classification of Reactor Zone Components of the Chernobyl Nuclear Power Plant Unit 1 after Final Shutdown. *Nucl. Technol.* **136** (2001) 76–81.
- [16] INTERNATIONAL ATOMIC ENERGY AGENCY, Estimation of Global Inventories of Radioactive Waste and Other Radioactive Materials, IAEA-TECDOC-1591, IAEA, Vienna (2010).
- [17] U.S. EPR FINAL SAFETY ANALYSIS REPORT; 11.0 Radioactive Waste Management <https://www.nrc.gov/docs/ML1322/ML13220A880.pdf>
- [18] KLEVINSKAS G., JUODIS A., PLUKIS A., PLUKIENĖ R., AND REMEIKIS V., Determination of I-129 activity in the RBMK-1500 main circulation circuit, *Nucl. Eng. Des.* **238** 7, (2008) 1518–1524.
- [19] JUODIS L, MACEIKA E., PLUKIS A., DACQUAIT F., GENIN J.B., BENIERG., Assessment of radioactive contamination in primary circuit of WWER-440 type reactors by computer code OSCAR for the decommissioning case, *Prog. Nuc. Energ.* **110** (2019) 191-198.
- [20] LEWIS B. J. AND HUSAIN A., Modelling the activity of ¹²⁹I in the primary coolant of a CANDU reactor, *J. Nuc. Mat.* **312** 1 (2003) 81–96.
- [21] Leskinen, A., Salminen-Paatero, S., Rätty, A., Tanhua-Tyrkkö, M., Iso-Markku, T., Puukko, E., “Determination of ¹⁴C, ⁵⁵Fe, ⁶³Ni and gamma emitters in activated RPV steel samples – a comparison between calculations and experimental analysis”, *J Radioanal Nucl Chem* **323** (2020) 399-413.
- [22] Roberto P.G. Monteiro ,Thiago C. Oliveira, Ângela M. Amaral and Raquel M. Mingote, Radiochemical Determination of ⁹³Zr in Low and Intermediate Nuclear Wastes, 2009 International Nuclear Atlantic Conference – INAC 2009, Rio de Janeiro,RJ, Brazil, September 27 to October 2, 2009.
- [23] T. C. Oliveira, R. P. G. Monteiro, A. H. Oliveira, A selective separation method for ⁹³Zr in radiochemical analysis of low and intermediate level wastes from nuclear power plants, *J Radioanal Nucl Chem* (2011) 289:497–501.
- [24] Szabolcs Osvath, Nora Vajda, Zsuzsa Molnar, E va Kovacs-Szeles, Mihaly Braun, Mate´ Halasz, Determination of ⁹³Zr in nuclear power plant wastes, *J Radioanal Nucl Chem* (2017) 314:31–38.

4.4 Encapsulation of reactive metals in magnesium phosphate cement-based matrices (Task 4.6.)

MPC were identified as a promising alternative to Portland cements in encapsulation of nuclear wastes having high reactivity in alkaline media. To use MPC as a conditioning matrix, research has to be developed. In the frame of the task 6 of the WP4, studies concern formulations, leaching behaviour, stability under irradiation, and the reactivity of reactive metallic waste (Al, Be) and a steel drum in MPC. A reference formulation was provided by the CEA to begin the studies [1].

Keywords: magnesium phosphate cement, formulation, cost, leaching, irradiation, corrosion of Al, Be and steel

4.4.1 Development of magnesium phosphate cement formulations

R. Fernández, M. Dieguez, P. Padilla, A. I. Ruiz, J. Cuevas (UAM), raul.fernandez@uam.es
 M. Cruz Alonso, C. Fernández (CSIC), mcalonso@ietcc.csic.es

The reference formulation uses a MgO imported from outside the European Union, fly ash (FA) as filler and a Mg/P molar ratio = 1. The work was focused on the MPC formulation optimisation based on these aspects: 1) evaluate of alternative fillers to replace FA due to its decreasing availability, 2) study the MPC formulations with increasing Mg/P molar ratio to increase the physical and chemical stability of the cement paste, and 3) evaluate the behaviour of additional MgO sources within the European Union. CSIC has contributed to the study on the influence of Mg/P molar ratios in pore solution composition and curing conditions.

Out of 5 different fillers evaluated, including two types of metakaolin and pumite powder, wollastonite and volcanic ash originated from the eruption of the volcano of La Palma in 2021 were selected due to their better rheological and mechanical properties. MPC matrices elaborated with any of these two fillers require less water in the formulation than the reference MPC and achieve similar (with wollastonite) or higher compressive strength (with volcanic ash). These two fillers were selected to evaluate the increase in the molar Mg/P ratio in MKPC. Regardless the ratio, K-struvite is the only crystalline mineral phase formed as a result of the acid-base chemical reaction between MgO and KH_2PO_4 , with none or neglected contribution of the filler compounds. However, excess of MgO is observed with the increasing Mg/P ratio (Figure 17).

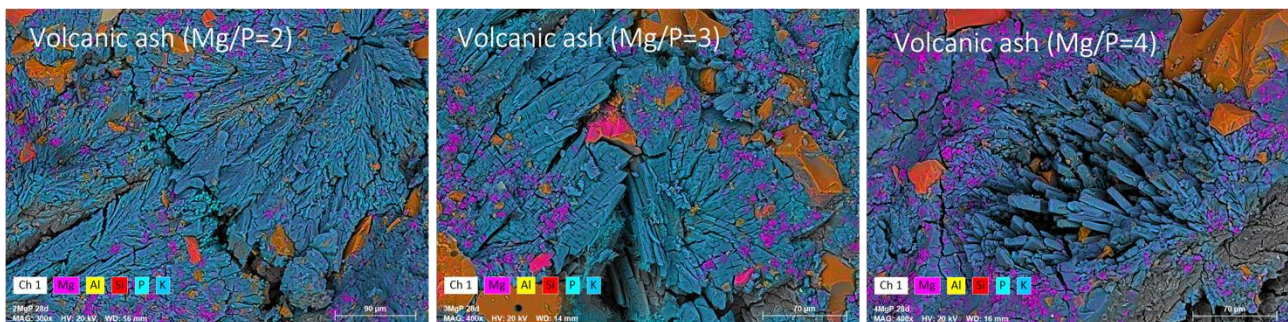


Figure 17. SEM-EDX aspect of K-struvite in MPC matrix using volcanic ash. Excess of Mg with the increasing Mg/P molar ratio is observed by the increasing pink colour on the surface of K-struvite.

CSIC confirmed improved mechanical strength and physical stability of MPC at Mg/P = 2 and 3 M associated to the increase of capillary pores < 0.1 μm . The pH varies according to the curing conditions and the Mg/P ratio within a range between 7 (Mg/P = 1) and 10 (Mg/P = 3). Phosphate and Magnesium content decrease with curing advance accordingly with pH changes. Borates also decrease its content with the aging (Figure 18).

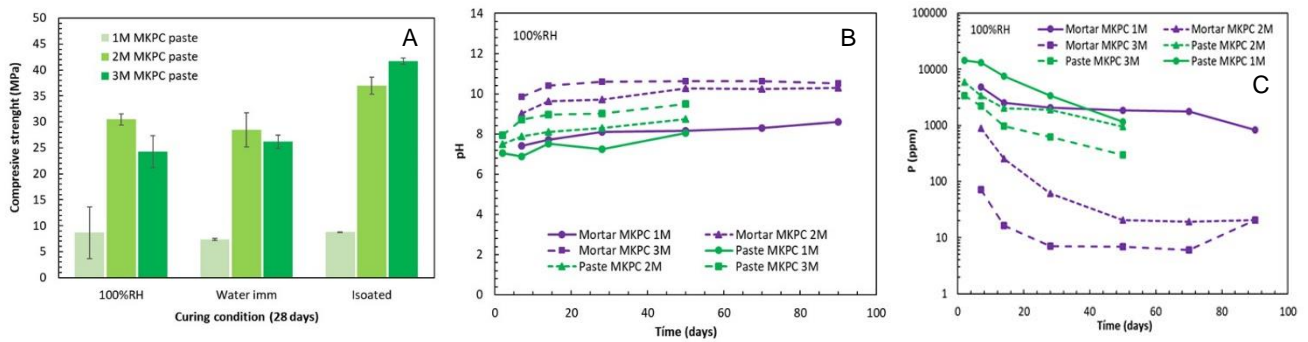


Figure 18. Effect of Mg/P molar ratio: A) Compressive strength, B) pH evolution and C) phosphate ion content.

Different MgO sources are currently under consideration. Four other commercial products are included and at least two of them exhibit potentially good rheological properties.

4.4.2 Magnesium phosphate cement cost optimization

L. Stefan (Orano), lavinia.stefan@orano.group.fr

K. Le, S. Delpech, D. Rodrigues, C. Cannes (CNRS), kim.le@ijclab.in2p3.fr

The high MPC cost higher is a barrier to an industrial scale. A low-cost MPC formulation (LC-MPC) was then developed using reactive MgO instead of dead-burned (DB) MgO, the latter being more expensive and sourced from fewer providers. Reactive MgO has also good durability and a lower carbon footprint. However, its high reactivity (specific surface up to 100 times greater than DB MgO) leads to flash set time, making it impossible to use when large volumes need to be cast. Classic retarders, such as borax are not efficient when it comes to reactive magnesia. The previous work aimed to replace DB MgO with reactive magnesia, while keeping other parameters similar to the reference formulation and using sodium thiosulfate as retarder.

The primary focus was on optimizing the retarder for high purity industrial grade reactive MgO to achieve a set time within a reasonable range. Two optimized formulations were developed for this purpose: one consisted of 3% thiosulfate and 2% boric acid by weight relative to the cement content (B2T3), and a second one with a thiosulfate concentration of 5% (B0T5). Both formulations successfully provided control over the setting time, ensuring it fell within an acceptable range for practical applications (Table 2).

Table 2. Setting time and compressive strength of optimized LC MPC.

| Sample | Final setting time (min) | Compressive strength of solid samples after 7d curing, (MPa) |
|--------|--------------------------|--|
| B0T5 | 86 | 41.0 |
| B2T3 | 128 | 53.4 |

Recent work has focused on adjusting the volumes of aggregates (A) and cement paste (C) to achieve the required strength and reduce the cost. Increasing the A/C ratio from 2 to 4 can result in a significant 24% reduction in formulation costs (Figure 19). Despite maintaining a high cement dosage of 461 kg/m³ with an A/C ratio of 3, literature data suggest that the desired mechanical strength (>20 MPa) can be attained. (Figure 20) [1] Experiment works showed that increasing the Aggregate-to-Cement (A/C) ratio, with values such as 2.5, 3, and 4, resulted in a significant reduction in the setting time of the formulation. This indicates that as the proportion of sand increased in relation to cement, the setting process accelerated (Figure 21). When FA was replaced by sand, the setting time significantly decreases. Then, lowering the FA/C ratio accelerates the setting process. FA have an influence on the setting characteristics of the formulation. Increasing the A/C ratio does not necessarily decrease the setting time to the same extent as the impact of FA replacement. The influence of fly ash on the setting time was found to be much more significant.

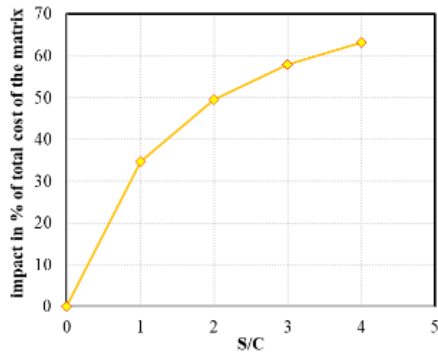


Figure 19. MPC formulation's cost in function of A/C ratio

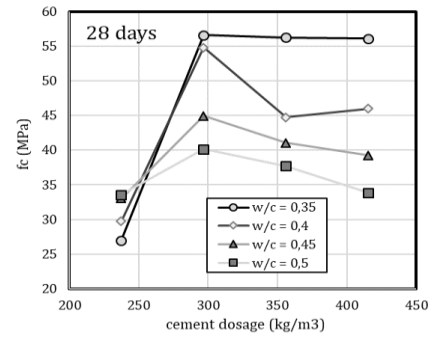


Figure 20. Effects of different cement quantities on compressive strength for different water/cement [2]

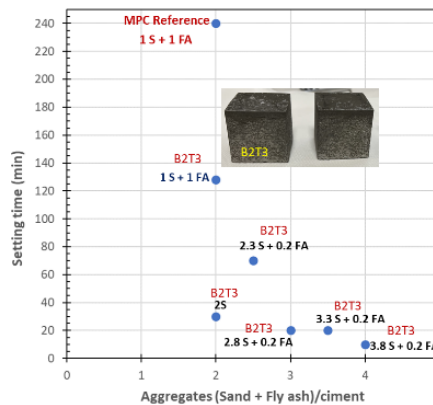


Figure 21. Setting time in function of of A/C ratio.

In future work, several aspects can be explored:

- Investigate the use of superplasticizers can help maintain workability while increasing the A/C ratio.
- Design a broader grain size distribution of the aggregates can improve the compacity of the the mortar.
- Study the influence of fly ash and other fillers on the setting time is crucial.

4.4.3 Behavior of magnesium phosphate cement under irradiation

I. Moschetti, L. Sarrasin, G. Blain, A. Abdelouas, (IMTA), moschett@subatech.in2p3.fr
 E. Mossini, F. Fattori, A. Santi, G. Magugliani, M. Giola, E. Macerata, M. Mariani (POLIMI),
eros.mossini@polimi.it

At IMTA, the radiation-induced modification of MPC under γ irradiation has been investigated with two configurations: (i) configuration #1, samples exposed to the same total dose (200 kGy) at different curing time (7, 11, 18 and 28 days), and (ii) configuration #2, samples with a complete curing time (28 days) exposed to different total dose (50, 100 and 200 kGy). Gamma irradiations (137-Cs) were performed at Arronax facility (France) with dose rate around 400 ± 80 Gy/h. X-Ray Diffraction (XRD) and Scanning Electron Microscopy (SEM) coupled with Energy Dispersive X-Ray (EDX) were performed before and after irradiation. No changes were observed: all K-struvite peaks do not change after exposure to γ irradiation up to 200kGy and irradiating starting from different curing times, in agreement with previous works on similar formulation irradiated up to 10 MGy [1,3]. The Mg/P, Mg/K, and K/P molar ratios for configuration #2 were determined by EDX. The molar ratios for the non-irradiated samples are closer to the stoichiometric values (Mg/P = 1, K/P = 1, and K/K = 1), but the quantification for the irradiated samples reveals a wider range of values. These ranges may be brought on by the discovery of various K-struvite morphologies, such as needles or tabular crystals, as reported in a prior article [4, 5], or by γ radiation-induced changes.

The hydrogen release was quantified by μ -Gas Chromatography immediately after the irradiation for configuration #1. The $G(H_2)$ yields measured from the early irradiation (1 d curing) to later one (28 d curing) do not shown greater differences indicating good matrix stability even with a fresher matrix. Leaching test were performed according to ANSI ANS 16.1 procedure [6] to accomplish the durability of the irradiated matrices

after irradiation. Quantification of the Mg^{2+} and K^+ were evaluated by Ion Chromatography. For all the configurations and elements, the values are stabilized after 90h of immersion, and the Li calculated are above 6 ensuring acceptable leaching resistance.

At POLIMI, the MPC samples were prepared and cured following the reference formulation [1]. One of the two series of specimens was spiked with four stable contaminants to emulate radionuclides frequently found in nuclear power plants, namely Cs-137, Eu-152 and Eu-154, Co-60, and Sr-90. These contaminants represent different chemical groups, and possibly different chemical behaviours. Absorbed doses of 100, 200, and 500 kGy have been delivered by a Co-60 source (2.5 kGy/h), keeping some unirradiated samples for reference. Three-dimensional leaching test were performed in accordance with the ANSI/ANS-16.1-2003 protocol (90-days duration), followed by compressive tests carried out in conformity with the UNI EN 12390-3:2019. The total leached fractions for K, P, and Mg at the end of the test are in the range of 20%, 10%, and 2%, respectively. Instead, for the contaminants, the total leached fractions are in the range of 5% for Cs, 1% for Co and Sr, and 0.05% for Eu. All of the leachability indices are higher than the Italian WAC (7) for heterogeneously encapsulated ILW. As expected, the leachability index of Cs, a highly mobile element, has the lowest value, around 10 (\gg the WAC limit) both for unirradiated and 500 kGy irradiated samples. Hence, no noticeable alterations can be attributed to radiation damage. The compressive tests were carried out at the Nucleco laboratories. All samples showed no significant signs of deterioration that can be linked to irradiation, respecting the Italian WAC (10 MPa). Additionally, at least 70% of the initial strength is maintained after 90-days of leaching, still meeting the Italian WAC.

The Mercury Intrusive Porosimetry analyses highlighted a slight porosity increase after irradiation, as expected, and the average pore diameter is decreased. On the other hand, a more evident porosity increase was evidenced for leached samples. This result may explain the loss in terms of mechanical properties.

Finally, thirty freeze-thaw cycles between -40 and +40 °C, following the UNI 11193:2006 as requested by the Italian authority, were performed on both unirradiated and 200 kGy samples. After thermal cycles, a slight loss of mechanical property was evidenced, more evident for the irradiated sample. However, the Italian WAC is still met with satisfactory safety margin.

Radiation stability of reference MPC samples irradiated up to 500 kGy and subjected to leaching was confirmed. All the specimens respected the current Italian WACs for leaching, compression, and freeze-thaw resistance, without alarming signs of radiation-induced alterations. The reference MPC formulation is therefore a promising immobilisation matrix for RRMW. Further studies are required to investigate higher doses and new contaminants (e.g. actinides), as well as to test low-cost formulations.

4.4.4 Leaching behaviour of magnesium phosphate cement pastes

L. Diaz Caselles, C. Cau Dit Coumes, P. Antonucci, A. Rousselet (CEA, France), A. Mesbah (IRCELYON, France), V. Montouillout (CNRS, France), laura.DIAZCASELLES@cea.fr

This work focuses on understanding the leaching behaviour of MPC pastes using demineralized water as the leaching solution. To this end, various semi-dynamic leaching tests were performed for 28, 90 and 210 days. The chemical composition of the leachates was determined over time, and mineralogical and microscopic characterizations were performed on the solid before and after leaching to assess the degradation mechanisms. Reactive transport modelling was used to further elucidate the degradation mechanisms of the MPC paste samples. MPC paste samples were prepared using the reference formulation. The paste was cast into hermetic and cylindrical plastic containers, and placed in a controlled chamber at 20 °C and 95% RH to avoid desiccation. Samples were stored for six months until characterization and leaching. MPC paste was characterized by the presence of K-struvite ($MgKPO_4 \cdot 6H_2O$, 53.8%), MgO (1.8%), quartz (2.6%), mullite (8.2%) and amorphous content (33.6%). Quartz and mullite were present in FA. The amorphous content could include contributions from FA, but also from transient magnesium phosphate phases or poorly crystallized K-struvite. EDS analyses suggested that not only the formation of K-struvite took place during hydration but also the formation of at least one intermediate hydrate such as $Mg_2KH(PO_4)_2 \cdot 15H_2O$.

Figure 22 presents the evolution of cumulated leached concentrations of K, P, Mg and B at 7 for 28, 90 and 210 days of leaching as well as the cumulative HNO_3 concentration added by titration to the leaching solution. Data were obtained by experimental (circle markers) and modelling (dotted line) approaches. As a first modelling approach, fly ash was omitted and only K-struvite was considered as the main hydrate. The pore solution composition was defined based on experimental data and had a pH of approximately 8. The initial porosity of the matrix was set to 15.5% as experimentally determined. The effective diffusion D_e and the Archie's power coefficient α were adjusted to fit the cumulative release of Mg observed experimentally. In this first modelling approach, D_e and α were set at $4.5e^{-11} m^2/s$ and 2.0, respectively.

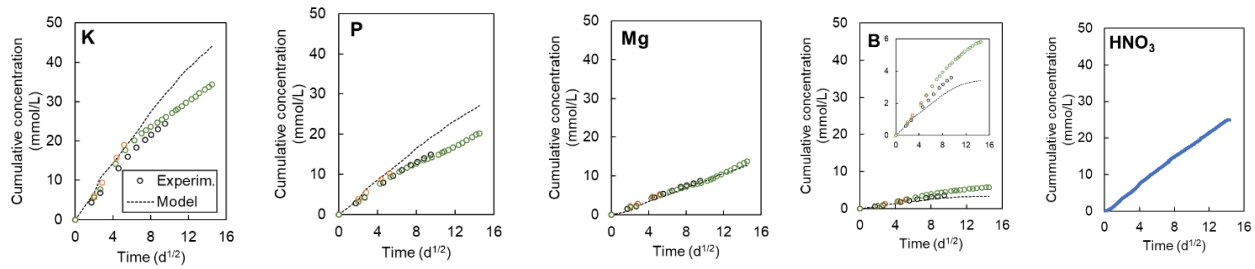


Figure 22. Evolution of the concentration of K, P, Mg and B and the cumulative HNO₃ concentration added by titration (in mmol/L). Data were plotted against the square root of time in days.

As shown in Figure , the immersion of the MPC paste into demineralized water (pH 7) induced a continuous leaching of the sample and thus, a gradual increase in the concentrations of K, P, Mg and B in the leachates. The cumulative concentrations showed a linear trend when plotted against the square root of time, meaning that the leaching rate was controlled by diffusion through the pore network. The leached fluxes decreased in the following order: K > P > Mg > B, meaning that leaching did not simply result from dissolution of K-struvite (MgKPO₄·6H₂O). A change in the slopes of the K and P curves occurred at approximately 40 days, possibly due to the exhaustion of soluble potassium brought by the FA. Since the leached fluxes of Mg²⁺ and OH⁻ remained constant, a decrease in the leached flux of K⁺ should result indeed in a decrease in the leached flux of HPO₄²⁻ to keep electrical balance. Predictions of K, P and B concentrations agreed with experimental data for the first 40 days of leaching. After this point, some discrepancies were observed, possibly because fly as was neglected in the model. Work is under way to improve the modelling.

Figure presents a SEM image and XRD patterns obtained at different depths of the 28 days leached solid. The MPC leached solid presented a zonation process, mainly characterized by three different regions:

- An irregular residual layer of about 200 μm thick all along the exposed surface, mainly composed of mullite and quartz, and exhibiting holes resulting from a mass loss,
- An intermediate zone comprised between 200 μm and approximately 1.5 mm, where cattite (Mg₃(PO₄)₂·22H₂O) precipitated as a secondary phase and coexisted with K-struvite,
- A sound core containing K-struvite, where cattite was not observed anymore.

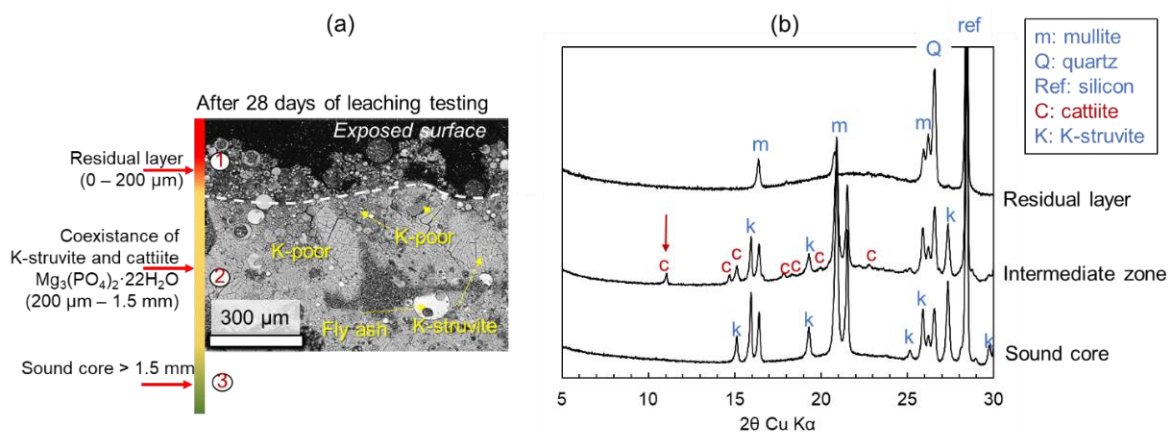


Figure 23. MPC paste section after 28 days of leaching (a) SEM image, and (b) XRD patterns obtained at different depths.

Figure 24 presents modelling results of the mineralogical changes in the leached MPC paste after 210 d of leaching. In agreement with the experimental results, the model predicted a retreat of the interface in contact with the leachant, the transient precipitation of cattite, and a porosity increase due to the dissolution of K-struvite retreat of interface in the MPC sample when in contact with the leaching solution. Nevertheless, the interface retreat was underestimated (0.5 mm instead of 2 mm observed experimentally), as well as the depth of the intermediate zone (0.6 mm, against approximately 1.5 mm observed experimentally).

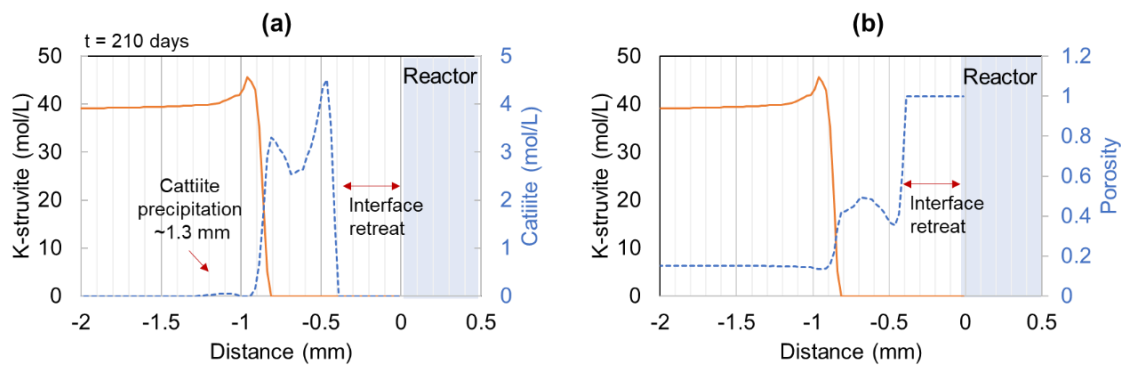


Figure 24. Modelling results of MPC leaching, (a) evolution of K-struvite and cattiiite, and (b) porosity within the sample.

The leaching behaviour of MPC was investigated for 28, 90 and 210 days using semi-dynamic leaching tests and demineralized water (pH 7) as the leaching solution. Chemical analyses of the leachates, recovered after each renewal, indicated that leaching was kinetically controlled by the diffusion of dissolved species through the pore network of the cement paste. The flux of dissolved K exceeded that of Mg and P by factors of 3.15 and 1.8, respectively during the first 40 days, which was explained by the transient precipitation of cattiiite, a K-free and Mg-rich phosphate phase ($\text{Mg}_3(\text{PO}_4)_2 \cdot 22\text{H}_2\text{O}$), and the release of K from fly ash. After 40 days, a change in the leached fluxes of K and P was noticed, possibly because of the exhaustion of soluble K from the fly ash. The basis of a reactive transport model has been set. The model describes fairly well the leaching phenomenology (mineralogical evolution, retreat of interface, released species), but still needs to be optimized to reproduce the extent of degradation observed at 210 days.

4.4.5 Al corrosion in magnesium phosphate cements

M. Cruz Alonso, C. Fernández (CSIC, Spain), mcalonso@ietcc.csic.es

M. Fulger, A. David, V. Lautaru (RATEN, Romania), manuela.fulger@nuclear.ro

J. L. Leganés (ENRESA, Spain), JLEN@enresa.es

The Al alloy corrosion risk is focused on three main objectives:

Al & AlMg passivation and corrosion related to H_2 evolution:

Studies on Simulated Pore Solutions (SPS) were performed by measuring the corrosion potential (E_{corr}) and Linear Polarization Resistance (LPR). RATEN studied the Al-Mg corrosion in MPC (reference formulation) and $\text{Ca}(\text{OH})_2$ saturated solution by comparing the volume of H_2 released from electrochemical and chemical methods. CSIC carried out studies in SPS of 7d hydrated 1 molar ratio M PC and $\text{Ca}(\text{OH})_2$ sat. for 150 d. The effect of borates and phosphates is also considered in MPC pore solution for Al and AlMg alloys. SPS considered are: borates: 500-200ppm, pH 8.5, phosphates: 10000-500ppm, pH 4.5, and phosphates + KOH, 6500ppm, pH 8.5, using electrochemical impedance spectroscopy (EIS) at 25d.

The main outputs are:

- Higher corrosion risk and hydrogen released was confirmed in OPC than in MPC SPS (Figure 25A).
- Borates content does not affect the E_{corr} but the corrosion current increases with the borate content and so the hydrogen evolution. The corrosion rate depends on the phosphate content: more anodic E_{corr} and lower I_{corr} for higher phosphate content. In absent of phosphate (KOH) more cathodic E_{corr} and higher corrosion current were measured in the initial stage. The inhibition effect of phosphates is confirmed (Figure 25B). The mechanism of the inhibition is under study by fitting the EIS data with equivalent circuit.
- Borate and phosphate concentration influence the Al passivation process resulting in different EIS responses.

1. Influence of M/P molar ratio in Al alloy corrosion:

CSIC prepared MPC mortars with 1, 2, 3M M/P cured at 100%RH for 90d. Corrosion risk and H_2 evolution was obtained by LPR and E_{corr} measurements. More cathodic E_{corr} are initially observed with higher M/P ratio associated to the higher pH and lower phosphate content in the pore solution. The corrosion densities increase

at short-term for 2 and 3 M/P molar ratio that approach after 40 days for all cases. The phosphates and magnesium content in the pores affect the H₂ released.

2. Long-term corrosion behaviour in MKPC & OPC binders:

MPC and OPC mortars were considered. ENRESA studied Al corrosion in El Cabril mortar for 200d. CSIC studied by electrochemistry Al and AlMg corrosion in 1M MPC, CEM I, CEM IV and CEM I+SF mortars, first exposed under water for 300 d and then immersion in alkaline water for 250 d. Physical-chemical stability of the matrices and the interaction of metal/matrix interface was evaluated at the end of the test. Microstructure was characterized using XRD and MIP, and the metal-matrix interface with SEM/BDX.

The main outputs are:

- Corrosion of Al in El Cabril mortar significantly decreases with time showing lower corrosion that in alkaline SPS (Figure 25C). The formation of an Al₂O₃ layer is confirmed by SEM (Figure 25E).
- After 300 d water immersion the MPC mortar shows a lower corrosion (lower *i*_{corr} and more anodic *E*_{corr}) than in Portland. A leaching of phosphates on MPC with increase of pH from 7 to 9 is appreciated. The CEM I+SF pore pH also decreases close to 10 with decrease in the *i*_{corr} more that CEM I and CEM IV that remain more alkaline (pH>12.7). In the alkaline water immersion, the MPC pore increases the pH to 10, remaining constant in OPC systems.
- The alkaline media interaction confirmed the corrosion risk and H₂ reactivation (Figure 25D). Less hydrogen is estimated to be released in CEM I+SF followed by MPC as better alternatives matrices to OPC for Al alloy immobilization.
- Evolution in capillary pores exist and K-struvite in MPC and Portlandite and Ettringite in OPC were identified. The SEM-BS confirmed the formation of Al oxide layer in all OPC matrices that is not appreciated in MPC. Besides, Al release during corrosion process penetrates in the cement paste of OPC, as well as precipitating as ettringite (Figure 25F).

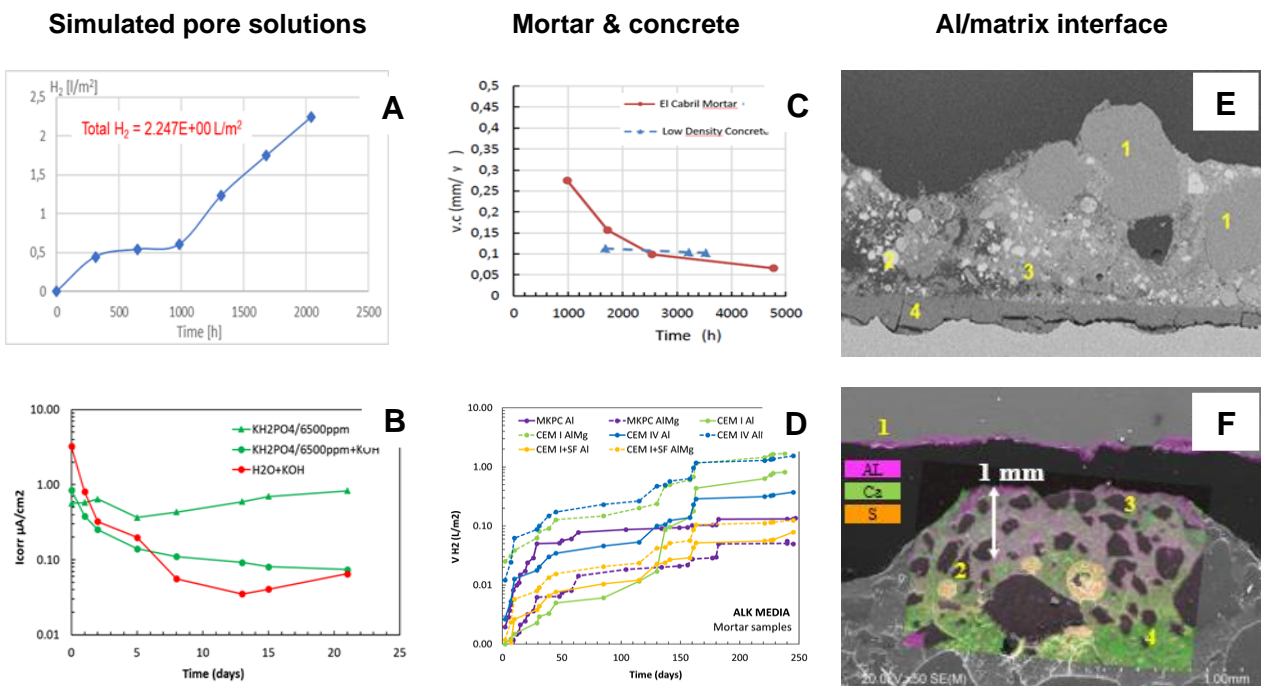


Figure 25. A) Volume of H₂ generated of AIMg in MKPC/SPS (RATEN). B) Corrosion kinetic of P-6500ppm with and without KOH (CSIC). C) Corrosion kinetic in El Cabril mortar (ENRESA). D) Volume of H₂ gas generated of Al and AlMg alloy in MKPC and OPC mortars in immersed in alkaline water (CSIC). E) Al₂O₃ oxide layer in Al/El Cabril mortar interface (ENRESA). F) Al/OPC mortar interface Al oxide layer, Al enrichment in cement paste and ettringite formation (CSIC).

4.4.6 Steel corrosion in magnesium phosphate cements

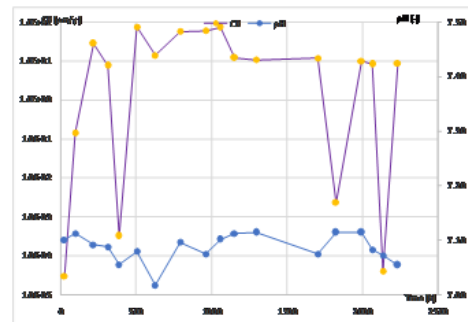
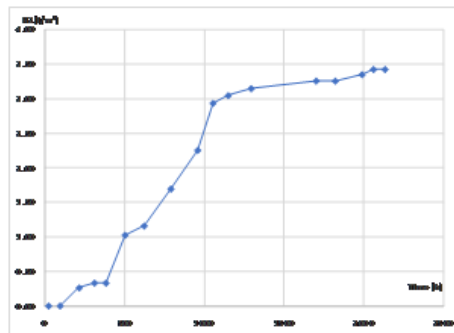
A. David, L. Lautaru, M. Fulger, C. Bucur (RATEN), crina.bucur@nuclear.ro
 K. Le, S. Delpech, D. Rodrigues, C. Cannes (CNRS), kim.le@ijclab.in2p3.fr

As usually the carbon steel is the material used for primary waste packages, the reactivity of steel in chemical conditions characteristic for the MPC matrices is studied, for two types of carbon steel: DC01 (material of the primary package in Romania) and S235JR (material of the primary package in France).

The DC01 steel corrosion was studied by RATEN under chemical conditions characteristic for the porewater of the reference MPC matrix with the MgO/KH₂PO₄ molar ratio of 1 and pH_{25°C}= 7.11 and in saturated portlandite water with pH_{25°C}= 12.6, as relevant for the OPC porewater. Two types of tests were performed: electrochemical tests (linear polarization – LPR) to measure the corrosion rate and chemical tests in which the H₂ generated by corrosion was collected and measured. For the chemical tests, the H₂ pressure was measured using a high-resolution barometer. The normalized H₂ volume was used to calculate the corrosion rate. For the electrochemical tests the parameters measured by LPR were used to estimate the volume of H₂ generated by corrosion ($V = (M_{\text{loss}} \times R \times T / P) / S$). For the chemical tests, the normalized volume of H₂ was used to estimate the mass loss ($m_{\text{loss}} = M_{\text{Fe}} \times V_{\text{H}_2 \text{ measured}} / V_0$) and the corrosion rate.

The results obtained for the MPC porewater are summarized in Figure 26. Similar values for the H₂ volume generated by DC01 steel corrosion was obtained by the two types of tests: ~ 3L/m² measured from the chemical tests (after 85 d) and 3.6 L/m² estimated based on the LPR results (after 94 d). For saturated portlandite water the H₂ volume generated by corrosion is one order of magnitude lower than in the MPC porewater (0.2 L/m² measured from chemical tests and 0.3 L/m² estimated based on LPR results).

LPR tests



Chem. tests

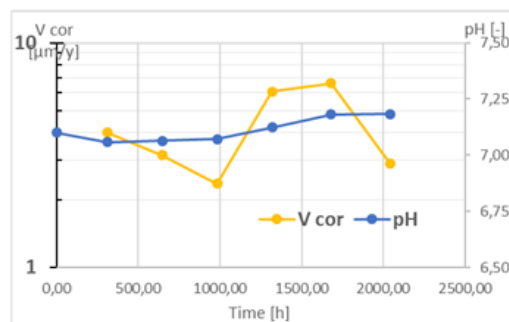
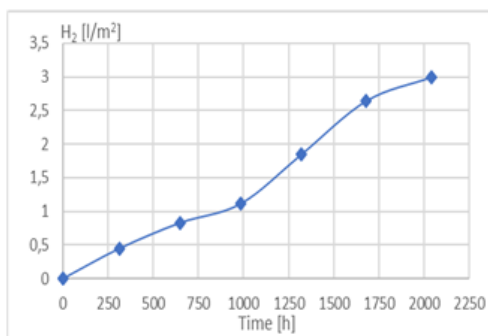


Figure 26. The evolution of H₂, corrosion rate and pH during the LPR and chemical tests on DC01 steel.

For the S235JR steel, CNRS assessed its behaviour in a low cost MPC formulation based on reactive MgO and KH₂PO₄, with Mg/P molar ratio of 1 and thiosulfate (5wt% / cement) as a set retarder, compared to the MPC reference formulation in which boric acid is used as retarder. Impedance measurements were first performed on Pt electrode to be able to discriminate from the contribution of LC-MPC to electrochemical impedance. In contrast to the typical capacitive behaviour seen on Pt in reference MPC formulations, in LC-MPC a unique capacitive loop on the Nyquist diagrams recorded on Pt was observed (Figure 27). This loop is likely characteristic of a charge transfer phenomenon. The potential of Pt electrode is fixed by a redox system (certainly thiosulfate) and the presence of an electroactive species in the medium is also indicated by the increase in the charge transfer loop over time.

After 45 days, S235JR steel has the same behaviour as an inert metal in the reference MPC (Figure 28) while it seems to be more corroded in LC-MPC than in MPC as the magnitude of impedance in the reference MPC

($3.5 \times 10^5 \text{ Ohm.cm}^2$) is higher than in LC-MPC ($3.5 \times 10^4 \text{ Ohm.cm}^2$). However, in LC-MPC, impedance seems to increase slowly from day 1 to day 45. The electrochemical tests will be continued to evaluate the steel behaviour in the proposed formulation for LC-MPC.

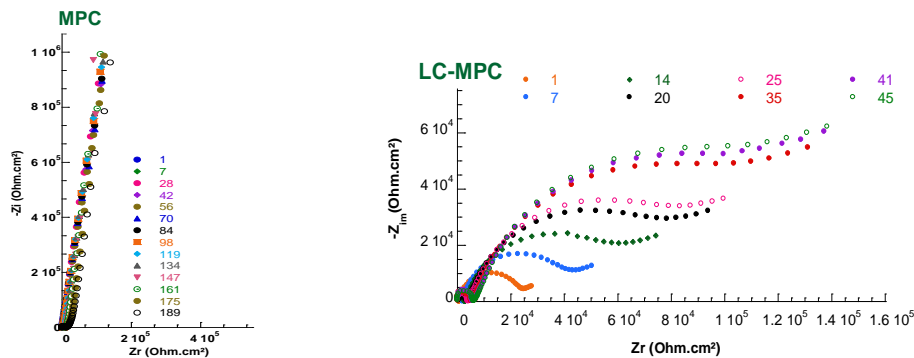


Figure 27. Nyquist diagrams recorded on Pt in reference MPC formulation (left) and in the LC-MPC (right).

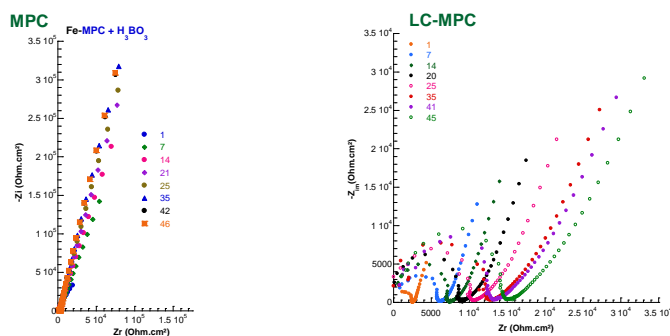


Figure 28. Nyquist diagrams recorded on steel in reference MPC formulation (left) and in the LC-MPC (right).

Corrosion tests in solution with boric acid and thiosulfate (pH 7.2) showed that after 17 d of immersion the boric acid protects the steel while the thiosulfate solution doesn't inhibit it and a black layer was formed on the steel surface, possibly identified as FeS [7]. To gain a comprehensive understanding of the impact of thiosulfate on steel corrosion, further electrochemical tests will be performed complemented with analysis of the metal surface, analysis of the solution and measurement of the pH evolution. Furthermore, the corrosion behaviour of steel will be examined in the LC-MPC formulation containing boric acid.

4.4.7 Be corrosion in magnesium phosphate cements

S. Caes, V. de Souza, B. Kursten (SCK CEN, Belgium), sebastien.caes@sckcen.be
 A. Bukaemskiy, G. Deissmann, G. Modolo (FZJ, Deutschland), a.bukaemskiy@fz-juelich.dea

The beryllium corrosion was studied in solution (simulated MPC and OPC pore media and NaOH solutions) and in contact with OPC and MPC matrices. In high pH solutions, the corrosion rate calculated by H_2 measurement and ICP-MS at SCK CEN, and by gravimetry and ICP-MS at FZJ are comparable. For OPC pore solution the H_2 measurement revealed a decrease of the corrosion rate with time to reach a steady state at $1.8 \mu\text{m/y}$ after one year. Tests performed in simulated MPC pore media (pH 8) revealed a higher corrosion rate (around $12 \mu\text{m/y}$) which is relatively constant during the first 120 days of the test (Figure 29). Electrochemical impedance spectroscopy (EIS) revealed the same trend. However, an optimisation of the method is still needed to quantify the corrosion rate. When beryllium samples are embedded in cement pastes, the corrosion rate is lower than in solution, probably due to the mass transfer limitation, and reach an initial value lower than $2 \mu\text{m/y}$. This corrosion rate decreases further during the curing period (28 days) in humid atmosphere, and later, when a dry atmosphere is set up. At that moment, the corrosion rate is equal or lower than $0.1 \mu\text{m/y}$. Finally, after resaturation of the cement pastes by adding the corresponding simulated cement pore media, the corrosion rate in OPC directly increased up to $2.6 \mu\text{m/y}$ before to decrease again to $0.6 \mu\text{m/y}$, while the corrosion rate in MPC remains low until 4 days after immersion (Figure 30). Finally, scanning electron microscopy was made to observe the surface of the samples before and after the corrosion tests. All unaltered samples possess some stripes and defects due to the sawing process used to prepare the samples, as well as intermetallic impurities. After immersion of the beryllium samples in high pH solutions (OPC pore media (pH 13.5; 1 year) or NaOH (pH 13.95; 30 days)), pitting corrosion is observed with small and large pits (Figure 31).

The pit size distribution possesses a logarithmic normal distribution for both small and large pits, indicating that their growth occurs due to their agglomeration.

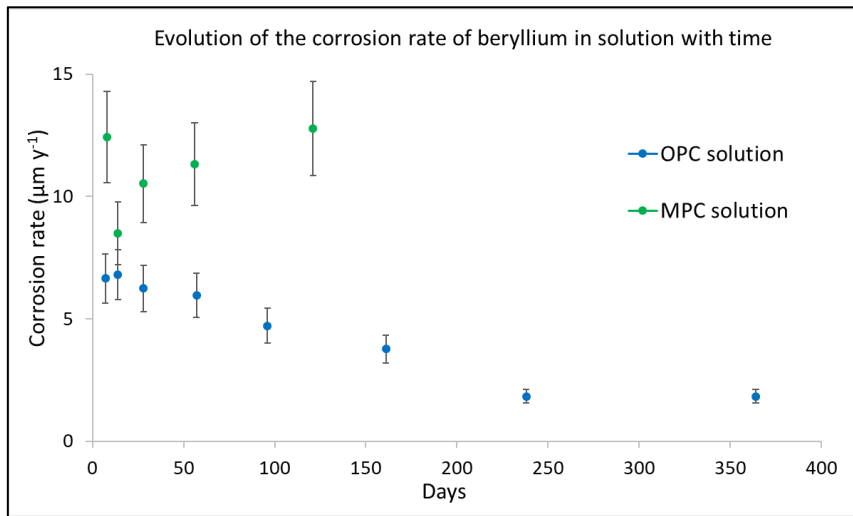


Figure 29. Evolution of the Be corrosion rate in solution with time.

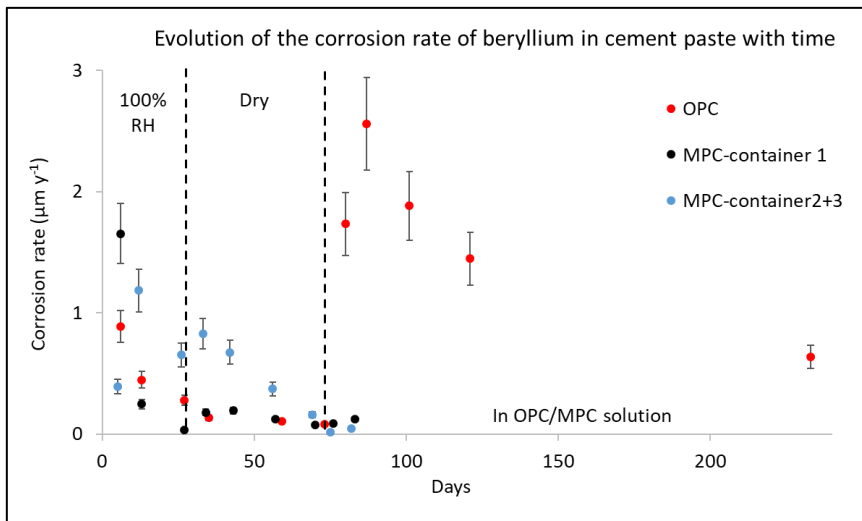


Figure 30. Evolution of the corrosion rate of Be embedded in cement paste with time.

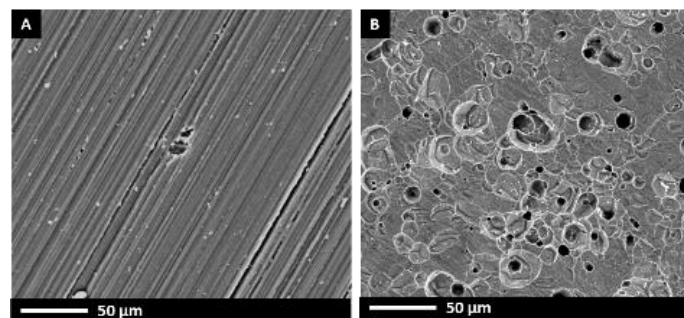


Figure 31. Surface of the Be sample (A) before corrosion and (B) after 30 days in NaOH solution at pH 13.95.

Acknowledgements

The author thanks Gammatom S.r.l. for the support to irradiation.

References

- [1] Chartier, D., Sanchez-Canet, J., Antonucci, P., Esnouf, S., Renault, J-P., Farcy, O., Lambertin, D., Parraud, S., Lamotte, H. and Coumes, C. *Cau Dit. J. Nucl. Mater.* 541 (2020) 152411.
- [2] E. Yurdakul, "Optimizing Concrete Mixtures with Minimum Cement Content for Performance and Sustainability", Iowa State University, 2010.
- [3] Bykov, G.L., Abkhalimov, E.V., Ershov, V.A. and Ershov, B.G. *Radiation Physics and Chemistry* 190 (2022) 109822.
- [4] Gardner, L. J., Bernal, S. A., Walling, S. A., Corkhill, C. L., Provis, J. L. and Hyatt, N. C. *Cement and Concrete Research* 74 (2015) 78.
- [5] Xu, Biwan, Ma, Hongyan, Shao, Hongyu, Li, Zongjin and Lothenbach, Barbara. *Cement and Concrete Research* Vol. 99 (2017) 86.
- [6] ANS. "Measurement of the leachability of solidified low level radioactive wastes by a short-term test procedure." Technical Report No. ANS/ANS-16.1. American Nuclear Society, La Grange Park, IL. 2003.
- [7] L. Choudhary, Digby Macdonald, A. Alfantazi, *Corrosion* 71. 150602132136005. 10.5006/1709, 2015.

5 Scientific progress Innovations in liquid organic waste treatment and conditioning (WP5)

5.1 Geopolymer cements for the immobilisation of radioactive liquid organic wastes

J. McWilliams*¹, B. Walkley², J. L. Provis¹

¹Department of Material Science and Engineering, University of Sheffield, United Kingdom

(E-mail jmcwilliams1@sheffield.ac.uk, j.provis@sheffield.ac.uk)

²Department of Chemical Engineering, University of Sheffield, United Kingdom

(Email: b.walkley@sheffield.ac.uk)

Keywords: Geopolymers, Radioactive waste, Tributyl phosphate (TBP), Dodecane, Nevastane

1. Introduction

Pickering emulsion with fumed silica has been investigated as a potential immobilisation route for liquid organic oils. The potassium geopolymers developed were based on a NNL (National Nuclear Laboratory) formulation with 1 wt% of fumed silica and 10/20/30/40 wt% of either TBP (tributyl phosphate)/Dodecane or Nevastane. The initial observation highlights a clear difference in the immobilisation of the two oils. The Nevastane appeared to be immobilised successfully whilst TBP/Dodecane separated from the potassium geopolymer matrix. This separation was found to get worse with an increasing weight percentage of the TBP/Dodecane with a significant quantity of the oil sitting above the cement, For Nevastane, when the weight percentage was increased from 10 to 30 wt%, there was an increase in the viscosity of the sample; 30 wt% Nevastane was the most viscous of all the samples made and was difficult to pour. Further characterisation will be vital to understand the nature of these samples and how they interact with the oil.

2. Description of work and main findings

This work has investigated creating Pickering emulsions with silica fume (1 wt%) with TBP/Dodecane and Nevastane at 10, 20, 30 and 40 %wt at the three NNL (National Nuclear Laboratories) formulations, Table 3. For the pre-leaching samples, FTIR, XRD and SEM-EDX will be conducted for samples at seven, 28 and 90 days, and compressive strength and rheology determined. The 28-day cured samples are immersed in deionised water for the leaching test, with regular replacement of the deionised water. Work is ongoing to compare GC-MS, TOC and UV-Vis as potential techniques to analyse the leached solutions.

Table 3. The three NNL formulations adopted in this work.

| Metakaolin | Activator SiO ₂ /K ₂ O | Bulk H ₂ O/K ₂ O | Bulk K ₂ O/Al ₂ O |
|------------|--|--|---|
| Metamax | 1 | 11 | 1 |
| Metamax | 1.2 | 13 | 1.2 |
| Metamax | 1 | 15 | 1 |

Results

Samples of Metamax potassium geopolymers of the NNL formulation 1.2/13/1.2 were prepared. From the initial observation of the preparation process, it was observed that at 10 wt% TBP/Dodecane there was a layer of liquid above the cement. It is likely that a quantity of oil was not incorporated in the geopolymer matrix and separated due to the unfavorability of the O/W emulsion. When the weight fraction of TBP/Dodecane was increased from 10 wt% to 40 wt%, there is a clear separation of the liquids with a significant quantity of the oil sitting above the cement. This suggests that the silica fume was not successful in aiding the immobilisation of the TBP/Dodecane by Pickering emulsion. There is a clear difference between the immobilisation of Nevastane and TBP/Dodecane within the potassium geopolymer. From initial observation, Nevastane looks to be immobilised successfully with the geopolymer matrix, whilst the TBP/Dodecane has separated from the matrix,

and more so at higher oil loading. Further characterisation will be vital to understand the nature of these samples and how they interact with the oil.

3. Conclusions and way forward

Further experimental work is required to further understand the effects of the Pickering emulsion on the organic oils.

Acknowledgements

The authors would like to express appreciation for the financial support of PREDIS project and the EPSRC GREEN CDT, and the constant support of colleagues in the Cements@Sheffield team.

5.2 Robustness tests for immobilization of oils in alkali activated slag

Thi Nhan Nguyen^{1,3*}, Lander Frederickx¹, Mejdí Neji², Alexandre Dauzères², Quoc Tri Phung^{1**}

¹Institute for Environment, Health, and Safety, Belgian Nuclear Research Centre (SCK CEN), 2400 Mol, Belgium

²Institute of Radiation protection and Nuclear Safety (IRSN), 92260 Fontenay-aux-Roses, France

³Department of Materials Engineering, KU Leuven, 3001 Leuven, Belgium

[*thi.nhan.nguyen@sckcen.be](mailto:thi.nhan.nguyen@sckcen.be), [**quoc.tri.phung@sckcen.be](mailto:quoc.tri.phung@sckcen.be)

Keywords: alkali activated slag, mineral oils, immobilization, organic liquid waste, robustness tests

1. Introduction

Lubricating oils, TBP, dodecane, and other radioactive liquid wastes produced by nuclear power reactors are frequently contaminated with hazardous radionuclides (such as ⁶⁰Co and ¹³⁷Cs). These types of waste are frequently encapsulated for final disposal to prevent and delay the leakage of these radionuclides into the environment [1]. Due to its low cost of consumption, ordinary Portland cement (OPC) is one of the most popular matrices [2]. OPC, however, is ineffective at capturing the oily wastes. When using indirect mixing techniques, such as absorbents, the OPC appears to function with lubricating oils but not with organic substances, such as hydrocarbons [3]. However, it was shown that adding merely 10 wt.% of mineral oil or crude oil to waste forms with OPC significantly reduced their compressive strength, falling by 75% and 50%, respectively. Once more, immobilizing organic liquid molecules would not be a good use for OPC as a matrix.

Alkali-activated materials (AAMs) or geopolymers, as opposed to OPC, have demonstrated a great capacity for integrating oily wastes. A potential encapsulation of up to 70% vol.% of lubricating oil in metakaolin-based geopolymer was reported by Lambertin et al. [4]. Although the reduction is less than that of OPC, the addition of oil also weakens the compressive strength. According to Cantarel et al. [5], if the waste forms contain 20% oil, the compressive strength will fall by 35% in comparison to MK-based geopolymers without oil. When less oil is loaded (14 vol.%), the strength loss is likewise less noticeable (12.5%). To determine whether the waste forms are appropriate, it is also necessary to study and evaluate other aspects of them, such as setting time, heat release, workability, and so forth, in addition to their mechanical strength. Notably, these qualities depend on a number of additional elements in addition to the waste loading. In order to create the best waste-form design, a huge number of investigations may be necessary.

This study carried out robustness tests with 14 recipes that cover the impact of key parameters on the fresh properties and mechanical strength of the waste-forms in the context of optimizing waste-form recipes between lubricating oils and alkali activated slag (AAS), which has been lacking in information in the application of liquid waste immobilization.

2. Description of work and main findings

Robustness tests

AASs were made from granulated blast furnace slag (GGBFS) and activating solutions (produced from solid NaOH pellets, solid sodium disilicate, and water). The AAS slurries were mixed with Nevastane EP 100 (NEV) and Shellspirax (SHE) oils using tween 80 as a non-ionic surfactant. Then, river sand with a particle size smaller than 2 mm as an aggregate was added. Details of robustness design are shown in Table 4. The waste-forms were then tested for their fresh properties, including setting time, heat release, and workability; and mechanical strengths after 28-day curing in sealed condition at 20 °C.

Table 4. Robustness design of waste-forms between AASs and lubricating oils.

| Sample ID | SS | NH | WB | WL, vol. % | SF, wt. % | Oil type |
|-----------|------|-----|------|------------|-----------|----------|
| DoE 1 | 2.79 | 4.2 | 0.45 | 30 | 3 | NEV |
| DoE 2 | 2.59 | 4 | 0.35 | 30 | 5 | NEV |
| DoE 3 | 2.59 | 4.2 | 0.35 | 25 | 3 | SHE |
| DoE 4 | 2.69 | 4 | 0.45 | 25 | 4 | SHE |
| DoE 5 | 2.79 | 3.8 | 0.35 | 30 | 4 | SHE |
| DoE 6 | 2.59 | 4.2 | 0.55 | 20 | 4 | NEV |
| DoE 7 | 2.69 | 3.8 | 0.35 | 20 | 3 | NEV |
| DoE 8 | 2.59 | 3.8 | 0.55 | 30 | 3 | SHE |
| DoE 9 | 2.69 | 4.2 | 0.55 | 30 | 5 | SHE |
| DoE 10 | 2.69 | 4 | 0.45 | 25 | 4 | NEV |
| DoE 11 | 2.79 | 3.8 | 0.55 | 25 | 5 | NEV |
| DoE 12 | 2.59 | 3.8 | 0.45 | 20 | 5 | SHE |
| DoE 13 | 2.79 | 4 | 0.55 | 20 | 3 | SHE |
| DoE 14 | 2.79 | 4.2 | 0.35 | 20 | 5 | NEV |

SS and NH: sodium silicate and NaOH (wt.%, per 100 g GGBFS), respectively

WB: w/b ratio

WL: waste loading (vol.%, volume of oil per total volume of waste-form)

SF: surfactant Tween 80, (wt.%, per mass of oil)

Results

AASs showed as an outstanding candidate for oil immobilization. Most recipes observed a relatively homogeneous slurry with good viscosity during mixing, except for a slight separation in DoE 11 (Figure 32). SHE seemed to incorporate easier in AAS matrices than NEV, potentially due to a slight higher viscosity of this oil. The Vicat tests provided information about the setting time of all mixtures which was significantly longer than AASs without oils. This was consistent with the delay of geopolymerization in the waste-forms as indicated by their heat release results. Notably, the setting was influenced mainly by the w/b ratio and much less by the other factors, with the final setting time being lower than 8h, ~15h and ~25h for waste-forms with w/b ratios of 0.35, 0.45, and 0.55, respectively.

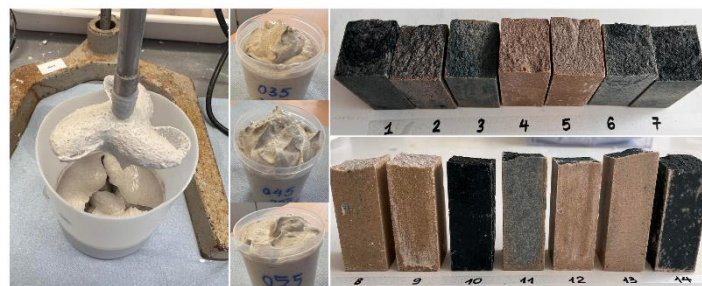


Figure 32. Waste-form slurries and 28-day cured specimens of 14 formulations of waste-forms between AASs and oils

Although SHE was profound in workability, the waste-forms with NEV presented higher mechanical strength than the ones with SHE at a similarity of other designed parameters (Figure 33-left). In general, both the flexural and compressive strengths of most of the recipes met the Belgium acceptance criteria (2 MPa and 8 MPa for flexural and compressive strengths, respectively). In addition to the type of oils, the strengths were also affected by other parameters, in which the w/b ratio and waste loading were very important. To have a better understanding to what extent the effect of these factors on the strengths, factorial analysis was applied and, it was found that the waste-form obtained from AAS with 0.35 w/b ratio, 20 vol.% NEV, and 4 wt.% tween 80 can allow for optimal flexural and compressive strengths.

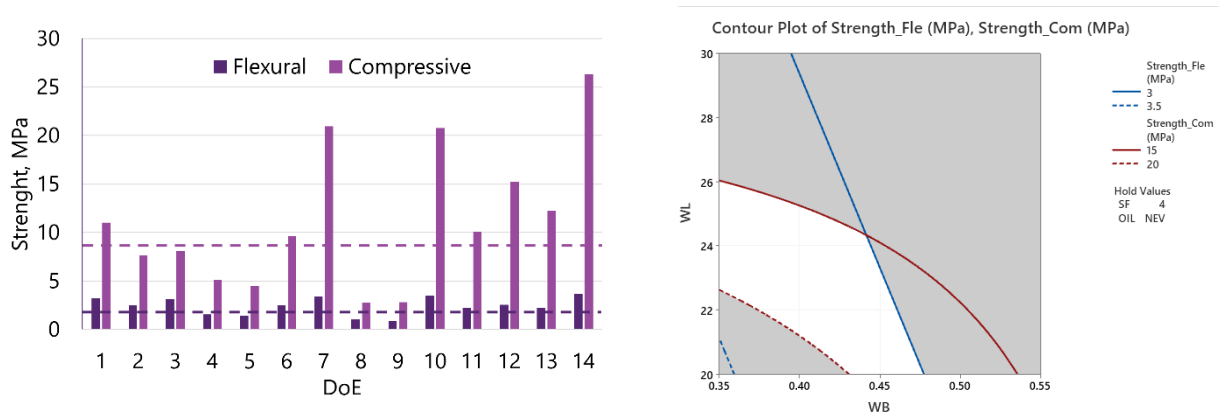


Figure 33. The 28-day mechanical strength of 14 recipes (left) and factorial analysis for optimal strengths (right) of waste-forms.

3. Conclusions

Both NEV and SHE oils can be well immobilized in AASs using a very small amount of tween 80 as a surfactant. Up to 30 vol.% oil can be encapsulated in the matrices, and almost all of obtained waste-forms achieved mechanical strengths higher than the acceptance criteria values. The waste-forms also presented good fresh properties, implying the applicable capacities of these recipes. Notably, the robustness tests indicated w/b ratio, waste loading, and type of oil as three important parameters affecting significantly the strength of waste-forms, in which AAS with the w/b ratio of 0.35 containing 20 vol.% NEV oil can allow to achieve an optimal flexural and compressive strength.

Acknowledgements

This work has received funding (in parts) from the Belgian Energy Transition Fund (ASOF project), IRSN (France), and the PREDIS project.

References

1. Cuccia, V., C.B. Freire, and A.C.Q. Ladeira, *Radwaste oil immobilization in geopolymer after non-destructive treatment*. Progress in Nuclear Energy, 2020. **122**.
2. Phung, Q.T., N. Maes, and D. Jacques, *Current concerns on durability of concrete used in nuclear power plants and radioactive waste repositories*, in *Proceedings of the 4th Congrès International de Géotechnique – Ouvrages -Structures, Lecture Notes in Civil Engineering 8*, H.-H. Tran-Nguyen, et al., Editors. 2018, Springer Nature Singapore: Singapore. p. 1108–1121.
3. Reeb, C., et al., *Incorporation of organic liquids into geopolymer materials – A review of processing, properties and applications*. Ceramics International, 2021. **47**(6): p. 7369–7385.
4. Lambertin, D., A. ROOSES, and F. Frizon, *Process for preparing a composite material from an organic liquid and resulting material*. 2014, Google Patents.
5. Cantarel, V., et al., *Solidification/stabilisation of liquid oil waste in metakaolin-based geopolymer*. Journal of Nuclear Materials, 2015. **464**: p. 16–19.

5.3 Robustness tests and optimization of BFS based geopolymers (Task 5.3)

Crina Bucur, Carmen Manolescu, Ionut Florea

Institute for Nuclear Research Pitesti (RATEN ICN), Romania

e-mail of main contact: crina.bucur@nuclear.ro <mailto:pancotti@sogin.it>

Keywords: Radioactive Liquid Organic Waste, direct conditioning, geopolymer, blast furnace slag

1. Introduction

Conditioning matrices based on ordinary Portland cement (OPC) are the most used in the radioactive waste conditioning but there are some so called problematic radioactive waste, including different categories of Radioactive Liquid Organic Waste (RLOW), that can not be incorporated in OPC based matrices or the waste loading in OPC based matrices is too low. Different geopolymer matrices are studied under PREDIS WP5 for direct conditioning of RLOW. In RATEN ICN, the oil waste and liquid scintillation cocktails are conditioned in a quick setting mixed binder system, based on Portland composite cement type CEM II/A-M(S-LL) 32,5 R and calcium aluminate cement type GORKAL 70 [1]. To increase the waste loading and consequently decrease the volume of the conditioned radioactive waste that need to be disposed of, geopolymer matrices based on granulated blast furnace slag (BFS) and volcanic tuff are investigated in RATEN ICN under PREDIS WP5 for RLOW conditioning.

The work performed in RATEN ICN and reported during this annual workshop focuses on the robustness of the reference formulation based on Ecocem BFS developed by SCK CEN (reference formulation #2 developed under Task 5.3.2), to study the impact of RLOW type, raw materials and process variability. In the previous tests on geopolymer formulation performed in RATEN ICN under Task 5.3.2, BFS from Liberty Steel Galati (Romania) was used together with Romanian volcanic tuff from Barsana as aluminosilicate precursors and a mixture of commercial Na₂SiO₃ solution and 8M NaOH as alkaline activation solution. As the tests performed to reproduce/optimize the reference formulation with Romanian BFS didn't give satisfactory results a BFS received from CEA (produced by Ecocem) was also used in the tests performed in RATEN ICN.

2. Description of work and main findings

The RLOW considered for the robustness tests consists in pump oil (Shellspirax S2A80W90) and liquid scintillation cocktail (UltimaGold AB and XR), for loading rates ranging between 10 wt.% and 20 wt.%. Two types of BFS were used: Romanian BFS produced by Liberty Steel Galati (not commercially available and received directly from the producer) and an Ecocem BFS received from CEA, whose oxide compositions are reported in Table 5.

Table 5. Main oxide content in Romanian BFS and in the BFS used in the reference formulation tested and the BFS received from CEA.

| wt.% | BFS in the reference formulation | RO_BFS (3) | Ecocem_CEA |
|---|----------------------------------|------------|------------|
| CaO | 43.4 | 41.60 | 42.7 |
| SiO ₂ | 32.4 | 38.20 | 36.7 |
| Al ₂ O ₃ | 11.1 | 9.20 | 11.3 |
| MgO | 7.77 | 7.50 | 7 |
| Fe ₂ O ₃ | 0.6 | 0.55 | 0.6 |
| Na ₂ O | 0.27 | 0.30 | 0.7 |
| SO ₃ | 2.41 | 0.32 | 0.2 |
| (CaO+MgO)/SiO ₂ | 1.58 | 1.29 | 1.35 |
| CaO/SiO ₂ | 1.34 | 1.09 | 1.16 |
| Al ₂ O ₃ /SiO ₂ | 0.34 | 0.24 | 0.31 |
| (CaO+MgO)/(SiO ₂ +Al ₂ O ₃) | 1.18 | 1.04 | 1.04 |

The fresh mortars were analysed regarding the setting time and bleeding while for the hardened mortar mechanical strength was measured. The mortar compositions tested are summarized in Table 6.

Table 6. Geopolymer composition tested.

| Mortar composition | Wt.% |
|----------------------------------|------------------------|
| BFS | 36.4–46.0 |
| Na ₂ SiO ₃ | 1.2–4.7 |
| NaOH (10M) | 5.2–10.1 |
| Additional water | 6.9–15.2 |
| Sand | 23.3–25.0 |
| oil | 10.0–20.0 |
| Tween 80 | 5% of the waste volume |
| scintillator | 8.0–20.0 |
| W/B | 0.35–0.45 |

All the geopolymer formulations obtained with Romanian BFS had good workability and normal fluidity composition for waste loading rates of up to 15%wt. for oil waste and up to 9%wt. for liquid scintillator, with setting times < 24 hours. After 24 days of curing at room temperature, protected in plastic bags, the mortars with 15%wt. oil incorporated developed a mechanical strength between 5 MPa and 6 MPa, at the limit imposed in Romania for WAC (5MPa).

The geopolymer mortars obtained with the Ecocem BFS received from CEA had better rheological properties for waste loading rates of up to 19%wt. for oil waste and up to 10%wt. for liquid scintillation cocktail, with mechanical strength after 24 days of curing (for oil waste forms) between 5 MPa and 14 MPa.

For the formulations tested with liquid scintillation cocktail, due to the limited amount of BFS available only small specimens were produced to test the properties of fresh mortars.

The optimum formulation obtained in our laboratory for oil incorporation in geopolymer based on BFS, for both types of BFS investigated is the following:

| | |
|--------------------------------------|---|
| BFS (Ecocem / Ro_BFS) | 42.9 wt.% |
| Na₂SiO₃ | 4.4 wt.% |
| NaOH 10M | 8.6 wt.% |
| Additional water | 7.5 wt.% |
| Sand | 23.3 wt.% |
| oil | 30 vol.% |
| Tween 80 | 5% of the oil volume |
| W/B | 0.35 |
| Mechanical strength | 14 MPa – for Ecocem BFS received from CEA |
| | 6 MPa – for Ro BFS |

For mechanical strength measurements on mortars with liquid scintillation cocktail incorporated a new batch of BFS received from SCK CEN will be used in the tests that will be further carried out.

3. Conclusions and way forward

As it can be seen in Table 6, the Romanian BFS has an oxide composition similar with the BFS used in SCK CEN for the reference formulation #2 and with BFS received from CEA, with slightly lower calcium oxide and alumina and a higher silica content compared with the one used in the reference formulation. But a major

difference among the Romanian BFS and the BFS received from CEA and the BFS used for the reference formulation #2 (both commercially available and produced by Ecocem) is the finesse of the BFS particles. The Romanian BFS is not commercially available and was obtained directly from the Liberty Steel Galati in form of a powder with coarser particles that required grinding and sieving. The finest powder that we were able to obtain using a laboratory ball mill was particles with dimensions up to 75 μ m, significant coarser than the commercially available BFS.

Supplementary optimization tests will be performed for liquid scintillation cocktail incorporation in geopolymer based on BFS using a slag received from SCK CEN.

5.4 Encapsulation of Nevastane oil and TBP/Dodecane using the mix formulation (KIPT formulation) (Task 5.3)

Abdelaziz HASNAOUI, CEA, France, abdelaziz.hasnaoui@cea.fr

Abstract

The work presented during this annual workshop focuses on the encapsulation of radioactive liquid organic wastes (RLOW) using the mix formulation developed by KIPT. Two types of organic liquids, namely Nevastane EP100 and 30/70 TBP/Dodecane, were subjected to testing with varying loading rates ranging from 30 to 50% of the total mixture volume. Additionally, three different surfactants were evaluated to enhance/ensure the emulsification process. A key aspect of the investigation was dedicated to analysing the rheological behaviour of the emulsions and examining the size and distribution of the organic liquid droplets within the geopolymer matrix. The results obtained from the experiments allowed for the identification of an appropriate surfactant for the mix formulation, thereby validating its suitability for the encapsulation process. Furthermore, the microstructural properties of the hardened emulsions were thoroughly characterized and assessed. In summary, this study demonstrates the successful application of the KIPT-developed mix formulation for encapsulating radioactive liquid organic wastes.

Keywords: direct conditioning, radioactive liquid organic wastes (RLOW), geopolymer, surfactant, mix formulation

1. Main Findings

The results obtained from the conducted experiments provide valuable insights into the encapsulation process using the KIPT Formulation. It was determined that up to 30% of Nevastane could be successfully incorporated into the formulation without the need for a surfactant. However, for higher incorporation rates or when dealing with low viscosity liquids such as TBP and Dodecane, the use of a surfactant became necessary, as demonstrated in *Figure 34*.

In this study, the efficiency of the Glucocon surfactant in the KIPT Formulation was examined, revealing its remarkable effectiveness in both emulsification and ensuring the stability of the composite. The rapid setting of the KIPT formulation played a crucial role in maintaining the composite's stability. These findings highlight the significance of selecting an appropriate surfactant, such as Glucocon, to facilitate the emulsification process and ensure the overall stability of the encapsulated material.

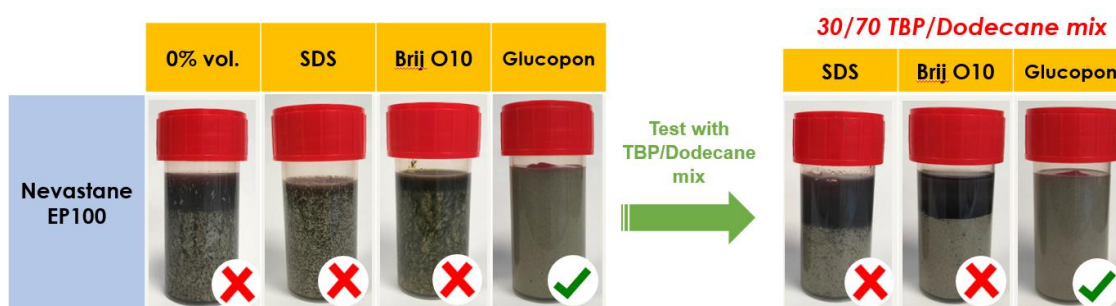


Figure 34. Visual evaluation of the initial stability of fresh emulsions with a loading rate of 50% vol. using different surfactants.

In terms of rheological behaviour, the incorporation of organic liquids in the mixtures resulted in a significant increase in the consistency index and yield stress, while also accentuating the shear-thinning behaviour with a flow index decrease of approximately 50%. Despite these changes, the emulsions exhibited sufficient workability to be poured adequately.

Microstructural characterization of the mixtures revealed notable effects of the surfactant on droplet size, as depicted in *Figure 35*. It is worth mentioning that even though the mixture with 30% Nevastane remained stable without surfactant, the droplet size was considerably larger compared to the surfactant-enhanced mixture. Hence, the use of a surfactant is highly recommended, even for viscous oils, to reduce droplet size.

The effectiveness of Glucocon surfactant was further validated for mixtures containing TBP/Dodecane, as evidenced by droplet diameters typically below 20 microns (*Figure 36*). However, a less homogeneous

distribution of droplets was observed when compared to mixtures with Nevastane. This disparity can be attributed to the exceptionally low viscosity of the TBP/Dodecane mixture, which promotes droplet mobility and the coalescence.

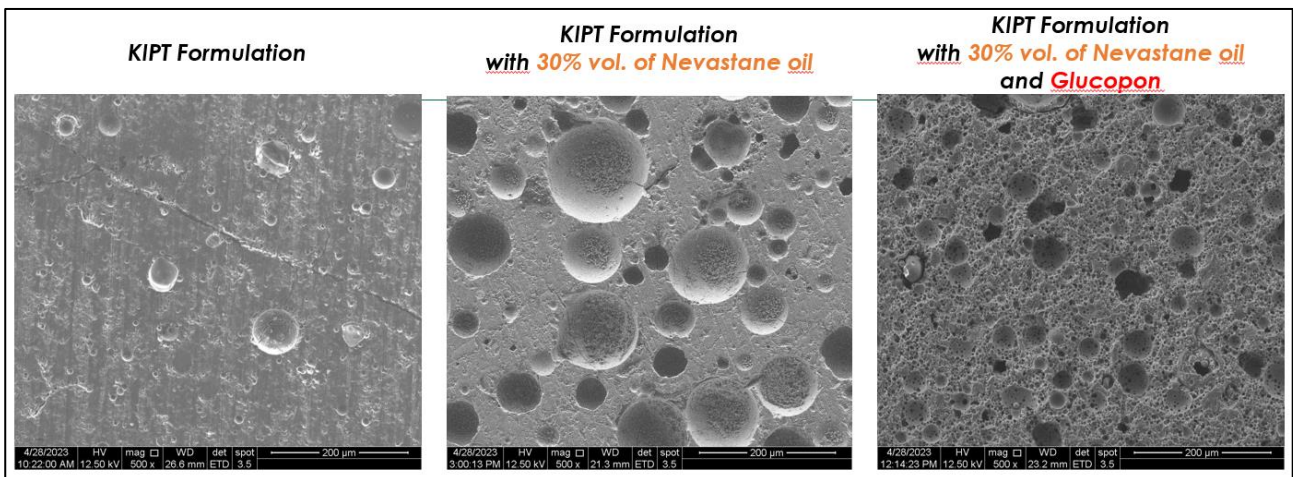


Figure 35. SEM micrographs of KIPT formulation with 30% vol. of Nevastane oil (with and without Glucocon).

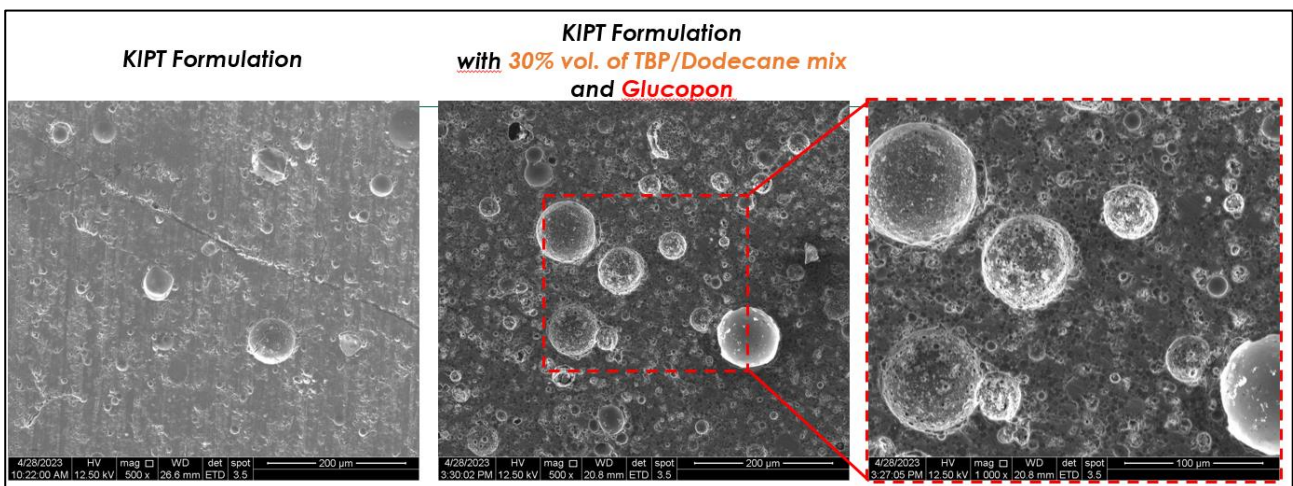


Figure 36. SEM micrographs of KIPT formulation with 30% vol. of TBP/Dodecane mix using Glucocon.

To assess the mechanical strength of the composites, compressive strength tests were conducted on cubic samples stored at 20 °C and 90% relative humidity for a duration of 28 days. The key findings can be summarized as follows:

Firstly, the use of surfactant resulted in a slight reduction in mechanical strength, primarily attributed to the formation of air bubbles. This observation was corroborated by density measurements, which indicated a decrease in density.

Secondly, the introduction of liquids led to a decrease in mechanical strength, which is an expected outcome. However, there was a minor discrepancy between the mixtures containing TBP/Dodecane mix and those containing Nevastane. This difference is likely due to variations in droplet size and distribution within the matrix.

Lastly, the obtained mechanical strengths were found to be largely acceptable, particularly in light of the fact that various nuclear waste regulations typically require a minimum compressive strength of approximately 8 MPa for solidified wastes. Thus, the composites exhibited satisfactory mechanical properties within the specified regulatory limits.

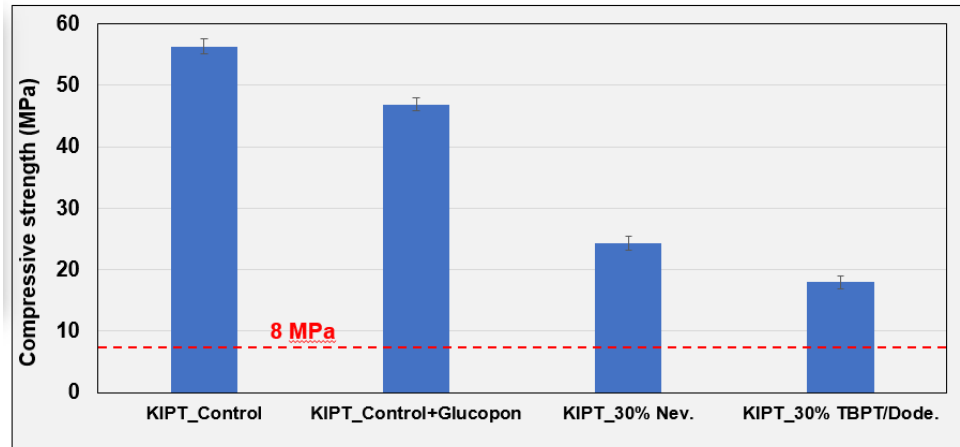


Figure 37. Compressive strengths of hardened emulsions at 28 days.

Regarding the impact of relative humidity on the storage of specimens, two different relative humidity levels were examined: 90% and 50%. The influence of relative humidity is clearly illustrated in Figure 38, where it is evident that macro cracks were observed on samples stored at 50% relative humidity. These cracks are attributed to drying shrinkage and should be carefully considered, especially in terms of test reproducibility among various collaborators. However, it is worth noting that these findings primarily apply to laboratory conditions, as the mixtures will ultimately be stored under endogenous conditions, eliminating the risk of cracking.

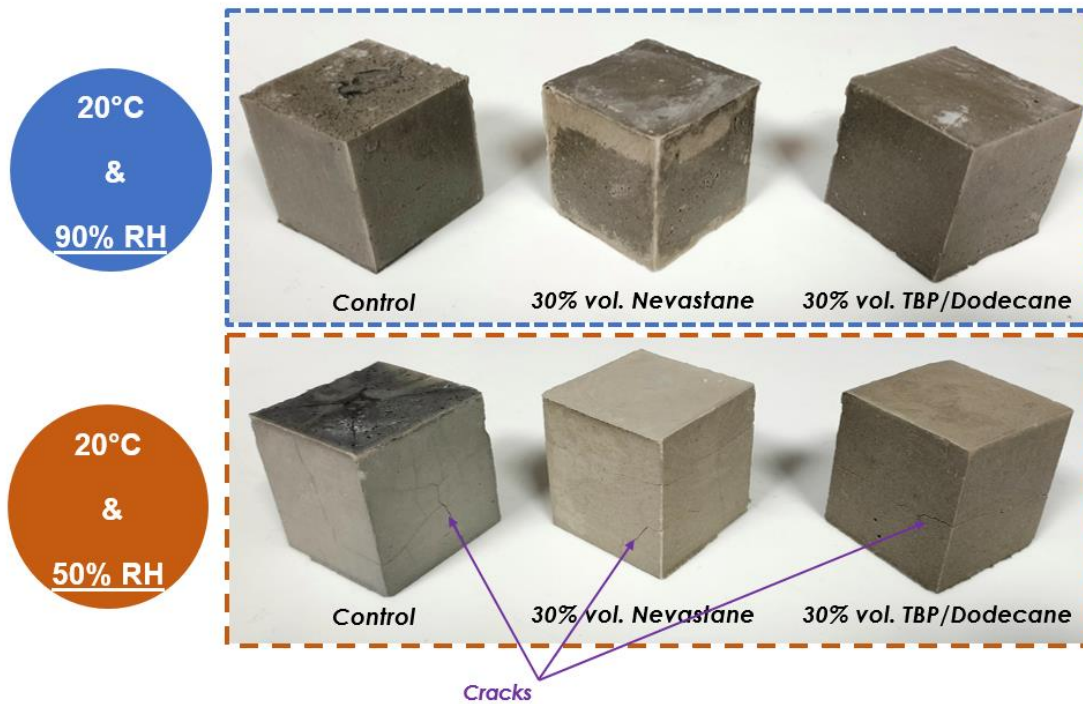


Figure 38. Effect of relative humidity on the properties of the composites.

5.5 Study of conditioning matrix durability – leaching experiments with BFS formulation and engine oil as waste

Anna Sears, Vojtěch Galek, Petr Pražák, Research Centre Řež, Czech Republic, anna.sears@cvrez.cz

Keywords: organic liquid radioactive waste, oil, blast furnace slag, geopolymer, leachability

1. Introduction

The management and disposal of liquid organic radioactive waste, such as scintillation cocktails and oils, present significant challenges due to their hazardous nature and long-term environmental impacts. Conventional methods like incineration and solvent extraction often lead to the generation of secondary waste streams or the release of harmful emissions. We have explored within WP5 a novel approach for directly treating liquid organic radioactive waste by incorporating it into a geopolymer matrix.

2. Description of work and main findings

The blast furnace slag (BFS) formulation developed by SCK CEN was used for our experiments. As a simulated organic radioactive waste, we used engine oil Mogul TB 32 mixed with blast-furnace slag, alkali activators, and other additives to create a homogeneous geopolymer mixture. Different raw materials were tested; one set was received from SCK CEN, and the other from the supplier in the Czech Republic. Different surfactants (Tween80, sodium dodecyl sulfate, and glucopone) were also tested. The mixture was then cured under controlled conditions (dry and sealed bag). The cured samples were characterised and placed in the demineralised water for a specific duration of time (2, 7, 2, 7, 14, 28, 56, and 91 days). At these set times, the demineralised water was replaced and analysed for the presence and concentration of the leached elements. After the leaching experiments, the samples will be subject to compressive strength tests according to CSB EB 12390-3.

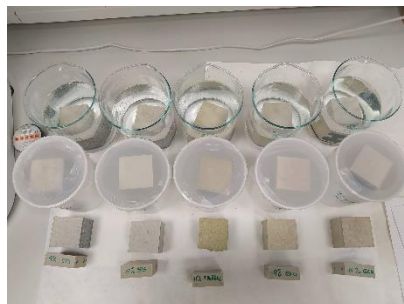


Figure 39. Prepared BFS samples.

A rapid decrease in oil leached from the samples was observed after the replaced leaching solution analysis. No oil was leached after day 14. We also observed less oil leached at samples cured in sealed bag conditions compared to those cured in dry conditions, as seen in Figure 40.

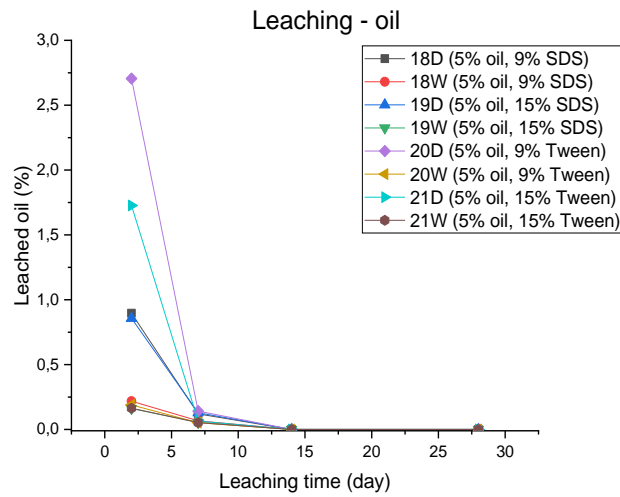


Figure 40. Leached oil from the samples.

The leached Si and Ca from the samples can be seen in Figure 41. As with the leached oil, there was a significant difference between the samples cured in dry conditions and sealed bags. In contrast, there was increased leached Ca from samples with time.

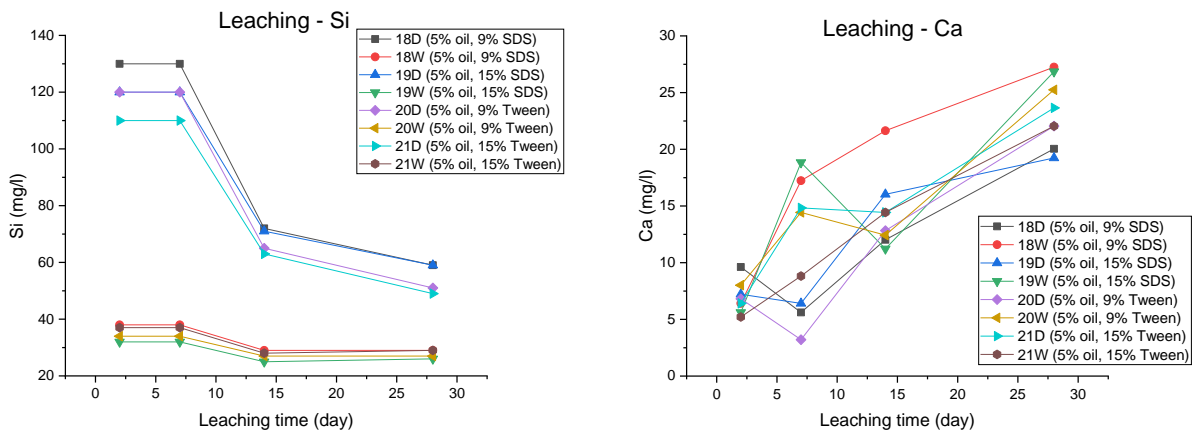


Figure 41. Leached Si and Ca from the samples.

3. Summary

The conducted leaching processes are still underway. We are also awaiting results from sample analysis for Fe and XRF. The compressive strength tests will be performed on the samples which underwent the leaching experiments. Additionally, SEM and XRD analysis will be performed on the samples.

5.6 Study of the effects of gamma irradiation on the behavior of GP

*Ilaria Moschetti, Lola Sarrasin, Guillaume Blain, Abdesselam Abdelouas, SUBATECH, CNRS-IN2P3, IMT Atlantique-Université de Nantes, France, moschett@subatech.in2p3.fr
Eros Mossini, Mario Mariani, Department of Energy, Politecnico di Milano, Italy*

Keywords: geopolymer, gamma irradiation

1. Introduction

Task 4.5 is then focus on the investigation of the possible radiation-induced modification of geopolymer (GP) under gamma irradiation using the three reference formulations developed in the WP4.

2. Description of work and main findings

Considering the different formulation and the relatively scarce literature on the behaviour of GP under irradiation [2-], investigation on the possible modification must be considered.

Water radiolysis from pore solution and hydrates must be investigated for the conditioning of radioactive waste in cement materials, since hydrogen is produced. Therefore, its ability to withstand representative levels of irradiation has to be evaluated carefully to validate the use of such a matrix and its compliance with WAC. The samples will be irradiated by using Cs-137 gamma-emitting sources characterized by different dose-rates up to relevant absorbed doses (up to 1 MGy).

The installation at IMT will allow several studies on irradiated samples, such as:

- The analysis by gas chromatography of H₂ produced during the radiolysis of the cement.
- The determination of the mechanical properties at the nanoscale (local hardness, elastic, topography).
- The characterization, structure and composition, of the samples by TEM, SEM, μ Raman, FTIR and XRD.

The leaching properties of irradiated solids (ICP and Ion Chromatography) will also be considered.

References

- [1] International Atomic Energy Agency. "Treatment and Conditioning of Radioactive Organic Liquids". In: Technical Documents 656 (1992). issn: 1011-4289.
- [2] Michelle L.Y. Yeoh et al. "Mechanistic impacts of long-term gamma irradiation on physicochemical, structural, and mechanical stabilities of radiation-responsive geopolymer pastes". In: Journal of Hazardous Materials 407 (2021). <https://doi.org/10.1016/j.jhazmat.2020.124805>
- [3] M. Ramadan et al. "Effect of high gamma radiation dosage and elevated temperature on the mechanical performance of sustainable alkali-activated composite as a cleaner product". In: Cement and Concrete Composites 121 (2021). <https://doi.org/10.1016/j.cemconcomp.2021.104087>
- [4] V. Cantarel et al. "On the hydrogen production of geopolymer wasteforms under irradiation". In: Journal of American Ceramic Society (2019). DOI: 10.1111/jace.16642
- [5] D. Lambertin et al. "Influence of gamma ray irradiation on metakaolin based sodium geopolymer". In: Journal of Nuclear Materials 443 (2013). <http://dx.doi.org/10.1016/j.jnucmat.2013.06.044>

5.7 Durability of alkali activated slag bearing organic liquid waste

Emile Mukiza^{1,2*}, Thi Nhan Nguyen^{1,3*}, Lander Frederickx¹, Mejdj Neji⁴, Alexandre Dauzeres⁴, Quoc Tri Phung^{1**}

¹ Sustainable Waste & Decommissioning Institute, Belgian Nuclear Research Centre, 2400 Mol, Belgium.

² Department of Structural Engineering and Building Materials, Ghent University, Belgium

³Department of Materials Engineering, KU Leuven, 3001 Leuven, Belgium

⁴Institute of Radiation protection and Nuclear Safety (IRSN), 92260 Fontenay-aux-Roses, France

*emile.mukiza@sckcen.be, **quoc.tri.phung@sckcen.be

Keywords: Alkali activated slag, wasteforms, durability, leaching, carbonation.

1. Introduction

Due to their advantages over conventional Portland cement (OPC)-based materials in terms of the environment and economy, alkali-activated materials (AAMs) are receiving more attention [1]. Alkali-activated slag is one of them and has been extensively studied for use in waste encapsulation. However, a crucial consideration in using AAS as waste conditioning matrices is the wasteform's durability. To ensure the integrity of the wasteform and guarantee safe waste containment, leaching and carbonation are the two most crucial durability factors that must be thoroughly understood. Previous investigations looking at the reference AAS (without waste) found that the decalcification of the AAS and consequent loss of strength were caused by leaching in a 6M NH₄NO₃ leaching solution [2]. However, carbonation of AAS revealed that the C-A-S-H structure of AAS underwent decalcification and increased cross-linking [1]. Nevertheless, nothing is known about how leaching and carbonation would affect organic waste that contains AAS. In this light, the current work aims to investigate the leaching and carbonation resistance of AAS containing organic oils, Nevastane (NEV) and Shell (SHE), as simulants of organic liquid waste.

2. Description of work and main findings

The durability performance in terms of carbonation and leaching resistance was evaluated on alkali activated bearing organic oil Nevastane (NEV) and Shell (she) as simulants of organic liquid waste. The wasteform formulations are shown in Table 7, which were developed in a robustness study [3]. The carbonation resistance was tested on AAS wasteforms after 28 days of curing by exposing them to accelerated carbonation at 1% CO₂ and 60% relative humidity. The leaching of AAS wasteforms was performed in 6M NH₄NO₃ solution [4] and the leachate was analysed by means of inductively coupled plasma optical emission spectroscopy (ICP-OES).

Table 7. AAS Wasteforms compositions.

| | Sample ID | SS | NH | w/b | WL Vol.% | % SF(Tween80) | Oil type |
|-----------------|-----------|------|-----|------|----------|---------------|----------|
| High SS, Low NH | DoE 11 | 2.79 | 3.8 | 0.55 | 25 | 5 | NEV |
| Low SS+NH | DoE 12 | 2.59 | 3.8 | 0.45 | 20 | 5 | SHE |
| High SS | DoE 13 | 2.79 | 4 | 0.55 | 20 | 3 | SHE |
| High SS+NH | DoE 14 | 2.79 | 4.2 | 0.35 | 20 | 5 | SHE |

SS: Sodium silicate, NH: NaOH, W/B: water-binder ratio, WL; waste loading, SF: Surfactant.

The leaching depth determined by phenolphthalein spraying after 28 day experiment is shown in Figure 42. The leaching results show that AAS wasteforms are generally more prone to leaching with DoE 11 (high sodium silicate and low NaOH content) fully leached.

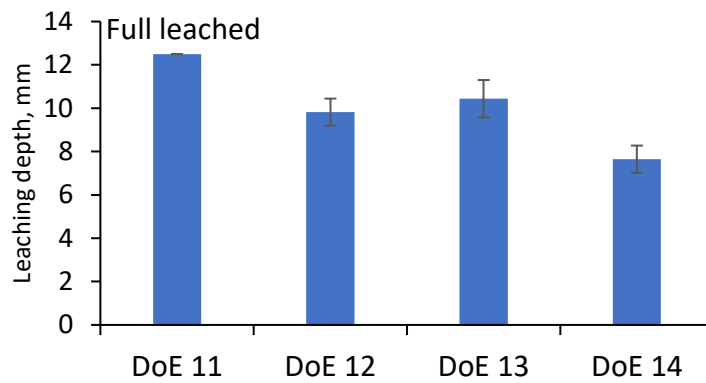


Figure 42. Leaching depth (28D).

Moreover, ICP-OES results showed that Ca and Na were the main leachable elements. It was also observed that the higher the w/b ratio, the more the leaching of AAS.

The carbonation results are presented in Figure 43. It can be seen that the strengths of wastefoms seemed stable than that of reference AAS (without oil) under carbonation.

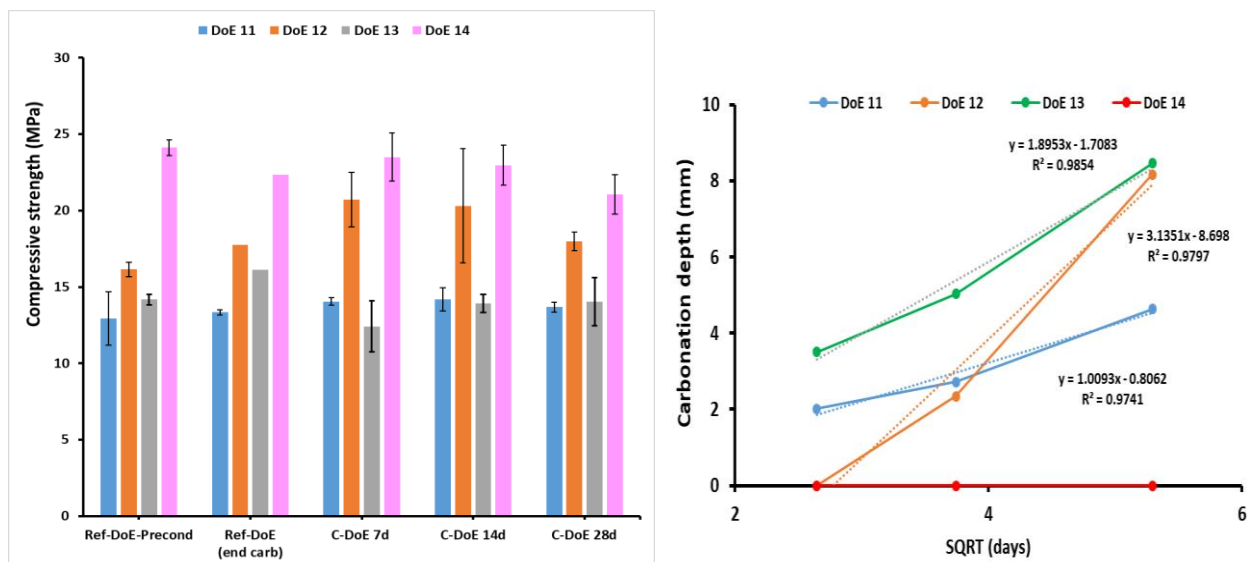


Figure 43. Compressive strength of carbonated AAS matrices (left) and carbonation depth after 28d of carbonation (right).

It was also noticed that wastefoms bearing SHE are more vulnerable to carbonation than those containing NEV, while a higher w/b ratio also led to a higher carbonation susceptibility.

3. Conclusions and way forward

The accelerated leaching and carbonation of AAS wastefoms were performed. It was noticed that both carbonation and leaching resistance of waste forms depend significantly on oil type, waste loading, and w/b ratio. The leaching was greatly affected by the w/b ratio. Ca and Na were the main leachable elements of waste forms in 6M NH₄NO₃ solution. On the other hand, carbonation was predominantly affected by oil type. Wastefoms with NEV showed a better carbonation resistance than those with SHE. The mechanical strengths of wastefoms seemed stable under carbonation. Future work will focus on extensive characterization to examine the evolution in microstructure and mineralogy of AAS wastefoms exposed to both accelerated leaching and carbonation.

Acknowledgements

This work has received funding (in parts) from the Belgian Energy Transition Fund (ASOF project), IRSN (France), and the PREDIS project.

References

1. Nguyen, T.N., et al., *Alteration in molecular structure of alkali activated slag with various water to binder ratios under accelerated carbonation*. Scientific Reports, 2022. **12**(1).
2. Komljenović, M.M., et al., *Decalcification resistance of alkali-activated slag*. Journal of hazardous materials, 2012. **233**: p. 112-121.
3. Nguyen, T.N., et al., *Robustness tests for immobilization of oils in alkali activated slag in Proceedings of the PREDIS MAY 2023 WORKSHOP 2023*: Mechelen, Belgium. p. 3.
4. Phung, Q.T., et al., *Investigation of the changes in microstructure and transport properties of leached cement pastes accounting for mix composition*. Cement and Concrete Research, 2015. **79**: p. 217-234.

5.8 PREDIS 4th Workshop GSL WP5 update

Tim Harrison, Steve Wickham

Galson Sciences, UK

e-mail of main contact: th@galson-sciences.co.uk

Keywords: Radioactive Liquid Organic Waste, geopolymer, life cycle analysis, disposability assessment

1. Introduction

WP5 of the PREDIS project investigates the use of geopolymers for conditioning of radioactive liquid organic waste. GSL is currently involved in sub-tasks 5.4 – Study of conditioning matrix performances and 5.5 – Preliminary technical, economic and environmental analysis.

2. Description of work and main findings

Study of conditioning matrix performances (Sub-task 5.4)

In the coming year, Galson Sciences (GSL) will lead sub-task T5.4.9. This sub-task involves developing a preliminary disposability assessment on the use of geopolymers for direct conditioning of liquid organic waste and will result in the production of a disposability assessment report. This work has not yet formally begun but GSL has undertaken an internal planning exercise to determine the best approach for this work.

When conducting the disposability assessment for WP5, GSL plans to follow the procedure used by Nuclear Waste Services (NWS) in the UK as this approach is reasonably mature and flexible, having been developed for assessing a wide variety of waste forms for various disposal concepts. In the NWS approach, the disposability assessment is broken into multiple smaller evaluations and safety assessments. The long list of evaluation areas to consider are:

- Nature and Quantity of Waste;
- Wasteform;
- Container Design and Storage Conditions;
- Container integrity and Durability;
- Impact Accident Performance;
- Fire Accident Performance;
- Data Recording;
- Management System;
- Policy;
- Concept Compatibility;
- Criticality Safety;
- Nuclear Security;
- Nuclear Safeguards; and,
- Sustainability.

These assessment areas will be screened to eliminate those which are not relevant to WP5. The outputs of the evaluations will be used to inform high-level transport, operational and post-closure safety assessments.

A similar approach was taken by GSL when conducting research into the factors affecting the disposability of thermally treated waste products in the THERAMIN project [1]. Some adjustment to the UK process is required, i.e., where there are quantitative limits within the UK disposability assessment guidance, there will need to be discussion on the benefit of comparison against these limits to the wider European community.

Preliminary technical, economic and environmental analysis (Sub-task 5.5)

Work over the past year has focused on the provision of case study input to the Life Cycle Analysis (LCA) being undertaken in Work Package 2.

A questionnaire was developed to collect information salient to the LCA case study and circulated to the groups developing treatment technologies. For each group, the questionnaire collected data quantifying the raw material inputs, energy inputs, waste loadings, secondary waste streams and final product characteristics.

The returned questionnaires were synthesised into a spreadsheet recording the data provided by the experimentalists, and an excerpt of this sheet is shown in Figure 44, including contact details of the individuals providing the information. Where further information was required beyond that included in the questionnaire response, further clarification was obtained directly from the experimentalists. A brief overview of the organisations providing inputs, as well as the waste types and treatment routes, is shown in Table 8. Treatments of organic liquids involving cementation will be used as an LCA baseline for comparison against geopolymer techniques. The spreadsheet and underlying questionnaires were shared with the LCA case study team lead as well as being made available on the [Teams group](#).

| Waste | Waste Overview | | | Material Inputs | | Treatment Method | Conditioned Waste | | | Energy Used Energy Used/kwh | |
|-------------------------|-------------------------|----------------|---|---|--|---|-------------------------------|--------|---------------|--------------------------------|---------|
| | Total Amount | Waste Units | Waste Comments | Components | Amount/kg | | Output | Amount | Waste Loading | | Comment |
| Pump Oil | | per 220 l drum | Small amount of pump oil was generated from TRIGA reactor operation and few more liters are expected to be generated when TRIGA reactor will be | CEM II B/M (S-LI) 32.5 R GORKAL 70 cement Pump oil water NEOPAL MA 3 NEOPAL MA 9 220 l stainless steel drum | 210 16 44.5 4.5 4.64 4.64 | Emulsifying before embedding in cement based matrix. The emulsion of oil, water and non-ionic surfactants (NEOPAL MA 3 + NEOPAL MA 9) is mixed directly in the conditioning drum (220 l carbon steel drum). NEOPAL MA 3 and NEOPAL MA 9 are alcohols C12-14 ethoxylated with 3 and respectively 9 moles of ethylene | Cemented oil in standard drum | 325 kg | ~ 13.7 %wt | | 7.5 |
| Scintillation cocktails | 10 l generated per year | per 220 l drum | The main radionuclides in these scintillation cocktails are H-3 and C-14 and to a less extent other pure beta emitters such as Sr-90 and alpha emitters | CEM II B/M (S-LI) 32.5 R GORKAL 70 cement Scintillation cocktails water lime sodium silicate 220 l stainless steel drum | 135 91 47 35 17 5 | Emulsifying before embedding in cement based matrix. The emulsion of scintillation cocktails, water and additives (lime and sodium silicate) is mixed directly in the conditioning drum (220 l carbon steel drum). | Cemented oil in standard drum | 330 kg | ~ 14.2 %wt | | 7.5 |

Figure 44. Excerpt from the LCA case study input spreadsheet showing, as an example, entries for cemented waste oils and scintillation cocktails.

Table 8. Brief overview of inputs from WP5 organisations noting the waste type and treatment.

| Organisation | Waste | Treatment Type |
|--------------|---------------------------|---------------------|
| RATEN ICN | Pump Oil | cementing |
| RATEN ICN | Scintillation cocktails | cementing |
| Sogin | unspecified RLOW | cementing |
| Sogin | unspecified RLOW | cementing |
| UJV Rez | solvents & cocktails | sorbent & cementing |
| CEA | unspecified RLOW | cementing |
| CEA | unspecified RLOW | geopolymer |
| NNL | oils & solvents | geopolymer |
| NSC KIPT | Various contaminated oils | geopolymer |
| Ciemat | oils & cocktails | geopolymer |
| CV Rez | oils & cocktails | geopolymer |

Engagement with the LCA researchers has continued since the synthesis was shared with the LCA case study team. This engagement is focused on determining what assumptions should be made in the LCA, and what conditioning scenarios should be considered. Future engagement will also focus on how value assessment work to be undertaken in WP5 (and in other PREDIS WPs) can be aligned with LCA work (see below).

3. Summary

Study of conditioning matrix performances (Sub-task 5.4)

Initial planning work for sub-task 5.4 has been completed. The planned approach is presented in Figure 45. The next step in the approach is to conduct a screening of evaluation and assessment areas. This will be conducted in a workshop with SOGIN, GSL's partners in T5.4.9.

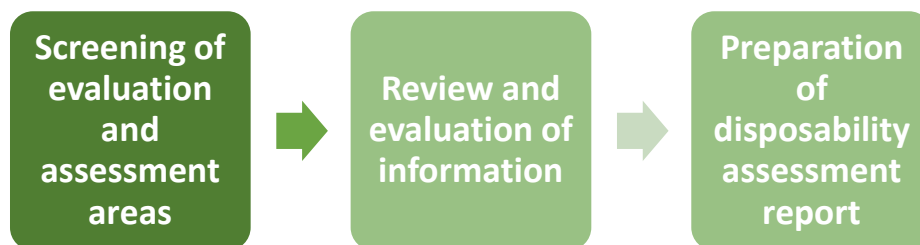


Figure 45. Overview of planned disposability assessment approach.

Preliminary technical, economic and environmental analysis (Sub-task 5.5)

The LCA case study input has been provided to WP2 (MS37). Engagement with the WP2 LCA case study team is on-going in order to further refine the scope of this task. The outputs of the LCA will be a key input to D5.5 (Report on Direct conditioning of liquid organic waste route. Another key input will be a value assessment workshop, to be run in the coming year. GSL will lead the development of D5.5 and organise and facilitate the value assessment workshop.

Acknowledgements

Thanks to Joel Kirk and Laurence Stamford (University of Manchester), Federica Pancotti (Sogin), Karel Prchal (UJV Rez), David Lambertin (CEA), Sergey Sayenko (NSC KIPT), Lara Esperanza (Ciemat), Martin Hayes (NNL), Vytech Galke (CV Rez) and Quoc Tri Phung (SCK CEN) for their collaboration on the LCA case study task.

References

- [1] THERAMIN Project, *THERAMIN Project Synthesis Report*. THERAMIN Deliverable no. D5.4, June 2020.

5.9 Study of direct conditioning process coordination (Task 5.3)

Federica Pancotti, Rossella Sciacqua, Francesco Troiani
Sogin SpA, Italy
e-mail of main contact: pancotti@sogin.it

Keywords: Radioactive Liquid Organic Waste, direct conditioning, geopolymer, alkali activated materials

1. Introduction

Sogin as Task Leader coordinated the activities related to Task 5.3 "Study of direct conditioning process" and was in charge for organising the work between the different partners, developing work methodologies to compare, analyse and assess the different formulations, monitoring the progress status and ensuring that the scientific milestones and deliverables are reached in a timely manner.

2. Description of work and main findings

The description is focused on the activities conducted in the framework of Sub-task T5.3.3 – Formulation of conditioning materials: optimization and robustness of reference formulations.

As reported in the Milestone (MS32 “Choice of 3 reference formulations to be further studied” – 14.07.2021), the experimental work started without a clear definition of the three specific formulations, but just considering 3 families of formulations based on the different raw materials included in the conditioning options studied. They are mainly based on Metakaolin, Blast Furnace Slag and mixture of different raw materials.

For each family, 2-3 Partners were identified to work in the Optimisation and Robustness testing activities in the scope of the sub-task 5.3.3 (see Figure 46).

| | | Optimization (7 months) - selection of the three Reference Formulations for Robustness DECEMBER 2021 | | | |
|------------------------------|--|---|-------------------------------------|----------------------------------|-----------------------|
| Reference Formulation/Family | PARTNER | TBP/Dodecane (30%) | Pump Oil (low viscosity - not pure) | Pump Oil (high viscosity - pure) | Scintillation Liquids |
| | | A | B | C | D |
| 1 | Metakaolin based geopolymers MK | NNL | X (1-A1) | X(Nevastane EP100) (1-C) | |
| | | CIEMAT | | X (Shellspirax) (1-B) | X (1-D) |
| | | SCK-CEN | X (1-A2) | | |
| 2 | Blast Furnace Slags based alkali activated materials - BFS | NUC | | X (Shellspirax) (2-B) | X (2-D) |
| | | SCK-CEN | X (2-A) | | |
| | | POLIMI | X (3-A) | | |
| 3 | Mixed - (VT-MK-BFS) | RATEN | | X (Shellspirax) (3-B1) | X (3-D1) |
| | | KIPT | | X (Shellspirax) (3-B2) | X (3-D2) |
| | | | | X(Nevastane EP100) (3-C) | |

Figure 46. T5.3.3 organisation of the work for the optimisation study.

The activities were split into two main parts:

1. Optimisation study: 7 months (from June 2021 to December 2021)
2. Robustness study: 10 months (from January 2022 to October 2022).

At the end of the Optimisation phase (see PREDIS Meeting minute – WP5 Task 5.3.3 progress on-line meeting 15.12.2021) a review and an agreement on the 3 Reference Formulations, among the reference families, was achieved and the Robustness study plan was defined (see Figure 47).

| | Jan-22 | feb-22 | mar-22 | apr-22 | may-22 | Jun-22 | Jul-22 | Aug-22 | Sep-22 | Oct-22 | nov-22 |
|---|--|--------|--------|--------|-----------|--------|--------|--------|--------|--------|--|
| 1) RLOW variability | | | | | | | | | | | MS34 Optimised formulations for reference formulations |
| Fixed incorporation rate (for example 30 % volume) and fixed raw materials | | | | | | | | | | | |
| *Different RLOW as reported in the table | 1st stage | | | | 2nd stage | | | | | | |
| 2) Raw materials variability | | | | | | | | | | | |
| Fixed incorporation rate (for example 30 % volume) and fixed RLOW | | | | | | | | | | | |
| *Different raw materials depending on local availability | 1st stage | | | | 2nd stage | | | | | | |
| 3) Process variability | | | | | | | | | | | |
| Fixed incorporation rate (for example 30 % volume), fixed raw materials and fixed RLOW | | | | | | | | | | | |
| *Variability of aluminosilicate source-to-activation source ratio (for example ± 2 %) | 1st stage | | | | 2nd stage | | | | | | |
| *Variability of water-to-binders ratio (for example ± 2 %) | 1st stage | | | | 2nd stage | | | | | | |
| *Variability of sand-to-water ratio (for example ± 2 %)(at fixed incorporation rate) | 1st stage | | | | 2nd stage | | | | | | |
| *Variability of emulsifier, if needed (for example ± 2 %) (at fixed incorporation rate) | 1st stage | | | | 2nd stage | | | | | | |
| Improved understanding of emulsification process and influence on hardened materials properties and identification of the most suitable emulsifier (if needed) - CEA, ECL | in close collaboration with all the other partners | | | | | | | | | | |

Figure 47. T5.3.3 robustness study plan.

The three reference formulations were tested in the Robustness phase to study the impact of RLOW, raw materials and process variability. As reported in Figure 48, two Partners were identified to work on each formulation, considering the previous experiences of the different partners and the need for a complete evaluation of the robustness of the three reference formulations. It was agreed to leave POLIMI outside the selected formulations in order to continue with the study of an alternative solution (pre-impregnation) based on sustainable principles.

| Partner | Form. 1 (MK) | Form. 2 (BFS) | Form. 3 (MIX) | RLOW Surrogate | |
|---------------|----------------------------|---------------|---------------|-------------------------------|-------------------------------|
| | | | | 1° stage (Jan-May) | 2° stage (Jun-Oct) |
| CIEMAT | X | | | TBP – Scintill | Oil (Nevastane – Shellspirax) |
| NNL/UoSF | X | | | Oil (Nevastane – Shellspirax) | TBP – Scintill |
| RATEN | | X | | TBP – Scintill | Oil (Nevastane – Shellspirax) |
| SCK-CEN | | X | | Oil (Nevastane – Shellspirax) | TBP – Scintill |
| NUCLECO/SOGIN | | | X | TBP – Scintill | Oil (Nevastane – Shellspirax) |
| KIPT | | | X | Oil (Nevastane – Shellspirax) | TBP – Scintill |
| POLIMI | Recycled polymers and Tuff | | | TBP – Scintill | Oil (Nevastane – Shellspirax) |

CEA – ECL (in close collaboration with all the other partners): Improved understanding of emulsification process and influence on hardened materials properties and identification of the most suitable emulsifier (if needed)

Figure 48. T5.3.3 organisation of the work for the robustness study.

In November 2022 Milestone 34 “Optimised formulations for reference formulations” (30/11/2022) was completed. The goal of the milestone was the selection of a limited number of optimised formulations to be used in Subtasks T5.3.4 and T5.3.5 for the investigation of reference formulations with real RLOW and direct conditioning process scale-up.

The selection of the most promising formulations was based on qualitative analysis of the available data. A matrix (see Figure 49) was created with a predefined set of criteria. A colour-based scale was used for the qualitative analysis of proposed formulations and different priorities (high and medium) were assigned to the defined criteria. The matrix was discussed, and additional information was given by the partners during the meeting to focus the selection of the optimised formulations to a limited number of options.

| Option | Formulation | Waste | Criteria | Priority | | | | | | | | | | | | | | |
|--------------------|--------------------------------------|--------------------------------|----------|--------------|------------|------------|---------------------|------------|--------------|----------------|--------------------------|-------------|-----------|-------------------|-------------------|--|--|--|
| | | | | WL %, (vol%) | Surfactant | Bleeding % | Supplying materials | Robustness | Heat release | Setting time h | Compressive strength MPa | Workability | Viscosity | Calorimetric data | Flexural strength | | | |
| OIL | 1 MK - Metamax | Nevastane oil | | H | M | H | H | M | M | H | H | H | H | M | M | | | |
| | 2 MK - Argicem | Nevastane oil | | | | | | | | | | | | | | | | |
| | 3 MK - Metamax | Repsol supertauro 100 oil | | | | | | | | | | | | | | | | |
| | 4 MK-BFS-FA (Ukr) | Nevastane oil | | | | | | | | | | | | | | | | |
| | 5 MK-BFS-FA (Ukr) | Shellspirax oil | | | | | | | | | | | | | | | | |
| | 6 MK-BFS-FA (metamax-Ecotrade-FA IT) | Nevastane oil | | | | | | | | | | | | | | | | |
| | 7 MK-BFS-FA (metamax-Ecotrade-FA IT) | Shellspirax oil | | | | | | | | | | | | | | | | |
| | 8 MK-BFS-FA (metamax-Ecocem-FA IT) | Nevastane oil | | | | | | | | | | | | | | | | |
| | 9 MK-BFS-FA (metamax-Ecocem-FA IT) | Shellspirax oil | | | | | | | | | | | | | | | | |
| | 10 BFS + Sand | Nevastane oil | | | | | | | | | | | | | | | | |
| TBP-dodecane | 11 BFS + Sand | Shellspirax oil | | | | | | | | | | | | | | | | |
| | 12 MK - Metamax | TBP-Dodecane (70-30) | | | | | | | | | | | | | | | | |
| | 13 MK - Argicem | TBP-Dodecane (70-30) | | | | | | | | | | | | | | | | |
| scintill cocktails | 14 MK-BFS-FA (metamax-Ecocem-FA IT) | TBP-Dodecane (30-70) | | | | | | | | | | | | | | | | |
| | 15 MK-BFS-FA (MK-BFS-FA IT) | scintill | | | | | | | | | | | | | | | | |
| | 16 MK - Metamax | scintill INSTAGEL plus | | | | | | | | | | | | | | | | |
| | 17 BFS + Sand | scintillation cocktail (UG AB) | | | | | | | | | | | | | | | | |

Figure 49. T5.3.3 matrix for qualitative evaluation of formulations.

In February 2022, Subtasks T5.3.4 and T5.3.5 Kick off Meeting was held and a discussion on the structure of the final Deliverable D5.2: Report on Synthesis of formulation & process studies results, in the scope of Subtask 5.3.6, started.

3. Summary

The experimental activities conducted for the investigation, development, and assessment of innovative direct conditioning solutions for Radioactive Liquid Organic Waste, showed that specific formulations based on metakaolin, blast furnace slags and innovative mixes of raw materials have very promising results in terms of improving waste loadings and waste form properties in comparison with traditional cementitious waste forms.

The outcomes of the work conducted for the optimisation and robustness studies have been collected and a paper “Investigation, development and assessment of innovative direct conditioning solutions for radioactive liquid organic waste within the PREDIS project” has been accepted for the ICEM 2023 conference (October 3-6, 2023, Stuttgart, Germany).

The conditioning matrix durability study and the preliminary technical, economic, and environmental analysis for the Life Cycle Assessment are ongoing. Moreover, investigation of the reference formulations with real RLOW and process scale-up tests are planned for the last year of the project.

5.10 Study of direct conditioning matrix performances: Study of thermal behaviour and "fire hazard" (Task 5.4)

*Salvatore Angelo Cancemi, Rosa Lo Frano, Sandro Paci
University of Pisa, Italy
e-mail of main contact: rosa.lofrano@ing.unipi.it*

Keywords: Radioactive Liquid Organic Waste, direct conditioning, temperature, integrity, durability, simulation, experiments

1. Introduction

UniPi as Sub-Task Leader coordinated the activities related to Task 5.4.7" Study of thermal behaviour and fire hazard" aimed at investigating the thermophysical, mechanical and deformation properties of RLOW/conditioning matrix composites caused by the elevated temperature/fire hazard.

Numerical methodology to compare, analyse and assess the different matrix formulations/simulants of RLOW was implemented, and preliminary testing on concrete material (aged/unaged) was developed to investigate the effects of both the elevated temperature and aging to assure milestones and activities will be performed in timely manner.

2. Description of work and main findings

The description is focused on the activities conducted in the framework of Sub-task T5.4.7 – Study of thermal behaviour and fire hazard".

The solidification of the RLW (LOW) is one of the WACs to be respected so that both the liquid content and voids of the immobilized waste streams are reduced to a minimum. These wastes that cannot longer be successfully treated as liquids are converted into a solid state suitable for the intended purpose for safe storage. At the same time, the porosity (voiding) of the solid waste must be reduced to make the immobilization more efficient. The heterogeneity of the conditioning matrix due to the presence of various structural components and constituents, differing in composition, strength, durability, fire resistance, and non-combustibility properties requires a proper investigation.

Figure 51 shows SEM results of a conditioned matrix made of cemented resins: cracks formed because of growth of voids into the solidified matrix [1]. Cracking unavoidably affects the strength of conditioned matrix and consequently its durability under real storage conditions. Damage could become even worst under ageing and thermal actions.

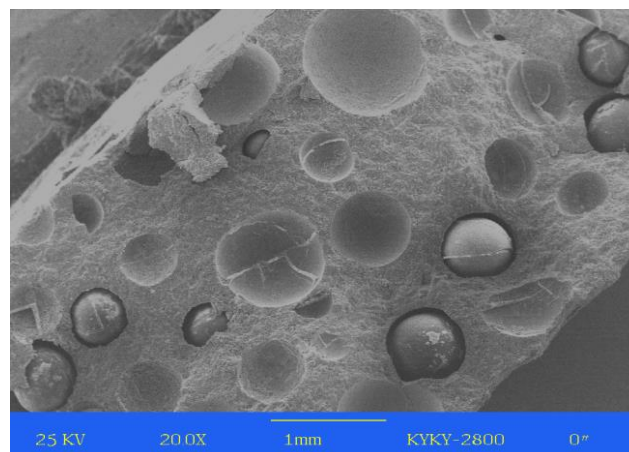


Figure 50. SEM results of resins immobilized into a specific cement type matrix.

The thermo-mechanical behaviour of waste matrix and its evolution, which are crucial aspects affecting the long-term performance, the compatibility and capability to dispose the waste forms (RLW/geopolymers composites [2][3]) in the disposal facilities are so investigated numerically and experimentally.

Figure 51 shows the methodology used for the assessment of the deterioration of concrete-cemented waste under high temperature exposure. The FEM used to represent the behaviour of a real scale of analogue matrix is shown in Figure 51 b)[4].

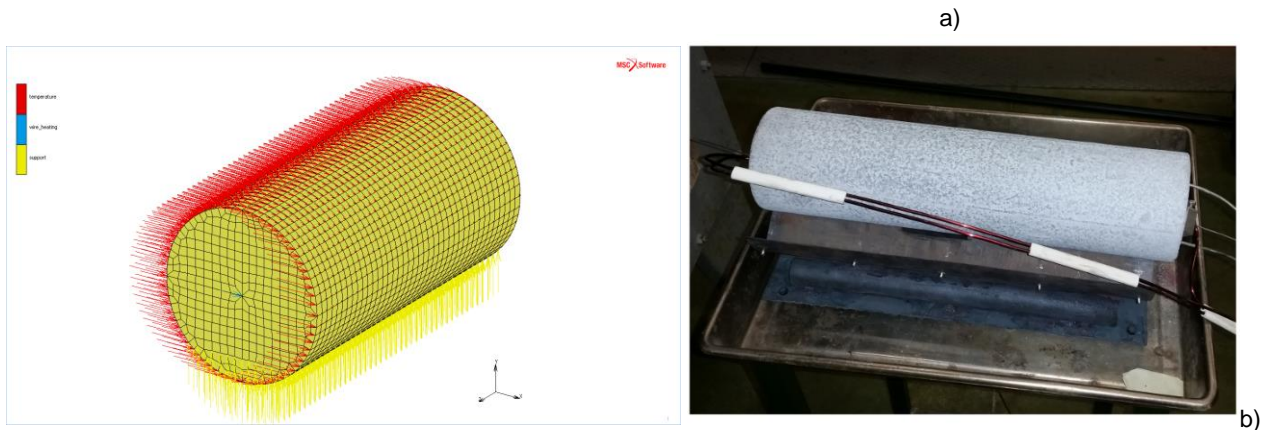
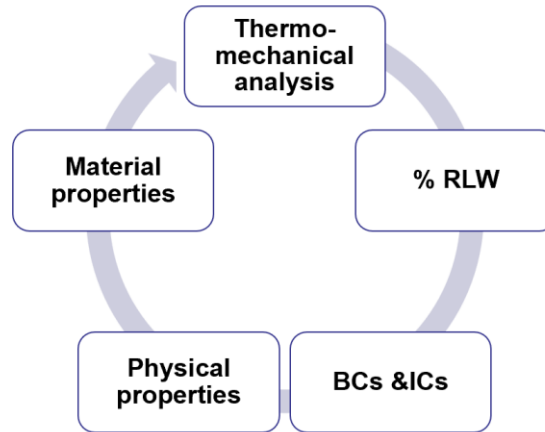


Figure 51. a) Methodological approach for numerical study of the thermal performance of a possible conditioned matrix and b) FE model and real specimen used for thermal tests [5].

The activities performed consisted of:

1. Numerical study.
2. Preliminary thermo-mechanical tests.

The numerical study highlights the importance of the liquid content in impairing the structural bonding and reducing the strength (and durability) of conditioned matrix (Figure 52).

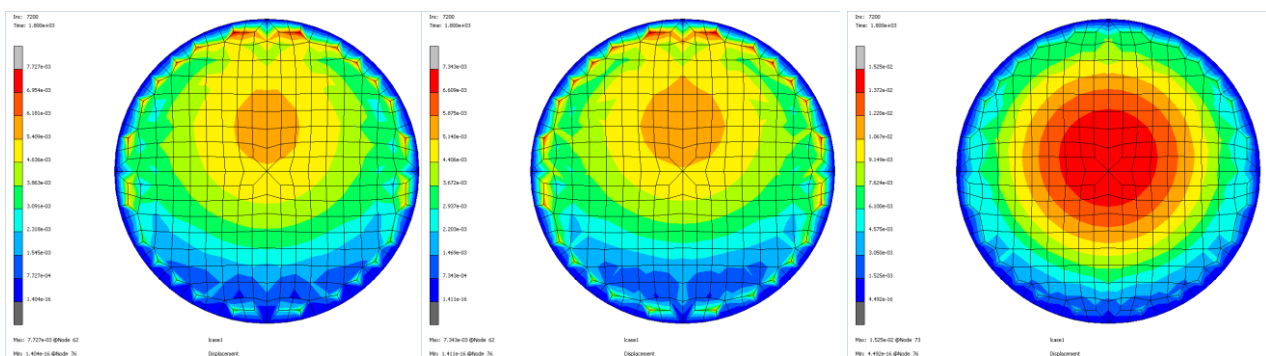


Figure 52. Overall displacement of RLW incorporating increasing percentage of organic waste analogue.

Preliminary thermo-mechanical tests (waiting for other different RLOW analogues to be provided by CEA and SCK CEN) were carried out by adopting standardized and new procedures (defined within Sub-task 4.1 – e.g., ASTM E1530, ASTM C1269, SSR-6, etc.). The cylindrical samples were prepared (see previous Figure 51 b) equipping each of them with at least two thermocouples (TC) and a central wire resistor.

The hot-wire method [6][7] was also used to determine the thermal conductivity. Fourier equation is then used to calculate the k-value based on the rate of temperature increase of the wire and power input. Temperatures are measured in thermal steady state condition. k-values determined at one or more temperatures were used for ranking concrete material in relative order of their thermal conductivities.

The obtained results in terms of thermal conductivity are shown in Figure 52 as a function of temperature. The first important observation relates to the reduction of the thermal conductivity as the temperature increases: 20% decrease in the range from 100 °C and 800 °C. Explanation lies on de-hydration process occurring at elevated temperature and that leads to an increase of porosity.

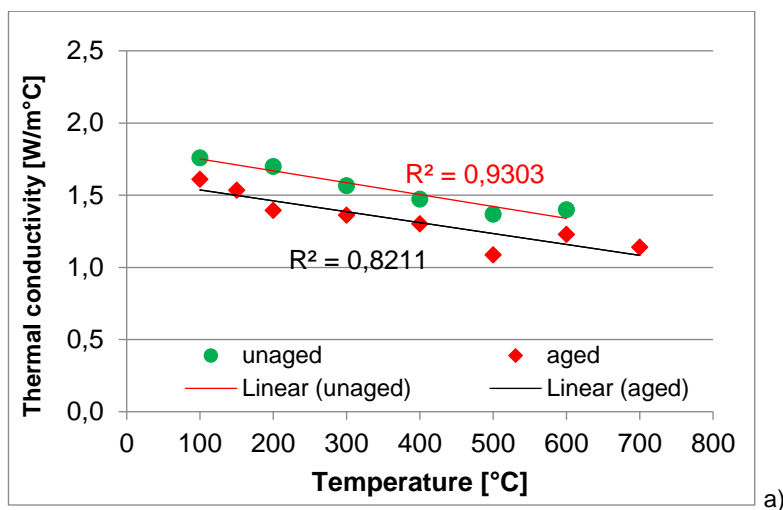


Figure 53. T5.4.7 Thermal conductivity trends with linear interpolation for (un)aged (a) concrete. In b) image from thermal test execution on RLOWs simulant/concrete.

The role of aging was analysed by repeating the same thermal tests on specimens obtained from the same materials constituents and aggregates (same input materials, wt. %). The decrease of bulk and matrix density is not remarkable. The open porosity increases and is responsible for the worsened mechanical properties. The compressive strength was also affected by the internal porosity of the solidified forms: the rupture load resulted about 405 kN.

The selection of the most promising formulations for RLOW was the basis for the forthcoming thermo-mechanical testing campaign. The new matrices to analyse were discussed, and additional information on the material properties are provided by the partners during the meeting.

3. Conclusions and way forward

Elevated temperature exposure has a significant impact on the mechanical and physical properties of RLW examined. The numerical results indicate that stiffer the conditioned matrix lower the deformation capacity. This creates distortion in the cemented microstructures, that may be responsible under specific conditions of crack propagation and spalling of matrix surfaces. The liquid waste stream degrades the durability and structural performances of RLOW analogue.

The testing results instead highlights that the thermal conductivity monotonically decreases of about 32.5% as temperature increases (effects of de-hydration process). The open porosity increases and determines the reduction of the mechanical strength.

The outcomes of the work performed have been collected in the two papers: "Preliminary thermo-mechanical characterization of cement-based materials for LLW immobilization"(ICEM2023-110093) and "Preliminary thermo-mechanical characterization of cement-based materials for LLW immobilization- Part II"(ICEM2023-110086) that have been accepted at the ICEM 2023 Intl. conference (October 3-6, 2023, Stuttgart, Germany).

The conditioning matrix durability study and the preliminary technical, economic, and environmental analysis for the Life Cycle Assessment are ongoing. Moreover, the investigation of the effects of the exposure to elevated temperature or to the fire flame condition of the reference formulations with real RLOW are planned for the last year of the project.

References

- [1] Li, J. (2013). Cementation of Radioactive Waste from a PWR with Calcium Sulfoaluminate Cement (IAEA-TECDOC-CD--1701(Companion CD)). International Atomic Energy Agency (IAEA).
- [2] Natsuda, M., Nishi, T., Solidification of ion exchange resins using new cementitious material (1) swelling pressure of ion exchange resin, Journal of Nuclear Science and Technology 29 (1992) 883-889.
- [3] Nishi, T., Advanced solidification system using high performance cement: ICEM'95, ASME Part, Proceedings of the Fifth International Conference on Radioactive Waste Management and Environmental Remediation, New York (1995) 1095-1098.
- [4] Lo Frano R and S. A. Cancemi. "Preliminary thermo-mechanical characterization of cement-based materials for LLW immobilization", Proceeding of ICEM2023, October 3-6, 2023, Stuttgart, Germany 2023
- [5] Lo Frano R et al. "Thermo-mechanical test rig for experimental evaluation of thermal conductivity of ceramic pebble beds", Fusion Engineering and Design 89, Issues 7–8, 2014, 1309-1313 <https://doi.org/10.1016/j.fusengdes.2014.03.007>
- [6] ASTM International, Standard Test Method for Thermal Conductivity of Refractories by Hot Wire (Platinum Resistance Thermometer Technique) ASTM-C1113/C1113M-09(2019).
- [7] EUROPEAN STANDARD. Testing hardened concrete Part 1: Shape, dimensions and other requirements for specimens and moulds, BS EN 12390-1:2012.

5.11 Geopolymer cements for the immobilisation of radioactive liquid organic wastes

¹Department of Material Science and Engineering, University of Sheffield, United Kingdom

(E-mail jmcwilliams1@sheffield.ac.uk, j.provis@sheffield.ac.uk)

²Department of Chemical Engineering, University of Sheffield, United Kingdom

(Email: b.walkley@sheffield.ac.uk)

Keywords: Geopolymers, Radioactive waste, Tributyl phosphate (TBP), Dodecane, Nevastane

1. Introduction

Pickering emulsion with fumed silica has been investigated as a potential immobilisation route for liquid organic oils. The potassium geopolymers developed were based on a>NNL (National Nuclear Laboratory) formulation with 1 wt% of fumed silica and 10/20/30/40 wt% of either TBP (tributyl phosphate)/Dodecane or Nevastane. The initial observation highlights a clear difference in the immobilisation of the two oils. The Nevastane

appeared to be immobilised successfully whilst TBP/Dodecane separated from the potassium geopolymer matrix. This separation was found to get worse with an increasing weight percentage of the TBP/Dodecane with a significant quantity of the oil sitting above the cement, For Nevastane, when the weight percentage was increased from 10 to 30 wt%, there was an increase in the viscosity of the sample; 30 wt% Nevastane was the most viscous of all the samples made and was difficult to pour. Further characterisation will be vital to understand the nature of these samples and how they interact with the oil.

2. Description of work and main findings

This work will investigate creating Pickering emulsions with silica fume (1 wt%) with TBP/Dodecane and Nevastane at 10, 20, 30 and 40 %wt at the three NNL (National Nuclear Laboratories) formulations, Table 9. For the pre-leached samples – FTIR, XRD and SEM-EDX will be conducted for samples at seven, 28 and 90 days. Compressive strength and rheology will be carried out by a selection of these samples to investigate their strength and workability. For the leaching test, the samples will be cured for 28 days and placed into deionised water. Where allocates of the deionised water will be removed at set time points and the samples placed in fresh deionised water. This is the first leach test of this PhD, it would be interesting to compare GC-MS, TOC and UV-Vis as potential techniques to analyse the leached solutions. For further investigation of these techniques, known oil concentrations in deionised water should be prepared and analysed by each technique. This work alongside the leached samples from the Pickering work should identify the most suitable technique.

Table 9. The three formulations used by NNL.

| Metakaolin | SiO ₂ /K ₂ O | H ₂ O/K ₂ O | K ₂ O/Al ₂ O |
|------------|------------------------------------|-----------------------------------|------------------------------------|
| Metamax | 1 | 11 | 1 |
| Metamax | 1.2 | 13 | 1.2 |
| Metamax | 1 | 15 | 1 |

Results

Samples of Metamax potassium geopolymers of the NNL formulation 1.2/13/1.2 were prepared. From the initial observation of the preparation process, it was observed that at 10 wt% TBP/Dodecane there was a layer of liquid above the cement. It is likely that a quantity of oil was not incorporated in the geopolymer matrix and separated due to the unfavourably of the O/W emulsion. When the weight fraction of TBP/Dodecane was increased from 10 wt% to 40 wt%, there is a clear separation of the liquids with a significant quantity of the oil sitting above the cement. This suggests that the silica fume was not successful in aiding the immobilisation of the TBP/Dodecane by Pickering emulsion. In conclusion, there is a clear difference between the immobilisation of Nevastane and TBP/Dodecane within the potassium geopolymer. From initial observation, Nevastane looks to be immobilised successfully with the geopolymer matrix. Whilst, the TBP/Dodecane has separate out from the matrix which only gets worse as the weight percentage of the oil increases. Further characterisation will be vital to understand the nature of these samples and how they interact with the oil.

3. Way forward

Further experimental work is required to further understand the effects that the Pickering emulsion has of the organic oils.

Acknowledgements

The authors would like to express appreciation for the financial support of PREDIS project and the EPSRC GREEN CDT, and the constant support of the Cements@Sheffield team.

5.12 Results of oil and liquid scintillation immobilization with NNL formulation

*Esperanza Lara Robustillo, CIEMAT, Spain, esperanza.lara@ciemat.es
Eva M^a Márquez Franco, CIEMAT, Spain, evamaria.marquez@ciemat.es*

Keywords: Metamax, potassium activator, oil, liquid scintillation.

1. Introduction

Ciemat has participated in the study of immobilisation of organic liquid wastes, in particular industrial oil and scintillation liquid (Instagel). These wastes not only need to be managed according to their activity, but also according to their chemical content. The presence of organic liquids prevents the hydration of the cement and lead to structural defects that may allow the waste to leak out. This is one of the reasons for studying of new cementitious matrices for the immobilisation of this type of waste.

The formulation selected in task 5.3 was developed by NNL, based in metakaolin Metamax and potassium activator to immobilise, at least, 30% liquid organic waste.

2. Description of work and main findings

The immobilisation of the organic waste was carried out by adding the liquid waste to the prepared geopolymer (direct method). From the different variables affecting the formation of the geopolymer, the time and speed of stirring were optimised to obtain better geopolymer properties. The optimized time of stirring was 15 minutes for the geopolymer preparation. Then the waste was added at low speed until reach one hour of stirring. A homogeneous mixture of geopolymer and waste was obtained, so it was not necessary to use surfactants.

The cured were performed in endogeneous conditions to avoid the exchange of water with the surrounding environment (without saturation or evaporation of water) to simulate the real case of use of the geopolymer during the encapsulation of radioactive waste. The samples, wrapped in a film, were cured in a climatic chamber at 20 °C and 90% humidity until the mechanical strength assay.

The studies carried out for the characterisation of the manufactured geopolymers were mechanical strength, water stability and leaching tests.

Mechanical strength

The waste immobilisation was carried out with different percentages of the waste. The maximum amount of immobilised waste was considered as the one with a mechanical strength higher than 10 MPa after 28 days of curing. In this way it was possible to immobilise up to 30% in vol. of scintillation liquid and 40% vol. of oil.

The mechanical strength results with the immobilised waste are shown in Figure 54. In the case of the oil samples, the results are shown for 30 and 40% waste and the geopolymer without waste, while for the liquid scintillation samples, the results are shown for 10, 20 and 30% and the geopolymer without waste.

At least 3 prismatic samples were prepared and broken in half to obtain 6 data (UNE-EN 196-1:2005). The data with the largest deviation were discarded, but the average data obtained were at least 4 measurements.

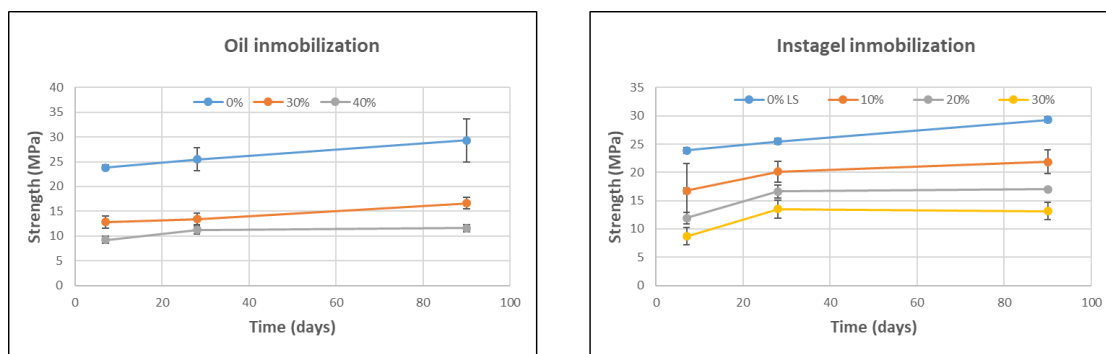


Figure 54. Mechanical strength results at different curing days and different content of waste.

The results show that as the amount of waste increases, the mechanical strength decreases with both wastes. It is also observed that the curing time does not significantly influence the mechanical strength after 28 days of curing in both types of samples.

Stability of geopolymer in water. Leachate measurements in milliQ water

In order to analyse how stable are the samples and if there is leaching of the waste immobilised in the geopolymer, leaching tests of the samples in milliQ water have been carried out. Cylindrical geometry samples with a height of 4 cm and a diameter of 2 cm were prepared. The leachant has to be totally renewed after 1, 3, 7, 10, 14, 21, 28, 35, 42, 72, 98, 126, 156, 182 until to reach 375 days from the start of the test.

The ratio between the volume of leachant and exposed area of specimen ranges from 10-20 cm. The specimen has to be totally- submerged in the leachant.

The analytical determinations on the leachant are: pH, conductivity and carbon content. Figure 55 shows the results of the carbon determination (Total Organic Carbon (TOC), Total Carbon (TC) and Inorganic Carbon (IC)) in both types of wastes. The graphs show that for the samples with oil the organic carbon content is non-existent in the leachate. In the case of the samples with scintillation liquid, organic carbon was measured in the leachate due to the diffusion of the organic molecules that form the waste. In addition, when stirring the leach solutions, foam formation was observed, indicative of the presence of surfactant contained in the Instagel.

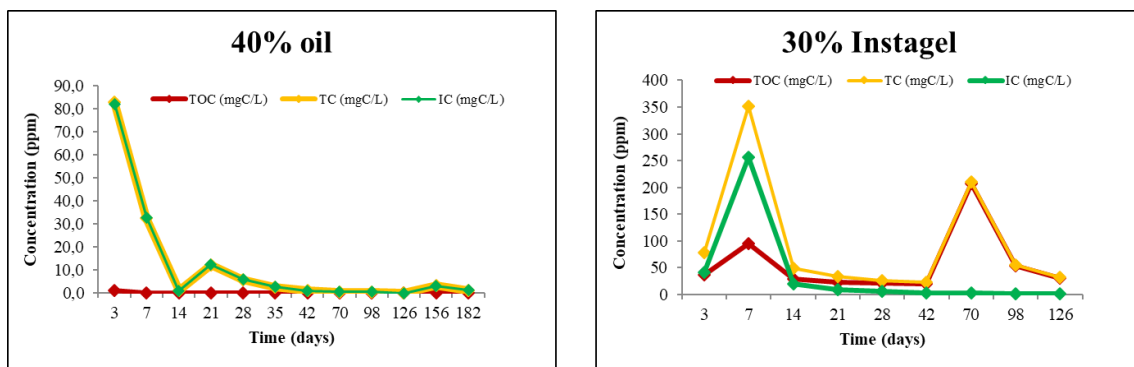


Figure 55. Studies of the carbon content in milliQ water in oil samples and Instagel immobilised with potassium geopolymer.

Due to samples containing Instagel leach, the use of Nochar was studied to try to avoid diffusion of the liquid scintillation’s components. The Nochar 910 is an efficient and effective polymer formulated to solidify oils, organics, solvents and other hydrocarbons into a solid mass for storage.

The polymer was impregnated with Instagel, in a 1:2 ratio. The results showed that the setting time was greatly increased, up to 2 days of hardening and the mechanical strength decreased appreciably, with a result of 4 MPa with 30% Instagel at 28 days of curing, being out of waste acceptance criteria.

3. Conclusions

The potassium geopolymer formulation based on the formulation developed by NNL shows very good mechanical characteristics, stability and immobilisation up to 40% in vol. of the immobilised industrial oil, but the immobilisation of liquid scintillation, although it presents good mechanical resistance (up 30% in vol.), shows a low stability in water, producing cracks and breakages soon after immersing the samples in water, and the leaching studies show that the components of the scintillation solution pass into the leachant. The use of Nochar to solidify the liquid scintillation make decrease the mechanical strength, with values below 10 MPa, so its use was discarded.

References

[1]. Duxon, P., Mallicoat, S.W., Lukey G.C., Kriven, W.M., Van Deventer, J.S.J., 2007c. The effect of alkali and Si/Al ratio on the development of mechanical properties of metakaolin-based geopolymers. *Colloids and Surfaces. A, Physicochemical and Engineering Aspects* 292, 8-20.

- [2]. Charles Reeb, Christel Pierlot, Catherine Davy, David Lambertin. Incorporation of organic liquids into geopolymer materials – A review of processing, properties and applications. *Ceramics International* 47, 7369-7385, 2021.

5.13 Innovations in liquid organic waste treatment and conditioning

Samantha Irving, NNL, samantha.irving@uknnl.com
 Martin Hayes, NNL, martin.hayes@uknnl.com

Keywords: Geopolymer, MetaMax®, Argicem®, Nevastane EP 100, TBP, Dodecane, Tween 80

1. Description of work and main findings from work at NNL/USFD

4L mixing trials incorporating both Nevastane EP 100 paraffin oil and TBP/ dodecane (70/30 vol/vol%) solvent mixture have been incorporated into two different geopolymer (GP) systems, one incorporating a pure, rotary calcined metakaolin (MK) powder (MetaMax®) and one containing a MK powder containing a relatively large quartz (SiO₂) fraction (Argicem®). The GP formulations tested were based on a potassium silicate/potassium hydroxide activator solution (K₂SiO₃/KOH) and covered a range of formulation ratios developed in previous UK studies. The formulation ranges assessed covered a SiO₂:K₂O ratio of 1.0–1.4, a H₂O:K₂O molar ratio = 11–15 and a K₂O:Al₂O₃ molar ratio = 1.0–1.5. In addition, preliminary scoping studies indicated that a surfactant (Tween 80) was required to incorporate TBP/dodecane solvent into both GP systems. The aim of the trials was to assess a range of Radioactive Liquid Organic Waste (RLOW) loadings that could be achieved for both organics tested using a preferred order of addition method for each RLOW which was determined from small scale (~160 mL) polypot studies. GP formulation studies were carried out at 4L scale, in which typical grout processing properties (fluidity, viscosity, residual bleed and set time) was assessed in addition to products cast and tested to assess preliminary product properties up to 90 d curing under endogenous conditions of 20±1 °C and > 90% RH.

Mixing methods:

Nevastane EP 100 4L Trials:

A total of thirty-seven 4L scale mixes were undertaken, covering both GP systems and incorporating 10–50 vol% Nevastane loading based on total GP wasteform volume in both GP systems. For each mix, in which components were stored at 20±1 °C prior to mixing, the appropriate amount of MK powder pre-cursor to give the correct K₂O:Al₂O₃ molar ratio for a particular mix was added to pre-prepared K₂SiO₃/KOH activating solution (including additional deionised water to give the correct H₂O:K₂O molar ratio) in a Hobart N50 planetary mixer with stirring over a 5 min period at 62 rpm. The mixer was stopped, scraped down to ensure all materials were incorporated into the mix, and then started again. At this point, Nevastane oil was incorporated into the grout while mixing over a 2 min period and mixing continued for a further 13 min at 62 rpm to give a total mix time from addition of MK powder of 20 min (defined as t=0). These were denoted as “low” shear mixes. Alternatively, after the initial mixing of activator solution and MK powder over 5 min at 62 rpm and scraping down the mix bowl contents, the grout mix was then transferred to a Silverson L5 mixer, Nevastane oil added over 2 min whilst mixing at 4500 rpm with a standard mixing head, with mixing then continuing for a further 13 min to give a 20 min total mix time from addition of MK powder (denoted as t=0). These were denoted as “high” shear mixes. The low shear mixes were all carried out at the mid-point formulation ratio of SiO₂:K₂O=1.2, H₂O:K₂O=13, K₂O:Al₂O₃=1.2 with a 20 vol% Nevastane loading. In addition, a further low shear mix was also carried out with 50 vol% Nevastane loading, with MetaMax® pre-cursor in the GP system to assess the effect of shear on mix properties at the highest Nevastane addition level.

TBP/dodecane (70/30 vol/vol%) 4L Trials:

A total of twenty-four 4L scale mixes were undertaken, with nineteen mixes undertaken using the MetaMax® GP system covering the full formulation envelope range (SiO₂:K₂O = 1.0–1.4, H₂O:K₂O = 11–15 and K₂O:Al₂O₃ = 1.0–1.5) and five mixes using the Argicem® MK powder at the mid-point formulation only (SiO₂:K₂O = 1.2, H₂O:K₂O = 13 and K₂O:Al₂O₃ = 1.2). All mix components were stored at 20±1 °C prior to mixing, with the greater focus on MetaMax® mixes resulting from improved performance characteristics observed in preliminary ~160 mL polypot studies in comparison to the Argicem® GP system. In these studies, 10–30 vol% TBP/dodecane loading based on total GP wasteform volume was assessed with a surfactant (Tween 80)

loading of 1–3 vol% (based on RLOW loading). TBP and dodecane (70/30 vol/vol%) of appropriate quantity for a given formulation were weighed into a Hobart bowl followed by the appropriate quantity of Tween 80. The bowl was transferred to a Silverson L5 mixer with emulsifying head attachment and mixed for 10 mins at 3500 rpm. This was defined as the **pre-emulsion** step. The bowl was then transferred back to the Hobart mixer where pre-weighed activator solution of appropriate quantity for the particular mix design was added to the planetary mixer whilst stirring at 62 rpm over a 2 min period. The MK powder to give the correct $K_2O:Al_2O_3$ molar ratio for a particular mix was then added gradually over a 5 min period with continued stirring at 62 rpm. The mixer was then stopped, scraped down to ensure all materials were incorporated into the mix and the Hobart bowl was transferred back to the Silverson L5 mixer and mixed for a further 13 mins using the standard mixing head at 4500 rpm to give a total mix time of 20 mins from addition of activator solution to the TBP/dodecane/surfactant solution. The culmination of mixing was again denoted as $t=0$.

Mixes were assessed as follows:

- Grout fluidity based on EN 13395-2 at $t=0$
- Grout viscosity at 106 s^{-1} using UK standard test and at 100 s^{-1} in accordance with ASTM C 1749 at $t=0$
- Initial and final set from $t=0$ in accordance with EN 196-3
- Bleed liquor at $t=0$ monitored as vol/vol% of total grout volume on 100 mL sealed samples at 24 h and 48 h. Samples stored at $20\pm 1\text{ }^\circ\text{C}$ and $> 90\%$ RH between measurements
- Heat of reaction from $t=0$ using isothermal conduction calorimetry at $25\text{ }^\circ\text{C}$, with data normalised to reactive material content in the mix (MK powder mass, KOH mass and K_2SiO_3 solids content mass)
- Compressive and flexural strength testing up to 90 d curing in accordance with EN 196-1, with samples cured at $20\pm 1\text{ }^\circ\text{C}$ and $> 90\%$ RH
- Dimensional stability of prism samples up to 90 d curing in accordance with ASTM C 490, with samples cured at $20\pm 1\text{ }^\circ\text{C}$ and $> 90\%$ RH

Summary of Results

Nevastane EP 100 Trials:

Encapsulation of up to 50 vol% loading was achieved for mid-point formulations ($SiO_2:K_2O = 1.2$, $H_2O:K_2O = 13$, $K_2O:Al_2O_3 = 1.2$) for both GP systems, including MetaMax® and Argicem® metakaolin powders, yielding products that achieved final set within 24 h. Low viscosity grouts were produced with high fluidity, with a trend of increasing viscosity and decreasing fluidity as the oil loading was increased. Mixes at the low point of the formulation range, $H_2O:K_2O = 11$ and $K_2O:Al_2O_3 = 1$, could not incorporate oil and should be avoided in future studies for these GP systems for this oil. Less than 1.25 vol% bleed was present at 48 h on mixes in which Nevastane could be incorporated into the GP system, although some bleed was present in the large majority of samples at 48 h, and bleed volumes tended to increase slightly between 24 h and 48 h curing. It was noted that at higher RLOW loadings (50 vol%) mixing methodology appeared important as Nevastane could be successfully incorporated in MetaMax GP at low shear but not under high shear conditions. The mixes were characterised by an initial high heat of dissolution of the MK powder followed by a much smaller secondary peak associated with the GP polymerisation reaction, and relatively high cumulative heats of hydration were obtained at $25\text{ }^\circ\text{C}$ for MetaMax® GP mixes (240–257 kJ/kg at 24 h curing for mid-point formulations) which will require further assessment on scale-up. These heat outputs are greater than typical UK PC formulations for Higher Active Waste encapsulation processes (~100 kJ/kg) and so the effects on resultant product performance characteristics with scale will need to be assessed. The data showed the effect of oil loading and shear was negligible on heat output based on reactive material content as defined.

Typical of GP systems, a significant proportion of the compressive strength was developed by 7 d which then plateaued and strengths of all products in which oil could be incorporated were deemed acceptable at 90 d curing ($>5\text{ MPa}$), up to 50 vol% Nevastane loading. As the oil loading was increased the compressive strength of the products was reduced. Flexural strength results showed more variability with curing time and all oil loadings but strengths of greater than 2 MPa at 90 d curing were obtained for all formulations in which Nevastane could be incorporated into the GP system which are considered acceptable. In addition, products showed moderate shrinkage at 90 d for both GP systems which are comfortably within historic accepted guideline values for PC blended grouted products. The shrinkage range was small ranging from 0.03–0.11% shrinkage at 90 d curing with negligible effect of shear for mid-point formulations, and the large majority of samples attaining stability by 90 d curing. However, it should be noted that a small number of samples (3 off) had not fully stabilised at 90 d and therefore longer-term monitoring was recommended in these cases. Further, ‘sweating’ was noticeable on the surface of a number of samples covering a range of formulations, although

of insufficient quantity to establish if any organic content was expelled. Hence, further optimisation of mix designs may be achievable.

TBP/dodecane (70/30 vol/vol%) Trials:

Encapsulation of up to 30 vol% TBP/dodecane loadings at a 70/30 vol/vol%) ratio was achieved with 1-3 vol% Tween 80 surfactant added to the RLOW prior to addition of GP mix components, to yield products that achieved final set within 24 h. As in the case of Nevastane mixes, this RLOW could not be incorporated into the MetaMax® GP system at the low H₂O:K₂O molar ratio = 11 and low K₂O:Al₂O₃ molar ratio = 1 point of the envelope at a 30 vol% RLOW loading and again indicates this region of the envelope should be avoided for this RLOW in future studies. The results showed that for mixes in which TBP/dodecane could be incorporated, high fluidity grouts could be produced which had viscosities of <1000 mPa·s. The trend showed that viscosity increased (and fluidity decreased) with increased RLOW loading. Less than 1.75 vol% bleed was observed on all mixes at 48 h in which RLOW could be incorporated across the range of formulations and GP systems studied, with less than 1.25 vol% bleed observed on mid-point mixes with a 20 vol% RLOW loading. However, there was a tendency for bleed to increase slightly between 24 h and 48 h and gelation of bleed was observed at formulations which had 3 vol% surfactant incorporated. The mixes were characterised by an initial heat of dissolution peak for the MK powder followed by a secondary peak associated with the GP polymerisation reaction, and again relatively high cumulative heats of hydration were obtained at 25 °C for MetaMax® GP mixes (247–250 kJ/kg at 24 h curing for mid-point formulations) which will again require further assessment on scale-up. In the case of MetaMax® mixes there appears a reduction in heat output and elongation of the polymerisation reaction as the SiO₂:K₂O molar ratio increases from 1.0–1.4. The data showed the effect of oil loading appeared less significant on heat output based on reactive material content as defined.

Typical of GP systems, a significant proportion of the compressive strength was again developed by 7 d curing. The strengths for all products in which TBP/dodecane could be incorporated were considered acceptable against historic guideline values for cemented products, with MetaMax® mixes exhibiting increased strength in comparison to Argicem® mixes at equivalent mid-point formulations with 20 vol% RLOW loading. Strengths also reduced with increased RLOW loading as expected. At the mid-point formulations MetaMax® products showed flexural strengths of 1.9–2.8 MPa at 90 d, and Argicem® mid-point mixes had strengths between 2.0 and 3.5 MPa at 90 d curing, both of which are considered acceptable. However, it was noted that the flexural strength for both GP systems dropped from 28 to 90 d, which was not observed in compressive strength data and, whilst reasons for this behaviour are not clear at present, it is possibly arising from microcracking within the geopolymer product structure.

Products showed dimensional changes at 90 d for both GP systems which are within historic accepted guideline values for PC blended grouted products, with shrinkage values ranging from 0.05% – 0.15% obtained for MetaMax® mid-point formulations at a 20 vol% RLOW loading and Argicem® products ranging from 0.06% expansion and 0.12% shrinkage over a 10–30 vol% TBP/dodecane loading. However, several samples had not fully stabilised at 90 d curing, although there was no sign of any loss of integrity of the samples, or, in contrast to Nevastane mixes, any evidence of TBP/dodecane expulsion at 90 d curing suggesting good incorporation of RLOW.

2. Conclusions

GP systems based on both MetaMax® and Argicem® MK powders appear possible alternative encapsulation matrices for the RLOW tested, in which up to 50 vol% Nevastane oil and 30 vol% TBP/dodecane solvent (70/30 vol/vol%) have been encapsulated in mid-point formulations (SiO₂:K₂O = 1.2, H₂O:K₂O = 13, K₂O:Al₂O₃ = 1.2) to give products with generally acceptable properties up to 90 d curing. However the TBP/dodecane solvent required the addition of a surfactant (Tween 80) into the mix design to enable successful incorporation of this RLOW.

Both GP systems produced small amounts of residual bleed on setting in a large majority of mixes, with a tendency for a slight increase in bleed from 24 h to 48 h curing. In addition, some evidence of ‘sweating’ of a small volume of liquid across a range of formulations for Nevastane oil samples was observed. Hence, further optimisation of mix design (change/add- surfactant) or mix method may serve to further improve product performance.

Longer term monitoring of samples required to ensure long term RLOW retention is established and product dimensional stability attained for those mixes that had not achieved stability by 90 d curing.

Acknowledgements

PREDIS project and Sellafield Ltd for funding these studies.

5.14 Study of direct conditioning process

*Andrea Santi, Eros Mossini, Gabriele Magugliani, Francesco Galluccio, Michele Brini, Elena Macerata, Marco Giola, Mario Mariani
Politecnico di Milano, Italy
Corresponding author: eros.mossini@polimi.it*

Keywords: radioactive liquid organic waste, conditioning, waste acceptance criteria, geopolymer, tuff

1. Introduction

Within Task 5.3, POLIMI contributed to Sub-task T5.3.2 “Formulation of conditioning materials: feasibility study & screening of conditioning options” and Sub-task T5.3.4 “Investigation of reference formulations with real RLOW”. Within T5.3.2, POLIMI has been asked to investigate alternative approaches for the incorporation of organic liquids in tuff-based geopolymers exploiting preliminary emulsification or impregnation steps. For the emulsification strategy, the use of surfactant Tween80 was tested. The impregnation approach was investigated with greater efforts, to differentiate the work from other partners. As absorber, recycled polyurethane (rPU) was first proposed, but discarded afterwards due to incompatibility with the alkaline geopolymeric grout. As an alternative, the commercial N910 polymer has been investigated, with both POLIMI’s tuff-based geopolymer and SCK CEN’s BFS-based formulation. Within T5.3.4, POLIMI has been asked to investigate the reference formulation with real waste. So far, the work consisted in the characterization of the available real waste, in terms of physico-chemical properties and radiological content.

2. Description of work and main findings

Within T5.3.2, two challenging organic liquids have been considered as surrogate waste: 30%v. tributyl phosphate in kerosene (TBP-k) and Ultima Gold LLT liquid scintillation cocktail (UG-LSC). Weighed amounts were absorbed on rPU or N910 polymer at different weight ratios and then encapsulated in tuff-based geopolymeric grouts prepared following the already published method [1]. Few samples were also prepared with the BFS-based formulation developed by SCK CEN. Compression tests were performed following UNI EN 12390-3:2019 on cubic specimens (5-cm sized). Static water-immersion tests were performed following ANSI/ANS-16.1-2003 protocol, by immersing almost equilateral cylindrical samples (2.8-cm sized) in ultrapure water for one month. The leachates were characterized to assess the released of matrix constituents and organic matter. Examples of cubic samples are reported in Figure 56.



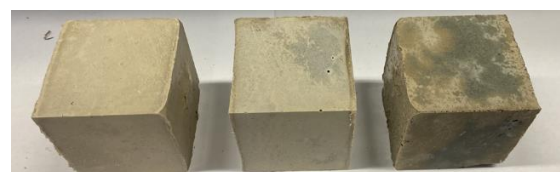
a) Geopolymer samples containing 0, 5, and 10 %wt. of rPU.



b) Geopolymer samples containing rPU previously pre-impregnated with 10, 10, and 20 %wt. of TBP-k.



c) Geopolymer samples containing rPU previously pre-impregnated with 10, 10, and 20 %wt. of UG-LSC.



d) Geopolymer samples containing N910 previously pre-impregnated with 0 or 10 %wt. of UG-LSC or TBP-k.

Figure 56. Picture of tuff-based geopolymer encapsulating organic liquids pre-absorbed on rPU or N910 polymer.

As clearly visible in the pictures, the samples containing rPU presented evident cavities and defects. Moreover, a non-negligible amount of organic liquid has already been released during setting and curing. The cause was attributed to rPU degradation in alkaline medium, as demonstrated by X-Ray Diffraction and ThermoGravimetric Analysis. The low density and high porosity of rPU samples affected the mechanical properties. Indeed, the compressive strength was compromised by the addition of rPU and organic liquids, dropping far below the Waste Acceptance Criteria (WAC, 10 MPa). The specimens were not stable toward 1 month of water immersion, and release of organic liquid was evident. Replacing rPU with N910 solved the issues of cavities formation and organic liquid bleeding. Hence, the compressive strength was higher, but still not compliant with the WAC for TBP-k. The issue was linked to N910 swelling when in contact with TBP-k, generating a gel difficult to be homogeneously incorporated into the geopolymer matrix. Different protocols have been tested. The most promising seemed to be skipping the pre-impregnation by mixing the powders – N910 polymer and geopolymer precursors – directly with the liquids – activation solution and RLOW. This absorbing material resulted in higher stability during water immersion than rPU, as evidenced from limp leachates and stable specimens. Besides, to further improve the compressive strength, preliminary attempts were made by replacing the tuff-based geopolymer with the BFS-based formulation. The compressive strength promisingly reached the WAC, with 10 %wt. of waste loading.

Within T5.3.4, the real radioactive liquid organic waste (RLOW) available at POLIMI have been collected:

- Solvent: kerosene + 5% 1-octanol, containing complexing ligand and 1-100 kBq/L of ^{241}Am , ^{244}Cm , and ^{152}Eu ;
- LSC: «aqueous» cocktails mainly containing ^3H , ^{63}Ni , ^{137}Cs (about 1-1000 Bq/L) and «organic» cocktail for organic solutions containing TBP and natural uranium (about 10 Bq/L).

Given the real RLOW available and the results provided by T5.3 colleagues, the metakaolin (MK)-based formulation developed by NNL has been selected. The waste is being characterized, especially to accurately determine the water and radionuclides content. These data will be important for the sample preparation and for the leaching tests.

3. Conclusions

Within T5.3.2, further experiments are needed to confirm the promising properties of N910 as RLOW absorber. The new mixing protocol and the use of BFS-based formulation will be investigated, especially to improve the waste loading while still meeting the WAC.

Within T5.3.4, the experiments of encapsulation of real RLOW into MK-based formulation will be performed. In particular, different waste loading factors will be tested. Some issues, such as adjustment of water content (for real RLOW already containing water) and optimization of surfactant (for real RLOW more lipophilic than those tested by T5.3 colleagues), will be faced. The leaching experiments will be performed following the ANSI/ANS-16.1-2003 protocol, preliminarily using ultrapure water as leachant.

References

- [1] A. Santi, E. Mossini, G. Magugliani, *et al.* “Design of sustainable geopolymeric matrices for encapsulation of treated radioactive solid organic waste”. *Frontiers in Materials* 9, p. 1-17 (2022). DOI: <https://doi.org/10.3389/fmats.2022.1005864>

5.15 Study of conditioning matrix performances

Andrea Santi, Eros Mossini, Gabriele Magugliani, Francesco Galluccio, Michele Brini, Elena Macerata, Marco Giola, Mario Mariani
Politecnico di Milano, Italy
 Corresponding author: eros.mossini@polimi.it

Keywords: radioactive liquid organic waste, conditioning, waste acceptance criteria, geopolymer, tuff

1. Introduction

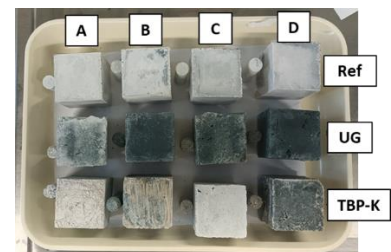
Within Task 5.4, POLIMI contributed to Sub-task T5.4.6 – “Study of radionuclides binding and leaching”. POLIMI has investigated the influence of organic substances, present in radioactive liquid organic waste

(RLOW), on radionuclides binding and leaching. The experiments have been performed on SCK CEN's BFS-based formulation.

2. Description of work and main findings

The experiments on BFS-based formulation were performed using the same raw materials and protocols of the developer (SCK CEN). Three series of samples were prepared: 1) without organic liquids for reference; 2) containing 10 %wt. of Ultima Gold LLT liquid scintillation cocktail (UG-LSC); 3) containing 10 %wt. of PUREX solvent (kerosene + 30 %v. tributyl phosphate). To emulsify the organic liquid waste and the activation solution, 0.5 %wt. of surfactant (Tween80) was used in a planetary mixer. Nevertheless, being the emulsion unstable, an in-oven curing (50 °C) of few hours was performed to partially set the grout and improve the incorporation of the organic liquid. On the other hand, beside complicating the preparation protocol, this step makes the casting more problematic due to the increased viscosity of the partially set grout. Compression tests were performed following UNI EN 12390-3:2019 on cubic specimens (5-cm sized). To investigate the effect of gamma irradiation and/or water immersion on the compressive strength, some samples were irradiated by a Co-60 source (dose rate of 2.5 kGy/h) up to 200 kGy and/or immersed in water for 1 month, following the scheme reported in Figure 57. The compressive strength of the reference samples resulted to be slightly degraded by irradiation, more by water immersion, still meeting the waste acceptance criteria (WAC, 10 MPa for the Italian regulator) with reassuring safety margin. Conversely, the addition of surrogate RLOW dropped the mechanical strength below the WAC.

| Sample #A | Sample #B | Sample #C | Sample #D |
|---------------|-------------------------|---------------|-------------------------|
| Curing (28 d) | Curing (28 d) | Curing (28 d) | Curing (28 d) |
| Storage | Storage | 200kGy | 200kGy |
| Storage | Immersion (28 d) | Storage | Immersion (28 d) |
| Compression | Compression | Compression | Compression |



a) Legend of the samples prepared for the compressive strength tests.

b) Three series of samples prepared.

Figure 57. Scheme and pictures of the prepared BFS-based geopolymers samples.

Semi-dynamic water-immersion tests were performed following ANSI/ANS-16.1-2003 protocol on almost equilateral cylindrical samples (2.8-cm sized) containing some contaminants (including Cs, Sr, Co, Ni, U, Th, Ce, Eu...), representative of fission or activation products. The leachant was ultrapure water at 22 ± 2 °C, periodically renewed according to the protocol, for a total duration of 3 months. The leachates have been tested for pH and conductivity. ICP-OES and ICP-MS analyses were performed to determine constituents (including Na, K, Ca, Si, Al...) and contaminants release, respectively. Moreover, COD was evaluated to assess the organic release. The leachability indices of constituents and contaminants are well above the WAC (equal to 6 for the Italian regulator), regardless of whether the sample contains the organic liquid waste or has been gamma irradiated. Remarkably, the irradiation seems to limit the release of organic material. This result deserves further studies.

3. Conclusions

Some experiments with BFS-based formulation will probably be repeated with a high-shear mixing device, with the purpose of improving the emulsification step, possibly avoiding in-oven curing to obtain more easily castable samples. This would allow to obtain more homogeneous samples with better mechanical properties.

Similar experiments on the metakaolin (MK)-based formulation will start soon. The raw materials have been procured and preliminary meetings with partners have been performed to get acquainted with the protocol. The need for high-shear mixer has been evidenced. The experiments on the so-called MIX-based formulation (containing MK, blast furnace slag, and fly ash) will start once the other Partners have completed the preliminary investigations and provided the raw materials.

6 Scientific progress in Innovations in solid organic waste treatment and conditioning (WP6)

6.1 PREDIS 4th Workshop GSL WP6 update

Callum Eldridge & Shivangi Prasad, Galson Sciences Ltd, UK, ce@galson-sciences.co.uk

Keywords: Life cycle assessment, LCA, value assessment, disposability, solid organic waste

1. Introduction

Radioactive Solid Organic Waste (RSOW) is a prime candidate for thermal treatment as significant waste volume reduction can be realised. The properties of certain thermally treated RSOW can be challenging to dispose of using conventional cementation due to properties that affect the setting of grout or are not well immobilised by the cement matrix. WP6 of the PREDIS project investigates various immobilisation technologies for thermally treated wastes as well as developing certain thermal treatments.

The work presented here consists of three tasks:

- Input into the LCA work being undertaken in WP2;
- development of summaries of thermal treatment technologies and key data; and,
- economic, environmental and disposability impacts of novel treatment technologies.

The first task is complete, having delivered the input in Milestone 44. The other two tasks are underway and primarily focus on preparatory work.

2. Description of work and main findings

LCA Case Study Input

Work over the past year has focused on the provision of case study input to the LCA being undertaken in Work Package 2. A major complication is the diverse set of initial wastes, end points and paths which can be considered in WP6, which includes both thermal treatment and conditioning steps.

A meeting was arranged including the respective leads for WP6 and the LCA case study to identify which processes studied within the PREDIS project to target. The outcome was the decision to focus on treatment of ashes arising from the IRIS process, which is being pursued within WP6 with three technologies:

- Hot-Isostatic Pressing (HIP) at the University of Sheffield
- Encapsulation in Geopolymer at Politecnico di Milano
- Compaction at CEA

The common starting point for each of these processes (inactive ashes from the IRIS process developed at CEA) enables the processes to be directly compared against each other. Which is not possible for the full range of technologies pursued in WP6 due to the diversity of input waste types.

A questionnaire was developed to collect information salient to the LCA case study and circulated to the groups developing treatment technologies and to CEA for information about the IRIS process. The questionnaire collected data about the values for raw material inputs, energy inputs, waste loadings, secondary waste streams and final product characteristics.

The returned questionnaires were synthesised into a spreadsheet recording the data provided by the experimentalists, an excerpt of this sheet is shown in Figure 58. In some places the required data were not available and assumptions needed to be made to derive representative values. Where this occurred, the source and derivation of the presented values was recorded. Part of the sheet was also used to scale the processes to equivalent volumes to make them comparable. The spreadsheet and underlying questionnaires were shared with the LCA case study team lead as well as being made available in the PREDIS [Teams group for Task 6.7](#).

| Process, organisation and description | | Waste | | Material Inputs | | Provided values | | Product | | Energy Used | | Energy Used | | | | |
|---------------------------------------|------------------------------|--------------|--------------|-------------------------------|--|-----------------|--------------------|------------------|-------------|---------------|--|--------------------------|-----------------------|-----------------------------|---------------|-----------------|
| Operational Process | Treatment Method | Total Amount | Waste Unit | Waste Comments | Components | Amount | Unit | Output | Amount Unit | Waste Loading | Waste Category | Energy Used | unit | Comment | | |
| CEA | IRS | 4 | kg/h | The solids are composed of... | Nitrogen | 0.6 | Nm ³ /h | Ashes | 111 | g/h | N/A | The ashes produced | 120 | kJ/h (hour processing 1kWh) | | |
| University of HIP | Hot Isostatic Pressing (HIP) | 0.16 | kg per cycle | Total for all 8 canisters | stainless steel, per cycle (8 canisters) | 0.864 | kg | HIPed canisters | 1.024 | kg | 100% (51.2 vol %)/ HIP canisters, assume | 0.8 | kJ/h | Electricity/level | | |
| | | | | | Argon, per cycle (8 canisters) | 5.5 | m ³ | | | | | 43.2 | kJ/h | Electricity/bak | | |
| | | | | | | | | | | | | 15.5 | kJ/h | Electricity/HIP | | |
| | | | | | | | | | | | | 26.4 | kJ/h | Electricity/level | | |
| | | | | | | | | | | | | 1.3 | kJ/h | Electricity/HIP | | |
| | | | | | | | | | | | | 4.4 | kJ/h | Electricity/HIP | | |
| | | | | | | | | | | | | 4 | kJ/h | Electricity/HIP | | |
| | | | | | | | | | | | | 0.8 | kJ/h | Electricity/HIP | | |
| Polys | Encapsulation | 80 | kg Per 2000 | scaled from encapsulation | Zedtic Vibratic Tull (ZVT) | 3.36 | kg per 2000 drum | Geopolymerised | 200 | 400 | kg | 20% | The resulting product | 20 | kJ/h | IRS waste gen |
| | | | | | ground granulated blast furnace | 56 | kg per 2000 drum | | | | | | | 4.02 | kJ/h | Mixing of geop |
| | | | | | Ryask (FA, 14 wt%) | 56 | kg per 2000 drum | | | | | | | 4.02 | kJ/h | Cement mixing |
| | | | | | sodium hydroxide (7 wt%) | 28 | kg per 2000 drum | | | | | | | 3 | kJ/h | coating chamber |
| | | | | | water (30 wt%) | 100 | kg per 2000 drum | | | | | | | 9 | kJ/h | Water fill drum |
| | | | | | aluminium oxide (predominant) | 24 | kg per 2000 drum | | | | | | | 4.6 | kJ/h | handling oper |
| CEA | Compaction | 0.5 | g/ pellet | | none | | | cemented drum of | 0.5 | g | 100% | density of pellets: 1.58 | 0.034 | kJ/Mg | assume 2.2 kJ | |

Figure 58. Except from the LCA case study input spreadsheet.

Development of summaries of thermal treatment technologies and key data (Task 6.2)

Issues using non-public THERAMIN Deliverables have meant that the Task 6.2 listed in the grant agreement had to be rescoped to include only publicly available data. The new task will develop a high-level summary of wastes in the form of a report rather than a database, summaries will also be developed for each thermal treatment technology considered in WP6 and THERAMIN [1] as well as other thermal treatment technologies not within scope of either project.

Technologies within PREDIS for which data sheets have been developed include:

- Incineration / Gasification;
- Hot Isostatic Pressing HIP;
- Plasma Incineration;
- Molten Salt Oxidation; and,
- Wet Oxidation.

Technologies considered in THERAMIN for which datasheets have been developed include:

- SHIV A;
- In-Can Melter;
- Thermal Gssification;
- GeoMelt;
- HIP; and,
- Vitrification.

Further technologies that might be considered include:

- Calcination;
- Microwave;
- Plasma Arc;
- Pyrolysis;
- Thermal desorption;
- Thermochemical; and,
- Low temperature oxidation technologies including acid digestion and chemical oxidation.

The final datasheets on each of these technologies will describe how the technology works, the wastes it is appropriate for, the composition of the treated product and, if relevant, the applicable conditioning steps which would be required to make the product disposable.

Economic, Environment and disposability impact (Task 6.7)

This task will deliver a report on the economic, environmental and disposability impacts of novel treatment technologies for low-level and intermediate-level solid organic wastes. Work to-date has focused on defining the information need from experimentalists and the approach to be undertaken to evaluating the economic, environmental and disposability impacts.

Treatment and conditioning options will be grouped into a set of process flows, each of which take a waste from its initial form to a disposable condition (e.g. incineration, compaction then cementation in a disposal container). The evaluation of the impacts will consider the overall impacts of the grouped process.

Economic and environmental impact will be evaluated by both including quantitative outputs from the LCA task, as well as qualitative judgements informed by a value assessment workshop. The value assessment workshop will draw on the scoring criteria developed for THERAMIN [1] to rate operational safety, environmental impact, timescale, technical readiness, strategic impact, disposability and strategic cost impact as compared to a baseline solution (e.g. cement encapsulation). The content and structure of the value assessment workshop for WP6 will be developed in collaboration with the other work packages.

Disposability impacts will be evaluated by adopting a disposability assessment approach which will break the assessment into a series of smaller evaluations. The long list of evaluation areas to consider are:

- Nature and Quantity of Waste;
- Wasteform;
- Container Design and Storage Conditions;
- Container integrity and Durability;
- Impact Accident Performance;
- Fire Accident Performance;
- Data Recording;
- Management System;
- Policy;
- Concept Compatibility;
- Criticality Safety;
- Nuclear Security;
- Nuclear Safeguards; and,
- Sustainability.

These assessment areas will be screened to eliminate those which are not relevant and the remaining set will be evaluated against each process and the baseline. A further step will undertake a high-level post closure safety assessment for each wasteform, evaluating the natural evolution and human intrusion scenarios.

3. Summary and way forward

Overall, progress has been made against each task. The delivery of the LCA case study input and development of treatment data sheets will help to inform the planning and preparation for the economic, environmental and disposability task.

Further work in Task 6.2 will focus on collecting relevant data supporting volume reduction, long term behaviour and the composition of the treated products of the different technologies and on synthesising the data into a report. Further work in Task 6.7 includes developing the content of the value assessment workshop and undertaking disposability assessment of the thermally treated and conditioned products.

Acknowledgements

Thanks to Helene Nonnet (CEA), Samuel Walling (University of Sheffield), Eros Mossini (Politecnico di Milano), Thierry Mennecart (SCK CEN) and Laurence Stamford (University of Manchester) for their collaboration on the LCA case study task.

References

- [1] THERAMIN Project, *THERAMIN Project Synthesis Report*. THERAMIN Deliverable no. D5.4, June 2020

6.2 Densification and encapsulation of ashes from incineration of RSOW from IRIS process: characterizations of the samples and launch of the short term durability tests (WP6, tasks 3, 4, 5 and 6)

Hélène NONNET, Virginie ANSAULT

CEA, DES, ISEC, DE2D, Univ Montpellier, Marcoule, France

helene.nonnet@cea.fr

Keywords: RSOW, ashes, compaction, molten glass coating, SEM

1. Introduction

This paper summarizes the work carried out since the last workshop. Complete SEM characterizations of the conditioned ashes produced by molten glass coating and densification process have been achieved. The best matrices in terms of microstructural homogeneity and ability of waste encapsulation have been selected for the leaching tests evaluations. Short term leaching tests on two types of samples started in December 2022. First analysis have been available at end of April and have been briefly presented. In addition, two communications have been produced by USFD and POLIMI involving the IRIS ashes produced and delivered to the partners [1, 2].

2. Microstructural observations of the initial ashes and conditioned waste

SEM and structural characterizations have been done. The micro particles have a very porous aspect and are partially amorphous. The crystallized phase are composed of ringwoodite, anohrtite and chlorapatite $\text{Ca}_5(\text{PO}_4)_3\text{Cl}$

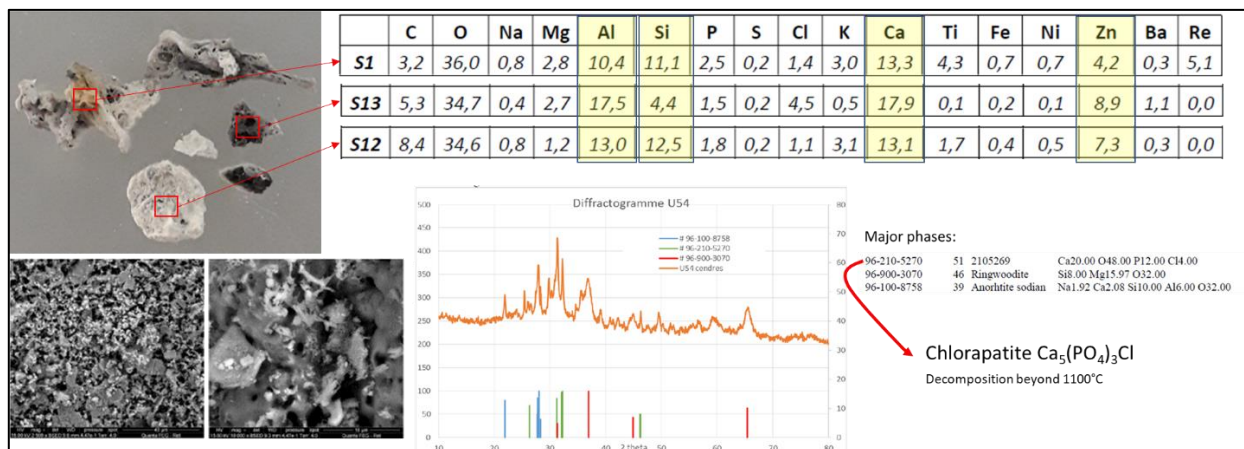


Figure 59. SEM and XRD characterizations of the IRIS ashes.

a. SEM observations of the densified pellets and granulates

- The immobilization of the ashes waste is studied according to different routes, with the objective to get a densified monolith.
- The first route is compaction and granulation. Ashes have been shaped to get pellets or granulates obtained either starting from the raw ashes, either from a mix of ashes and glass as vitrification agent.
- The pellets and the granulates are then heat-treated at 1100 °C during 3 hours to get a densified and sintered monolith.
- SEM observations have been achieved on the sintered samples.

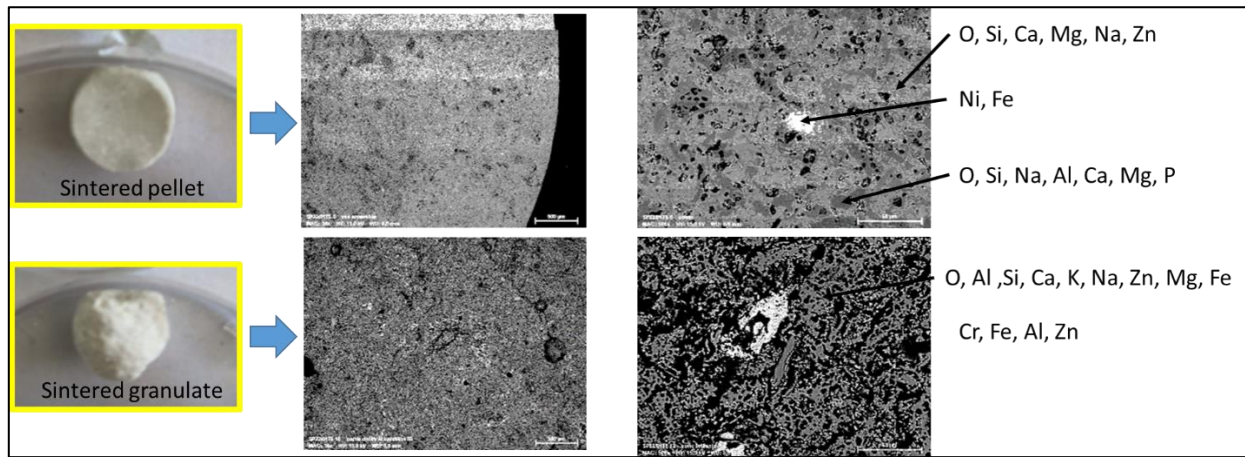


Figure 60. SEM observations of the sintered pellets and granulates.

- The microstructure of the densified samples has been achieved. For the sintered pellets 3 main phases are observed and the material is relatively dense with low porosity. As for the sintered granulates, only mainly 2 phases are observed with very large porosities.

b. SEM observations of the molten glass coating samples

The second route is the molten glass coating, using a glass in order to catch the ashes inside the glass. The idea here is to use low temperature melting glass, in order to avoid the volatilization of radionuclides and to get a monolithic form.

Specific glass frit made of sodium, silicon and boron having a very low melting temperature, has been carried out various morphologies both of the glass adjuvant and the ashes have been tested, as various mix ratio in order to assess the best way of shaping. The best macroscopic results have been achieved for the ratio ashes/glass 30/70 and 40/60. These 2 samples have been observed at microstructural scale (Figure 61, Figure 62).

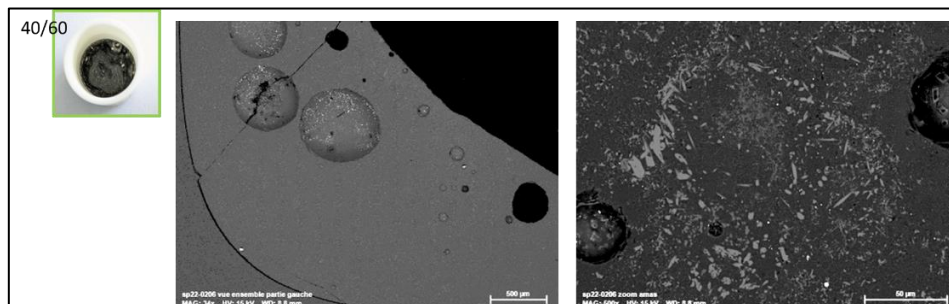


Figure 61. SEM observation of the molten glass sample 40/60 ratio (ashes/glass)

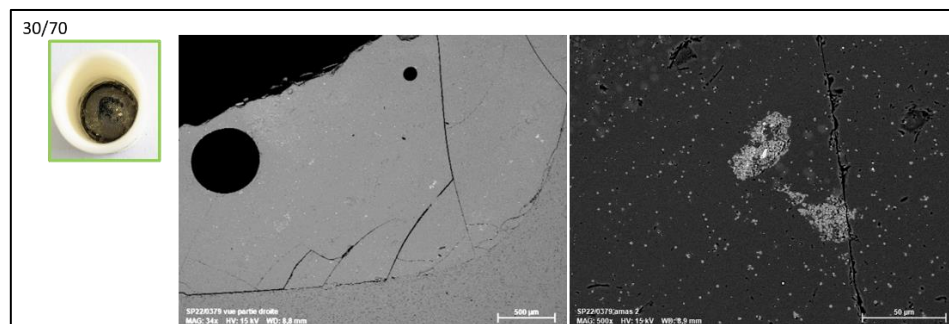


Figure 62. SEM observation of the molten glass sample 30/70 ratio (ashes/glass)

In the 40% load sample (Figure 61), we observe some millimetric bubbles included into the glassy matrix. Many crystals are imbedded inside these bubbles and also distributed everywhere inside the glassy matrix. The matrix is mainly composed of Si, Na, Al and Ca. The crystals are mainly made of P, Na and Ca.

Less bubbles are observed in the 30% load and the crystalline phases are more regularly distributed inside the glass matrix. No crystals are observed inside the bubbles. The glass matrix is also composed of Si, Na, Al and Ca. The crystals are mainly made of P, Na and Ca.

These microstructural observations led us to pick preferentially the sintered pellet and the 30% load molten glass for the leaching tests evaluations. Both seem to be the best densified and encapsulated forms of the waste.

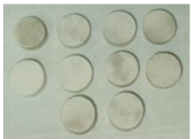
3. Stability testing (short term leaching experiments)

Short-term semi-dynamic leaching tests are performed according to the reference protocol defined by all partners and described in the Milestone 39.

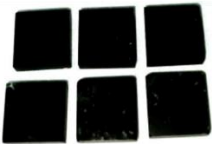
The samples are leached in a glove box under Ar at 22 ± 2 °C using a high pH solution (12.7 ± 0.2) containing potassium, calcium and sulphates. The sample surface area to solution volume is fixed to 10 m^{-1} by using 15 mL of leaching solution. Regularly, the solution is refreshed to prevent the accumulation of the elements released by the samples, which leads to a decrease of the affinity, and thus to a decrease of the dissolution rate. pH is measured and the elemental concentrations are measured by ICP/MS. The concentrations of the monomeric Si concentration is also determined by UV/Visible spectrophotometry.

From several square rods of 10 mm tablets were prepared by using a Minitom machine and Isocut fluid as cooling fluid. Then, the tablets were cleaned with ethanol, and dried overnight at 50 °C. Before starting the leaching tests, the unaltered samples were characterized by SEM-EDX and XRD (§2). SEM observations of the leached samples will also be achieved.

Densified pellet + thermal treatment





Molten glass coating 30/70



PREDIS leaching protocole: semi-dynamic leaching tests
(milestone 36)

- Glove box under inert atmosphere
- Savillex 60 ml ; S/V 10 m^{-1} ; 22°C
- synthetic cementitious water (50 mL of KOH 1 M; 1.886 g of K_2SO_4 ; 0.0774 g of $\text{CaSO}_4 \cdot 2\text{H}_2\text{O}$; Degassed Milli-Q® water)
- Sampling at 3, 7, 14, 21, 28, 56 et 91 day,
- filtration 0,45µm and acidification,
- Changing of the solution at each sampling
- B, Si, Na, Al, Zn analysis

Started: 2 Dec 2022 -> 3 March 2023
Analysis received 17 April 2023

Figure 63. Leaching samples and protocole for the short term tests.

First results were available at the very beginning of May 2023. They will be presented in more details during the next workshop of 2024.

4. Summary and way forward

The different ways of encapsulation have been achieved, testing densification process and molten glass coating. For densification, the most promising process seems to be the pellet shaping followed by a thermal treatment at high temperature to reach high-density material. For molten glass coating, the ratio 30/70 ashes/glass seems to be the most sensible way to get a correct waste encapsulation.

Short terms durability tests have been achieved and the results are going to be analysed.

The chemical durability of the samples will be compared to those obtained for other waste forms developed for solid organic low and intermediate level waste (e.g. geopolymers).

Acknowledgements

We would like to acknowledge Virginie Ansault (CEA DES/ISEC/DPME/SEME/LFCM) and Marie FENARD (CEA DES/ISEC/DPME/SEME/LFCM) who achieved the technical experimentations and the preparation of the leaching solution.

References

- [1] Santi Andrea, Mossini Eros, Magugliani Gabriele, Galluccio Francesco, Macerata Elena, Lotti Paolo, Gatta Giacomo Diego, Vadivel Dhanalakshmi, Dondi Daniele, Cori Davide, Nonnet H el ene, Mariani Mario "Design of sustainable geopolymeric matrices for encapsulation of treated radioactive solid organic waste" *Frontiers in Materials* VOLUME=9 YEAR=2022
URL=<https://www.frontiersin.org/articles/10.3389/fmats.2022.1005864>
DOI=10.3389/fmats.2022.1005864
- [2] Densification of nuclear waste incinerator ashes via Hot Isostatic Pressing Sam A. Walling*, H el ene Nonnet**, and Claire L. Corkhill* *NucleUS Immobilisation Science Laboratory, Dept. of Materials Science and Engineering, The University of Sheffield, UK **CEA, DES, ISEC, DE2D, Univ. Montpellier, Marcoule, France; poster MRS Fall Meeting Dec 2022

6.3 Gasification of Solid Organic Radioactive Waste

Yuri Zabulonov, Alexander Puhach, Borys Zlobenko

SI "Institute of Environmental Geochemistry" NAS of Ukraine, Kyiv, Ukraine

Email: 1952zyl@gmail.com

Keywords: gasification, plasma torch, cation exchange resins, radioactive waste

1. Introduction

When decommissioning nuclear facilities, it is necessary to process large volumes of solid organic radioactive waste, an industrial problem. Over the past few years, there have been several innovative projects to develop specific heat treatment processes [1–3]. The State Institution "Institute of Environmental Geochemistry" NASU (IEG) research group and partners have worked for several years to develop a hybrid process of gasification of IER with after-ash incineration by plasma torch and gas cleaning technologies for different applications.

These studies at the frame PREDIS focused on the gasification conditions that allow the retention of radioactive elements in a residue. Gasification – conversion of organic carbon-containing material to a gaseous product, with (0,9...0,1) limited oxygen available. One of the most promising areas that meet the requirements of environmental safety is the use of plasma technologies. The difference between the plasma technology of S. V. Petrov and other plasma waste processing processes is water vapour as a plasma-forming gas. Vapor-plasma conversion ensures complete thermal and concentration uniformity throughout the workspace. The plasma treatment process provides environmentally friendly waste processing without the formation of tar, dioxins, aerosols, etc. When IER is gasified with water vapour at high thermodynamic parameters, no sulfur compounds are in the gas phase – it entirely remains in the ash (slag).

The IER combustion method determines the gasification process's temperature for gradually converting mobile and volatile Cs nuclide into inorganic and thermally stable compounds. The transition time and the rate of temperature rise of the thermal process were optimised by conducting a preliminary thermogravimetric analysis. The combustion has carried out at different temperatures. The IEG developed innovative equipment for effective deep thermal treatment of waste containing organic substances and shows that the first must be into a gasification step at a temperature of 600– 800 °C to remove the significant organic gaseous compounds and then plasma torches incineration (1600 °C) till complete mineral ash. The radioactive ashes have been processed into solid waste forms.

2. Description of work and main findings

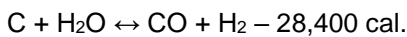
There have been many studies of conventional thermal treatment technologies such as incineration and other similar processes, which combust or gasify most organic constituents to final ash and have led to a very large volume of off-gas bearing unburned hydrocarbons, toxic, acid gases and vapourisation of radioactive elements. These processes result in a significant decrease in the volume of the final waste form.

Steam plasma gasification does not lose its destructive efficiency with a change in the moisture content of the IER. In the work of Dobrohotov N. N., three defining reactions for the main process are considered:

- the furnace at the bottom of the generator $C + O_2 + 3.8 N_2 = CO_2 + 3.8 N_2 + 97,650 \text{ cal};$
- decomposition of carbon dioxide in the next highest level of the generator



- decomposition of water vapour by hot carbon in the level water gas reaction



An essential gasification problem is the completeness of thermal treatment, which allows removing organic substances from IER without releasing large amounts of radionuclides. Fundamental experiments have refined the pyrolysis characteristics of anion- and cation-exchange resins. Introducing the principle of a multi-circuit gasifier in waste processing gives more profound destruction of waste, reducing the amount of waste with the accompanying decomposition of organic matter. As a result, toxic high molecular weight components have transformed into low molecular-weight ones, thereby reducing their toxicity. In addition, toxic volatile substances present in the pyrolysis gas are afterburner at a temperature of 1100–1400 0C, which ensures the complete decomposition of dioxins and furans.

The multi-loop circulating gasifier is a fundamentally new technology that provides a complete thermal decomposition of solid radioactive organic waste at high temperature in the reactor (1) without oxygen access (Figure 64). Toxic components formed in the form of a gas mixture circulate in a multi-circuit system (5, 6, 7, 8, 9) until complete decomposition to low molecular weight components. The resulting pyrolysis gas (2) has burned in a device that prevents toxic elements formation. The requirement for them, in this case, is determined by Directive 2000/76/EC.

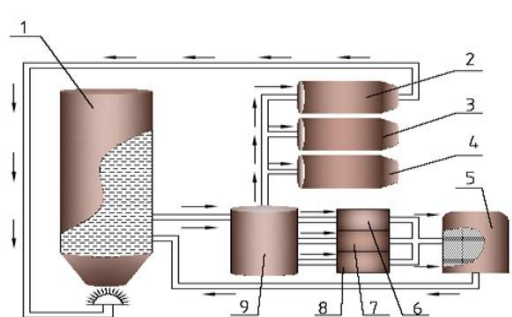


Figure 64. Scheme of technological stages of a multi-circuit circulating gasifier. 1 - reactor, 2 - outlet circuit of gaseous compounds, 3 – the closed circuit of solid compounds, 4 - dry residue outlet circuit, 5 - catalyst block, 6, 7, 8 - sectional circuits, 9 - multi-circuit coolant distribution unit.

This work proposes a novel for spent IER conducting a two-stage process of the carbonisation of organic constituents and high-temperature plasma.

The thermal treatment plant consists of a waste loading bin, a gasification chamber, a gas afterburner, a heat exchanger and a smoke exhauster (Figure 65). The lining is made of high-temperature ceramics and the heat exchanger is made of stainless steel. Plasma technologies require unique refractory lining materials which are durable to the extremely high temperatures and aggressive influence of the residue ash (slag).

The construction of a high-temperature reactor has provided the most effective heating slag and prevented superfluous heat losses.



Figure 65. The installation trials of plasma torch gasification.

The initial stage of thermal utilisation of organic radioactive waste is entering the processing system into operating mode, and loading into the bunker. Bunker with radioactive waste with humidity up to 80% preheated with a gas burner, and the heat treatment process starts. Hot water has supplied to air convectors heating

system. A smoke exhauster controls the process of removing gases. After gasification, ash has removed from the system and loaded into special steel containers for further sealing. The dimensions of the crucible play an important role. The most efficient treatment has been achieved in a long crucible with a small diameter. This design allows you to heat and ash the contents of the crucible evenly. The experiments have carried out using a plasma torch with a reactor with a spatially developed active zone. Temperature 1200–1250 °C for the plasma gasification to take below the boiling point of CsCl, which allows it to remain in the ash. The absence of ballast nitrogen and free oxygen in the reaction chamber eliminates the problem of the formation of nitrogen oxides, which ensures the high quality of the resulting synthesis gas and does not require additional measures for its separation and purification. An essential gasification problem is the completeness of thermal treatment, which allows removing organic substances from IER without releasing large amounts of radionuclides.

The phases of the primary cycle and the installation parameters are displayed on the LCD panel during the execution of the cycle. The main physical parameters of the process (e.g. temperature, pressure, time and gas composition) are controlled. The control system is easy to use as the plant control is programmable. The automatic operating system (automatic cycle selection) for the entire cycle guarantees maximum safety. During the experimental work, a surrogate waste cationic IER has used for loading. Processing occurs with the sintering of the IER ash (**Error! Reference source not found.**). Methods of DTA, SEM and XRF to study decomposition and the resulting ash (Figure 67). Synthesis gas, solid residue, and gaseous compounds are dependent on thermodynamic parameters and process speed.

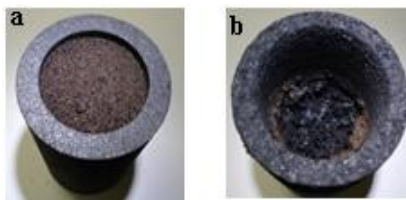


Figure 66. IER before heat treatment (a) and after (b).

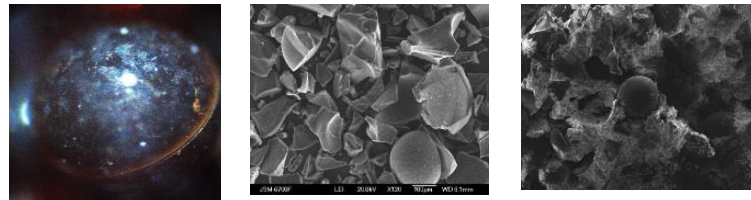


Figure 67. Snapshot of ash after thermal processing.

However, gasification residues bearing radioactive and hazardous elements should be further treated and transformed into a high-integrity waste form that can safely dispose of in a radwaste repository.

3. Conclusions

Thus, the thermal treatment process uses a plasma torch with a multi-loop circulating gasifier that provides a complete thermal decomposition of organic radioactive waste without access to oxygen at high temperatures. Synthesis gas, solid residue and gaseous compounds depend on thermodynamic parameters and process speed. The capability of this process with regard to the removal of radionuclides from spent IER was demonstrated using non-radioactive surrogates under an experimental test process. This study demonstrated that gasification of the IER would be a beneficial treatment to reduce the total volume of LILW requiring predisposal treatment.

References

- Nieminen M., et al. Gasification-based thermal treatment of Low and Intermediate Level Waste containing organic matter IOP Conf. Ser.: Mater. Sci. Eng. 818 012007, 2020
- Singare P., Lokhande R., Madyal R. Thermal Degradation Studies of Some Strongly Acidic Cation Exchange Resins. Open Journal of Physical Chemistry, 1, p.45–54, 2011.
- Jung, H.G., Brähler, G. & Slametschka, R., Pyro(hydro)lysis of Spent Ion Exchange Resins for Disposal of Organic-Free Radioactive Waste. IGD-TP 7th Exchange Forum, October 25–26th, 2016, Córdoba, Spain, 2016

6.4 Stability and Physico-Chemical Characterisation of Reconditioned Waste Forms Relevant to Radioactive Wastes

Gianni F. Vettese, The University of Helsinki, Finland, Gianni.vettese@helsinki.fi; Taavi Vierinen, UH; Tandre Oey, VTT Technical Research Centre of Finland, Finland; Suvi Lamminmäki, VTT; Sami Hietala, UH; Matti Nieminen, VTT; Markku Leivo, VTT; Tapio Vehmas, VTT; Jaana Laatikainen-Luntama, VTT; Emmi Myllykylä, VTT; Gareth T. W. Law, UH, Gareth.law@helsinki.fi

Keywords: Geopolymer, leaching experiments, Low- and Intermediate Level Nuclear Wastes.

1. Introduction

Current conditioning methods for the predisposal of low- and intermediate-level radioactive waste (LILW) streams generate complex waste forms whose safe, and long-term stewardship is difficult to achieve. Spent solid organic LILW typically includes operational wastes and spent ion-exchange resins. Finland generates over 300 m³ of LILW annually, this only represents ~1% of the countries total waste by radioactivity, but by volume it represents more than 95% of the total volume generated annually (STUK, 2020). Currently, spent ion exchange resins are immobilised in a solid matrix (cement or bitumen) and contained in a steel drum where it is held in interim storage until the final disposal concept is ready. In Finland final disposal of LILW proceeds via burial in geological disposal, with waste emplaced in rock caverns ~ 100 m below surface. During final disposal passing water will come into contact with concrete structures present in the facility creating a high ambient pH (~12, CaOH buffered) rich solution that may leach the immobilised radionuclides from the host matrix. Recently, geopolymers have been proposed as more economic and sustainable alternatives to OPC, and in this experiment we will assess the short- and long-term (1 month – 2 years) physico-chemical behaviour of several novel geopolymer formulations. These proceedings discuss the chemical stability of the geopolymer and the stable Cs as an analogues for radioactive ¹³⁴⁺¹³⁷Cs contained within. Here, we share early results (up to 6 months) on the characterisation and leachability of a novel geopolymer form leaching experiments carried out by the University of Helsinki (UH). We achieved this through: (1) Pre-characterisation of the physico-chemical properties of geopolymer; (2) Assessment of leaching behaviour of waste-form in repository conditions; and (3) Post-mortem characterisation of the physico-chemical properties of the leached geopolymer.

2. Description of work and main findings

2.1. Methods

Spent ion-exchange resins have been thermally treated via gasification and immobilised in a series of novel metakaolin-based geopolymers by VTT e.g., (Vehmas *et al.*, 2020). Here, treatment enables substantially higher loading of the LILW (>90% volume reduction) into the geopolymer without loss of matrix strength or cohesion. Briefly, a metakaolin binder, sodium silicate and a potassium hydroxide activator were mixed at room temperature with a thermally treated (inactive) ion-exchange resin ash containing simulant radionuclides. The geopolymer is loaded with a 1.2%_{wt} loading of organic ion-exchange resin ash and uses a modified version of the PREDIS leachant solution (Table 10).

Physico-chemical pre-characterisation and post-mortem characterisation was conducted using powder field emission – scanning electron microscopy and energy dispersive x-ray (FESEM EDX) and X-ray diffraction (XRD). FESEM EDX samples were mounted on Al holders using carbon tape and a 10 nm layer of carbon coating was applied using a Leica EM ACE 200 vacuum coater. FESEM EDX was conducted using a Hitachi S-4800. Thin layer samples for XRD were prepared by creating a uniform powder of crushed geopolymer which was put on a glass slide. Once dry, the samples were measured from 5–70 2θ using an XRD Panalytical X'Pert3 Powder, X-ray powder diffractometer with Cu Kα radiation. XRD patterns were referenced using the ICDD PDF4 Minerals reference database. Geopolymer leachability and stability were then assessed via leaching experiments and post mortem analyses. Leaching experiments were performed in agreement with the ANSI/ANS-16.1-2019 protocol (American Nuclear Society, 2019). Here, 1 cm³ geopolymer samples were prepared in quintuplet for each leaching experiment, each cube was immersed in 60 mL of leachant (Table 10). The leachant solution was replenished after 7, 14, 21, 28, 60, 90, 120, 150 and 180 days. During replenishing the leachant was sampled, geopolymers were rinsed with de-ionised water (15 or 18 MQ), and fresh leachant replaced the solution. Electrical conductivity, pH and Eh was measured on the leachant and leachate solutions using electrodes that were calibrated daily. Inductively Coupled Plasma Mass Spectrometry (ICPMS) and Microwave Plasma Atomic Emission Spectroscopy (MPAES) were used to monitor changes in the cation concentrations of the leachant and leachate solutions. Here, aqueous samples were diluted in 5%

HNO₃ prior to analysis. In the de-ionised water and fresh leachant rinses cation concentrations were below the limit of detection. Dynamic Light Scattering (DLS) was used to assess for colloid formation in the leachant and leachate samples on a Malvern Zetasizer Nano ZS using filtered leachant and leachates (0.2 µm Whatman filters) in DTS1070 disposable sample cuvettes.

Table 10. Geopolymer (left) and leachant (right) details in leaching experiments.

| Geopolymer details | | Leachant details (per L) | |
|-----------------------------|------------------|-------------------------------------|----------|
| Ash (% _{wt}) | 1.2 | Na ₂ SO ₄ | 0.9799 g |
| Precursor | Metastar | CaCl ₂ .H ₂ O | 0.5353 g |
| Added Fe (% _{wt}) | 0 | NaOH (1M) | 16.6 mL |
| Cs in ash (ppm) | 180 | KOH (1 M) | 15.2 mL |
| Ni, Cr, Cu in ash (ppm) | 3000, 3000, 3000 | pH | 12.6 |

a. Results

Pre-characterisation of the ashed resin via FESEM EDX shows that the ash contains dense agglomerations approximately 5–10 microns in size that contain trace contaminant metals Ni, Cr and Cu. These dense agglomerations were also observable in the geopolymer matrix. Cs was not detectable in the dense agglomerations via ESEM suggesting it was homogeneously distributed in the ash and geopolymer matrix. Following 6 months of dynamic leaching experiments the pH and conductivity remain stable at 12.5 and 8.5 mS/cm respectively. Colloidal analysis showed no detectable presence of colloids in the leachates. The bulk geopolymer components (Na⁺, Al³⁺, Si⁴⁺) leach into solution, whilst K⁺ and Ca²⁺ are removed from the leachant into the solid phase geopolymer (Figure 68). Cs⁺ also leaches into solution, although its leaching index (9.1) was significantly above waste acceptance criteria of (6.0) prescribed by US NRC for radioactive waste (American Nuclear Society, 2019). Ni, Cr and Cu levels remain below the limit of detection in all leachate samples.

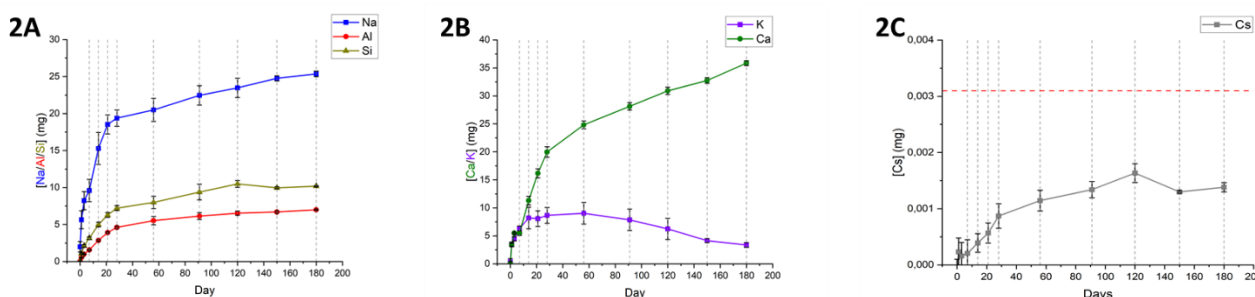


Figure 68: [A] Cumulative leaching of Al, Si, and Na; [B] Cumulative absorption of K and Ca; [C] cumulative leaching of Cs. The horizontal lines represent a sample refresh and the red line in [C] shows the total added Cs.

Post-mortem analyses after 1, 6 and 12 months of leaching experiments identify: (1) weakening of structural integrity of the sample, (2) cracking, and (3) precipitation of secondary CaCO_{3(s)} phases, all of which increase with time.

3. Conclusions

We have successfully developed experimental methodology for geopolymer characterisation, leaching experiments, and post-mortem analyses. When combined, these can accurately describe (1) the evolution of the geopolymer matrix with time and (2) the leachability of surrogate radionuclides. These leaching experiments show that Cs was retained within the criteria to US NRC. Further analyses are required before the experiments are complete including aqueous analyses up to 24 months (ICPMS, MPAES, DLS/zetapotential), and solid-phase characterisation methods (Electron microprobe analysis, magic angle spinning nuclear magnetic resonance for ²⁹Si and ²⁷Al).

References

- American Nuclear Society (2019) 'Measurement of the leachability of solidified low-level radioactive wastes: ANSI/ANS-16.1-2019'.
- STUK (2020) Joint Convention on the Safety of Spent Fuel Management and on the Safety of Radioactive Waste Management : 7th Finnish National Report as referred to in Article 32 of the Convention. Available at: <https://urn.fi/URN:ISBN:978-952-309-488-8>. Accessed 08/06/2023.
- Vehmas, T. *et al.* (2020) 'Geopolymerisation of gasified ion-exchange resins, mechanical properties and short-term leaching studies', in *IOP Conference Series: Materials Science and Engineering*. Institute of Physics IOP, p. 012017. doi: 10.1088/1757-899X/818/1/012017.

6.5 Immobilization of thermally treated ionic exchange resins in geopolymer matrices

Pedro Perez-Cortes¹, Francisca Puertas¹, Ines Garcia-Lodeiro¹, Maria Cruz Alonso¹

¹Agencia Estatal Consejo Superior de investigaciones Científicas (CSIC), Spain

pedro.perez@ietcc.csic.es, puertasf@ietcc.es, iglodeiro@ietcc.csic.es, mcalonso@ietcc.csic.es

Keywords: immobilization, geopolymer, cement, radioactive nuclear wastes

1. Introduction

One of the main objectives of the WP6 is to demonstrate the reliability of alkaline cementitious binders for conditioning nuclear wastes. This document describes the experimental work and compiles the main findings presented by CSIC, regarding to task T6.4.

2. Description of work and main findings

The aim of this work was to optimize “one-part” geopolymer formulations for conditioning of thermally treated ionic exchange resins (IER). Table 11 shows the geopolymer matrices that were prepared and tested to optimize the concentration of alkaline activator (%Na₂O) and the proportion of the metakaolin/blast furnace slag (MK/BFS) precursors for developing materials with low porosity and high mechanical strength. Prismatic paste specimens of 1*1*6 cm³ were prepared after mixing precursors, solid Na₂SiO₃ activator (Na₂O/SiO₂=1) and water, with a liquid/solid (L/S) mass ratio of 0.3. Samples were cured in a climatic chamber, at 21 °C and 99% RH, and the compressive strength development was measured after 3, 7 and 28 days of curing; at this last age, microstructural changes in the geopolymer matrices were studied before and after incorporating 20% of IER.

Table 11. Geopolymer matrices studied for the immobilization of the thermally treated IER wastes.

| Formulation | G1 | G2 | G3 | G4 | G5 | G6 | G7 | G8 | G9 | G10 |
|--------------------|----|----|----|----|-----|----|----|----|----|-----|
| %Na ₂ O | 6 | 9 | 12 | 12 | 6 | 6 | 9 | 12 | 12 | 6 |
| MK/BFS | 1 | 1 | 1 | 3 | 1/3 | 1 | 1 | 1 | 3 | 1/3 |
| %IER | 0 | 0 | 0 | 0 | 0 | 20 | 20 | 20 | 20 | 20 |

Figure 69 shows the compressive strengths of the geopolymer pastes without and with the incorporation of 20% IER. The reference matrices, at 3 days of curing, achieved mechanical strengths higher than 70 MPa, with G1-G5 undergoing a slight increase over time. As expected, the incorporation of 20% IER reduced the compressive strengths, but this effect was not the same for all the systems; matrices G6 and G10 showed the most substantial reduction while the opposite behaviour was observed for G7 and G9. In this way, the geopolymer composition of 9%Na₂O and MK/BFS=1, and 12%Na₂O and MK/BFS=3 underwent the best mechanical performance when the IER was incorporated; both formulation samples far exceed the waste acceptance criteria (WAC) of compressive strengths (10 MPa) [1], and substantially overcome those previously reported elsewhere [2].

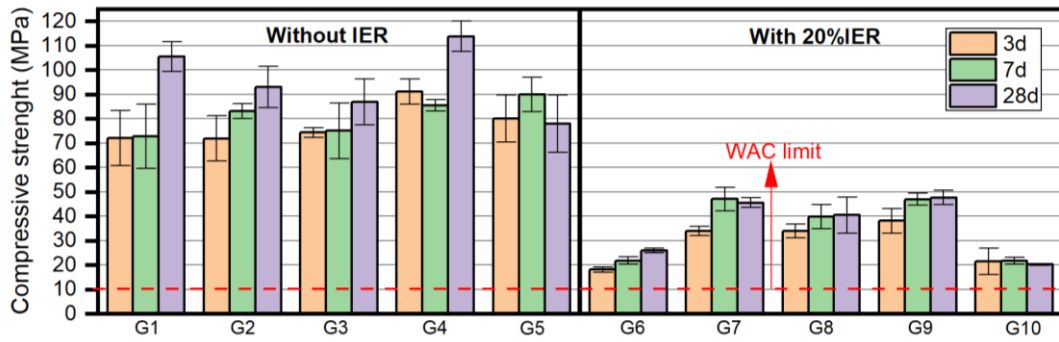


Figure 69. Compressive strength at 3, 7 and 28 days of paste samples without and with 20%IER.

In agreement with the above, the reference samples with 9%Na₂O-MK/BFS=1, and 12%Na₂O-MK/BFS=3 showed very low total porosity (Figure 70a). The incorporation of 20%IER increased the total porosity and changed the pore size distribution, which was more remarkable in G9. The deleterious effects of the IER agree well with the remarkable interface porosity between the IER and the geopolymer matrix (Figure 70b and c). It should be noted that the IER does not affect the chemical composition of the reaction products, composed of a mixture (N,C)-A-S-H and C-A-S-H gels (Figure 70d).

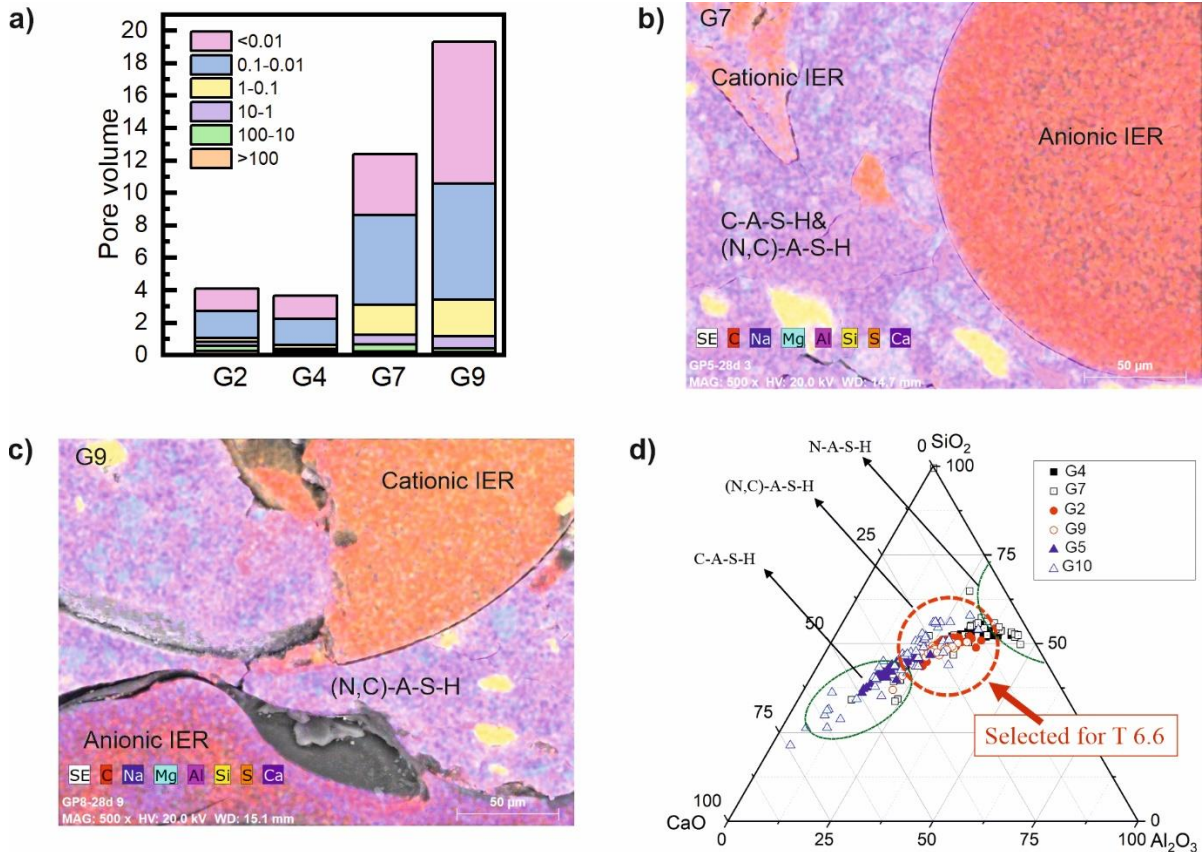


Figure 70. a) Pore volume (%) of samples with the best mechanical performance; mapping BSEM analysis of samples with 20%IER: b) G7 and c) G9, and d) chemical composition of the reaction products.

As shown in Figure 71, the XRD pattern of the geopolymer pastes formulated with a) 9%Na₂O-MK/BFS=1, and b) 12%Na₂O-MK/BFS=3 showed, in all cases, the formation of an amorphous hump between 25 and 37°2θ, which is associated with the precipitation of geopolymer gels ((N,C)-A-S-H + C-A-S-H) as identified in the BSEM/EDX analysis. Small diffraction lines of calcite and others phases associated with gismondine were also identified as secondary reaction products. It is noteworthy that the incorporation of 20%IER does not introduce the formation of new crystalline phases. However, solid-state MAS NMR characterization has shown that the amount of amorphous reaction products can be seriously affected after incorporating IERs.

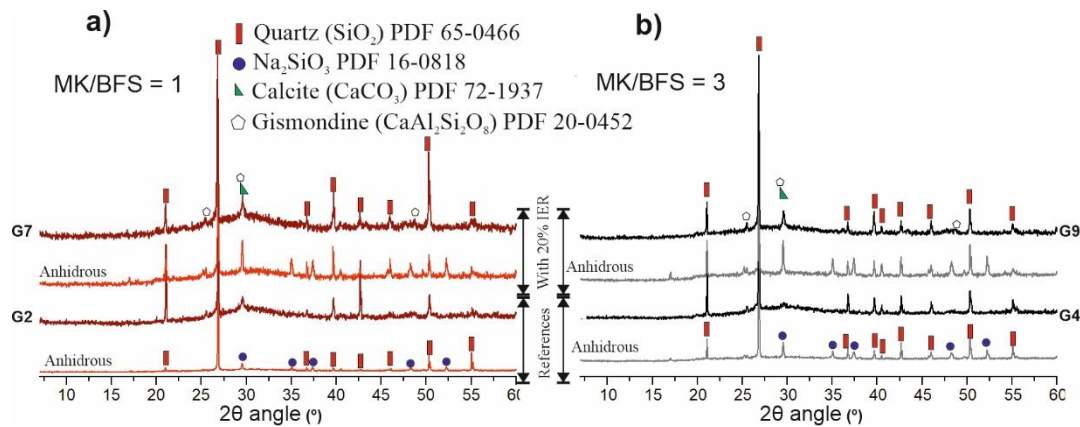


Figure 71. XRD patterns of geopolymer, without and with 20% IER, formulated with a) 9%Na₂O-MK/BFS=1, and b) 12%Na₂O-MK/BFS=3. The anhydrous corresponds to solid powders before the alkaline activation.

3. Conclusions and way forward

The findings of this study highlight the significance of considering the composition of precursors and the concentration of alkaline activator when developing geopolymer matrices for confining thermally treated ion exchange resins (IER). These variables play a crucial role in determining the properties of the resulting cementitious matrix.

Although the chemical and mineralogical composition of the cementitious matrix was found to be minimally affected by the presence of IER, its influence on the pore structure, structure and mechanical properties of the samples was significant. This observation underscores the importance of considering the impact of IER when designing geopolymer matrices.

Among the various formulations tested, the one-part geopolymer paste matrix, formulated with metakaolin and blast furnace slag in a mass precursor ratio of 1, and activated with 9% of Na₂O in the form of solid Na₂SiO₃ powder, exhibited remarkable performance. It surpassed the waste acceptance criteria for compressive strength by recording >40 MPa when 20% of IER was incorporated. This particular formulation was selected for the subsequent leaching test, as specified in T6.6.

References

- [1] ENRESA. Criterios de Aceptación de Unidades de Almacenamiento. Referencia 031-ES-IN-0002 rev. 1. July 2008.
- [2] Alonso, M.C., Puertas, F., Garcia-Lodeiro, I., Perez-Cortes, P. Immobilization of the treated wastes by geopolymer or cement-based materials encapsulation, PREDIS Proceedings of April Workshop 2022, Espoo, Finland.

6.6 Immobilization of molten salt residue using alkali-activated and cement-based materials

Lander Frederickx, SCK CEN, Belgium, lander.frederickx@sckcen.be
 Eduardo Ferreira, SCK CEN, Belgium
 Quoc Tri Phung, SCK CEN, Belgium

Keywords: alkali-activated materials, geopolymer, cementitious materials, molten salt oxidation

1. Introduction

Some radioactively contaminated solid organic waste streams are problematic to dispose of by direct immobilization in known matrices (e.g. cementitious binders), as they can potentially degrade after disposal, possibly resulting in the release of radionuclides. Within work package 6 of the PREDIS project, techniques for the treatment and disposal of these waste streams are investigated [1]. One of the possible ways of treatment is the molten salt oxidation (MSO) process, in which the bulk of the organic waste can be oxidized

at a high temperature in the presence of a sodium carbonate salt [2]. The residue after the MSO process is a salt containing radionuclides in carbonate forms. The goal of this study is to investigate whether it is possible to immobilize this salt residue in an alkali-activated or blended cementitious matrix resulting in a waste form with good mechanical properties and long-term durability. Previous experiments with direct immobilization of the salt into these matrices has been proven to be ineffective. Therefore, the salt will first be pre-treated to increase the compatibility with its matrix. After ensuring good mechanical properties, thermodynamic modelling of the system will be performed to understand the stability of the salt-related phases. Future work will include carbonation, leaching and resistance to alkali-silica reaction tests to ensure long-term durability of the waste forms.

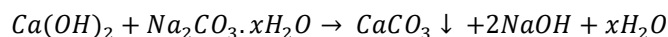
2. Description of work and main findings

Methods

Sample preparation & characterization

Initial characterization of the salt revealed it to be highly waterlogged at a water content of 60 wt.% after drying at 100 °C. In order to improve reproducibility of the tests, the salt was air-dried, after which the residual water content was approximately 16 wt.%. Detailed characterization of the air-dried salt revealed it to consist of different hydration states of sodium carbonate (Na₂CO₃), with thermonatrite (Na₂CO₃·H₂O) being the most dominant. Additionally, trona (Na₂CO₃·NaHCO₃·2H₂O) occurred in addition to small quantities of natron (Na₂CO₃·10H₂O) and gaylussite (Na₂Ca(CO₃)₂·5H₂O).

As initial experiments revealed that direct immobilization of the salt was ineffective due to the strongly hygroscopic nature of sodium carbonate, a pretreatment was necessary. As sodium carbonate is highly soluble, a double displacement reaction to form the insoluble calcite (CaCO₃) was proposed to be an effective way to improve the compatibility with the cementitious and alkali-activated matrices. A number of possible reagents exist, such as CaCl₂, Ca(NO₃)₂ and Ca(OH)₂. The former two were found to be ineffective as they either introduce new complications to the waste form (chloride attack in case of CaCl₂), or negatively impact the properties of the waste form (in the case of Ca(NO₃)₂). Ca(OH)₂ was therefore chosen as a reagent, with an additional benefit that the reaction (shown below) produces NaOH, which acts as an activator for the precursor of the alkali-activated matrices.



The pre-treatment was tested in two ways. Firstly, Ca(OH)₂ and the salt residue were both mixed together in water for three days (P1). Secondly, the salt residue was slowly added to a Ca(OH)₂ suspension over the course of three weeks (P2), to allow a more gradual reaction between both components, to prevent an overly Na-rich environment due to the low solubility of Ca(OH)₂.

After -, the resulting sludges were incorporated into either an alkali-activated or blended cementitious matrix. Waste loadings, expressed as the weight percentage of air-dried salt residue relative to the total mass of the waste form, varied from 10 to 20 wt.% in case of the alkali-activated matrices and 10 to 14 wt.% for the cementitious matrix. The fresh waste forms were cured in humid conditions (nearly 100% RH, room temperature) for 28 days to ensure that the waste form can withstand a high humidity environment.

Table 12. Details of the recipes used for the immobilization of the molten salt residue. Abbreviations are as follows: BFS = blast furnace slag; MK = metakaolin; LF = limestone filler; L = limestone; LS = limestone sand; SF = silica fume; SCM = supplementary cementitious material.

| Recipe | Activator/SCMs | Precursor/Binder | Waste Loading (wt%) |
|--------|-------------------------------------|------------------|---------------------|
| AAS | Na ₂ O·2SiO ₂ | BFS | 10–20 |
| CEM | BFS, LF, L, LS, SF | OPC (CEM I) | 10–14 |

The waste forms were characterized by X-ray diffraction. Thermodynamic modelling was performed using HP Geochemistry.

Results

Synthesis of waste form

Both the alkali-activated slag and blended cementitious waste forms showed good mechanical properties after 28 days curing, with the compressive strength of AAS at 42 and 37 MPa (for 10 and 20 wt.% waste loading) and 15 MPa for the CEM waste forms (for both 10 and 14 wt.% waste loading). The samples also did not show any signs of bleeding or efflorescence, proving their good resistance to high humidity environments. Mineralogical characterization of the waste forms (Figure 72) revealed that, in both cases, all the sodium carbonate species had reacted away. Instead of everything transforming into calcite, an important crystallization of gaylussite was also observed. The crystallization of gaylussite was found to be more prominent relative to the amount of calcite formed in case of pre-treatment P1, in which $\text{Ca}(\text{OH})_2$ and the salt residue were directly mixed.

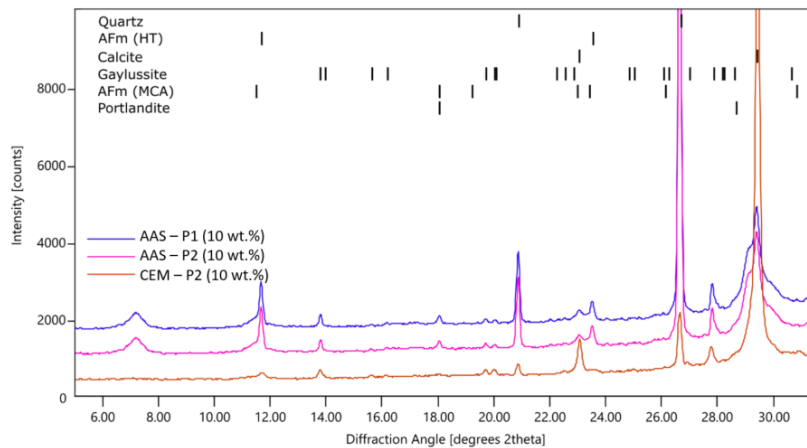


Figure 72. XRD analysis of the waste forms containing 10 wt.% of salt residue. P1 and P2 indicate the type of pre-treatment.

To understand the mechanism behind the formation of gaylussite, thermodynamic modelling was performed. In a simulation of pre-treatment P1, it was found that, in the case only a small amount of $\text{Ca}(\text{OH})_2$ (or portlandite) is in solution, gaylussite will be the preferred phase to precipitate due to the sodium rich nature of the solution. As more Ca comes into solution, calcite will be more stable. By contrast, a simulation of pretreatment P2 revealed that gaylussite should never be stable, as the gradual addition of salt to a Ca-rich suspension ensures the stability of calcite.

The observation of gaylussite in the P2 waste forms can be attributed to the fact that, after pre-treatment, the sludges are mixed with other phases, i.e. the binder, activator, SCMs, ... which can affect the stability of the gaylussite. In the case of the AAS waste form, the addition of $\text{Na}_2\text{O} \cdot 2\text{SiO}_2$ as an activator ensures that the system contains sufficient sodium for gaylussite to be thermodynamically stable. In the case of the CEM waste form, no additional source of sodium is added, so the continued presence of gaylussite can best be understood as that of a metastable phase, which will on the long term react with the available $\text{Ca}(\text{OH})_2$ to form additional calcite crystals.

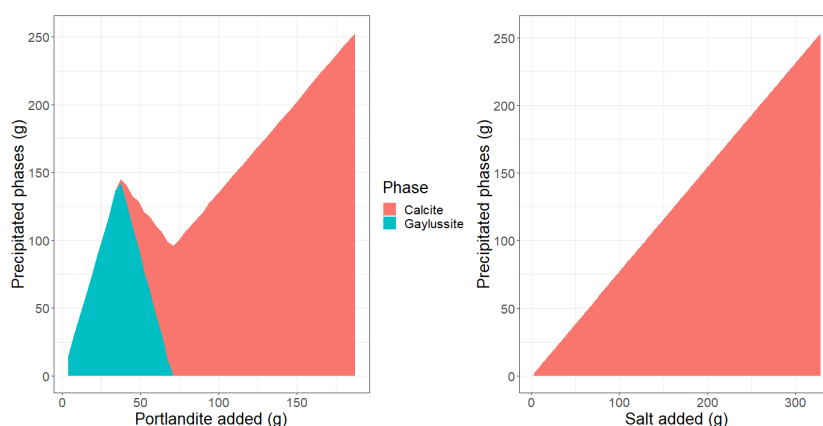


Figure 73. Thermodynamic simulation of the precipitation of calcite and gaylussite during the pre-treatment. The diagram on the left simulates pre-treatment P1, while the one on the right simulates pre-treatment P2.

3. Conclusions & way forward

This study has shown that it is possible to design both cementitious and alkali-activated matrices which are able to retain a highly hygroscopic sodium carbonate salt after pre-treatment. The waste forms showed good mechanical properties which are unaffected by changes in temperature or humidity. The pre-treatment was effective in eliminating all hygroscopic sodium carbonate from the system, although an intermediary Na-Ca carbonate phase, gaylussite, was still present. Through thermodynamic modelling, its presence can best be explained by the low solubility of $\text{Ca}(\text{OH})_2$ artificially creating a high-sodium rich environment in which gaylussite is more stable than calcite, combined with the additional contribution of Na from the sodium disilicate used as an activator in the AAS waste form.

Now a set of stable waste forms has been attained, durability tests will be performed, including carbonation resistance experiments, leaching experiments and alkali-silica reaction experiments (in the case of the CEM waste form).

References

- [1] M. Oksa, E. Holt, EU-project PREDIS: Predisposal management of radioactive waste, 2023. <https://predis-h2020.eu/>. 2023).
- [2] A. Akin, J. Dymačková, P. Pražák, R. Trtílek, P. Kovařík, E. Sulejmanov, Molten Salt Oxidation of Ion Exchange and Oils in Carbonate Salts and Evaporator Residue–16531, WM Symposia, Inc., PO Box 27646, 85285-7646 Tempe, AZ (United States), 2016.

6.7 Characterisation of the ash and their encapsulation after thermal treatment of IER

B.P. Zlobenko, Yu.G. Fedorenko, A.N. Rozko

*State Institution "Institute of Environmental Geochemistry of National Academy of Sciences" of Ukraine,
Kyiv, Ukraine*

Email: borys.zl@gmail.com

Keywords: IER, ash, encapsulation, geopolymer

1. Introduction

Spent ion exchange resins (IERs) represent a waste stream generated during NPP operation. Direct solidification is commonly used to treat spent IERs due to simple operation and equipment and has been widely accepted cementation using Ordinary Portland Cement (OPC). Removal of organic matter by thermal gasification results in significant volume reduction demonstrated successfully in many projects [1]. The remaining radioactive ashes must be transferred to treated waste forms. Cementation, traditionally used for encapsulation, is a conventional method to bind the gasified resin ash. TECDOC of IAEA reported that geopolymers were used to solidify radioactive wastes at Dukovany NPP [2]. The last time, many works indicated that alkali-activated geopolymer binders might be suitable matrices for encapsulating and stabilising IERs. Geopolymer is amorphous to a semi-crystalline three-dimensional Si–O–Al framework. It is synthesised by a polycondensation reaction of solid aluminosilicate materials such as metakaolin (MK) or blast furnace slag (BFS), and alkaline solutions known as the geopolymerisation process [3]. Potassium hydroxide and sodium silicate solution have been used as activators. The potential to combine gasification as thermal treatment and various inorganic binders as encapsulation matrices were tested in the VTT [4]. This work aims to evaluate the application of the geopolymerisation to ash after gasification of the IER and the problems associated with the specificities of the ash.

2. Description of work

A significant gasification problem is the completeness of thermal treatment, which allows removing organic substances from IER without releasing large amounts of radionuclides. The ion exchange resin combustion method is optimised by determining the temperature of the gasification process for the gradual conversion of mobile and volatile Cs species into inorganic and thermally stable compounds. The transition time and the rate of temperature rise of the thermal process are optimised by conducting a preliminary thermogravimetric analysis. The combustion was carried out at different temperatures. The resulting ash was characterised using FTIR spectroscopy, SEM and DTA to monitor the decomposition of organic matter. Previously, it was

established by the DTA method that with a small mass of the sample, it is wholly heated with a minimum temperature gradient over the sample volume. At a temperature of about 600 °C, the fragments are separated from the original and, at the same time, the particles are sintered into 5–10 mm in size aggregates. Incineration of significant volumes of spent ion-exchange resins can be problematic, also taking into account the uncertainty of the behaviour of radionuclides depending on the temperature and duration of gasification. In Figure 74, the sequence of destruction of spherical particles of the cation IER during heat treatment is given. When heated, the particles of an IER crack from them, separating scales, and they decrease in size. In the future, cracking continues while the scales begin to burn out. At sufficiently high temperatures, particles of a spherical shape can be preserved in the samples. The presence of such particles in the samples significantly reduces the ultimate compressive strength of the geopolymer matrix; reducing their number in the samples of compounds is an urgent problem and requires a higher temperature after the first gasification.

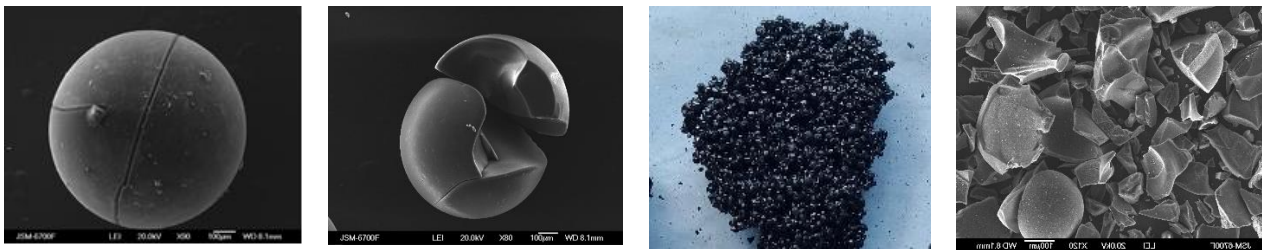


Figure 74. Destruction of IER under gasification.

By about 900 °C, the mass sample decreases and remains at 13% of the initial, Figure 75. Repeated studies showed that complete decomposition (99%) could occur at a temperature of more than 1000 °C (Figure 76).

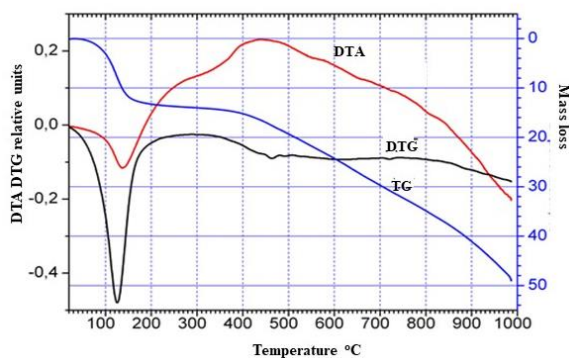


Figure 75. DTA analysis of samples of IER of the burnout

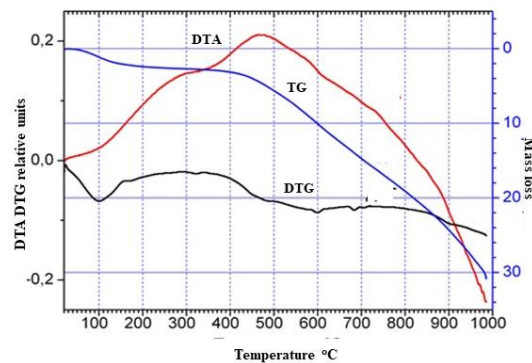


Figure 76. DTA of samples ash after the burnout of IER.

These analyses suggest that the degradation of IER can be separated into three primary stages: weight loss between 25 and 150 °C is ascribed to dehydration. Most weight loss results from decomposing the functional groups from 250 to 350 °C for cationic exchange resins. The last stage (temperatures above 400 °C) is associated with the degradation of the organic matrix and its subsequent mineralisation. The cationic IER is characterised by releasing more significant quantities of a degradation product, mainly SO₂. In the article Matsuda the lower mass reduction of the cationic IER to the stabilisation processes of the residual matrix associated with the formation of sulfur structures [5].

After gasification, the ash was homogenised and mixed with the geopolymer. Experiments have been carried out on geopolymer matrices with a marker of inactive caesium. The work used metakaolin (MK) obtained from kaolinite by heating kaolin for 4 hours at a temperature of 800 °C and Blast Furnace Slag (BFS), the raw material of the Mariupol metallurgical plant, which has been used and practically no longer exists, as a result of the current war. The BFS was granulated, dried, grounded and sieved (<125 μm). The slag was a fine-grained powder with a specific surface area of 288 m²/kg, and the residue on a 0.08 sieve was 1.26%. Table 13 shows the chemical composition of the raw material (oxide wt. %) used in the work. The geopolymer matrix binder was made from BFS and MK with water, alkaline activators, and added IER ash. The modification was done by mechanical activation main binding component – BFS, treatment for 15 min at 14,000 rpm. As previously established, the treatment allows a 1.5 times increase limit compressive strength. First, pre-mixed alkaline activators and water, as activators used hydroxide potassium and solution silicate sodium.

Table 13. Chemical composition of the raw material (oxide wt. %).

| | SiO ₂ | Al ₂ O ₃ | CaO | MgO | Fe ₂ O ₃ | MnO | SO ₂ | Na ₂ O+K ₂ O | TiO ₂ |
|-----|------------------|--------------------------------|-------|------|--------------------------------|-----|-----------------|------------------------------------|------------------|
| MK | 52,9 | 41,92 | 0,19 | 0,27 | 1,64 | 0,1 | - | 0,69 | 1,87 |
| BFS | 36,53 | 7,92 | 42,94 | 9,47 | 0,24 | 0,1 | 0,54 | 1,29 | 0,47 |

The MK/BFS geopolymer pastes were prepared with different Al:Si:Na/K: H₂O ratios. Using KOH as an activator led to higher compressive strength than NaOH. The optimal amounts of water, activator, MK, and BFS have been determined based on the literature study and experimentally. The composition of such samples is shown in Table 14.

Table 14. Composition of binder, %.

| Sample composition | WP6-26 | WP6-54 | WP6-55 | WP6-56 |
|---------------------|--------|--------|--------|--------|
| BFS | 68.5 | 34.4 | 22.7 | 45.3 |
| Metakaolin | - | 1.3 | 0.85 | 1.7 |
| Liquid glass | 5.5 | 7.9 | 5.2 | 10.4 |
| Hydroxide potassium | 15.8 | 3.1 | 2.0 | 4.1 |
| Water | 10.3 | 19 | 23.9 | 16.0 |
| IER ash | - | 45.9 | 22.6 | 22.7 |

The geopolymer binder has measured on viscosity after mixing according to ASTM C1749 and set time based on EN 196-3. The setting time of geopolymer pastes should be at least the duration of the technological cycle – the time from the beginning to the end of compounds mixing and pouring into moulds. After mixing components, the mixture was put into moulds – a general view of the sample in Figure 77.



Figure 77. Geopolymer compound with ash IER (WP 6-54).

Compressive strength measurements evaluated matrices after curing on an electromechanical press (ZD 10/90) according to EN 13791 [6]. The definition of compressive strength was carried out on the 7th and 28th days after manufacturing. Received blank samples matrices size 5 x 5 x 5 cm had a limit compressive strength of more than 51 MPa with porosity of about 0.5%. With such low porosity, samples dry up slowly, and when gradient distribution water in samples may take place, they crack. To prevent this modified slag-alkaline binder was added metakaolin, which increased porosity up to 15% and reduced limit compressive strength up to 19.3 MPa. Table 15 shows the properties of the above samples.

Table 15. Properties of samples.

| | WP6-26 | WP6-54 | WP6-55 | WP6-56 |
|----------------------------|--------|--------|--------|--------|
| Density, g/cm ³ | 2.3 | | | |
| Porosity, % | 0.5 | 14.0 | - | - |
| Setting time, min | 180 | 190 | 160 | 180 |
| Compressive strength, MPa | 51 | 4.4 | 9.6 | 10.9 |
| Degree gasification of IER | - | 0.81 | 0.87 | 0.81 |
| Fraction ash | - | <0.3 | <0.3 | <0.3 |

Due to the dependence of the ash on processing IER waste, one of the main goals concerning the ash characterisation was to select those factors responsible for the compressive strength. For this purpose, the original ash sample has been fractionated by sieving. Measurement of the compressive strength after drying

to constant weight showed that with an increase in the amount of added ash fraction < 0.2 mm, in the amount of 16.6%, the strength was 10.5 MPa, and at increased to 29.6%, the strength decreased to 4.7 MPa. In the geopolymer matrix sample, when the ash fraction <0.6 mm was used in the composition, the strength limit was 0.9 MPa.

Thus, it has been found that the most challenging issue when solidifying ash after thermal processing of IER is ash homogeneity in composition. From physical and mechanical properties, ash depends primarily on strength indicators compounds. Before the measurements, the ash samples were ground in an agate mortar. The microstructure and morphology of the ash fractions have been investigated on SEM (JSM-6490LV). As was indicated above, the presence of the sample's compounds of spherical particles significantly reduces their limited compressive strength (Figure 78), so decreasing the quantities in a sample of particles is a current problem. On the other hand, thermal processing IER to high values requires additional energy costs that may be impractical. The work has studied compounds obtained by solidification IER ash burned to 81% and 87%. Selected degree firing 80÷90% proceeding, shows that when the IER in the samples amounts spherical particles many decreases, Figure 79.

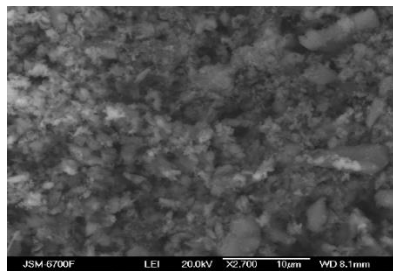


Figure 78. Ash of IER after thermal processing at 600 °C.

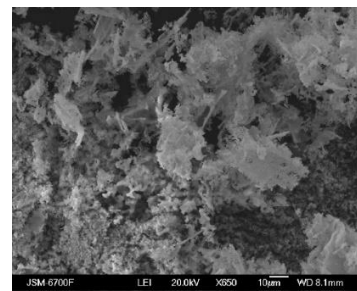


Figure 79. Ash of IER after thermal processing at 800 °C.

At the beginning of thermal processing at IER removed, a significant amount of adsorbed water was, and the degree of gasification on the amount of adsorbed water (Figure 78). Anyway, the strength of such specimens is extremely low, the same related significant dimensions particles ash. Results improved when selecting fractions by size 0,3mm, although large factions have been observed when studying distribution particle size.

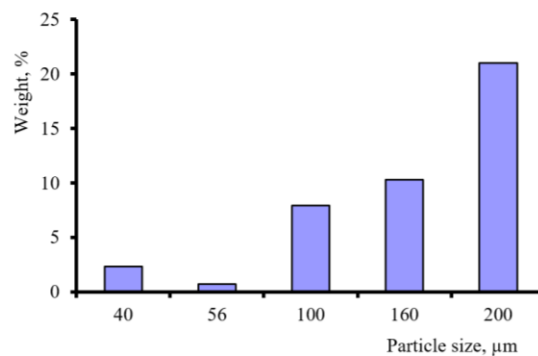


Figure 80. Size distribution in the fraction < 0,3 mm particles ash after burning 87% of the IER.

Table 15 shows that the best strength was the sample WP 6-56, which used the ash fraction <0.3 mm, a degree of gasification of 0.81. The amount of ash in the compound was 22.7%, and the amount of liquid glass increased to 19.4%. All samples were prepared for test leaching according to the previously described method. The characteristics of the samples are given in Table 16. The stable Cs-133 has been used as doping nuclides for leaching from MK/BFS matrix samples.

Table 16. Characteristics samples for leaching.

| Sample number | Mass of the test sample, g | Mass of Cs, g | Area of the contact surface, sm ² |
|---------------|----------------------------|---------------|--|
| WP6-56 (1) | 2.4 | 0,04 | 6.0 |
| WP6-56 (2) | 3,19 | 0,06 | 6,6 |

The leachability was conducted as a short-term test according to standard [7]. For leaching, samples have taken after 28 days of hardening in an atmosphere of saturated water vapour and dried for 10 days at room conditions. The surface of the sample has been cleaned of small particles or dust. The polypropylene containers have been used for leaching and the samples were suspended in containers filled with deionised water. The amount of deionised water was 10 times the specimen's surface area. After certain intervals, as specified in the standard, the specimens were withdrawn from the containers and immediately transferred to the next leaching container filled with fresh leachate. The used leaching containers containing all leached material has been closed and transmitted for analysis. Analytical data obtained for the leaching of the surrogate Cs are based on ICP-MS results. To measure the leaching rate, it is necessary to know the total leaching from the samples. According to these results, the values of the leaching rate were calculated and presented in Figure 81. Concentrations of caesium measured in the solution were negligible after one month of leaching in both samples.

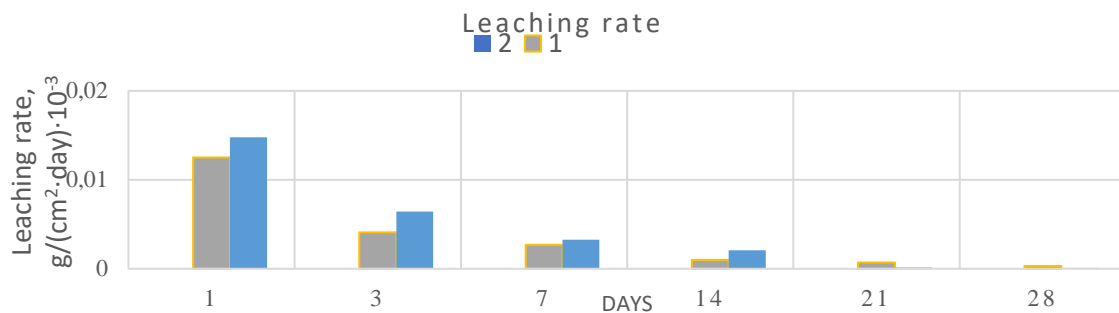


Figure 81. Leaching rate.

3. Conclusions / Summary / Way forward

The properties of binders' compositions of geopolymers intended to immobilise thermally treated organic wastes have been studied. The strength indicators of the compositions primarily depend on the physical and mechanical properties of the ash. It established that preliminary mechanical processing of precursors is necessary to increase the strength of the compounds to increase the efficiency of waste conditioning.

The leaching test showed that the MK/BPS geopolymer compound has good leaching resistance and that the Cs leaching rate does not exceed the standard.

References

- [1] M. Nieminen, et al., Gasification-based thermal treatment of Low and Intermediate Level Waste containing organic matter IOP Conf. Ser.: Mater. Sci. Eng. 818 012007, 2020
- [2] International Atomic Energy Agency, The Behaviours of Cementitious Materials in Long Term Storage and Disposal of Radioactive Waste. IAEA TECDOC No. 1701.
- [3] J. Davidovits, Geopolymer Chemistry and Applications, Publisher: Geopolymer Institute, Saint-Quentin, France, Editor: Joseph Davidovits, 2020
- [4] T. Vehmas, et al., Geopolymerisation of gasified ion-exchange resins, mechanical properties and short-term leaching studies, IOP Conf. Ser.: Mater. Sci. Eng. 818 012007, 2020
- [5] M. [Matsuda](#) et al., Decomposition of Ion Exchange Resins by Pyrolysis, Vol. 75, [Issue 2](#), 1986
- [6] EN 13791 – Assessment of in-situ compressive strength in structures and precast concrete components
- [7] ANS 2003 Measurement of leachability of solidified low-level radioactive wastes by short-term procedure American Nuclear Society, Illinois, USA, ANSI/ANS-16.1-2003

6.8 Physico-chemical characterization of the resulting waste forms

Elena Torres Álvarez, Esther Marugán, CIEMAT, Spain, elena.torres@ciemat.es

Pedro Perez-Cortes, María Cruz Alonso, Inés García-Lodeiro, Francisca Puertas, Instituto de Ciencias de la Construcción Eduardo Torroja (IETcc, CSIC), Spain, mcalonso@ietcc.csic.es

Raúl Fernández, Ana Isabel Ruiz, Mikel Dieguez, Pilar Padilla, Jaime Cuevas, Universidad Autónoma de Madrid (UAM), Spain, raul.fernandez@uam.es

Keywords: one-part geopolymer, qualification protocol, waste forms, doped IERs, leaching tests

1. Introduction

Several technical and economic issues are considered when implementing new pre-treatment/conditioning processes. Performance assessment of the resulting waste form in realistic disposal conditions, considering both, normal operation and accident conditions, is a key point.

Laboratory testing of waste form materials involves the application of tests to waste form materials to gain a better understanding of their degradation behaviour and release of constituents or to provide the information needed to model the performance of waste forms in disposal systems [1]. For instance, leaching tests can be used for the evaluation of the confinement ability of conditioning matrices. But also, this type of experiments can be used for tracking leaching process of matrix elements, which allows determining its stability in the leaching solution.

2. Description of work and main findings

During this last year of project, CIEMAT-CSIC-UAM have continued working on the physico-chemical characterization of the selected conditioning matrices for WP6. Mechanical and immersion tests have been performed according to national waste form qualification protocol. Since last Annual Meeting, 84 short-term leaching tests have been dismantled. Post-mortem characterization of the solids and the monitoring and analysis of the leachates from the short-term leaching tests has been carried out.

For task 6.6, 3 types of binders were selected: two OPC-based matrices, CEM I and CEM III, and the optimized geopolymer formulated in task 6.4 by CSIC. CEM I has been used as control in this set of leaching tests, as it is the reference formulation used for the backfill and sealing mortar in the Spanish disposal facility. In order to assess the economic and technical feasibility of the one-part geopolymer as conditioning matrix, performance of CEM III, typically used for the conditioning of SIERs, was compared with the geopolymer one.

In order to track the leaching behaviour and the matrix durability of the waste forms with time, four test durations were set, 3, 6, 12 and 24 months, and for each duration, 4 replicates have been tested. Two waste loads have been chosen: 0 and 20%wt. of waste.

Three different leaching media have been used: deionized water (UAM), *in situ* water sampled from *El Cabril* disposal facility and synthetic CEM I porewater according to PREDIS leaching protocol (CSIC).

These leaching media were selected in order to assess both, the compatibility of the waste forms with existing Engineered Barrier Systems (EBS) and the performance under disposal conditions, both in normal operation conditions and operational occurrences:

- *Synthetic CEM I porewater:* as a representative example of normal operational conditions, from CEM I backfill in disposal cells
- *Water sampled in disposal platforms:* porewater representative of the cementitious EBS in disposal facility
- *Deionized water:* worst case scenario

A complete characterization of the leachates and specimens from dismantled short-term leaching tests has been performed according to the leaching protocol defined in WP6 [2]. Additional ORP monitoring and TOC measurements have been carried out in leachates.

Monitoring of pH in the leachates showed different behaviours as a function of the chemical composition of the leachate. For disposal site water, pH reaches equilibrium after 5 months and stabilizes around 8.5 (initial pH 7.1). In tests using synthetic CEM I porewater, despite slight fluctuations, pH keeps constant, in a range

between 12.6 to 13.0 (initial pH 12.6). For degassed deionized water, different tendencies are observed depending on the conditioning matrix (Figure 82).

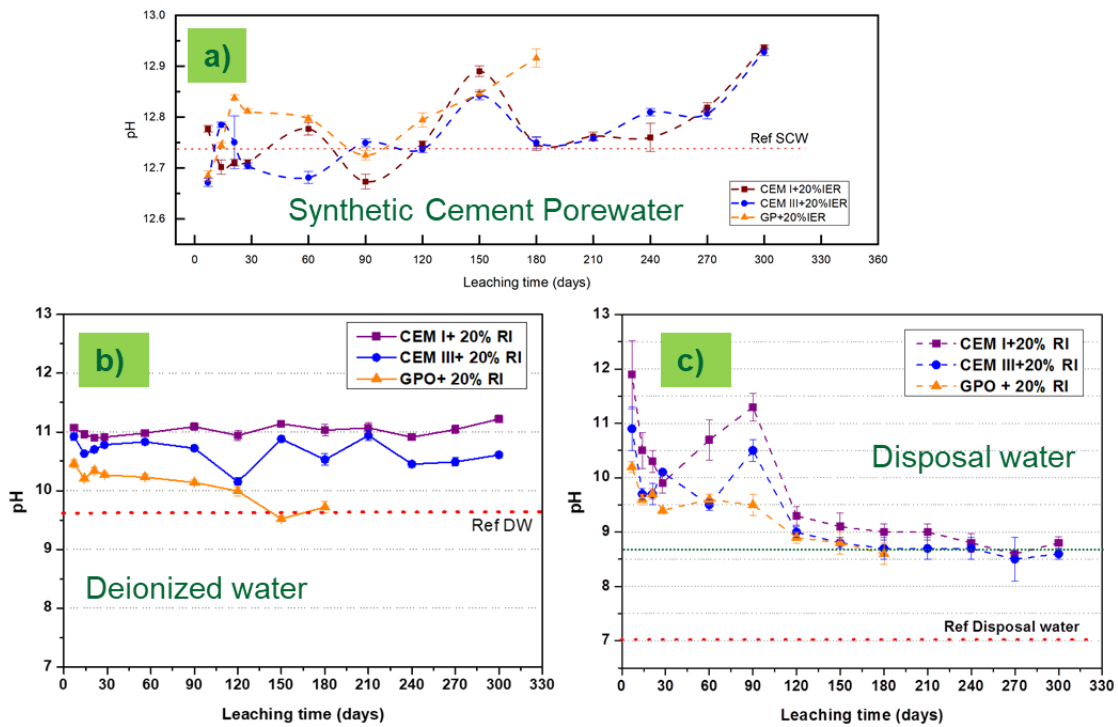


Figure 82. pH monitoring of leachates in the three leaching media selected for WP6: a) synthetic cement porewater (WP6 leaching protocol); b) deionized water and c) water sampled in disposal site.

Analogous behaviours are observed for Electrical Conductivity (EC) for the 6 waste forms and the 3 leaching media. Redox monitoring has shown that during the leaching tests, slightly reducing conditions were achieved, due to slags and fly ashes in the binders. No evidence of microbial growth were found in the leachates and no gas release was observed during leaching time. Biodegradation can be an issue of interest for further studies.

Chemical analysis of leachates shows moderate leaching of main cations: Ca in CEM I and CEM III-based waste forms and Na in geopolymer specimens, with and without waste. Comparing results of Ca analysis obtained for the three leaching media and the six waste forms, Ca leaching is higher for CEM I-based waste forms and highest Ca concentrations were measured for deionized water medium. For CEM III waste forms, similar leaching behavior of calcium were observed for disposal site and deionized water leachates. No significant differences are found between specimens with and without immobilized waste. In the case of geopolymer-based waste forms, Ca measured in leachates remains not affected (Figure 83).

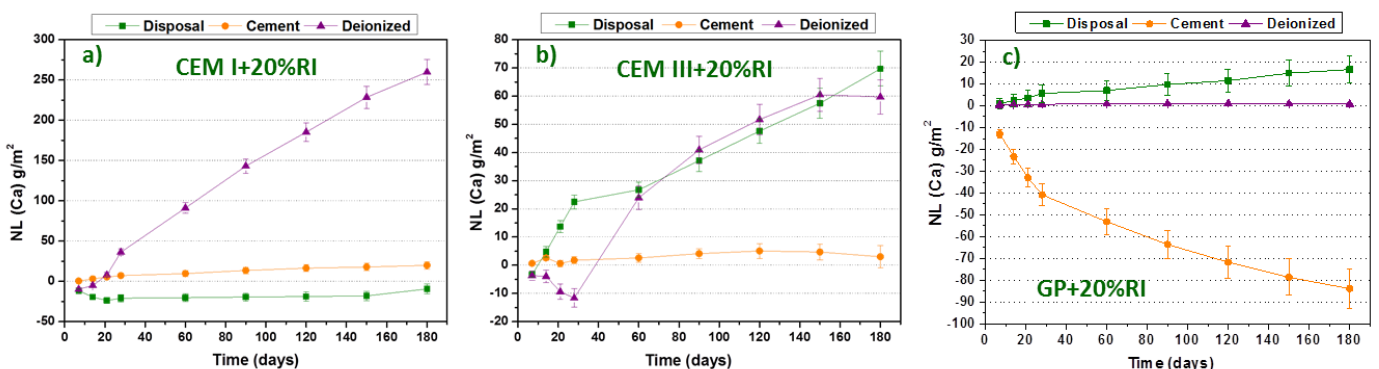


Figure 83. Normalised losses calculated for Ca measured in leachates from the short-term leaching tests for the three types of waste forms (a) CEM I+20 wt.%RI, b) CEM III+20 wt.%RI and c) Geopolymer+20 wt.%RI in the three leaching media: (disposal site water (disposal), synthetic cement porewater (cement) and deionized water (deionized)).

Calculated Si and Al normalized losses are similar for all matrices and leaching solutions. Regarding the type of conditioning matrix, greater leaching is observed for geopolymer rather than for CEM I and CEM III. When

comparing concentrations measured in the three leaching media, synthetic CEM I porewater seems to favour alkaline dissolution of the matrices, especially in the case of geopolymers.

In the case of trace analysis of doping elements of the IERs surrogates, concentrations range from tens of ppbs to few ppms, depending on the leaching media, type of conditioning matrix and analytical equipment. In any case, calculated leaching rates are remarkably lower than national WAC values.

Probes from the dismantled leaching tests were mechanically tested, previously to the microstructural characterization of the solids. In general, in specimens with immobilized waste, no significant differences were found between compressive strength values of as-cured specimens and the ones from the already leaching tests. Besides, post-leaching compressive strength does not seem to be conditioned by the type of leaching solution.

Due to the short duration of the tests, XRD analysis performed in the 3-month leached samples for the different type of waste forms and leaching media did not allow identifying the formation of new phases. Semiquantitative analysis by RIR neither showed significant variations in the mineral phase assemblage (Figure 84).

SEM observations of CEM I and CEM III-based specimens confirmed the occurrence of longitudinal surface cracking. EDX mapping of the polished sections showed the occurrence of different processes depending on the type of leaching solution used in the tests. Synthetic CEM I porewater seems to promote the advance of the hydration front, resulting in the potassium enrichment of the outer layer of the sides exposed to the solution. In the case of samples leached with deionized water, Ca depletion of the matrix was detected as well as the formation of a diffusion front towards the exposed surfaces. For the geopolymer-based probes leached in the synthetic cement porewater solution, lower Al, Na and Ca contents were determined in samples exposed to the cementitious solution. Again, cracking was observed on the surfaces exposed to the leachant (Figure 85).

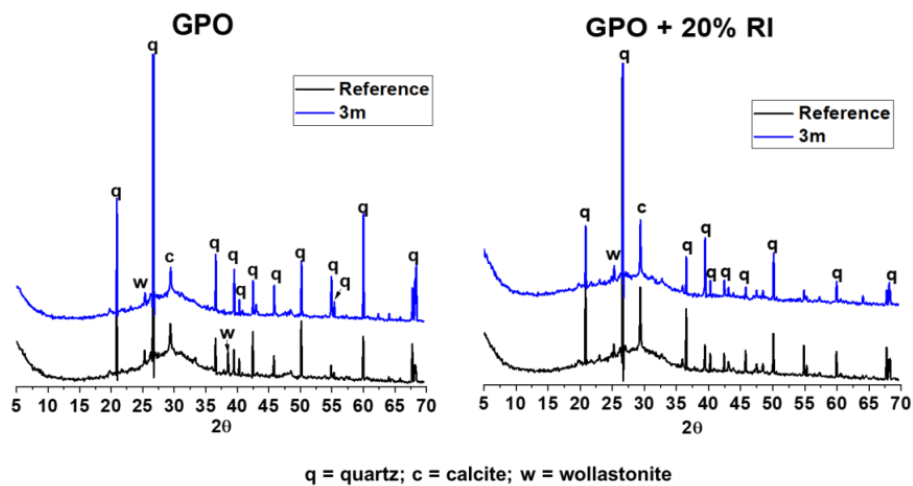


Figure 84. DRX pattern of the geopolymer specimens with and without waste load after 3-month leaching test in deionized water.

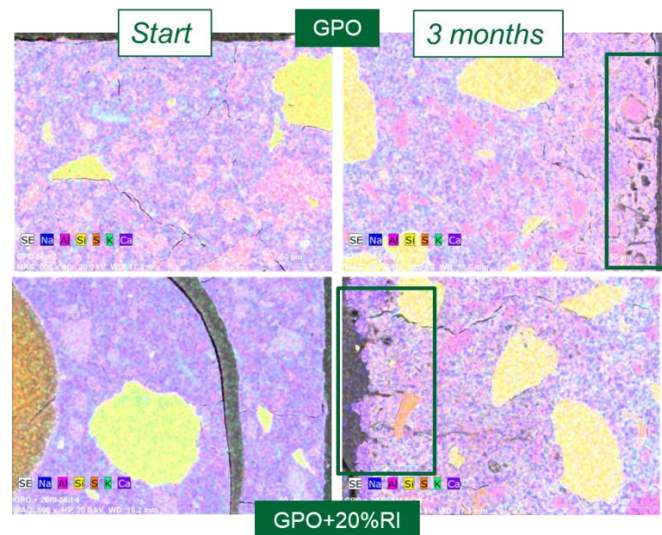


Figure 85. BSEM mapping analysis of the geopolymer samples before and after 3-month leaching tests in synthetic cementitious water.

3. Way forward

For the next coming months, CIEMAT-CSIC-UAM plan to continue with the on-going:

- characterization of the solids from the dismantled leaching tests (3, 6 & 12 months).
- analysis of leachates: both major and trace elements

A special coordination effort will be made to integrate the obtained results in the leaching tests, considering the three types of waste form and three leaching media. In parallel, freeze-thaw testing is scheduled as part of the qualification process of new waste forms. Results obtained in task 6.6. are expected to provide some insight about the durability and performance of the new geopolymer matrix compared with the commonly-used for the conditioning of SIERs (CEM III).

References

- [1] Chapter 5. Waste Form Testing." National Research Council. 2011. Waste Forms Technology and Performance: Final Report. Washington, DC: The National Academies Press. doi: 10.17226/13100.
- [2] E. Myllykylä, E. (2021). Milestone 39. Definition of the leaching procedure for the short-term experiments and the long-term durability experiments. PREDIS internal report. 7 pp.

6.9 Short and long-term leaching tests with HIPed ashes (Task 6.6)

*Karine Ferrand, Sébastien Caes, Karel Lemmens
SCK CEN, Belgium
karine.ferrand@sckcen.be*

Keywords: short and long-term leaching tests, synthetic cementitious water, HIPed IRIS ashes, glass ceramic, PREDIS reference protocol, Milestone 49

1. Introduction

After thermal treatment of inactive solid organic waste and ionic exchange resins in the IRIS incineration pilot process at CEA Marcoule, the ashes were HIPed at the University of Sheffield. To do this, 95 wt.% of IRIS ashes was mixed with 5 wt.% of Na₂B₄O₇ in stainless steel cans. Then, the welded cans were heated at 300 °C for ~12 hours under vacuum, and sealed. Afterwards, they were HIPed at 250 °C and 100 MPa for 2 hours. Two cans were sent to SCK CEN to perform short and long-term leaching tests, as described in the Milestone 39.

2. Description of work and main findings

Before starting the leaching tests, the HIPed samples were characterised by SEM-EDX and XRD analyses. SEM-EDX analysis shows the presence of crystalline phases, identified as magnesium / zinc aluminium oxide ($\text{MgAl}_2\text{O}_4 / \text{ZnAl}_2\text{O}_4$) and calcium chloride phosphate $\text{Ca}_5(\text{PO}_4)_3\text{Cl}$ by XRD, in an amorphous matrix composed of O, Si, Al, Ca, Na, Mg and K. Consequently, the HIPed wasteform is a glass-ceramic. The presence of many pores in the samples is also observed, with a pore diameter that can reach up to 45 μm .

Semi-dynamic tests are carried out at 22 ± 2 °C in a glove box under Ar atmosphere with one cubic sample (5 mm side) and 15 mL of synthetic cementitious solution at pH 12.7 ± 0.1 , which contains 2800 mg/L of K, 18 mg/L of Ca, and 1080 mg/L of SO_4^{2-} . After durations specified in the reference protocol, the solution was renewed and the pH and the elemental concentrations were measured in the leachates.

No significant pH change between two solution renewals was measured. The concentrations of K, Mg, Ca, SO_4^{2-} were similar to those in the leaching solution. Due to the low temperature, the low sample surface area to solution volume ratio and the renewal of solution, the release of the elements constituting the sample is also low. Consequently, some elements were not detected in solution or their concentration was below the quantification limit (P, Ti, Cr, Ni, Cl). However, the concentrations of three of the four main elements of the ashes, *i.e.* Si, Al and Zn, were measured by ICP/MS. Boron coming from the addition of $\text{Na}_2\text{B}_4\text{O}_7$ with the ashes in order to form a glass-ceramic by HIPing was also quantified in the leachates.

The normalised loss (NL) and the cumulative fraction leached (CFL) were calculated for the elements measured in the leachates using a theoretical sample composition. From the boron NL a maximum dissolution rate of 0.47 ± 0.05 g/m²d was determined between 0 and 28 days, which is about 5 times higher than the one for SON68 and ISG glasses altered in KOH at pH 12.5 and 30 °C by performing dynamic tests. The maximum dissolution rate of the HIPed samples is however quite similar to that measured for the Al-rich glass SM539 (0.58 g/m²d). The dissolution rate is slightly decreasing with time due to the formation of a protective alteration layer. After 1 year SEM analysis shows the presence of an alteration layer with an average thickness of 25 μm . Due to the presence of pores at the surface of the sample the alteration layer thickness can reach up to 100 μm . In the alteration layer, mainly composed of O, Al, Ca, P, Na, Mg, Zn, Cl and Si, the same crystalline phases as those present in the unaltered sample are visible. Note that very different compositions of the alteration layer were measured by EDX analysis, so an average composition cannot be reported.

According to the ANSI/ANS-16.1-2019 procedure, an effective diffusion coefficient of $\sim 2.5 \times 10^{-10}$ cm²/s and a leachability index of ~ 9.6 were calculated for boron and silicon.

3. Summary

The last renewal after 18 months will be done on July 2023 and the long-term leaching tests will be finished in January 2024. Data that have not been received yet will be processed and samples altered for 2 years will be characterised by SEM-EDX and XRD analysis.

6.10 Geopolymer characterization from immobilization of MSO waste

Vojtěch GALEK¹, Anna SEARS¹, Petr PRAŽÁK¹, Tomáš ČERNOUŠEK¹, Martin VACEK¹, Jan HADRAVA¹

¹Research Centre Řež, Hlavní 130, Husinec-Řež, 250 68, Czech Republic, cvrez@cvrez.cz
Vojtech.galek@cvrez.cz

Keywords: Geopolymer, volcanic tuff, molten salt waste, Molten Salt Oxidation

1. Introduction

Radioactive waste generated during the operation and decommissioning of nuclear facilities can include both organic and inorganic solid and liquid waste. Molten Salt Oxidation (MSO) is a promising thermal treatment process identified as one of the potential routes for volume reduction of organic radioactive waste such as oils, ion exchange resins, and other hazardous wastes.[1].

For immobilization techniques, cementation using Portland-based cement is a common solidification process. Cement, however, is subject to chemical degradation due to water or acidic condition, which can cause calcium from the solid matrix to leach out. This phenomenon challenges waste storage safety and sustainability [2].

Geopolymers are inorganic polymers that can challenge cementitious materials as a possible route for waste immobilization. Geopolymers are prepared by the polycondensation reaction of an aluminosilicate precursor with an alkali activator solution at normal temperature and pressure. Various aluminosilicate precursors are available for geopolymer manufacturing, such as metakaolin, blast furnace slag, fly ash, etc. [3][4]. Besides curing at the normal temperature (21 °C), the geopolymers have other advantages, such as but not limited to high acid and heat resistance, higher leaching resistance, high structural integrity, and mechanical stability. Geopolymers are also considered class green due to producing less greenhouse gas than cement. [5] The setting mechanism of geopolymer is based on rapid polymerization rather than hydration as with cement and is, therefore, much faster. [6] These characterizations suggest that geopolymers could be long-term stable and potentially usable materials for radioactive waste solidification.

2. Description of work and main findings

This work aimed to stabilize the spent salt from the MSO process with high content of alkaline carbonates in the geopolymer matrix. The physical and chemical properties of the geopolymer and spent salt were measured.

CVRez continued with the characterization of prepared samples for statistics as our recipe LK10 was filled with molten salt waste from 5 to 25 wt.%. The samples were cured for four days in the mold before they were taken out and cured for another 28 days in three different ways: in a wet environment, in dry conditions, and in underwater immersion. Then the mechanical strength and modulus of elasticity were analysed. The XRD and SEM analysis were performed on dry-cured samples. The results on mechanical strength and modulus of elasticity of dry-cured samples are shown in Figure 86.

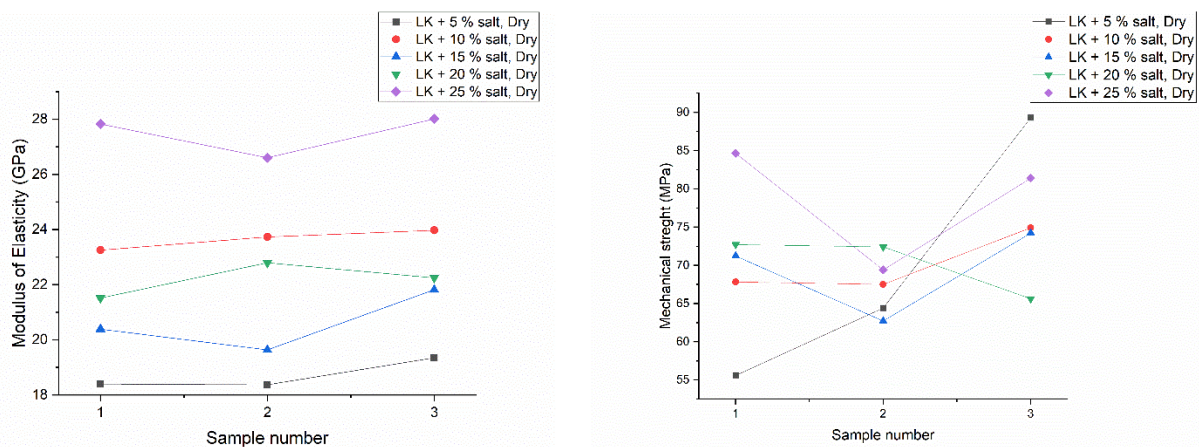


Figure 86. The modulus of elasticity and mechanical strength of cured samples with different waste loads.

The SEM and XRD analysis proved that all prepared samples show the homogenous distribution of chemical elements from surface to core, indicating good mixing technique. With higher amounts of waste load, the composition of Na-Ca-carbonates increases, and by the XRD, it is identified as pirssonite. Figure 87 shows the BSE and phase map of 25 wt.% of waste load.

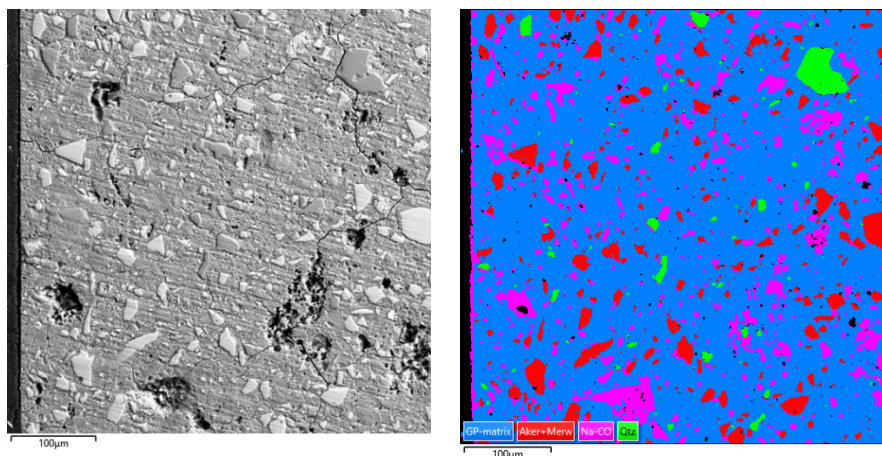


Figure 87. The BSE and phase map of 25 wt.% samples.

The following work aimed to substitute the 10 wt.% of geopolymer as filler with volcanic tuff obtained from POLIMI. The curing was set as regular LK geopolymer, but the first experiments proved longer curing in the mold, at least 14 days and then cured regularly for 28 days. The maximum possible waste load was set at just 15 wt.% due to the high viscosity during the mixing of the grout. The mechanical strength of prepared samples was performed. The waste load negatively affected the mixture, as only 15 wt.% waste load sample dry-cured was solid enough with 11,3 MPa of mechanical strength. The wet and water-immersed samples were not cured at all. The mechanical strength of 5 and 10 wt.% waste loads decreased with a high moisture environment. The recipe change for more water addition is needed for the possible waste load.

Waste enhancement was decided as the molten salts are chemically unstable with a geopolymer matrix in a wet environment. The process was done with the dissolution of molten salts in water with the slow addition of calcium hydroxide. This process took a few days as the calcium hydroxide in the solution was added as drops. During the process, the sediment formed, and the waste solution cleared. The sediment was then filtered and dried, and XRD analysis was performed. Figure 88 shows the results from the first experiment. Overall, the two experiments were performed with final sediment gain of around 500 g with a Na:Ca ratio of 55.9:44.1.

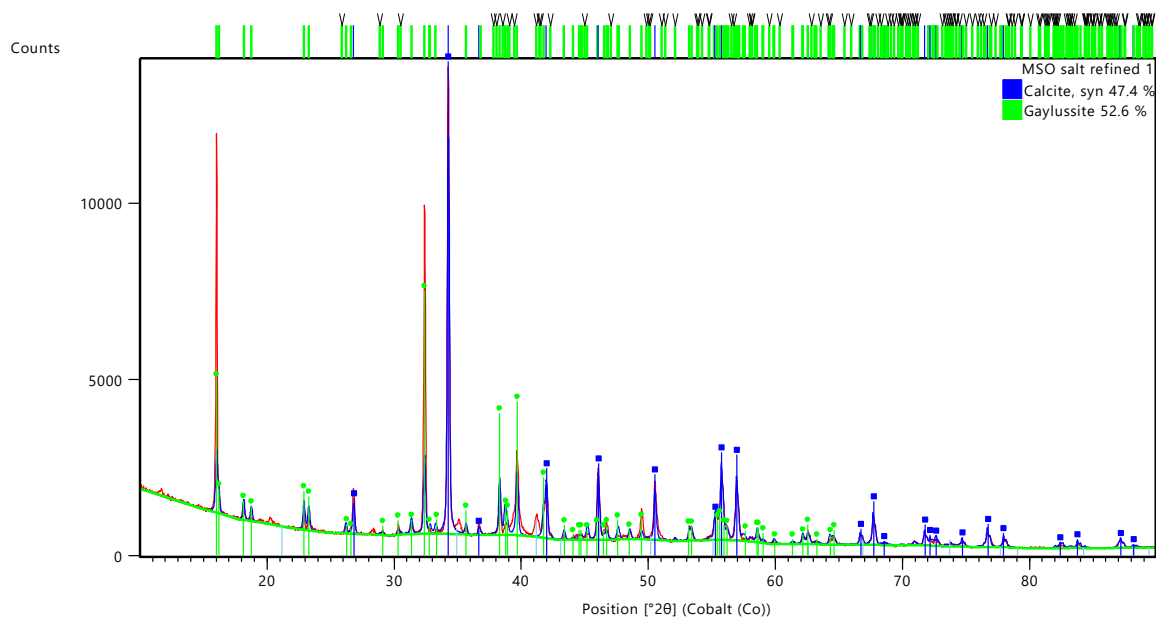


Figure 88. The XRD analysis of the first experiment of molten salt enhancement.

The enhanced molten waste was immobilized in the standard geopolymer matrix LK10. The waste load was set from 5 to 15 wt.%. The 15% wt. was the highest addition as the grout was very dense, had a fast reaction time, and was hard to mix. The samples were cured for three days in the mold and are now curing for 28 days regularly. The XRD and SEM analysis of the finished dry samples will be performed in a few weeks.

3. Conclusions

This work aimed to perform the XRD and SEM analysis on our recipe samples LK10 with waste load up to 25 wt. %. As expected, the higher phase distribution of pirssonite was present with a higher waste load in the matrix. The experiments with volcanic tuff added as filler were also performed. The final mixture could mix only with 15 wt. % of the waste load due to the high viscosity and fast setting time. The 15 wt. % waste load did not perform well, as only dry-cured samples could solidify enough for mechanical stress tests. The 5 and 10 wt. % waste load mechanical tests show decreasing strength with higher moisture environments. The waste salt was turned into enhanced salt with a chemical reaction with the lime solution. The final sediment was analysed, and Na:Ca was determined to be 55.9:44.1. This improved salt was immobilized in the LK10 geopolymer with 5, 10, and 15 wt.% waste load. The analysis of these samples was not yet performed.

References

- [1] C. Lin, Y. Chi, Y. Jin, X. Jiang, A. Buekens, Q. Zhang, J. Chen, "Molten salt oxidation of organic hazardous waste with high salt content", *Waste Management and Research*, 36(2), 2018, pp. 140–148.

- [2] F. J. Ulm, F.H. Heukamp, J. T. Germaine, "Residual design strength of cement-based materials for nuclear waste storage systems", *Nuclear Engineering and Design*, 211(1), 2002, pp. 51–60.
- [3] R. S. Krishna, J. Mishra, M. Zribi, F. Adeniyi, S. Saha, S. Baklouti, F. U. A. Shaikh, H.S. Gökçe, "A review on developments of environmentally friendly geopolymer technology", *Materialia*, 20, 101212, 2021.
- [4] S. S. Mohapatra, J. Mishra, B. Nanda, S. K. Patro, "A review on waste-derived alkali activators for preparation of geopolymer composite", *Materials Today: Proceedings*, 56, 2022, pp. 440–446.
- [5] E. R. Vance, D. S. Perera, "Geopolymers for nuclear waste immobilisation", *Geopolymers: Structures, Processing, Properties and Industrial Applications*, 2009, pp. 401–420.
- [6] N. A. Girke, H.-J. Steinmetz, A. Bukaemsky, D. Bosbach, E. Hermann, I. Griebel, "Cementation of Nuclear Graphite Using Geopolymers", (IAEA-TECDOC--1790(COMPANION CD-ROM)). International Atomic Energy Agency (IAEA), 2016

6.11 Oxidative pyrolysis and Fenton-like wet oxidation of spent ion-exchange resins

Francesco Galluccio, Andrea Santi, Eros Mossini, Gabriele Magugliani, Edoardo Rizzi, Elena Macerata, Marco Giola, Mario Mariani
Politecnico di Milano, Italy
 Corresponding author: eros.mossini@polimi.it

Keywords: radioactive solid organic waste, treatment, conditioning, oxidative pyrolysis, Fenton-like wet oxidation

1. Introduction

Ion-exchange resins (IERS) are employed worldwide for the control of the chemical purity of water in nuclear power plants and for the decontamination of radioactive aqueous effluents. Because of the harsh operating conditions – high temperatures, radiation fields, mechanical stresses – and contamination, spent IERS are preferably disposed of as low-level waste rather than being regenerated [1]. POLIMI investigates two different processes to treat the exhausted resin beads with the aim of obtaining stable products, suitable for conditioning in inert matrices, and achieving reduction of waste volumes. The two processes are an oxidative pyrolysis and a Fenton-like wet oxidation [2,3].

2. Experimental activity

2.1 Oxidative pyrolysis

A surrogate waste was prepared by doping nuclear grade cation-exchange AmberLite IRN77 beads (DuPont) with nitrate salts (Sigma-Aldrich, analytical grade) of stable elements, representative of fission and activation products, namely Co, Ni, Sr, Cs, Nd, Eu. Two types of surrogate waste are prepared: i) beads individually doped with each metal; ii) beads simultaneously doped with the six metals. The surrogate waste is treated in a muffle furnace; it is placed in a crucible, covered with a holed lid. Furnace temperature is then increased by 100 °C every 30 minutes up to 800 °C. After a certain residence time, an inverse temperature ramp is input until room temperature. The ashes are retrieved, weighed, and stored in a sealed vial for further characterisation and conditioning in the tuff-based geopolymer matrix developed at POLIMI.

2.2 Fenton-like oxidation

A surrogate mixed resin bed is prepared by doping nuclear grade cation-exchange AmberLite IRN77 beads (DuPont) with nitrate salts of stable Co, Ni, Sr and Cs. Anion-exchange resin is AmberLite IRN78 (DuPont) and is doped with KCl and KI salt (Sigma-Aldrich, analytical grade) solutions. The saturation factor with respect to the ion exchangeable resin sites ranges from 10 eq.% to 40 eq.%. The surrogate waste is transferred to a four-necked round-bottom flask, equipped with thermometers and an agitation system, and immersed in a thermal bath to control the reaction temperature of the process at increasing resin batches. A peristaltic pump is used to control the addition of the oxidant (H₂O₂) into the mixture. Two different catalysis systems are used to conduct a homogeneous and heterogeneous oxidative process, respectively:

- 0.1 mol/L FeSO₄ and 0.1 mol/L CuSO₄ (Sigma-Aldrich, analytical grade) aqueous solution;
- Fly ash (FA) powder or electric arc blast furnace slag (EA-BFS).

After adding the catalyst, the mixture in the boiling flask is heated up to 70 °C, before dropwise adding H₂O₂ to carry out the oxidation.

During the treatment, aliquots of the solutions are collected for further characterisation. At the end of the process, the liquor is recovered and evaporated at 70 °C. The residue is recovered and stored in sealed containers for further characterisation and conditioning in the tuff-based geopolymer matrix developed at POLIMI.

3. Results

Oxidative pyrolysis

Batches of 15 g of doped beads were treated for 39 h at 800 °C. Residues have been characterised via Raman spectroscopy and X-ray powder diffraction, and mass reduction and retention factor were derived from gravimetric and Q-ICP-MS measurements. Pictures of the residues taken with optical microscopy are reported in Figure 89. For the most part, resin beads undergo degradation into hollow, crystalline spheres. X-ray diffraction and Raman spectroscopy were employed to identify the contaminants' compounds present in the residues, mainly sulphates and oxides. Traces of graphitic carbon are found as well. Conversely, Raman spectra and X-ray diffractograms of resin samples doped with all the six cations (49.5 eq.% total doping) exhibit complex patterns, and only some compounds previously identified in single-doped samples are easily identifiable.

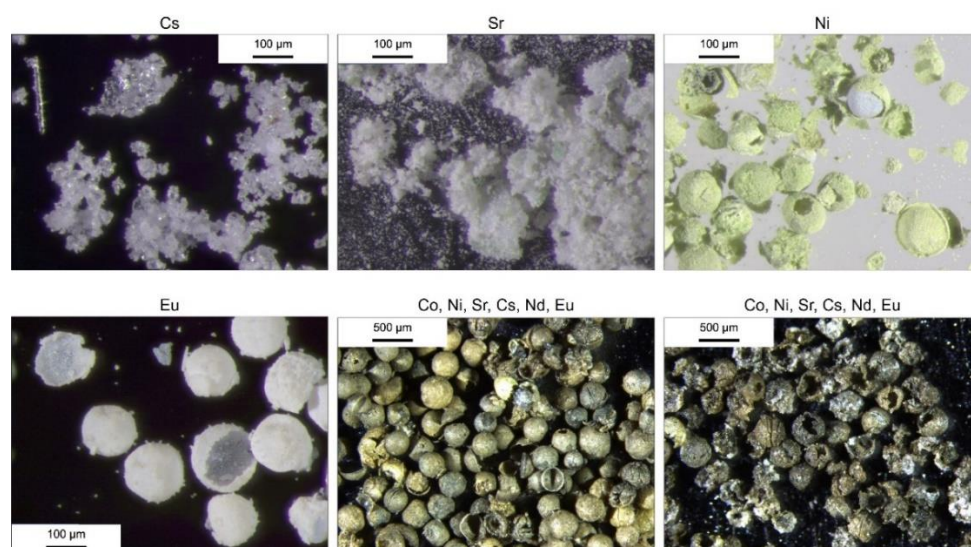


Figure 89. Optical microscopy of degraded resin batches.

Weight reduction ratios and contaminant retention factors for single-doped resin batches were calculated. The first always resulted above 97 %wt., the second was always higher than 94 %wt., with Cs as limiting case. Besides, residues of simultaneously doped resins were poorly dissolvable in concentrated acid mixtures (HCl and HNO₃), and an exact determination of the retention of the contaminants via Q-ICP-MS was not possible. However, more than 84.9 wt.% of Cs was found in the residues, and a mass reduction of 85.1% was measured. These results agree with the one obtained by single-doped batches of resin.

Fenton-like oxidation

Homogeneous wet oxidation

The management of a mixed resin bed required important adjustments in the operating parameters because of the presence of anionic resin. CuSO₄ · 5 H₂O was added to the FeSO₄ – H₂O₂ reaction system as co-catalyst to boost the oxidation yield. Furthermore, a larger amount of oxidant was needed and a longer time duration at increasing mass of surrogate waste was observed, in comparison with an equivalent mass of cationic resin bed.

A first trial run was performed with 20 g of mixed bed resin, where monitoring of temperature and colour shift of resin mixture was helpful to understand the evolution of the process. The double-peak reaction showed a great increase in the Chemical Oxygen Demand (COD) when the cationic IER dissolution occurs, while a second broader peak at a lower value can be observed and ascribed to the longer degradation of the anionic IER coherently with temperature profile and colour of the solution. At the end of the process, the COD almost reached the initial value measured before the occurrence of the IER dissolution. Moreover, a whitish and fine precipitate was found at the bottom of the reactor and identified as strontium sulphate by XRD analysis. A small scale-up of the process was attempted for the management of 100 g of mixed resin bed. The double-peak oxidative reaction clearly showed a first peak at about 90 °C due to the degradation of cationic resin, while a second peak at about 95 °C representative of the very long decomposition of anionic resin as observed in the small laboratory scale (Figure 90).

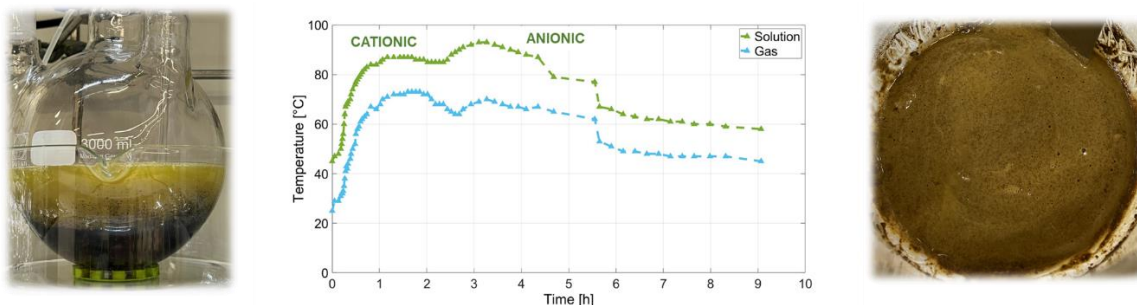


Figure 90. Oxidative transition from cationic to anionic resin (left). Temperature profiles of process solution and off-gases (middle). Residue obtained downstream of the evaporation process (right).

At large scale, intense formation of bubbles due to anionic resin decomposition occurs, and this became more pronounced with a batch of 200 g. Nevertheless, efficacy of the process was promisingly controlled. At the end of the oxidation, more than 95 wt.% of the initial Co, Ni and Cs was found in the resulting liquor, while part of the initial Sr (70 wt.%) was found in the precipitate. On the other hand, ~10 wt.% of I and Cl remains in the final solution since the larger part of them came out in the process off-gases and therefore need to be suitably collected downstream of the glass reactor (Figure 91). After evaporation stage, a brownish residue was obtained (Figure 90), thereby resulting in a weight reduction ratio (WRR) of about 80%. XRD investigations on the final residues mainly identified inorganic species like chalcantite $[CuSO_4 \cdot 5 H_2O]$, iron sulphate $[FeSO_4]$, and especially ammonium copper sulphate hydrate $[(NH_4)_2Cu(SO_4)_2 \cdot 6 H_2O]$ and ammonium iron sulphate $[NH_4Fe(SO_4)_2]$.

Overall processes conducted at small and intermediate laboratory scale showed the same WRR. However, the scale-up shifted the time duration of the process from 3 hours (20 g) to 10 hours (100 g) and towards 15 hours (200 g). In conclusion, research is in progress and a new version of wet oxidative process in a heterogenous way will be proposed soon, in search of more benefits for treatment and conditioning of RSOW.

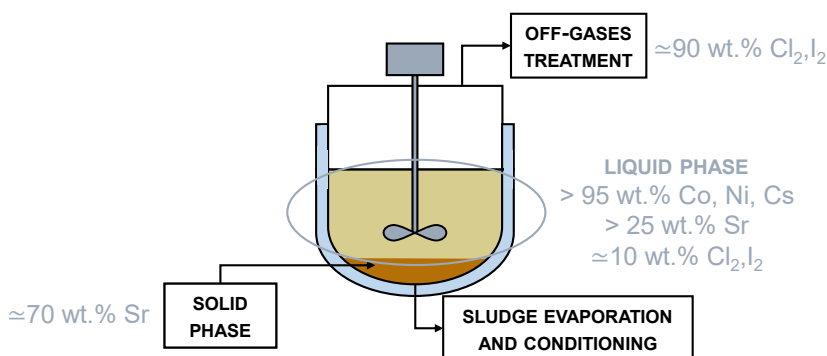


Figure 91. Distribution of contaminants at the end of the Fenton-like wet oxidation of a mixed bed resin.

Heterogeneous wet oxidation

Ongoing research aims at overcoming some of the drawbacks of homogeneous wet oxidation, such as high amounts of sulphates and volumes of the final liquor, strong acidity of the sludge and poor durability of waste forms, by exploring heterogenous ways based on the recycling of some iron-containing industrial by-products as potential catalysts and precursors of the used encapsulation matrix. At this stage, FA and EA-BFS are being investigated for a Fenton-like wet oxidation of 10 g of undoped cation-exchange resin.

From 3 g to 5 g of fly ash were tested. Increasing catalyst mass and keeping constant the oxidant flow rate, the single-peak reaction at about 100 °C is triggered earlier and lower amount of the oxidant is needed. The evolution of the process was visually inspected by the colour shift and the temperature of the mixture over time. After evaporating the yellowish liquor, a sludgy residue was obtained (Figure 92). Considering the added catalyst mass, a weight reduction ratio higher than 60% was calculated for each of the investigated experimental conditions.

Afterwards, a second series of experiments was run to investigate from 0.9 g to 1.5 g of EA-BFS. Similarly, the effect of increasing catalyst mass at constant oxidant flow rate brought the single-peak reaction at lower temperature (96 °C) forward. Moreover, the transient response resulted faster than that obtained with fly ash catalyst. The evaporation of the collected liquor resulted in a powdery residue (Figure 92), and a weight reduction ratio higher than 60% was similarly obtained.



Figure 92. Liquors and residues downstream of wet oxidation process by using fly ash (top) and steel slag (bottom) as a catalyst.

4. Concluding remarks

The management strategy based on a homogeneous Fenton-like wet oxidation calls for major efforts for the treatment of larger resin beds, encapsulation of the residue in a geopolymeric matrix, and complete characterization of the waste form. In this regard, POLIMI is going to equip its laboratory with a suitable chemical reactor to guarantee a complete mineralization of residual organic matter in the liquor and simplify the management of off-gases at very large scale of the process. Moreover, feasibility of a heterogeneous wet oxidation remains preliminary and implementation at large scale is going to be explored.

Acknowledgements

Collaborative Doctoral Partnership between Politecnico di Milano and European Commission's Joint Research Centre – Ispra site.

Department of Earth Sciences at University of Milan for performing X-ray Diffraction spectroscopy.

References

- [1] J. Wang, and Z. Wan "Treatment and disposal of spent radioactive ion-exchange resins produced in the nuclear industry". *Progress in Nuclear Energy* 78, p. 47–55 (2015). doi: <https://doi.org/10.1016/j.pnucene.2014.08.003>
- [2] U. Chun, K. Choi, K. Yang, *et al.* "Waste minimization pretreatment via pyrolysis and oxidative pyrolysis of organic ion exchange resin". *Waste Management* 18, p. 183–196 (1998). doi: [https://doi.org/10.1016/S0956-053X\(98\)00020-8](https://doi.org/10.1016/S0956-053X(98)00020-8)
- [3] S. A. Walling, W. Um, C. L. Corkhill, *et al.* "Fenton and Fenton-like wet oxidation for degradation and destruction of organic radioactive wastes". *Npj Materials Degradation* 5, p. 1–21 (2021). doi: <https://doi.org/10.1038/s41529-021-00192-3>

6.12 Encapsulation of treated organic wastes into tuff-based geopolymeric matrix

Andrea Santi, Francesco Galluccio, *Eros Mossini*, Gabriele Magugliani, Edoardo Rizzi,
Elena Macerata, Marco Giola, Mario Mariani
Politecnico di Milano, Italy
Corresponding author: eros.mossini@polimi.it

Keywords: radioactive solid organic waste, treatment, conditioning, waste acceptance criteria, geopolymer, tuff, Fenton-like oxidation, oxidative pyrolysis

1. Introduction

Downstream of the treatment processes, the radioactive solid organic waste (RSOW) residues undergo encapsulation in a suitable matrix, to confine the contaminants in durable, solid waste forms. To this purpose, POLIMI has developed a tuff-based matrix [1]. The latter consists of a geopolymer mainly synthesised with natural materials and recycled industrial by-products to pursue sustainability. A zeolitic volcanic tuff is used as a filler due to its low cost and worldwide availability. Besides, the zeolites provide an effective chemical barrier against certain mobile elements, namely Cs and Ni, by chelating the cations via selective cation-exchange processes. The encapsulation of four distinct treated wastes is ongoing:

- cation-exchange resins thermally degraded at POLIMI via oxidative pyrolysis;
- ion-exchange resins treated by Fenton-like wet oxidation at POLIMI;
- ashes coming from the IRIS pilot plant managed by the CEA;
- residues of solid organic waste treated at CVŘež by means of molten salt oxidation (MSO).

2. Experimental activity

The tuff-based matrix previously developed has been improved by decreasing the amount of activator, fly ash and blast furnace slag, while increasing the content of volcanic tuff. The updated composition of the matrix is reported in Table 17. The materials are used without any pre-treatment. Sodium hydroxide is technical grade with purity greater than 98%, sodium silicate technical grade aqueous solution with concentration 35 wt.%. Synthesis of the matrix remained unchanged [1]. Cast specimen underwent in-mould curing for 28 days when loaded with any waste.

Table 17. Composition of the tuff-based matrix.

| Component | Content [wt.%] |
|---------------------------|----------------|
| Volcanic tuff | 22.6 |
| Fly ash | 20.1 |
| Blast furnace slag | 21.0 |
| Alumina | 2.7 |
| Sodium hydroxide (pellet) | 5.0 |
| Sodium silicate solution | 2.4 |
| Water | 26.2 |

Waste loading factor is expressed in weight percentage as the ratio of the waste mass over that of the resulting waste form. The same matrix formulation was used for the four treated wastes under investigation.

Cation-exchange resins thermally degraded at POLIMI via oxidative pyrolysis

Because the oxidative pyrolysis is developed at a small laboratory scale and achieves significant volume reduction, the preparation of a surrogate representative product is necessary to investigate the encapsulation of this type of waste. Following the characterization of the residues obtained downstream of the treatment, a mixture of sulphates, oxides, and nitrates of representative stable contaminants namely Fe, Co, Ni, Sr, Ag, Cs,

Ce, Nd, Eu, Th, U, was prepared. Such a surrogate residue is added to the freshly activated grout before further mixing and casting.

Ion-exchange resins treated by Fenton-like wet oxidation at POLIMI

The concentrated sludge obtained downstream of the homogeneous Fenton-like oxidation has been preliminarily encapsulated at 10 and 20 wt.% by preparing cubic samples (side 5 cm) for compression tests. Prior to conditioning, the sludge is brought at pH 7 with sodium hydroxide and water; while the amount of required NaOH is determined by the initial pH of the sludge, which appreciably varies from batch to batch, the amount of water used for this neutralization is the water required for the preparation of the matrix grout. Afterwards, the sludge is mixed with the powdery precursors and, eventually, the activator is added.

Ashes coming from the IRIS pilot plant managed by the CEA

The IRIS ashes provided by CEA are blended prior to conditioning to break the agglomerates and obtain a finer powder. This is in turn added to the precursors before their activation. A preliminary set of small cylindrical samples (28 mm in diameter, 30 mm in height) was cast to assess the maximum loading factor. Explored waste loadings were: 10, 20, 30, 40, and 50 wt.%. Because of the substantial quantity of ashes required to run these experiments, it was not possible to cast cubic samples for compressive strength and more material was required.

Residues of solid organic waste treated at CVŘež by means of MSO

The MSO residues provided by CVŘež are blended prior to encapsulation in the tuff-based matrix to break the agglomerates and obtain a finer powder, and then added to the geopolymer precursors and mixed with them; activation of the grout follows. A set of samples (cubic for compression and cylindrical for leaching tests, respectively) has been prepared at 15, 25, and 35 wt.% waste loading.

3. Results

The decreased amount of activator resulted in several improvements: lower alkalinity implies lower carbonation effect. Besides, less hydration heat is developed during the activation phase, resulting in lower thermal stresses during hardening. The compressive strength has increased by approximately 37%, and the release rate of sodium during leaching tests dropped by 40%. The comparison of the two matrices is reported in Figure 93.

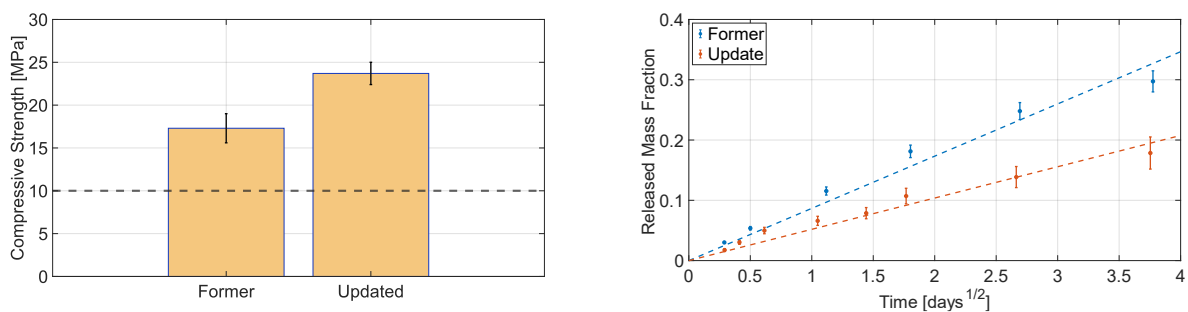


Figure 93. Compressive strength (left) and sodium leaching (right) for the former and updated tuff-based matrix.

Results concerning the encapsulation of surrogate pyrolyzed waste, Fenton-oxidized sludges and MSO residues are summarized in Figure 94. The presence of the surrogate pyrolyzed waste does not significantly affect the mechanical performance of the matrix, for a drop of about 16% in the compressive strength is measured when the matrix is loaded with 20 wt.% waste. This is attributable to the chemical stability of the waste, which poorly interfere with the geopolymerisation reaction. Preliminary hardening of the forms was tested and achieved also with 30 wt.% waste loading. Similarly, it was previously demonstrated that specimens encapsulating IRIS ashes maintain satisfactory compressive strength, at least up to 20 %wt. of waste loading.

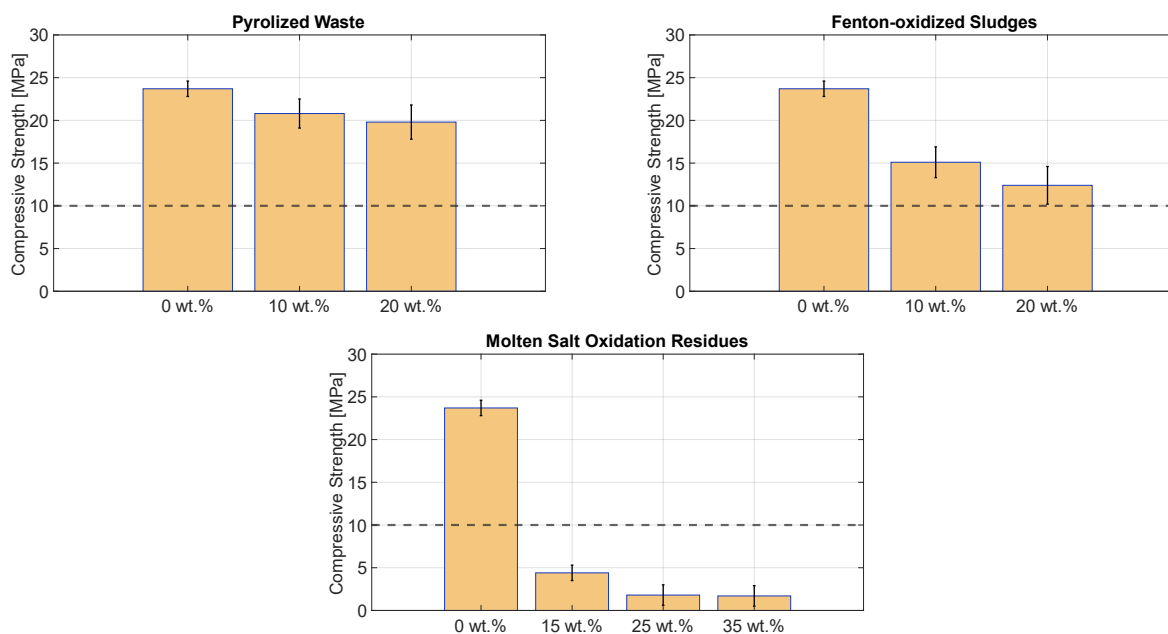


Figure 94. Compressive strengths of loaded waste forms. The 0 wt.% loading refers to the matrix, while the dotted line represents the 10 MPa acceptance limit adopted by the Italian regulator.

A different behaviour is observed in the case of Fenton-oxidized sludges, for which there is significant interaction with the matrix and the compressive strength rapidly decreases with increasing loading factor. This may be due to essentially two factors:

- The sludge has a high content of water which, because of the nature of the waste, cannot be easily determined. Hence, the loaded formulation has a higher water-to-binder ratio, which increases the porosity of the resulting waste form.
- The residual organic fraction in the sludge and the high content of sulphates interferes with the geopolymerisation reactions throughout hardening of the waste form, resulting in less crosslinked matrix.

The two proposed causes require further experimental activity for proper confirmation. Anyway, looking at the compressive strength 20 wt.% sludge-loaded waste form, this is the maximum loading factor achievable which satisfy the national acceptance criterion.

Concerning the residues downstream of MSO, a drop of about 80% with a loading factor of 15 wt.% is measured in the compressive strength of the waste form with respect to that of the unloaded matrix, and the drop increases to 90% with higher loadings. Because the waste is mainly constituted of sodium carbonate, the reasons for such a behaviour could be the hydration of carbonate phases. Further experimental confirmation is to be addressed.

4. Concluding remarks

The performances of the tuff-based matrix have been improved, and it shows to be versatile in the encapsulation of treated wastes with very different characteristics. In the case of pyrolyzed waste and IRIS ashes, the next step is the conditioning of higher loadings, while Fenton-oxidation sludges and MSO residues need improvements in the treatment step, and/or in the adjustment of the treated waste prior to conditioning. Anyway, the encapsulation step cannot be evaluated by itself, and needs to be addressed together with the corresponding treatment process.

References

- [1] A. Santi, E. Mossini, G. Magugliani, *et al.* "Design of sustainable geopolymeric matrices for encapsulation of treated radioactive solid organic waste". *Frontiers in Materials* 9, p. 1–17 (2022). DOI: <https://doi.org/10.3389/fmats.2022.1005864>

6.13 Leachability of nuclides of wastes conditioned in tuff-based geopolymeric matrix

*Andrea Santi, Francesco Galluccio, Eros Mossini, Gabriele Magugliani, Edoardo Rizzi,
Elena Macerata, Marco Giola, Mario Mariani
Corresponding author: eros.mossini@polimi.it*

Keywords: radioactive solid organic waste, treatment, conditioning, waste acceptance criteria, geopolymer, tuff, Fenton-like oxidation, oxidative pyrolysis

1. Introduction

Durability is the main feature waste packages must possess, and it often refers to a wide variety of properties which can be measured and related to their stability over time under specific conditions. POLIMI has lately focused on the leachability of radionuclides by carrying out tests in which the leaching behaviour of the wastes encapsulated in the tuff-based geopolymeric matrix is assessed. The waste forms under investigation are the ones synthesized in Task 6.4.

2. Experimental activity

The fresh pastes prepared in Task 6.4 are cast in cylindrical moulds (28 mm in diameter, 30 mm in height) and cured in it for 28 days. After demoulding, specimens are immersed in ultrapure water according to ANSI/ANS-16.1-2003 protocol. A preliminary verification of resistance may be run by means of static immersion. The leachates are analysed via ICP-OES and ICP-MS to determine the released fraction of each element. Stable isotopes of radionuclides of interest and matrix constituents are investigated, namely Na, Mg, Al, Si, P, S, K, Ca, Fe, Co, Ni, Sr, Ag, Ce, Nd, Eu, Th, and U. When not present in the treated waste, such elements were added during sample preparation in minor concentrations. Data are processed and presented in two ways: by means of leachability indices as reported in ANSI/ANS-16.1-2003 protocol, and through the determination of normalised losses (cumulative released mass fractions per unit surface area of the specimen) for better comparison with other partners in WP6.

3. Results

Cation-exchange resins thermally degraded at POLIMI via oxidative pyrolysis

The surrogate treated waste prepared for the investigation of encapsulation and durability comprises a mixture of sulphates, oxides, and nitrates of the element of interest. Samples at 10 and 20 wt.% loading were immersed, and the characterisation of the leachates was performed. Leachability indices were computed according to the ANSI/ANS-16.1-2003 protocol, and a minimum value of 6 was taken as the reference acceptance criterion. For certain elements, the amounts leached from the specimens were too low in concentrations to be detected using ICP-MS technique, and the quantification limit was used instead. As a result, only an upper limit of the releases could be inferred. Even with this artifact, leachability indices resulted to be greater than 8 for 20 wt.% loaded forms, both for matrix constituents and waste contaminants, thus satisfying the minimum requirement. Besides, samples showed integrity after three months of immersion, and it was decided to go on with the immersion tests. Normalised releases of some species are plotted against the square root of time in Figure 95. The linear regression shows R^2 values approximately equal to 0.90 ± 0.11 . However, it can be noted that a linear regression over the whole time is not the best way to interpret these data, for competitive release mechanisms simultaneously occur. In the first few hours, wash-off is predominant, then release of elements is governed by diffusion. Eventually, after three months, erosion begins to occur, as specimens started to lose their surface smoothness.

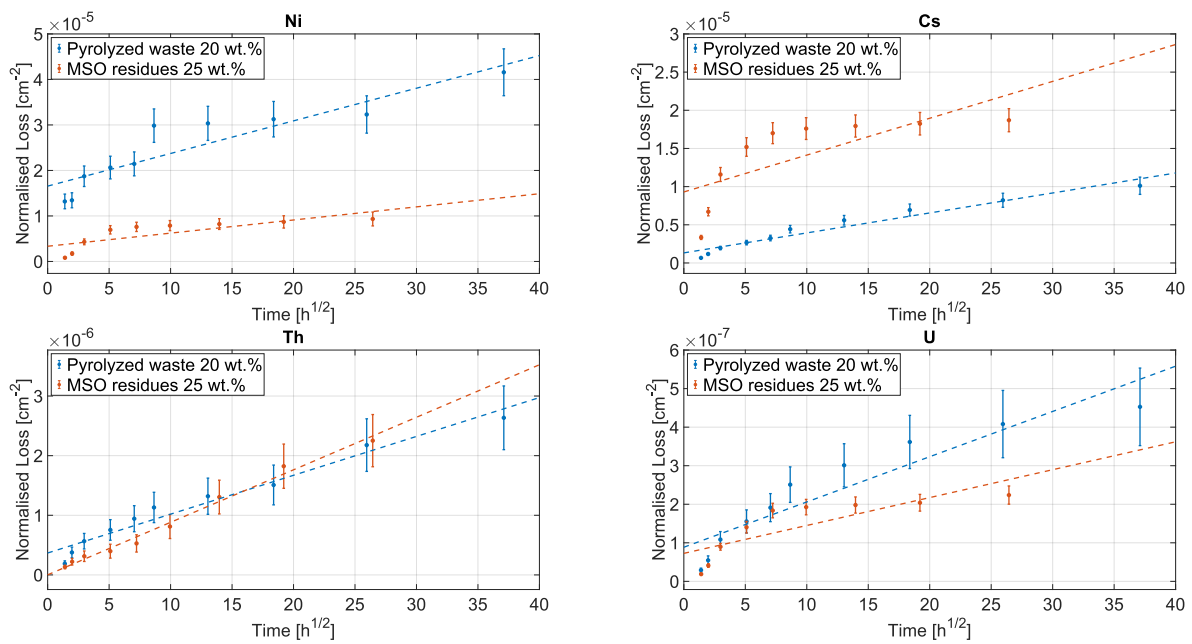


Figure 95. Cumulative leaching curves of nuclides in the waste forms for pyrolyzed waste (20 wt.% loading) and molten salt oxidation (MSO) residues (25 wt.% loading).

Mixed-bed ion-exchange resins treated by Fenton-like wet oxidation at POLIMI

Preliminary static immersion in deionised water of specimens loaded at 20 and 40 wt.% was carried out to assess the gross resistance toward immersion of the samples. The latter underwent swelling and cracking, and a significant amount of chloride and iodide was released, appreciably colouring the leachate in the first ten hours; debris was found at the bottom of the container. Hence, treatment and the encapsulation procedures must be reviewed to obtain more stable waste forms.

Ashes coming from the IRIS pilot plant managed by the CEA

The IRIS ashes provided by the CEA were encapsulated at 10, 20, 30, 40, and 50 wt.% in cylindrical specimens. These were used for static immersion in deionised water. Samples proved resistance towards immersion and exhibited no cracks at all after one month. More material is required to prepare representative samples and run further, more detailed tests.

Residues of solid organic waste treated at CVŘež by means of Molten Salt Oxidation (MSO)

Prior to hardening, specimens loaded at 15, 25, and 35 wt.% were spiked with ICP standards to introduce stable isotopes of radionuclides of interest. Preliminary, static immersion was run to assess the resistance. Samples at 35 wt.% loading, and after one hour of immersion were partially dissolved, with the formation of a fine particulate at the bottom of the container. After two hours of immersion, the specimens were fully degraded. Conversely, samples at 15 and 25 wt.% loading proved stability and underwent semi-dynamic leaching. Similarly to the waste forms loaded with pyrolyzed ion-exchange resins, for certain elements the leached amounts were too low in concentrations to be detected using ICP-MS technique, and the limit of quantification was used to estimate upper release values. The leachability indices resulted to be greater than the minimum required for 25 wt.% loaded forms, both for matrix constituents and waste contaminants. At visual inspection, after two months of immersion, samples did not exhibit major cracking nor surface erosion, and the test is still running. The normalised losses of some contaminants are plotted in Figure 95. The shape of the curves is similar to that of the samples loaded with pyrolyzed waste, and the values are comparable as well. Concerning the linear regression and the interpretation of leach mechanisms, the same considerations hold.

4. Concluding remarks

Samples prepared with pyrolyzed waste and MSO residues proved stable towards immersion and satisfy the leachability requirement up to 20 and 25 wt.% loading factors, respectively. However, because specimens with 25 wt.% MSO residues do not comply with strength criteria, the encapsulation step is to be reviewed and the

leaching test repeated. Similarly, major efforts should be devoted to improving the Fenton-like treatment of mixed-bed resins, in order to facilitate the encapsulation procedure and obtain stable, durable waste forms.

7 Scientific progress of Innovations in cemented waste handling and predisposal storage (WP7)

7.1 Radiation detection tools for radwaste characterization & monitoring

P. Finocchiaro (finocchiaro@lns.infn.it), INFN Laboratori Nazionali del Sud, Catania, Italy

M. Romoli (romoli@na.infn.it), P. Di Meo (pdimeo@na.infn.it), A. Pandalone (pandalone@na.infn.it), INFN Sezione di Napoli, Napoli, Italy

E. Conti (enrico.conti@pd.infn.it), P. Checchia (paolo.checchia@pd.infn.it), P. Andreetto (paolo.andreetto@pd.infn.it), F. Gonnella (francesco.gonnella@pd.infn.it), INFN Sezione di Padova, Padova, Italy

C. Sabbarese (carlo.sabbarese@na.infn.it), A. D’Onofrio (antonio.donofrio@na.infn.it), M. Di Giovanni (michele.digiovanni@unicampania.it), Università della Campania “L. Vanvitelli”, Caserta, Italy

Abstract

The subtask WP7.3 takes care of evaluating and demonstrating the quality assessment of cemented radioactive waste packages during their predisposal phase, to be performed by means of a non-destructive assessment technique and the external radiological monitoring. In particular INFN is following two guidelines: on the one hand the package tomography by exploiting the cosmic muons as penetrating radiation, and the other hand by externally monitoring the emitted gamma and neutron radiation carrying information from the inside of the packages. Suitable detection systems and electronics were developed ad hoc for these objectives.

Keywords: Muon tomography, SciFi gamma detector, SiLiF neutron detector, front-end electronics, wireless data acquisition.

1. Introduction

Two techniques developed by INFN are currently used in WP7 for external non destructive assessment and monitoring of cemented radwaste packages, namely the muon tomography and a low-cost gamma and neutron counting system. Muon Tomography is a powerful technique to detect denser materials inside a less dense medium, and to produce a corresponding 3D representation. It is the case, for example, of metal pieces (with density similar or greater than iron) cemented inside a radwaste drum that can thus be assessed in a non destructive fashion. As for monitoring, two kinds of gamma and neutron sensors can be installed outside single packages or on stillages to capture the radiological information coming from their inside, and a suitably developed front-end electronics and data acquisition system with WiFi interface can transmit the collected data to the database storage system.

2. Muon tomography

Muon Tomography exploits the natural flux of cosmic ray muons as scanning probes. Produced in the high layers of the atmosphere muons are highly penetrating particles which can cross large amount of dense material without being absorbed. However, they can experience Coulomb multiple scattering in materials and the resulting deflection, function of density and atomic number of the crossed material, can be measured event by event by means of two detectors above and two below the package (Figure 96).

Therefore the average scattering angle

$$\langle \theta_{\text{scatt}} \rangle = f(Z, \rho)$$

makes it possible to reconstruct the package density map [1].

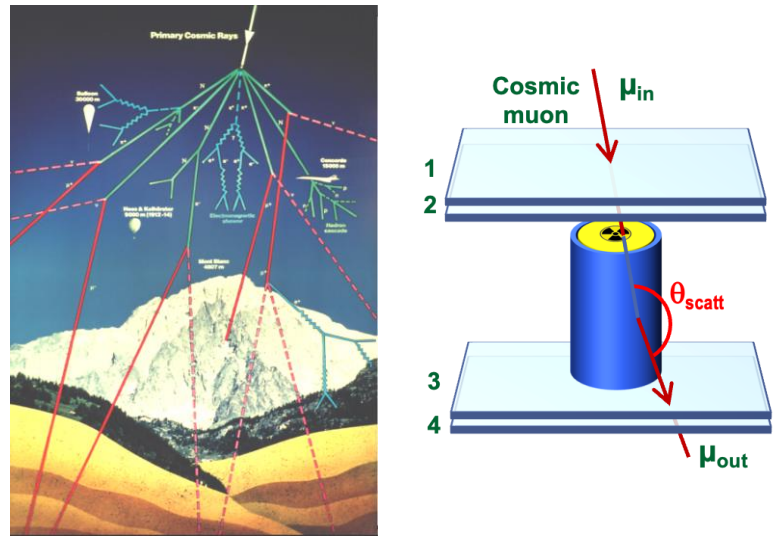


Figure 96. Sketch of the principles of muon tomography technique

Following a successful set of tests with preliminary prototypes, a mock-up cemented drum with several metal objects embedded in predefined positions was produced at UJV Prague and shipped to INFN Padova, where the final demonstration of the technique capabilities will take place with the existing tomograph.

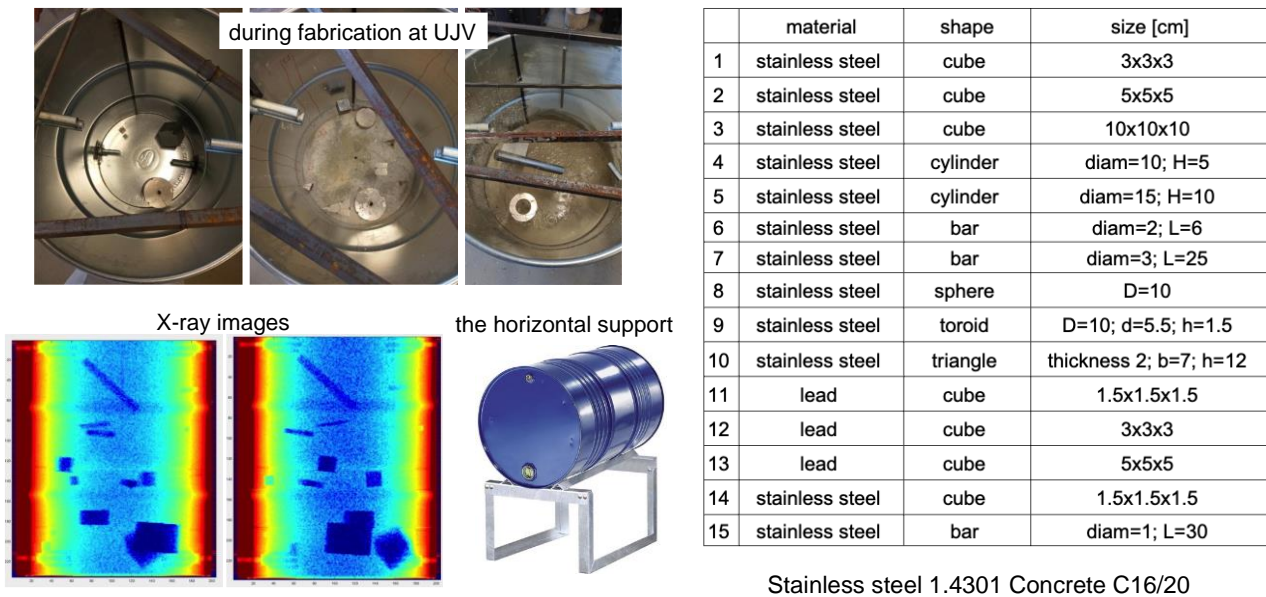


Figure 97. Left: the cemented mock-up produced at UJV Prague; two X-ray images were taken. Right: characteristics of the objects, embedded in the concrete, to be later detected by means of the muon tomograph at INFN Padova.

3. External radiological monitoring

The proposed system for external real-time monitoring consists of an array of gamma and neutron sensors to be deployed all around a number of radioactive waste drums, in order to collect counting-rate data in real time, following the developments done by the H2020 EU project MICADO. Such a system promises to be effective also in the case of cemented packages, as indicated by simulations, with added value in terms of safety, security, transparency with respect to the civil society expectation. As an evolution of the proof-of-principle systems discussed in [2–7], the SciFi and SiLiF detectors with their newly developed WiFi front-end and data acquisition electronics will be part of a prototype system to be installed in a radwaste storage to demonstrate the monitoring effectiveness (Figure 98).

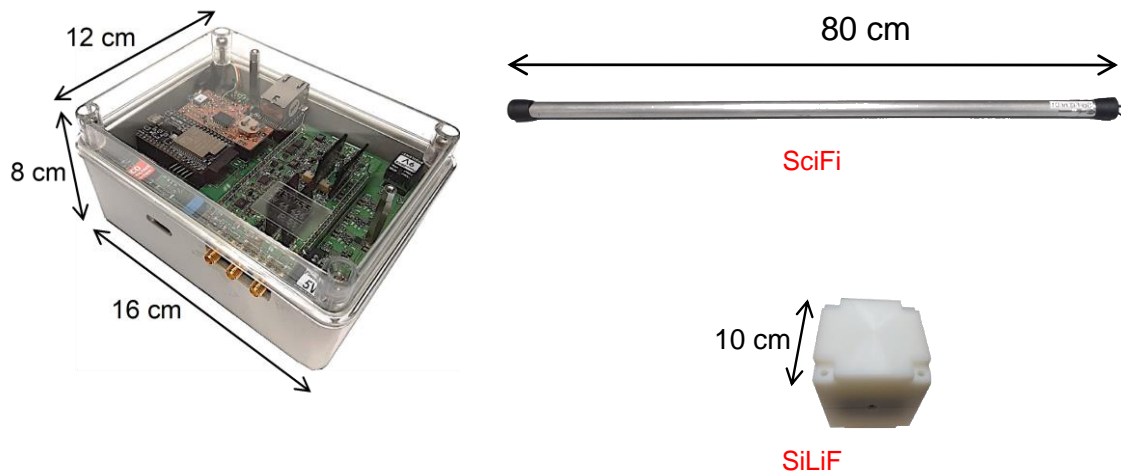


Figure 98. Left: the WiFi front-end and data acquisition electronics developed at INFN Napoli. Right: the SciFi and SiLiF detectors developed at INFN-LNS Catania, respectively for gamma rays and neutrons.

A successful radiological monitoring of radwaste has already been shown in MICADO, with partial limits due to the wired connections between the sensors and their front end electronics and then to the data acquisition hardware and software. The new developments done in PREDIS for aim at demonstrating the possible mass deployment of sensors in a modular and scalable fashion, so that one can tailor the system to small, medium, and large-scale storage configurations (Figure 99). In Figure 100 left we show an example of the so-called *radar plots* providing information about the anisotropy of the emission from radwaste packages in a 4x stillage configuration. Figure 100 right represents the timeline of the gamma emission, that provides indications about the stability of the measured emission of radiation, whose changes would hint at safety issues and/or at a security breach (tampering). The foreseen mock-up cemented drum, with holes for the insertion of radioactive sources and tiny wedges to simulate cracks, is in production at by UJV Prague and will be ready by the end of June 2023 for preliminary tests and the forthcoming final demonstration.

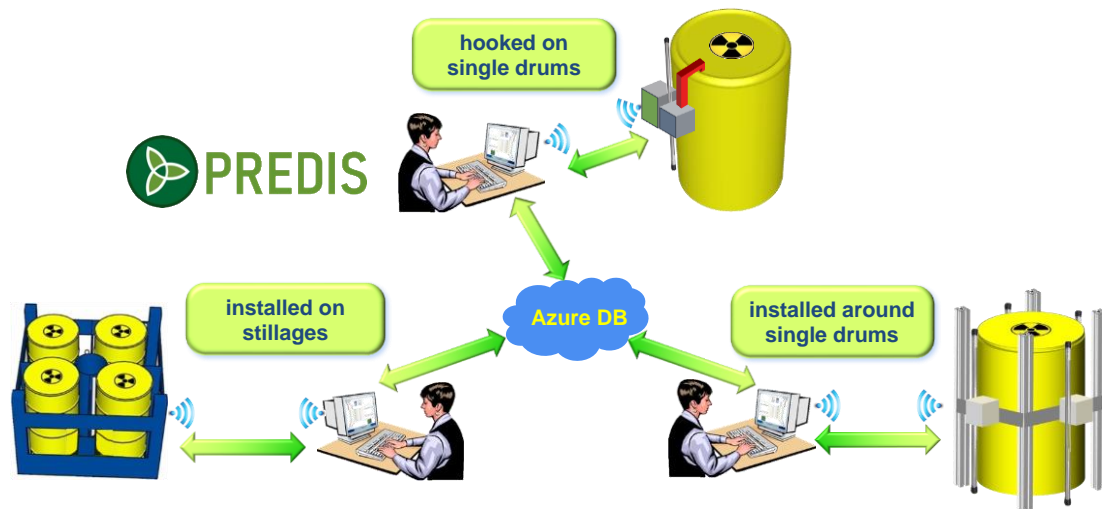


Figure 99. Three basic configurations for mass deployment of the external radiological monitoring system for gamma rays and neutrons, which could be freely mixed. The wireless front-end and data acquisition system allows for a remarkable flexibility.

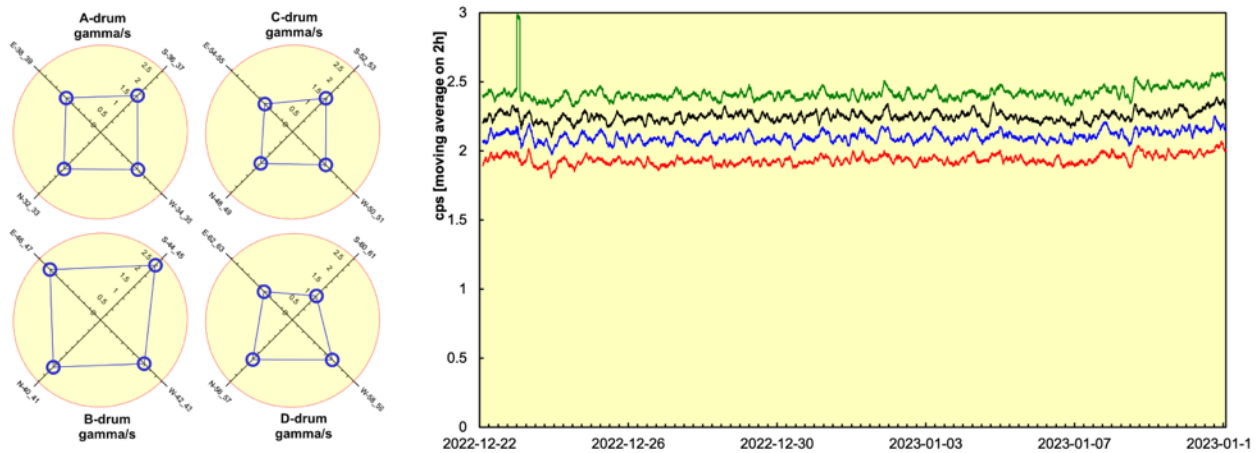


Figure 100. Left: example of the so-called radar plots providing information about the anisotropy of the emission from radwaste packages in a 4x stillage configuration. Right: timeline of the gamma emission from one package, that provides indications about the stability of the measured emission of radiation whose changes would hint at safety issues and/or at a security breach (tampering). Courtesy of MICADO.

4. Conclusions

Following the development activity so far conducted, we are now ready to start the field testing phase with mock-up cemented drums both for muon tomography and external radiological monitoring, in view of the final demonstration foreseen for PREDIS.

References

1. P. Checchia et al., “INFN muon tomography demonstrator: past and recent results with an eye to near-future activities”, (2018) Phil. Trans. R. Soc. A377: 20180065 <http://doi.org/10.1098/rsta.2018.0065>
2. L. Cosentino, Q. Ducasse, M. Giuffrida, S. Lo Meo, F. Longhitano, C. Marchetta, A. Massara, A. Pappalardo, G. Passaro, S. Russo, P. Finocchiaro, SiLiF Neutron Counters to Monitor Nuclear Materials in the MICADO Project. Sensors 2021, 21, 2630, doi:10.3390/s21082630.
3. L. Cosentino, M. Giuffrida, S. Lo Meo, F. Longhitano, A. Pappalardo, G. Passaro, P. Finocchiaro, Gamma-Ray Counters to Monitor Radioactive Waste Packages in the MICADO Project. Instruments 2021, 5, 19. DOI:10.3390/instruments5020019.
4. P. Finocchiaro, DMNR: A new concept for real-time online monitoring of short and medium term radioactive waste. In Radioactive Waste: Sources, Types and Management; Nova Science Publishers: New York, NY, USA, 2011; pp. 1–40.
5. P. Finocchiaro, Radioactive Waste: A System for Online Monitoring and Data Availability. Nucl. Phys. News 2014, 24, 34.
6. L. Cosentino, C. Cali, G. De Luca, G. Guardo, P. Litrico, A. Pappalardo, M. Piscopo, C. Scirè; S. Scirè; G. Vecchio, E. Botta, P. Finocchiaro, Real-Time Online Monitoring of Radwaste Storage: A Proof-of-Principle Test Prototype. IEEE Trans. Nucl. Sci. 2012, 59, 1426–1431.
7. P. Finocchiaro, M. Ripani, Radioactive Waste Monitoring: Opportunities from New Technologies. In Proceedings of the IAEA International Conference on Physical Protection of Nuclear Material and Nuclear Facilities, IAEA-CN-254/117, Vienna, Austria, 13–17 November 2017.

7.2 Embedded Monitoring System

Leone Pasquato¹, Esko Strömmer², Christoph Strangfeld¹, Christian Köpp¹, Vera Lay¹, Ernst Niederleithinger¹

¹ *Bundesanstalt für Materialforschung und -prüfung (BAM), 12205 Berlin, Germany*

² *VTT Technical Research Center of Finland, Espoo, 02150, Finland*

Abstract

BAM is developing an electronic measurement system to be placed inside a waste drum, which will be filled with concrete. The goal of this measurement system is to monitor the process of hardening and the evolution of the concrete itself over time to indirectly identify potential defects such as corrosion or cracking. The measured parameters are humidity, temperature, and pressure. In this regard, particular attention was given to the design of the electronic board's enclosure to allow the sensors to measure the state of the concrete without being in direct contact with it. In the scope of PREDIS, the supply of power to the battery-less sensors and the data acquired by such sensors are transmitted through the metallic waste drum by an innovative wireless technology developed by VTT (Technical Research Centre of Finland) to ensure long-term operation while keeping the integrity of the sealed container.

Keywords: Waste Drums, Embedded Sensors, Moisture, Temperature, Pressure, Concrete, RFID

1. Introduction

This measurement system aims to monitor the process of hardening and the evolution of the concrete itself over time and to indirectly identify potential defects such as corrosion or cracking of metallic waste drums by embedded battery-less sensors. Since the waste drums are completely sealed, it is necessary to develop a technology, which is able to transmit power and communicate through a metal layer, as well as to develop low-power sensors which can be embedded in concrete. These two main tasks have been carried out by BAM and VTT:

- BAM: development of a net of custom low-power measurement units (SensorNode) that allow the onboard sensors to measure the state of the concrete without being in direct contact with it.
- VTT: development of a customized RFID solution to power sensors and transfer data through solid metal structures based on its previous works (Strömmer, 2019).

2. Sensor instrumentation in the waste drum (BAM)

The sensing system is made of a chain of small units, called SensorNodes. Each SensorNode includes two off-the-shelf sensors: one for relative humidity and temperature and one for pressure and temperature. A SensorNode is designed to have a unique identifier and can be connected to other units while being uniquely addressable using a standard communication protocol. In this way, a distributed matrix of measurement points is created.

One of the most challenging tasks in designing a measurement system to run in a harsh environment (such as hardening concrete) is to let the sensors sense the external environment without being damaged themselves. To keep the external environment away from the electronic board, while still letting the sensors measure the concrete behaviour, holes have been drilled through the lid and were covered from the inside with a layer of porous membrane. The membrane's pores allow water and gas particles to pass through and let the enclosed air equilibrate with the external environment. With the help of the developed sensors, monitoring concrete in cemented waste drums will be possible. The derived data will also serve as the basis for ongoing modelling approaches for digital twins within the PREDIS project.

The energy consumption of one measurement cycle for each node is about 0.4mAs (20mW x 60ms).

- Limitations
 - Max 64 nodes on the same bus (Unique ID limit)
 - Max 6m water depth (Membrane's permeability limit)
 - Max 10m cable length (Communication protocol limit)



Figure 101. SensorNode (coin for scale).

3. Customized RFID (VTT)

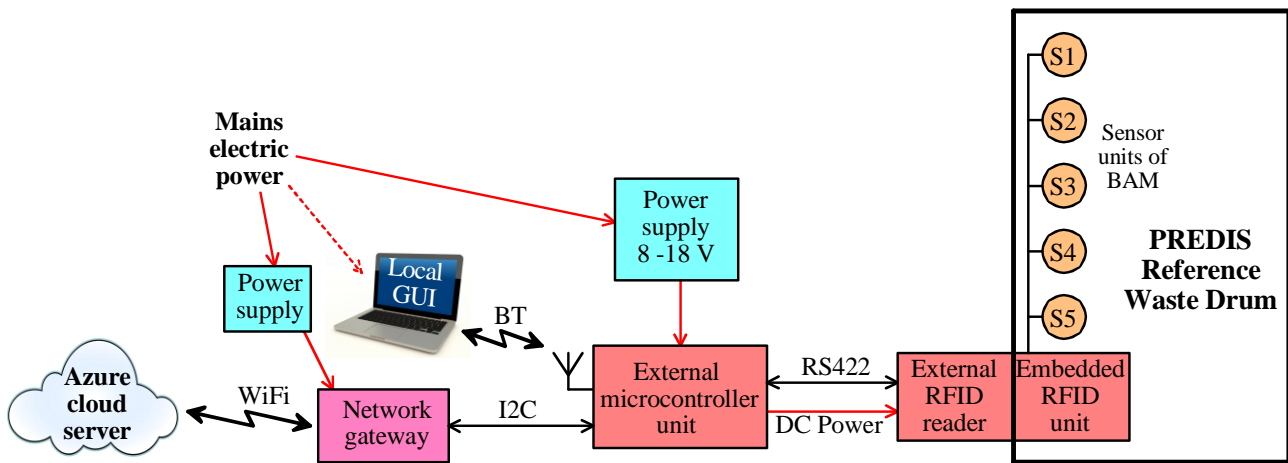


Figure 102. Data acquisition system layout.

The contactless powering and data uplink of the sensors in the drum is based on a couple of UR ferrite core antennas, symmetrically placed on the inner and outer surface of the drum.

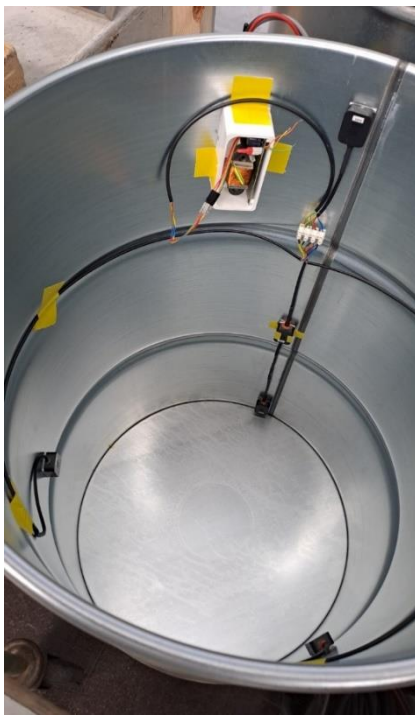
The maximum possible power transfer efficiency depends on the layer thickness, the gaps between the metal layer and the antenna cores, and the electromagnetic properties of the metal.

The PREDIS mock-up is a 1.4 mm thick steel drum, with a total gap between the antenna cores of about 2 mm. The maximum power transfer (about 1%) is achieved by super low frequency carrier (100 Hz). With a similar non-magnetic stainless steel drum, the power efficiency would be much higher.

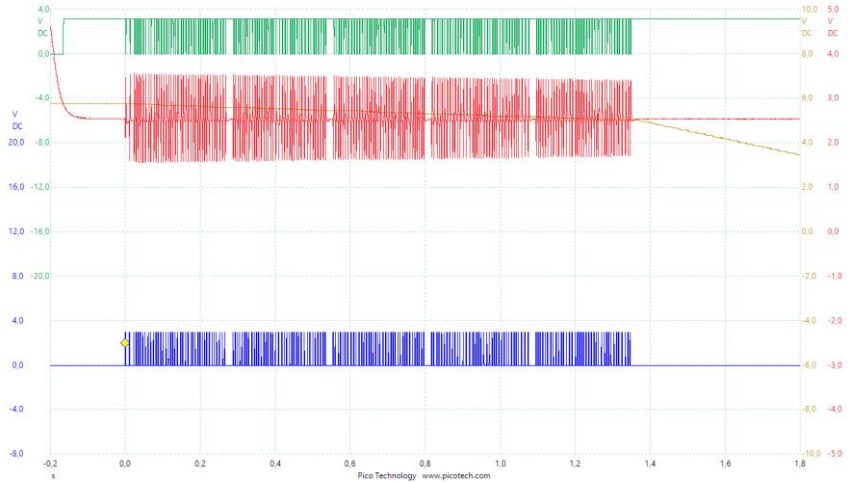
The required time to transmit enough energy to control up to 5 SensorNodes is about 30sec.

4. First drum integration at BAM 9-12/05/2023

The first integration of the Customized RFID data acquisition system and the chain of five SensorNodes has been made at BAM. The initial setup (not-waterproof, no concrete) showed that the Customized RFID technology is able to power five SensorNodes and transmits data through the drum skin. In the *Figure 103b*, it is possible to see the data transmitted by the embedded RFID unit (blue), the signal received by the External RFID unit (red) and the encoded binary data (red) converted from the analog signal (red).



a)



b)

Figure 103: a) Drum instrumentation, b) SensorNodes transmitted data

References

- [1] Strömmer, E. & Bohner, E., 2019. “Wireless energy transfer with data transfer add-on through low-conductivity host rocks”, Modern2020 Final Conference Proceedings: Deliverable n°6.3. Bertrand, J., Garcia, M. & Oltra, J. (eds.). European Commission EC, p. 411–417 7 p.

7.3 Experimental characterizations of old waste drums

Rainer Dähn, PSI, rainer.daehn@psi.ch

Wilfried Pfingsten, PSI

Dan Miron, PSI

Peter Szabo, KIT

Xavier Gaona, KIT

Marcus Altmaier, KIT

Keywords: old waste drums, spectroscopy, characterization

1. Introduction

Within task 7.4 it is foreseen to develop a digital twin of old waste drums. Such a digital twin should represent the evolution of radioactive waste packages during interim storage and takes into account modelling changes that happen on scales of tens of years due to the very slow processes involved. A PREDIS Digital Twin would contain a selection of independent and/or coupled processes, which can simulate the waste package evolution as a function of time. As input, the Digital Twin will require main waste package properties such as its chemical composition, physical dimensions, and storage conditions. Based on these input values, the Digital Twin will then select the appropriate evolution submodel(s) and use these models that calculate parameters that indicate integrity evolution of the waste package as a function of time (e.g. pressure and or volume changes).

2. Description of work and main findings

At PSI two waste drums prepared in 1994 have been taken out of the Swiss Federal Interim Storage Facility (BZL) at PSI. After approval of the Swiss Federal Nuclear Safety Inspectorate (ENSI) these drums were opened. Steel and cement samples were collected from the bottom, middle, top part and the lid of the drum

(Figure 104). These samples are currently under investigations with a variety of methods. In cooperation with EMPA we have tried to extract cement pore water with a heavy press from the bottom part. Unfortunately, the samples were too dry to extract any water. Successfully compression strength and young modul, TGA, mercury porosimetry, XRD and XRF have been performed. In addition at KIT X-ray microtomography was performed, which identified two well-defined regions, characterized by two different porosities (see Figure 105). Acquisition of XRD and TGA data have been completed (see Figure 106), and data evaluation is currently ongoing. XPS investigations are foreseen for summer 2023.

3. Conclusions

The preliminary results of the analysis from the concrete samples of almost 30 years old waste drums suggest that no significant alteration process have occurred in these real waste forms under the employed storage conditions at the BZL. Therefore, for the development of the digital twins the data obtained from the drum scale experiments of SCK CEN will be used. A git repository (<https://github.com/predis-h2020>) for the digital twin was set up, allowing for easier access and contribution to the project. Work on developing metadata and metadata schemas (<https://github.com/predis-h2020/metadata>) for waste package monitoring has been carried out, which will provide essential information about the location, sensors and the data collected from the sensors.



Figure 104. Cemented LLW drum considered for the characterization within this study. Samples were taken at PSI from upper, middle and bottom positions.

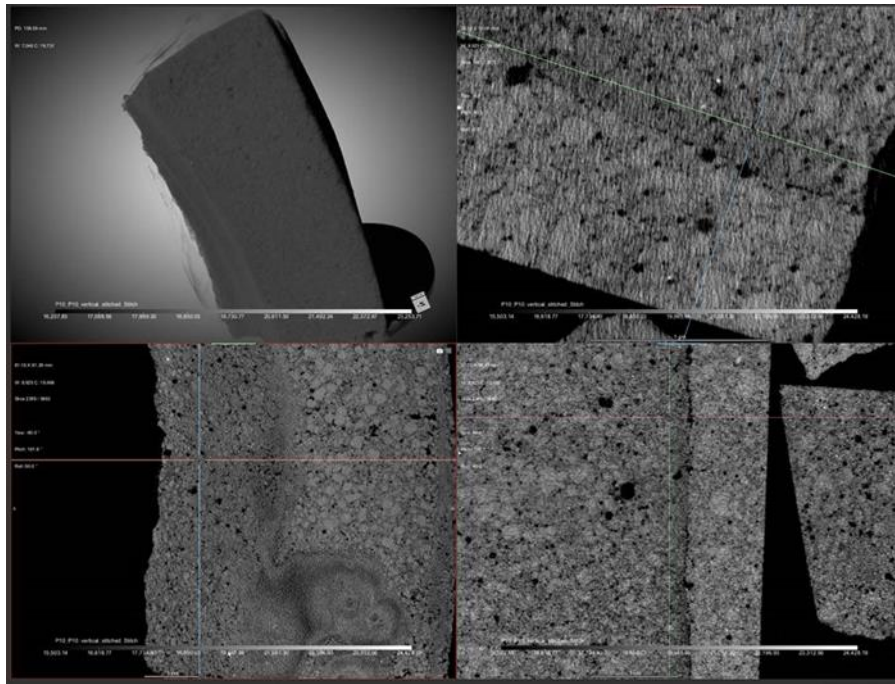


Figure 105. Microtomography of selected cement sample from LLW drum provided by PSI. Characterization conducted at the controlled area of KIT-INE.

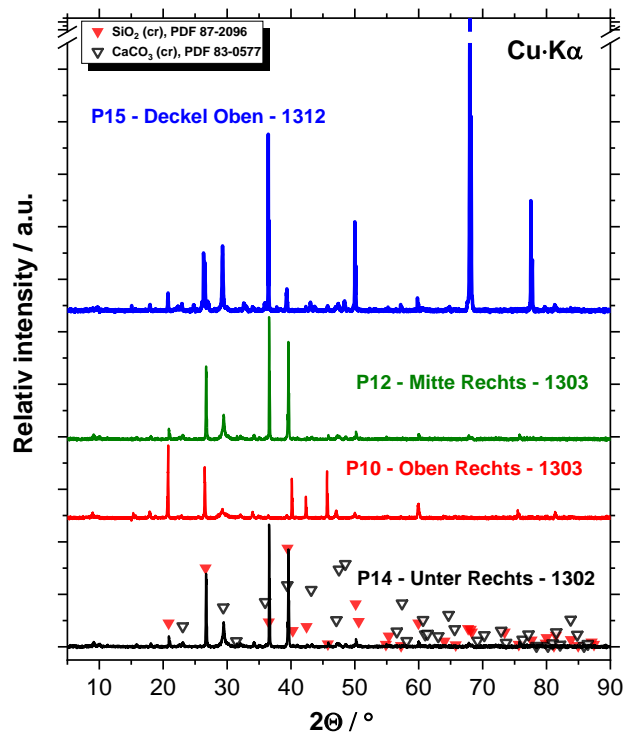


Figure 106. X-ray diffractograms of selected cement samples from LLW drum provided by PSI. Characterization conducted at the controlled area of KIT-INE.

7.4 CONDITIONING MONITORING FOR CEMENTED WASTE PACKAGE IN PREDISPOSAL STORAGE

Tuula Hakkarainen, Joonas Linnosmaa, Teemu Mätäsniemi, Jukka Aho & Tero Jokinen; VTT

Réka Szöke, Tom-Robert Bryntesen, Hans Olav Randem & Svein Tore Edvardsen; IFE

Enrico Botta & Paola Castagna; ANN

Bas Janssen; NRG

Keywords: Condition monitoring, decision support, cemented waste

1. Description of work and main findings

In PREDIS WP7, tools for monitoring cemented waste packages are researched and developed. The goal is to better understand and utilize the available data, with the possibility to detect and even predict important features from the measured data. The main questions to be answered are: 1) How long will the concrete last, 2) Which measurements are truly relevant, and 3) What is the current condition.

Monitoring systems are capable of providing ample data which is to be widely utilized. Advanced data handling helps to minimize potential errors and to reduce the risks related to data processing. Therefore, there is a need for a versatile data platform.

Figure 107 shows an overview of the condition monitoring system under development in PREDIS WP7. It illustrates the data and information transfer for monitoring technologies (T7.3), predictions from digital twin (T7.4) and decision support platform (T7.5). A joint demonstrator of these tasks will present the whole chain of data handling, processing and utilization. The novelty of the system will be in handling metadata so that it is useful and accurate, with good traceability.

From end-user viewpoint, the most important part of the condition monitoring system is the decision support platform. The processes at a radioactive waste storage are procedures-in-series where tasks and options must be selected. This selection will be more efficient when supported by a decision framework. The use of the decision support platform increases safety, reduces uncertainty, and supports decision making for intervention.

Figure 108 introduces the PREDIS Decision Platform which is implemented as a website. Dashboards give information about the quantities measured by sensors, e.g., temperature, pressure and humidity. Online analytical processing (OLAP) enables the user to analyse multidimensional data interactively from multiple perspectives. 3D analysis visualises the waste packages in three dimensions. Digital Twin models can predict the future state of the packages to support preparedness. The sensor view presents the state and time series of the sensors installed in the waste packages. The dose analysis visualises exposure to radiation based on “as low as reasonably achievable” (ALARA) principle. The optimisation tool calculates the optimal solution for packaging and logistics. The sensor deadman list reports the sensors which have not sent any data within a defined time limit. As a whole, the decision platform can be considered a holistic solution for enabling centralized decision management that incorporates data driven insights and analytics, along with human expertise.

Condition monitoring system

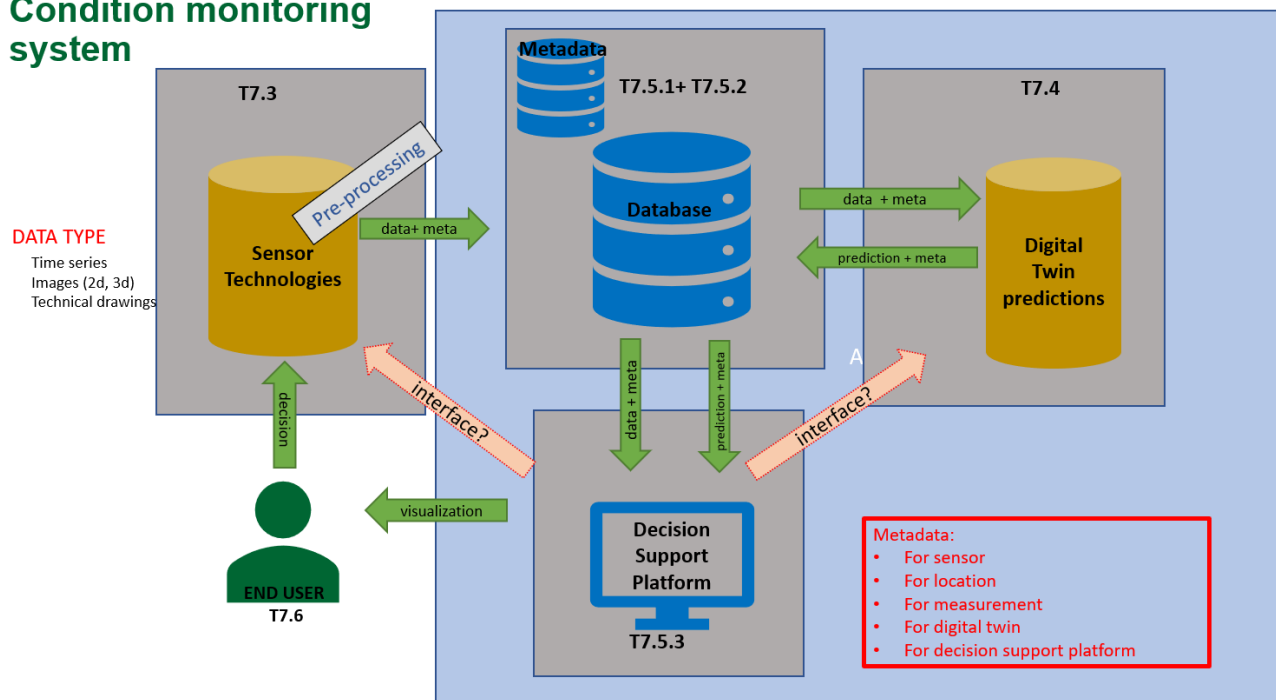


Figure 107. An overview of condition monitoring system for cemented waste package.

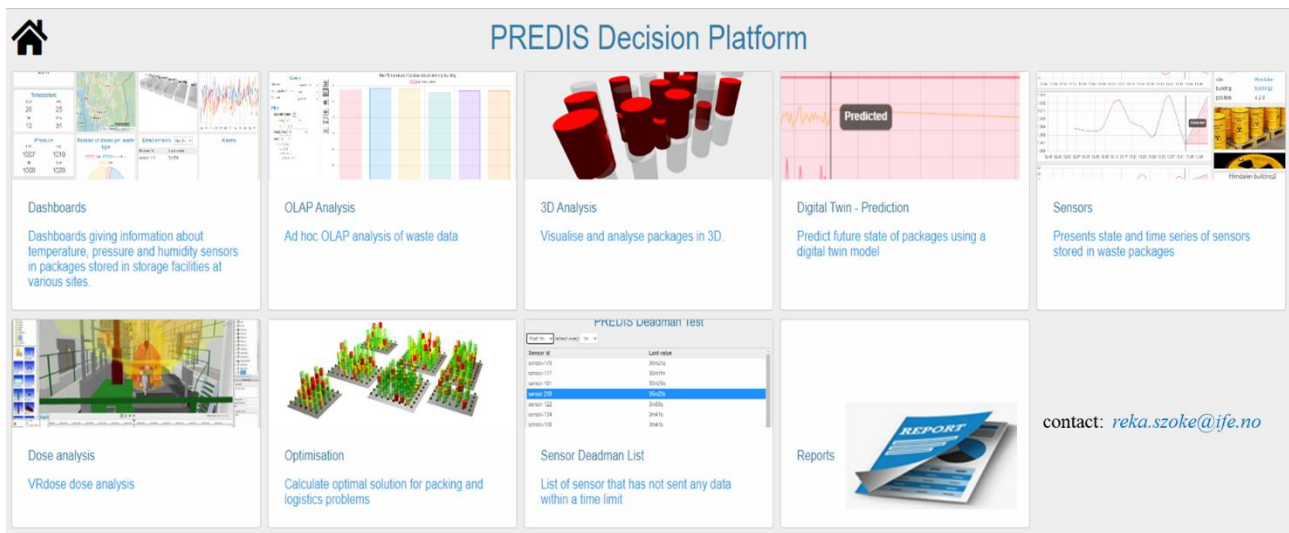


Figure 108. PREDIS Decision Platform, implemented as a website.

7.5 Demonstration and implementation of monitoring technologies

Elsa ABOU CHACRA, Orano, France, elsa.abou-chacra1.ext@orano.group
 Sabah BEN LAGHA, Orano, France, sabah.ben_lagha@orano.group
 Coralie CHAPUZET, Orano, France, coralie.chapuzet@orano.group

Abstract

During the PREDIS workshop of May 2023, Task 7.6's progress regarding the organisation of the demonstration tests was presented. The realisation of these tests is dependent on the mock-ups that will be used, the technologies that will be tested, and the locations at which they will be held.

Keywords: Demonstration, Mock-up, Technologies, technology comparison

1. Introduction

This document describes the work done by Task 7.6, which is composed of three major components:

- The results of the comparison study performed in order to evaluate and compare the technologies developed within WP7.
- The mock-ups that will be used to test out the technologies in a demonstration configuration
- The locations at which these demo tests will be performed

2. Description of work and main findings

Technology evaluation

To evaluate and compare the different non-destructive technologies of WP7, a comparison table was developed. It includes a set of criteria (universality level, measurement level, costs, safety, etc.). This table was sent to each WP7 technology developer to fill. After collecting the completed tables, the final scores for each technology were received and presented during the workshop.

The completion of the comparison table also required the participation of the End Users (EU) in scoring each technology according to several specific criteria such as whether the technology requires additional safety studies, if it could affect the behaviour of the package, and the duration and frequency of the measurements. These results, shown in the table below, were also obtained and presented at the workshop.

Table 18. Results of comparison table.

| | RFID embedded sensors | Sensorized RF identification box for radiation monitoring | Muon Tomography | SiLiF neutron monitor | SciFi gamma monitor | IoT Pressure sensor | AE wireless | US inspection |
|--------------------|-----------------------|---|-----------------|-----------------------|---------------------|---------------------|-------------|---------------|
| Global developers | C | A | B | A | A | B | C | B |
| Global EU criteria | B | A | B | A | A | C | A | A |

The table will be updated in 2023 in cooperation with the WP7 technology developers to include any updates and developments in the technologies.

2.1 Requirements for the realization of the demonstration tests

End User parameters

The first information required for the decision of which technologies to test came from EU needs. WP7 EUs identified a list of parameters of interest: cracks, internal and external corrosion of the metallic container, dose rate, leakage of liquid, gas emissions, and surface contamination.

Mock-ups

For the demonstration tests, three different packages will be used:

- >NNL: 30-year-old Magnox mock-up (non-active)
- 2 new mock-ups that will be produced by UJV:
 - Mock-up 1 will be used to test the RFID technology (non-active)
 - Mock-up 2 will be used to test SciFi, SiLiF, and RF technologies (active)

Test Locations

To fulfil the requirements of Task 7.6, the demonstration tests must be performed in a realistic environment. To do this, the characteristics of real storage facilities of the WP7 EUs were collected.

Using the information gathered, the two demonstration test locations and configurations were chosen.

2.2 The two demonstration tests

The performance of the demonstration tests will increase the technologies' TRL to a minimum of 5. Here, the technologies' efficiencies will be assessed over a longer period than in Task 7.3.

Demo at UJV

The demonstration test at UJV is planned for Q4 2023/Q1 2024. It will be ongoing for a period of three months. This demo test will use the mock-ups (mock-ups 1 and 2) as well as other cemented packages produced by UJV. The cemented packages will act as a screen in order to check the efficiency of the technologies' data transfer.

To meet the developers' specifications, stillages will be used to indirectly stack the packages on top of each other. The figure below presents the configuration that will be used for the UJV demo test.

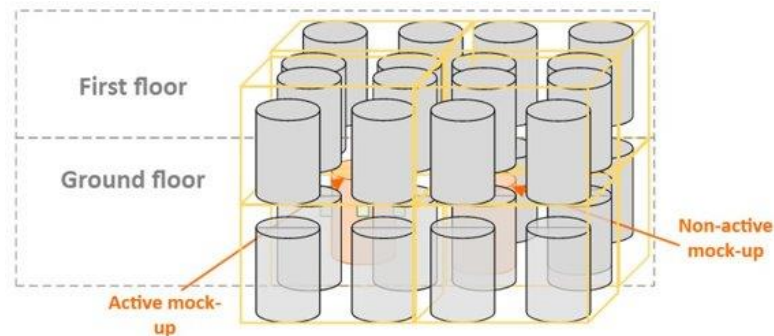


Figure 109. Configuration for UJV demo test.

Demo at NNL

NNL's feasibility trials of the automated scan, using 2D and 3D photogrammetry techniques of a 500L drum in a mock-up storage environment (shown in the figure below) has been completed, and a presentation including a video of the operation was presented during the Mechelen workshop May 2023. This initial operation of the works performed by NNL carries out the photogrammetry analysis whilst the drums remain within their stillage. In this setup, a stillage and paired drums obstruct the view of up to ~65% of the drum to be inspected. A 3D camera at the end of the robot arm collects a series of images at preset points in the current demonstration. These images are then stitched together to form a partial 3D point cloud map of the outer surface of the waste container using the camera's software.



Figure 110. NNL feasibility trial of stitching laser scanning.

Robot movements have now been pre-programmed for further inspections, and in the next few months the works at NNL will incorporate the results from ultrasonic trials once the system arrives from the manufacturer. Ultrasonic data will be coupled with the photogrammetry data to build up a 3D representation of a waste drum. The ultrasonics will be deployed using the same robotic system and without contact with the waste container. The next steps for the works will build on the recommendations from academic research performed originally by the NNL team at the University of Strathclyde. Scaling the technology to test if the ultrasonics can be applied to full size waste containers, with immobilized waste content, and using an automated deployment technique from a distance rather than by-hand methods.

Matlab software will then be used to extract the partial point cloud data from the photogrammetry analysis and then couple these measurements with those from the ultrasonic scans to generate a 3D digital representation of the waste container. This will provide results of any deformation from manufacturing tolerances. The work aims to identify cracking, swelling, deformation, or corrosion of the outer waste container, with an aim to increase the TRL of automated inspection for waste containers whilst in interim storage.

Showcase

The 7.6 showcase will be a collection of the results obtained from all of the tests performed during PREDIS in order to present them. It will consist of videos of test performances, pictures, as well as parts of the technologies if possible. In addition, posters to present each WP7 technology and their improvements obtained within PREDIS will be prepared to present the information as clearly as possible.

The showcase will be held before mid-2024 (the end of the project). Its location has not yet been decided.

3. Conclusion

As for the next steps, Task 7.6 will focus on the realization of the milestone M7.6 completion of the demo tests until their conclusion by Q1 2024. In addition to this, the poster template will be finalized so that all developers may complete it for the showcase.

There is also the milestone M7.5 value assessment to complete before the end of the project. Task 6 aims to hold a workshop-type meeting with the EUs to accomplish this.

The deliverable D7.8, which will report on the demonstration and implementation of the WP7 techniques for improving safety during the storage and handling of cemented waste packages, will also be completed before the end of the project.